This thesis is submitted to University College London
for the degree of Doctor of Philosophy

June 2014

The route taken by Wingless in secreting cells.

Lucy Palmer

Jean-Paul Vincent group
Division of Developmental Biology
MRC – National Institute for Medical Research
The Ridgeway, Mill Hill
London, NW7 1AA

Declaration

'I, Lucy Palmer, confirm that the work presented in this thesis is my own. Where information has been derived from other sources, I confirm that this has been indicated in the thesis.'

Abstract

Wingless (Wg), the major *Drosophila* Wnt, contributes to patterning, growth and cell survival during development. Wg is produced in a stripe at the dorsal-ventral boundary of the wing imaginal disc, a pseudostratified epithelium. Whole mount staining of permeabilised discs reveal that the Wg protein is tightly localized in the apical region of secreting cells. By contrast, extracellular Wg is barely detectable at the apical surface. Instead, extracellular Wg is mostly found at the basolateral surface of secreting, as well as surrounding, cells. These observations suggest that, in secreting cells, apically produced Wg traffics to the basolateral surface for release and gradient formation. This possibility has not been formally investigated. Nevertheless, specific regulators of Wg secretion have been identified. For example, Wntless (Wls)/Evenness interrupted (Evi) binds Wg in the ER and transports it to the plasma membrane. Without Evi, Wg accumulates within the secretory pathway. To test the transcytosis model, I have designed means of tracking Evi and Wg in secreting cells, using classical secretory and endocytic markers as guideposts. I have constructed tagged versions of Wg and Evi, which rescue *wg* or *evi* mutants when expressed at an endogenous level. In one set of experiments, I have produced a step of Wg expression and fixed discs at subsequent time points. With this approach I have determined that Wg moves from its apical production site towards the basolateral surface. This was confirmed with experiments utilising a temperature-sensitive dynamin mutant (*shibire*^{ts}) to control endocytosis. With this genetic tool, I have obtained data suggesting that Evi too transits through the apical surface of expressing cells before progressing basally. Unlike Wg, Evi is not released at the basolateral surface. I suggest that instead, it is recycled to replenish the secretory pathway, where it can escort more Wg to the apical surface.

Acknowledgements

The first and biggest thanks must go to my project supervisor **Jean-Paul Vincent** for taking a chance on me. Through our interactions I have learnt so much, not just about science but also about life! Thank you for pushing me to achieve more than I ever thought I was capable of, and for giving me confidence in both my science and myself. Working with you and the lab has been the best experience of my life and I will always be grateful for this opportunity.

None of this would be possible without the constant input, care, teaching and friendship of **Karen Beckett** and **Cyrille Alexandre**. Thank you Karen for being my science Auntie, the best collaborator one could wish for, and the best friend. Your patience has been never-ending and your support second to none. I have learnt so much from working with you and will always be thankful for that privilege. To Cyrille - the King of molecular biology. Thank you for teaching me so painstakingly and patiently everything I know about DNA, and still being prepared to field questions some four years later. Thank you for the support and laughter throughout this PhD, and for your constant enthusiasm and excitement in this project even when sometimes mine was running low!

To all past and present members of the **Vincent Lab**, thank you for making my time here so enjoyable! I owe a lot to our fantastic lab atmosphere and all the great input from so many talented people! Special thanks go to **Paul Langton**, **Satoshi Kakugawa**, **Alberto Baena-Lopez** and **Sam Crossman** for the constant laughter that is indeed the best medicine for a failed experiment! Also, big thanks must go to **Catherine Rabouille** for always encouraging me to look at things in a different way!

Thank you to my thesis committee: **Iris Salecker**, **Elke Ober and Tom Carter** for fruitful thesis committee meetings and great discussions. A big thank you must also go to **Hayley Wood** for her ability to turn my terrible drawings into works of art!

The collaborative atmosphere of the NIMR has also proved to be a blessing throughout my studies, and great thanks must go to the **fly-group members** from the labs of **Alex Gould** and **Iris Salecker**. Our stimulating meetings and fun fly room discussions have been invaluable throughout this

process. Not to mention the legendary Sex-lethal football team! The NIMR has also provided me with a wonderful group of friends who have helped me through the PhD, but thanks must go in particular to **Katherine Collins**, **Gemma Wildsmith** and **Harald Hartweger** for keeping me sane and fed in the more stressful moments.

Finally, the greatest thanks go to my parents, my boyfriend and **Eileen McCarthy**. I would be lost without them.

Table of Contents

List of Figures

List of Abbreviations

A compartment	Anterior compartment (see Figure 1.1)
AA	Amino acid
act	*actin*
AEL	After egg-laying
Ala	Alanine
A/P boundary	Anterior/posterior boundary (see Figure 1.1)
APC	Adenomatous polyposis coli
ARF	Auxin response factor
arm	*armadillo* (*Drosophila* homologue of β-catenin)
arr	*arrow* (*Drosophila* homologue of LRP5/6)
Asn	Asparagine
β-gal	β-galactosidase
β-cat	β-catenin
BAC	Bacterial artificial chromosome
BAR	Bin/Amphiphysin/Rvs domain
CAV-1/2	Caveolin-1/2
CCV	Clathrin coated vesicle
CD8	Cluster of differentiation 8 – transmembrane protein
CIE	Clathrin-independent endocytosis
CK1	Casein kinase 1
CLICs	Clathrin-independent tubulovesicle carriers
CME	Clathrin mediated endocytosis
colIV	*collagen-IV*
COP-I/II	Coat protein complex I/II
CRD	Cysteine-rich domain
CSC	Cargo-selective complex
Cu^{2+}	Copper
Cys	Cysteine
dally	*division abnormally delayed*
disp	*dispatched*
dll	*distal-less*
dlp	*dally-like protein*
DNA	Deoxyribonucleic acid
dpp	*decapentaplegic (Drosophila* homologue of the TGF-β family*)*
dsh	*dishevelled*

D/V boundary	Dorsal/ventral boundary (see Figure 1.1)
EC3	Extracellular loop 3 of the Evi 80kb BAC
ECM	Extracellular matrix
EE	Early endosome
EM	Electron microscopy
en	*engrailed*
ER	Endoplasmic reticulum
ESCRT	Endosomal sorting complex required for transport
evi	*evenness interrupted*
FBS	Foetal-bovine serum
FCS	Foetal-calf serum
fz	*frizzled*
FRT	Flp-recombinase target sequence
GEEC	GPI-anchored protein enriched early endosomal compartment
GFP	Green fluorescent protein
Gly	Glycine
GPI	Glycosylphosphatidylinositol
GSK3-β	Glycogen synthase kinase β
hh	*hedgehog*
hr	hours
HRP	Horse radish peroxidase
hs	heat shock
hsp70	heat shock protein 70
HSPG	Heparan sulphate proteoglycan
ILV	Intra-luminal vesicle
kb	kilobase
LB	Luria broth
LE	Late endosome
LRP5/6	Low-density lipoprotein receptor-related protein 5/6
LPP	Lipoprotein particle
MCS	Multiple cloning site
MDCK	Madin darby canine kidney cells
min	minutes
mop	*myopic*
MVB	Multi-vesicular body
NMJ	Neuro-muscular junction
P compartment	Posterior compartment (see Figure 1.1)

pA/PolyA	Polyadenylation tail added to mRNA
PBS	Phosphate buffered saline
PBT	PBS-Triton x100
PCR	Polymerase chain reaction
Pen	Penicillin
PFA	Paraformaldehyde
PIs	Phosphoinositides
PI-PLC	Phosphoinositide phospholipase C
porc	*porcupine*
Pro	Proline
PX	Phox-homology domain
RE	Recycling endosome
RFP	Red fluorescent protein
RNA	Ribonucleic acid
sens	*senseless*
Ser	Serine
shh	*sonic hedgehog*
shi^{ts}	$shibire^{ts}$ dynamin mutant
SNAREs	Soluble N-ethylmaleimide-sensitive fusion factor attachment protein receptors
SNX	Sorting nexin
srt	*sprinter*
Strep	Streptomycin
Swim	Secreted wingless interacting molecule
TCF/Lef	Transcription factor/lymphoid enhancer binding factor
TEB	Triton-extraction buffer
TGF-β	Transforming-growth factor β
tkv	*thick-veins*
TLE	Transducin-like enhancer protein
TM	Transmembrane
tub	*tubulin*
UAS	Upstream activating sequence
ubi	*ubiquitin*
UTR	Un-translated region
vg	*vestigial*
Vps26	Vacuolar protein sorting gene 26
Vps29	Vacuolar protein sorting gene 29
Vps35	Vacuolar protein sorting gene 35

wg	*wingless*
wg^{KO}	*wingless* knock-out
WLE	Wingless localisation element
wls	*wntless*
wnt	wingless-type integration site
YFP	Yellow fluorescent protein

List of Definitions

A compartment – the anterior compartment of the *Drosophila* wing imaginal disc (for schematic see Figure 1.1).

Apical – the region of a cell located on the luminal side of junctions.

A/P Boundary – the boundary separating the anterior and posterior compartments of the *Drosophila* wing imaginal disc (for schematic see Figure 1.1).

Basolateral – the region of a cell located on the haemolymph side of the junctions.

Confocal XY optical slice – a single confocal section of an image in the XY plane.

Confocal YZ reconstruction – an image produced from a stack of confocal sections reconstructing the YZ plane.

D/V Boundary – the boundary separating the prospective dorsal and ventral regions of the *Drosophila* wing imaginal disc giving rise to the wing margin (for schematic see Figure 1.1).

Extracellular staining – antibody staining protocol, which allows the detection of extracellular protein excluding intracellular epitopes.

Lateral – the region of a cell stretching from the junctions to the basal surface.

P compartment – the posterior compartment of the *Drosophila* wing imaginal disc (for schematic see Figure 1.1).

Planar Transcytosis – mechanism by which molecules move across the plane of the epithelium via internalisation by endocytosis and intracellular transport for release to the neighbouring cell. Molecules are passed from cell to cell via repeated rounds of internalisation and release.

Stop cassette – an FRT flanked DNA module containing a transcriptional termination sequence. Upon expression of Flp, FRT recombination causes cassette excision and expression of downstream genes.

Transcytosis – the process by which proteins are moved from one surface of a polarised cell to the opposite surface via endocytosis.

Total staining – antibody staining protocol, which detects both intra and extracellular protein present in a sample. In the case of Wg, the majority of protein detected is intracellular since intracellular Wg levels are much higher than extracellular Wg.

Wg secreting/producing cells – a stripe of cells along the D/V boundary, which produce and secrete Wg (for schematic see Figure 1.1).

Wg-HA step – a front of Wg-HA produced upon Flp expression, which can be tracked through the secretory pathway.

2A sequence – a short amino acid sequence, which can be inserted between two cDNA sequences for production of two separate proteins from the same transcript via ribosome "skipping" (see Chapter 5, section 5.2.5).

Chapter One

General Introduction

1.1 Importance of Wnts

1.1.1 General Roles of Wnt Signalling

The first *Wnt* gene identified was the oncogene *Int-1*, the locus of which was a frequent site for targeted retroviral insertion of the mouse mammary tumour virus (MMTV) (Nusse and Varmus, 1982). *INT-1* was later shown to be homologous to the *Drosophila* gene *wingless* (*wg*) (Rijsewijk et al., 1987), a gene which upon mutation prevents wing formation in flies (Sharma and Chopra, 1976), and so the name "WNT" was coined, a mnemonic for the Wingless-type Integration site (Nusse et al., 1991).

Wnt proteins are essential components of many complex developmental and homeostatic processes in tissues (Bartscherer and Boutros, 2008). Purified Wnt3a has been demonstrated to induce haematopoietic stem cell renewal (Willert et al., 2003). Wnt signalling is required for the maintenance of stem cell number in multiple contexts, for example, inhibition of Wnt signalling causes ablation of stem cells in the intestinal crypts of adult mice (Schepers and Clevers, 2012). Misregulation of the Wnt signalling pathway therefore has important consequences, and aberrant Wnt signalling has been implicated in the onset of many types of cancer, including colon cancer (Clevers and Nusse, 2012; Schepers and Clevers, 2012). A well-studied example of this is the mutation of the Adenomatous Polyposis Coli (APC) tumour suppressor gene (Polakis, 2012). In 80% of sporadic colon cancers APC is mutated, causing over-activation of the Wnt signalling pathway leading to overproliferation and

tumorigenesis (Oving and Clevers, 2002). However, further mutations are required for the transformation to a malignant carcinoma (Polakis, 2012).

A further role for Wnt proteins is during development. The *Wnt* gene family is well conserved through evolution, and *Wnt* genes influence many aspects of development in different animals (Miller, 2002). For example, Wnt signalling has been demonstrated to influence neuronal polarity in *C. elegans* (Prasad and Clark, 2006), to regulate anterior-posterior (A/P) patterning in the *Xenopus* embryo (Kiecker and Niehrs, 2001) and to be required for early stage mouse embryonic body axis formation (Fu et al., 2009). The role of Wnts has been well characterised in both the *Drosophila* embryo and wing imaginal disc, mainly focusing on the *Drosophila* homologue of mammalian *Wnt1*, *wg* (Rijsewijk et al., 1987).

Wingless (*wg*) was initially identified by Sharma et al. (1976) as required for wing formation in *Drosophila*. It was subsequently demonstrated to be a segment polarity gene, functioning as an important part of the genetic network that organises initial stages of *Drosophila* A/P patterning (Gonzalez-Gaitan, 2003; Nusslein-Volhard and Wieschaus, 1980). Secretion of Wg protein has been demonstrated to be important in both the *Drosophila* embryo and the wing imaginal disc (Couso et al., 1994; Gonzalez et al., 1991). Using immunocytochemistry, in embryos, Wg protein could be observed intracellularly at least two or three cells away from its source (Gonzalez et al., 1991; van den Heuvel et al., 1989). This signal was abolished upon treatment with monensin, an inhibitor of secretion, indicating that Wg protein is released from the cells in which it is made and spreads within the embryonic epidermis (Gonzalez et al., 1991). A similar situation is observed in the *Drosophila* wing imaginal disc. Wg is secreted from a source of expressing cells along the Dorsal-Ventral (D/V) boundary to activate target gene expression and subsequent patterning of the wing (Figure 1.1 B) (Couso et al., 1994). In both these contexts it has been proposed that target gene expression is concentration-dependent and that Wg acts as a morphogen.

Figure 1.1: Morphology of the *Drosophila* wing imaginal disc, morphogen gradient formation and Wingless (Wg) target genes.
Box 1 - (A) Schematic of the *Drosophila* wing imaginal disc. Two main compartment boundaries partition the disc: the anterior/posterior (A/P) boundary from top to bottom and the dorsal/ventral (D/V) boundary horizontally. (B) Wg is expressed in a stripe of cells along the D/V boundary and moves to form a gradient. Wg is also produced in a ring around the pouch. Box 2 – Each cell in a tissue has the potential to become red, white or blue. (C) The morphogen concentration provides positional information. (D) This positional information is converted into a response (i.e. red, white or blue) depending on the local morphogen concentration. Adapted from 'Principles of Development' by L. Wolpert. Box 3 – (E, F, G) Schematic outlining the expression patterns of Wg target genes Sens (E), Dll (F) and Vg (G). (E) Sens is a short-range target expressed around 4 cells away from the stripe of Wg expressing cells. (F, G) Dll and Vg are long-range target genes expressed around 20 cells away from the stripe of Wg expressing cells.

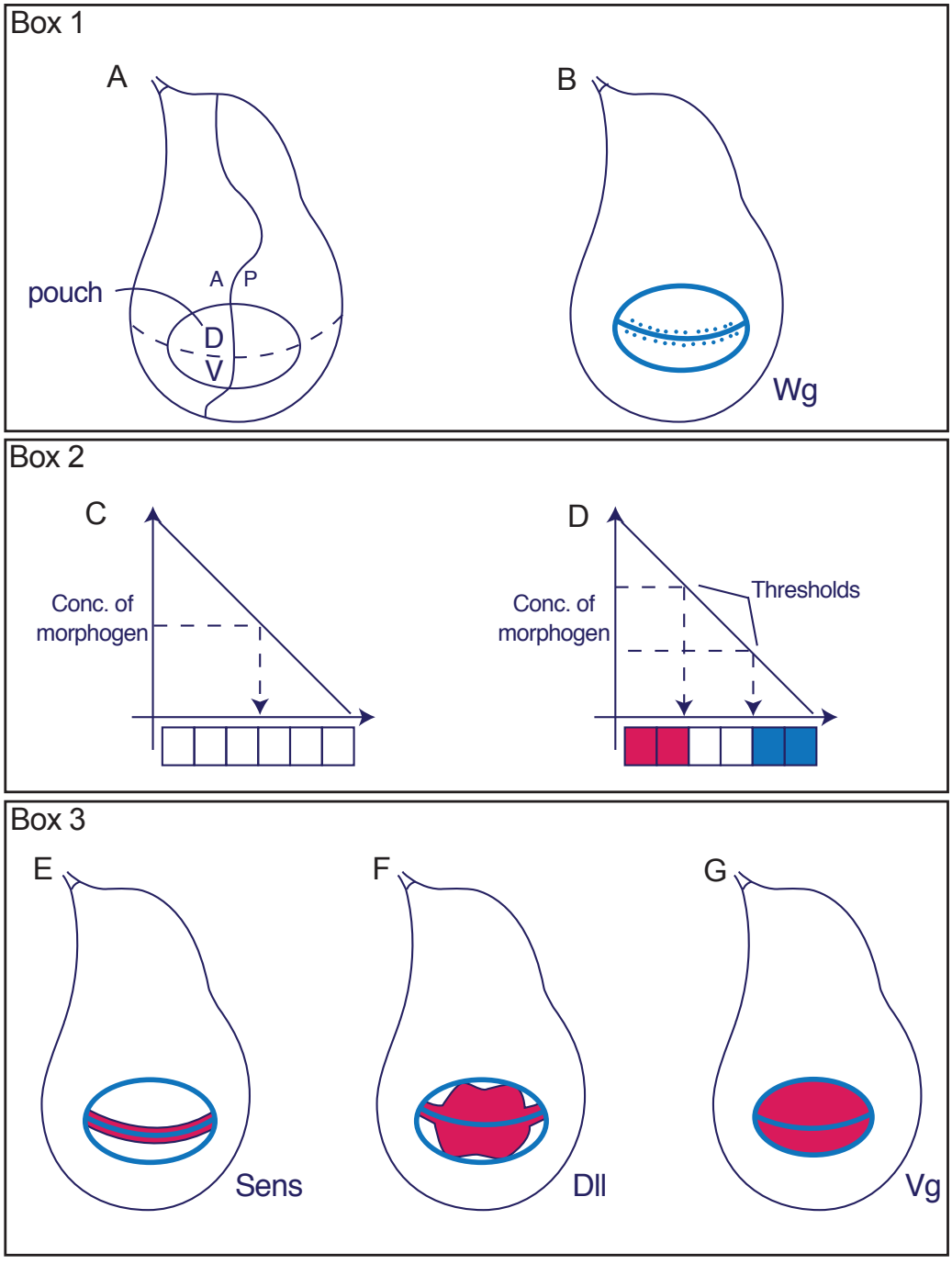
Box 1
A
pouch
A
P
D
V
B
Wg
Box 2
C
Conc. of
morphogen
D
Conc. of
morphogen
Thresholds
Box 3
E
Sens
F
Dll
G
Vg

1.1.2 Expression of the "morphogen" Wg and activation of its targets

The term "morphogen" refers to a substance that creates a concentration gradient, and in doing so provides cells with positional information to control pattern formation (Wolpert, 1998). This is illustrated in the "French flag model", whereby the different concentrations of a morphogen control expression of different target genes (Figure 1.1 C, D) (Wolpert, 1996, 1998).

There are many examples of morphogenetic gradient involvement in patterning during development. In the vertebrate limb bud, Sonic hedgehog (Shh) is secreted from a specific polarising region to form a gradient specifying digit formation along the A/P axis (Wolpert, 1996; Zeng et al., 2001). Shh also controls pattern formation in the vertebrate neural tube by forming a gradient along the D/V axis from its source in the ventral floor plate (Ulloa and Marti, 2010). This gradient of Shh is transduced into a gradient of target gene activity through the action of Gli proteins (Osterlund and Kogerman, 2006; Ulloa and Marti, 2010). Shh is cholesterol modified, however this modification does not perturb its ability to form a gradient via diffusion for long-distance signalling (Zeng et al., 2001). Activin, a member of the Transforming growth factor-β (TGF-β) family, is the best-characterised morphogen in *Xenopus* (McDowell and Gurdon, 1999). Different activin levels induce either high-level (*Xgoosecoid*) or low-level (*Xbrachyury*) target gene expression in the mesoderm (McDowell and Gurdon, 1999). Another member of the TGF-β family, Decapentaplegic (Dpp), forms a morphogen gradient centred at the A/P boundary of the *Drosophila* wing imaginal disc (Gonzalez-Gaitan, 2003; Kicheva et al., 2007), thus controlling growth and patterning (Baena-Lopez et al., 2012).

Morphogen gradients have been proposed to form in several different ways. For example, a morphogen may diffuse unhindered or move by "restricted diffusion", a process by which morphogens diffuse while being retained to the cell surface by interactions with the ECM (Kicheva et al., 2007; Schwank et al., 2011). Morphogenetic gradients may also form by endocytosis-dependent planar transcytosis without the need for extracellular release

(Kicheva et al., 2007; Tabata, 2001). Morphogens could also be directly delivered via projections from producing cells termed "cytonemes" (Ramirez-Weber and Kornberg, 1999)(see Section 1.6.4). Dpp has been demonstrated to bind glypicans and ECM components of the *Drosophila* wing imaginal disc, which may restrict extracellular Dpp diffusion and contribute to gradient formation (Schwank et al., 2011; Tabata, 2001). Another morphogen expressed in the *Drosophila* wing imaginal disc that has been suggested to move along cytonemes is Hedgehog (Hh). Hh is a cholesterol and lipid-modified protein that spreads away from its site of production (Callejo et al., 2011). Whether movement of Hh occurs via restricted diffusion (Gonzalez-Gaitan, 2003), or the action of cytonemes (Bischoff et al., 2013) requires further investigation.

Formation of Wnt morphogen gradients is important in many organisms. Wnt gradients contribute to the organisation of the *C. elegans* nervous system, through guidance of long-range migration of anteriorly directed neurons (Prasad and Clark, 2006). A/P patterning of the *Xenopus* neural plate also requires a Wnt morphogen gradient (Kiecker and Niehrs, 2001). In the vertebrate neural tube, Wnt is secreted dorsally to form an opposing gradient to Shh and specify dorsal identity (Ulloa and Marti, 2010). However, the best characterised role for Wnt in axial patterning is in D/V axis organisation in the *Drosophila* wing imaginal disc (Gonzalez-Gaitan, 2003; Zecca et al., 1996). Wg has been demonstrated to establish a patterning centre at the D/V boundary to control cell fate specification and wing growth (Neumann and Cohen, 1997). Wg is released from a stripe of expressing cells straddling the D/V boundary and moves across the wing pouch to activate target genes (Figure 1.1 B) (Strigini and Cohen, 2000; Zecca et al., 1996). *Senseless* (*sens*) is a short-range target of Wg and can be activated up to four cells away from the Wg source (Figure 1.1 E). *Distal-less* (*dll*) and *vestigial* (*vg*) are long-range targets and can be activated up to 20 cell diameters away from the Wg producing cells in the pouch (Figure 1.1 F, G) (Zecca et al., 1996). It has been suggested that the ability of Wg to spread and form an extracellular gradient (Strigini and Cohen, 2000)

may ensure differential target gene expression, as a result of a concentration gradient across the wing pouch (Zecca et al., 1996). Indeed, high Wg signalling levels are important for induction of *sens* (Baena-Lopez et al., 2009; Zecca et al., 1996), which is required for wing margin specification (Couso et al., 1994). At low levels of Wg signalling, the target genes Dll and Vg are induced for control of wing imaginal disc growth (Zecca et al., 1996). Therefore, the graded response of these long and short-range target genes is consistent with a dose-dependent requirement for Wg. However, upon a uniform low level of Wg expression across the wing pouch, adult wings are formed without proper margin since both Dll and Vg are expressed in response to low Wg levels, and only growth, but no margin specification occurs (Baena-Lopez et al., 2009). Therefore, the presence of two levels of Wg signalling may be enough to create these effects (Martinez Arias, 2003). Low-level signalling is needed for growth and high-level signalling is required for specification of the margin. A controversy in the field is whether the release and movement of Wg is required for this.

As described before, (and shown in Figure 1.1), Wg is released from a stripe of cells to form a concentration gradient across the wing imaginal disc at late 3rd instar (Strigini and Cohen, 2000). Zecca et al. (1996) suggested that this movement of Wg was important for target gene expression, since overexpression of a membrane-tethered form of Wg in clones only triggered target gene expression at a short range. However, later findings from Alexandre et al. (2014) suggest that long-range activity is not required since membrane-tethered Wg expressed at endogenous levels, in place of the wild type, produces viable adult flies that are almost identical to wild type (except for their slightly smaller wings). They propose a "cellular memory" model, in which early expression of Wg throughout the pouch (as observed in early wing development) stably turns on Dll and Vg target gene expression, which is then maintained throughout development (Alexandre et al., 2014). They suggest that expression of these target genes is maintained at levels that are sufficient for

growth and specification, but not as high as the wild type. Membrane-tethered Wg activates the short-range target gene *sens* in cells surrounding the D/V boundary and subsequent wing margin specification occurs (Alexandre et al., 2014). In this context, release of Wg is not required for patterning and growth, but spread of wild type Wg from the D/V boundary provides a proliferative enhancement for the final tempering of wing growth through maintenance of sufficient levels of Dll and Vg (Alexandre et al., 2014). Whilst two different levels of Wg are required, high levels for *sens* induction and low levels for *dll* and *vg* expression, a concentration gradient itself is not necessary for this induction and therefore Wg may not function within the category of a classical morphogen.

1.1.3 The Wnt Signalling Pathway

The canonical Wnt signalling pathway has been well characterised, and the general components and current model of signalling are summarised in Figure 1.2. In the absence of Wnt ligand, the destruction complex, which comprises Axin, APC, Glycogen synthase kinase 3 beta (GSK3-β) and Casein kinase 1 (CK1), is free to phosphorylate Beta-catenin (β-cat), and target it for degradation by the proteasome (Clevers and Nusse, 2012; Stamos and Weis, 2013). Signalling does not take place.

The Frizzled (Fz) family of seven-pass transmembrane receptors act as primary Wnt receptors (Wu and Nusse, 2002). Upon Wnt binding to Fz, recruitment of the single-pass transmembrane co-receptor LDL-related protein 5/6 (LRP-5/6) occurs (MacDonald and He, 2012; Piddini et al., 2005). Formation of the Wnt/Fz/LRP-5/6 ternary complex is required for signalling (Piddini et al., 2005), along with the action of the protein Dishevelled (Dsh) (Clevers and Nusse, 2012; MacDonald and He, 2012). Axin, a component of the degradation complex is recruited to the cytosolic domain of LRP-5/6 causing dissociation of the degradation complex and stabilisation of β-cat (Bejsovec, 2013; MacDonald and He, 2012). How inactivation or disassembly of the

destruction complex occurs is a subject of debate in the field. However, once β-cat is stabilised it enters the nucleus and binds to the TCF/Lef family of DNA-binding proteins thereby relieving the repression of Groucho/TLE on Wnt target genes (Bejsovec, 2013; Hlsken and Behrens, 2000).

Most studied Wnt target genes control cellular processes involved in growth and patterning (Martinez Arias, 2003). Mammalian Wnt targets include *Axin2*, a repressor of β-cat, and *LGR-5*, a known stem cell marker (Clevers and Nusse, 2012). *Drosophila* Wnt targets include *myc* and *vestigial* which are involved in cell proliferation, and *naked* and *notum* two feedback inhibitors of Wg signalling (Bejsovec, 2013; Hlsken and Behrens, 2000).

Figure 1.2: The Wnt signalling pathway.

A schematic outlining the general signalling pathway for Wnt/β-catenin. In the absence of Wnt, the destruction complex of APC, Axin, GSK3-β and CK1 is free to phosphorylate β-catenin. Phosphorylated β-catenin is targeted for ubiquitination and subsequent proteasomal degradation. Wnt target genes are not activated. However, upon binding of Wnt to the Fz2/LRP-5/6 receptor complex, recruitment and disassembly of the destruction complex occurs. This leaves β-catenin free to translocate to the nucleus for transcription of Wnt dependent target genes through the action of the TCF/Lef transcription factors. Adapted from (Clevers and Nusse, 2012).

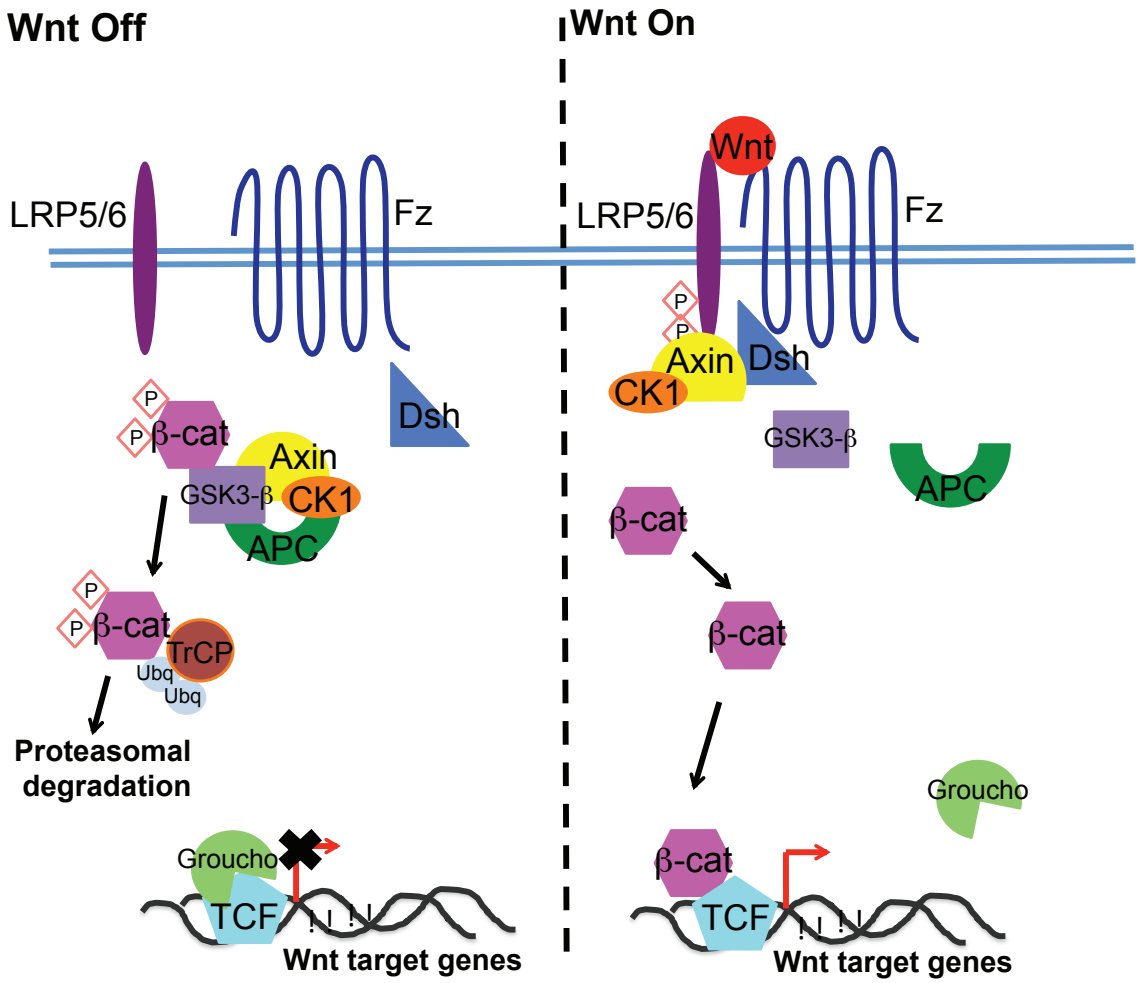
Wnt Off
Wnt On
LRP5/6
Fz
Wnt
Dsh
P
β-cat
Axin
GSK3-β
CK1
APC
TrCP
Ubq
Proteasomal degradation
Groucho
TCF
Wnt target genes

1.2 Secretion and Trafficking

The secretory and endocytic pathways are responsible for proper distribution of membrane proteins and lipids within cells. Trafficking within cells is well controlled and often highly specialised towards the cargo being carried. Several classical and non-classical pathways exist within cells for both movement of synthesised proteins to the surface, and internalisation and potential degradation or recycling of proteins from the cell surface. These processes are extensive and therefore cannot all be described in this section. An overview of the important features of these pathways is provided below.

1.2.1 General Secretory Routes

The Endoplasmic Reticulum (ER) is the site of secreted and transmembrane protein production due to the presence of ribosomes along some of its surface (Levine and Rabouille, 2005). Secreted proteins are translocated into the ER lumen during translation, from whence they commence their route of anterograde transport to the Golgi (Levine and Rabouille, 2005). Within the ER lumen initial protein modification occurs including lipid attachment, and quality control steps, which ensure correct protein folding (Alberts, 2002). Movement from the ER to the Golgi is conducted through specialised regions of the ER called transitional ER (tER) exit sites (Levine and Rabouille, 2005). These tER exit sites are enriched in COP-II coat proteins that will form COP-II vesicles, which mediate anterograde trafficking to the Golgi (Figure 1.3) (Brandizzi and Barlowe, 2013). Within these COP-II vesicles reside a family of proteins known as the p24 proteins (Figure 1.3) (Strating and Martens, 2009). p24 proteins are thought to act as cargo receptors, recruiting specific proteins to tER exit sites (Kaiser, 2000). However, upon removal of p24 proteins, COP-II vesicle budding still occurs, therefore

these proteins are not essential for COP-II carrier transport. They may instead play a role in cargo quality control and selection (Springer et al., 2000). In *Drosophila*, tER sites are associated with individual Golgi stacks forming tER-Golgi units, as illustrated in Figure 1.3 (Kondylis et al., 2011). Budding of COP-II vesicles for movement from tER sites to their respective Golgi stack appears to be dynamin-independent (Matsuoka et al., 1998a; Matsuoka et al., 1998b).

The Golgi is a complex of flattened, membranous compartments termed the cis, medial and trans cisternae, which form a single Golgi stack in mammals. *Drosophila* S2 cells have been described to contain many individual tER-Golgi stacks (Farquhar and Palade, 1998; Kondylis et al., 2001). COP-II coated vesicles from the ER enter the cis cisternae and cargo ultimately exits from the trans cisternae where it is sorted for onward movement (Figure 1.3) (Kondylis et al., 2001). The process by which cargo moves from the cis to trans cisternae is controversial, and several theories exist to explain cargo flow. One of the more popular ideas speculates that movement of cargo may happen through vesicle fusion between the cisternae, either via specialised vesicles, or through maturation of the cisternae themselves (De Matteis and Luini, 2008; Farquhar and Palade, 1998). Entry into the trans cisternae signals the start of sorting and segregation of cargo. Most of the final protein modification occurs within the trans cisternae, for example, pro-proteins are processed into their mature forms and O or N-glycan modifications are processed (De Matteis and Luini, 2008). O or N-glycan post-translational modifications often act as signals for apical targeting of cargo, but these modifications are 'secondary' to the stronger endosomal or basolateral targeting sequences such as di-Leucine (DXXLL) or Tyrosine (YXXΦ) based motifs (Rodriguez-Boulan et al., 2005). Certain proteins such as those containing Glycosylphosphatidylinositol (GPI)-anchors segregate to specialised membrane microdomains enriched in cholesterol due to their propensity for clustering (Rodriguez-Boulan et al., 2005).

Once segregated to an appropriate Golgi region, adaptor proteins facilitate movement of cargo-filled vesicles through association with clathrin

and microtubule motors (De Matteis and Luini, 2008; Deborde et al., 2008). Mature export domains associated with microtubule-based motors are extruded and fission occurs for vesicle release (Figure 1.3). It has been suggested that in polarised cells, fission of apically directed carriers is dependent on dynamin (De Matteis and Luini, 2008; Jones et al., 1998). Microtubule directionality has also been shown to be particularly important for the apical delivery of cargo. Studies have reported that upon microtubule disruption, problems with protein missorting of secretory and apically targeted proteins occur (Musch, 2004). Upon reaching the membrane, both apically and basolaterally targeted vesicles undergo fusion. This is dependent on the interaction between matching pairs of soluble N-ethylmaleimide-sensitive fusion factor attachment protein receptors (SNAREs), which are involved in all vesicular fusion events (Musch, 2004).

Figure 1.3: The General Secretory pathway.

A schematic outlining the general pathway of ER to plasma membrane movement. Proteins are translated by ribosomes on the surface of the ER and are simultaneously translocated into the lumen. Protein cargo is guided into COP-II coated vesicles through the action of p24 proteins for release and movement to the Golgi. Cargo moves through the Golgi cisternae and may undergo modifications such as glycosylation. In the trans cisternae, cargo is sorted and released in vesicles for fusion with the plasma membrane. Adapted from (Kondylis et al., 2011).

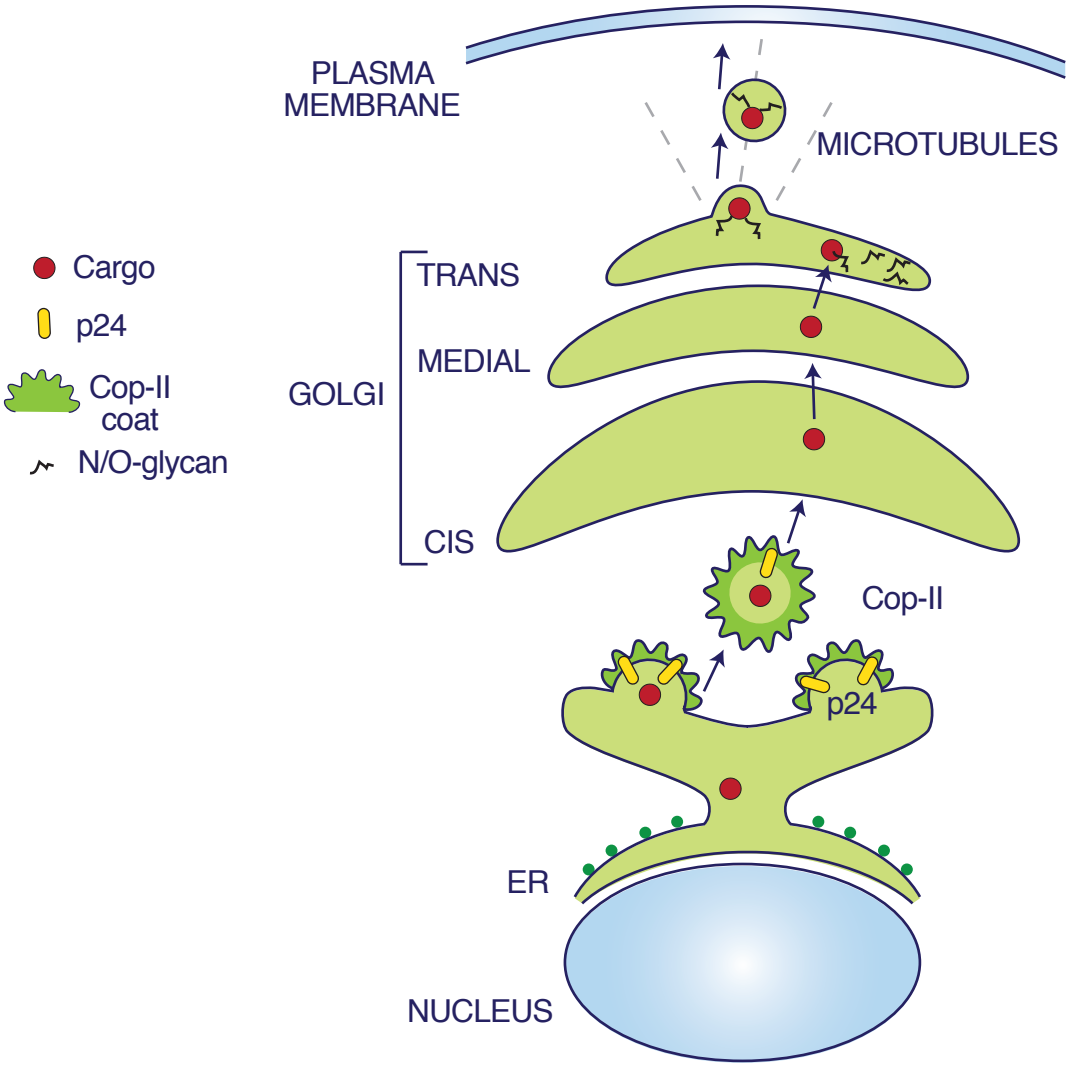
PLASMA
MEMBRANE
MICROTUBULES
Cargo
p24
Cop-II
coat
N/O-glycan
GOLGI
TRANS
MEDIAL
CIS
Cop-II
p24
ER
NUCLEUS

1.2.2 General Endocytic Trafficking Routes

Uptake of proteins from the plasma membrane to enter the endocytic pathway is a tightly regulated process. The best-characterised mode of internalisation from the cell surface occurs via clathrin-coated vesicles (CCV), this is termed clathrin-mediated endocytosis (CME) (McMahon and Boucrot, 2011). Cargo specific adaptors (such as AP2, which acts specifically at the plasma membrane) mediate cargo selection through binding of both phosphoinositides (PIs) and motifs in the cytoplasmic regions of transmembrane proteins destined for endocytosis (McMahon and Boucrot, 2011). AP2 and other adaptors then recruit clathrin from the cytosol and polymerisation occurs stimulating curvature of the membrane through the formation of a lattice-like structure creating a pit (Figure 1.4) (Kirchhausen, 2014). Severance of the CCV occurs via the action of the GTPase Dynamin, which constricts the neck of the vesicle causing scission (Kirchhausen, 2014; McMahon and Boucrot, 2011). Preventing dynamin function or recruitment arrests CME and no vesicle scission occurs (van der Bliek et al., 1993).

Upon CCV budding from the cell surface, rapid vesicle uncoating is facilitated by the actions of the ATPase Hsc70 and Auxilin, leaving a naked vesicle ready for fusion with its target endosome (Kirchhausen, 2014; McMahon and Boucrot, 2011). Initially, all uncoated vesicles fuse to form an early endosome (EE) that is marked by the small GTPase Rab5 (Figure 1.4) (Wandinger-Ness, 2014; Zerial and McBride, 2001). From this EE there are several routes the cargo could take. Proteins can enter either a degradative or recycling pathway. If destined for degradation, proteins enter a branch of the pathway characterised by the transition from a Rab5-positive EE to a Rab7-positive Late Endosome (LE) (Figure 1.4). LEs marked by Rab7 mature into multi vesicular bodies (MVBs) where most proteins destined for degradation are marked by ubiquitination (Wandinger-Ness, 2014). Ubiquitination causes their sorting into intra-luminal vesicles (ILVs) within the MVB via the endosomal sorting complex required for transport (ESCRT) machinery (Figure

1.4) (Rusten et al., 2012). Components of the ESCRT machinery recognise ubiquitin bound to cargo destined for degradation (ESCRT-0, I and II) and cause invaginations of the endosomal membrane (ESCRT-II), which can bud into the lumen of MVBs and are released via ESCRT-III mediated scission (Rusten et al., 2012). LEs and MVBs then undergo fusion with the lysosome and their contents are degraded (Figure 1.4) (Henne, 2014).

Following entry into Rab5-positive endosomes, cargo destined for recycling can traffic to compartments characterised by the presence of Rab4 and Rab35 before rapid return to the plasma membrane (Figure 1.4) (Grant and Donaldson, 2009). Cargo can also enter the slower moving recycling endosome (RE), which is characterised by the presence of Rab11 (Grant and Donaldson, 2009; Wandinger-Ness, 2014). In polarised epithelial cells, proteins destined for apical or basolateral targeting are sorted into separate domains within the RE (Thompson et al., 2007). Rab proteins are also thought to segregate into domains at the surface of the RE allowing both endosomal maturation (from Rab5 to Rab11) and cargo sorting, and movement back to the plasma membrane (Figure 1.4) (Sonnichsen et al., 2000; Zerial and McBride, 2001).

A further retrograde recycling route exists within cells, which can occur through either the EE, RE or LE to traffic cargo back to the Golgi. This is controlled by components of the retromer complex (Figure 1.4) (Johannes and Popoff, 2008). The retromer complex is formed from two main components. The first is a trimeric complex of Vps26, Vps29 and Vps35 known as the cargo-selective-complex (CSC), which recognises cargo proteins for recycling (Burd, 2014). The second are sorting nexin dimers (SNX), which possess Bin/Amphiphysin/Rvs (BAR) domains (SNX-BARs) (Burd, 2014; Johannes and Popoff, 2008). BAR domains have a curved structure and recognise regions of membrane curvature such as vesicles or tubular structures (Cullen, 2008). Association of SNX-BARs with tubular structures budding from endosomes stabilises membrane curvature through the addition of BAR domains, facilitating vesicle formation (Burd, 2014; Cullen, 2008). SNXs contain a phox-

homology (PX) domain, which binds PIs in the membranes of vesicles (Cullen, 2008). It has been suggested that different SNX-PX domains may recognise different PI compositions, directing certain SNXs to defined endosomal regions. SNXs have also been implicated in direct cargo recognition, and SNX3 (a non-BAR containing SNX) functions as a cargo-specific adaptor (Cullen, 2008). Once a region of membrane curvature has been stabilised, SNXs then recruit the CSC to endosomes, and specific Rab GTPases contribute to retrograde movement of the vesicles back to the Golgi, via the action of microtubules (Johannes and Popoff, 2008). Rab6 regulates retromer trafficking from the EE (Mallard et al., 2002; Maxfield and McGraw, 2004) and Rab9 regulates trafficking from the LE (Figure 1.4) (Johannes and Popoff, 2008).

Figure 1.4: The General Endocytic pathway.

A schematic outlining the core endocytic pathway that a protein can traffic through upon uptake. Internalisation from the plasma membrane can occur via clathrin-mediated endocytosis in a dynamin and AP2-dependent manner. Uncoating of the clathrin-coated vesicle occurs before fusion with a Rab5-positive early endosome. From the early endosome several trafficking routes are available, depending on the cargo destination. Cargo destined for degradation, move from an early endosome to a Rab7-positive endosome, which matures into a multi-vesicular body and undergoes lysosomal fusion for protein degradation. The ESCRT complex is required for MVB formation and protein degradation. Cargo destined for recycling can enter a Rab4 and Rab35-dependent rapid recycling route for movement back to the plasma membrane. Cargo can also enter a Rab11-positive recycling endosome for either movement back to the plasma membrane via the action of Rab8/Rab10, or movement back to the Golgi via Rab6/Rab9 and the retromer complex (orange arrows). Adapted from (Grant and Donaldson, 2009).

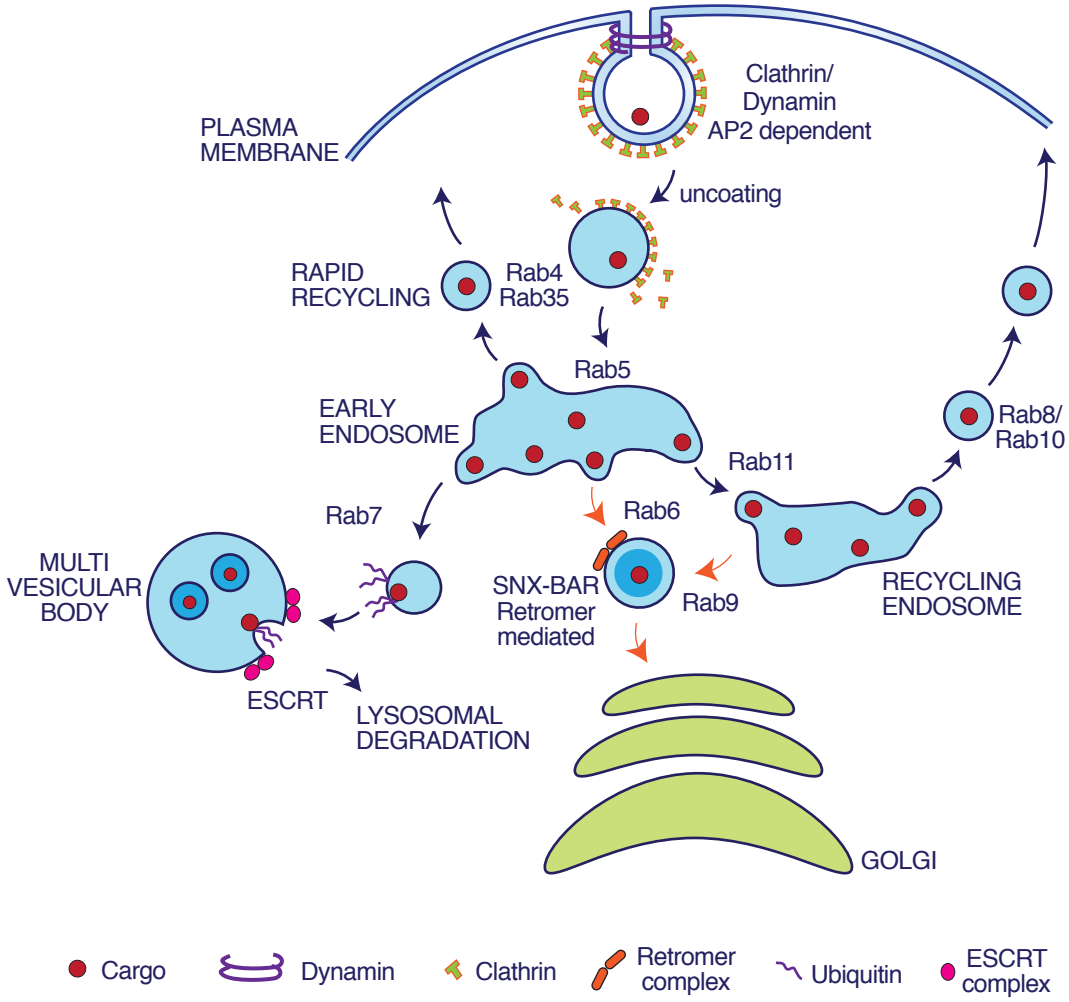
PLASMA
MEMBRANE
Clathrin/
Dynamin
AP2 dependent
uncoating
RAPID
RECYCLING
Rab4
Rab35
Rab5
EARLY
ENDOSOME
Rab8/
Rab10
Rab11
Rab7
Rab6
MULTI
VESICULAR
BODY
SNX-BAR
Retromer
mediated
Rab9
RECYCLING
ENDOSOME
ESCRT
LYSOSOMAL
DEGRADATION
GOLGI
Cargo
Dynamin
Clathrin
Retromer
complex
Ubiquitin
ESCRT
complex

1.2.3 Non Classical Secretory and Endocytic Routes

Most proteins are secreted through the conventional ER to Golgi route via COP-II coated vesicles as outlined above. However, there are several unconventional mechanisms of protein secretion present in cells. Proteins can be packaged into COP-II-coated vesicles, which bypass the Golgi and fuse directly with the plasma membrane, or with an intermediary endosomal compartment before delivery to the plasma membrane (Nickel and Rabouille, 2009). Soluble cytoplasmic proteins can also be released via unconventional secretory mechanisms. Secretory lysosomes are able to fuse with the plasma membrane for cargo delivery there (Nickel and Rabouille, 2009). Secretion of proteins can also occur through MVB fusion with the plasma membrane and subsequent release of exosomes, or through microvesicle shedding from the cell surface (Nickel and Rabouille, 2009).

CME is the best-understood route for endocytic uptake of cargo from the plasma membrane, however clathrin-independent endocytic (CIE) pathways also exist. Several of these are dynamin-dependent in a similar fashion to CME, including caveolar endocytosis (Grant and Donaldson, 2009; Mayor, 2014). Caveolae are membrane invaginations surrounded by oligomerisations of integral membrane proteins caveolin-1 (CAV1) and caveolin-2 (CAV2), and additional proteins termed cavins (Doherty and McMahon, 2009; Mayor, 2014). Caveolae appear to dynamically bud from the plasma membrane in a dynamin-dependent fashion with additional assistance from a BAR domain-containing protein Pacsin2, which recognises membrane curvature (Mayor, 2014). Caveolae are then able to fuse with the EE for cargo transfer. GPI-anchored proteins are endocytosed in a clathrin and dynamin-independent pathway. They are enriched in membrane regions associated with cholesterol and sphingolipids (Doherty and McMahon, 2009) and internalised via a cholesterol-dependent CIE pathway. This results in the fusion of clathrin-independent tubulovesicle carriers (CLICs) directly derived from the cell surface, with a GPI-anchored protein enriched early endosomal compartment (GEEC) (Mayor,

2014). This is referred to as the CLIC/GEEC pathway. In the absence of clathrin and dynamin the cytoskeletal protein actin appears to have an important role in endocytosis (Mayor, 2014; Merrifield, 2014). Inhibition of actin polymerisation affects the formation of CLICs (Romer et al., 2010), and in yeast (where clathrin is dispensable for endocytosis) an actin meshwork is important for endocytic uptake of proteins (Mayor, 2014; Merrifield, 2014).

1.2.4 Secretion, Endocytosis and Transcytosis within Polarised Epithelia

Epithelial cells depend on polarised protein distribution across their apical and basolateral surfaces for correct function. Madin-Darby Canine Kidney (MDCK) cells are the best-characterised model for polarised epithelial cells with specific apical and basolateral trafficking routes, leading to distinct protein and lipid compositions at the apical and basolateral membranes (Gould and Lippincott-Schwartz, 2009; Rodriguez-Boulan et al., 2005). Segregation of proteins to these distinct domains is performed within the Golgi and RE. Apical sorting signals tend to be modifications like N or O-glycans, or GPI-anchors (in vertebrates) (Traub, 2014). Basolateral sorting signals are usually localised to cytoplasmic regions of proteins and often contain Amino Acid (AA) motifs containing Leucine or Tyrosine that interact with adaptor proteins facilitating sorting (Rodriguez-Boulan et al., 2005). Basolateral signals tend to override apical sorting signals (Traub, 2014). In the polarised epithelium of the *Drosophila* follicle cell, proteins destined for the basolateral surface are secreted via a Rab10-dependent pathway. Lack of Rab10 does not affect apical secretion (Lerner et al., 2013), suggesting that basolateral secretion is determined by protein translation in a basolateral pool of ER and movement through basolateral Golgi to the plasma membrane. Therefore, the spatial distribution of mRNA could impact on polarised protein sorting (Lerner et al., 2013). Nevertheless, the RE can receive cargo from EEs both apically and basolaterally, and then must sort this cargo for recycling to the correct destination (Thompson et al., 2007). In addition to sorting signals, directional

protein trafficking can also occur through association with specific molecular motors. For example, a requirement for microtubules appears to be important for apical sorting (Musch, 2004; Sheff et al., 2002). Rab proteins are known to associate with microtubule motors for vesicle movement, therefore motor-dependent segregation may also require specific Rabs (Zerial and McBride, 2001). This may facilitate the efficient segregation of vesicle budding from the RE.

The apical-basolateral division of the plasma membrane in polarised epithelial cells requires proteins to traffic correctly. However, some proteins undergo a transcytosis step in their secretion and move to one membrane before being re-endocytosed and transported across the cell to the opposite membrane (Eaton, 2014; Rodriguez-Boulan et al., 2005). In a study following the movement of GPI-anchored proteins, transcytosis was observed from the basolateral to apical membranes of polarised hepatocytes (Galmes et al., 2013). The GPI-anchor is usually an apical sorting signal. However, in these cells, GPI-anchored proteins were first trafficked to the basolateral surface, where they oligomerise and associate with cholesterol-rich lipid domains in the membrane (Galmes et al., 2013). These domains were then endocytosed in a Flotillin-dependent manner, and transcytosed to the apical membrane (Galmes et al., 2013). Another example of transcytotic protein movement involves the trafficking of dimeric IgA (dIgA) (Rojas and Apodaca, 2002). In MDCK cells, dIgA is internalised basolaterally in a clathrin-dependent fashion and delivered to a basolateral EE. From here, dIgA moves to a RE in the apical region of cells via the action of actin and microtubules for delivery to the apical surface (Rojas and Apodaca, 2002).

1.3 Modification of Wnt

Human Wnts are highly conserved proteins that share a similar size range from around 39 to 46kDa (Clevers and Nusse, 2012; Miller, 2002). *Drosophila* Wnts also fall into this approximate size range with a few exceptions, the most notable being Wg, which contains an additional region not conserved in vertebrate Wnts, and therefore has a size of approximately 54kDa (Miller, 2002). Once secreted and released, Wnt proteins associate with the ECM and localise to cell surfaces away from their site of release (Bartscherer and Boutros, 2008). It is important to note that most Wnt proteins carry several post-translational modifications such as acylation and glycosylation (Coudreuse and Korswagen, 2007). Acylation is particularly relevant since the resulting hydrophobicity is expected to prevent extracellular spread.

1.3.1 Acylation of Wnt

It has long been known that Wnts associate with cell membranes through hydrophobic interactions with the ECM (Reichsman et al., 1996). The first Wnt site identified as potentially modified by acylation was a conserved Cysteine (Cys77) in Wnt3a (Willert et al., 2003). However, this was later found not to be the case, and in fact this conserved Cysteine is involved in di-sulphide bond formation and therefore is not thought to be modified (Janda et al., 2012). An alternative acylation site was identified by mass spectrometry in Wnt3a. Modification of a conserved Serine (Ser209) with palmitoleic acid was shown to be important for Wnt3a secretion (Takada et al., 2006). A version of Wnt3a with Ser209 mutated to Alanine is retained in the ER (Takada et al., 2006). Therefore, palmitoylation on the conserved Serine appears essential for secretion of Wnt3a. Subsequent work in *Drosophila* at the same conserved sites yielded similar results to those described above. Mutation of Ser239 in Wg to Alanine dramatically reduces signalling activity and affinity for the Wg receptor,

Fz2 (Tang et al., 2012). The conserved Cysteine (Cys93 in Wg) was found to play no role (Tang et al., 2012). Tang et al. (2012) demonstrated that previous reports which indicated a role for Cys93 in Wg signalling activity (Franch-Marro et al., 2008a), had simply incorporated an inappropriately placed HA tag in the construct that was affecting Wg secretion and therefore signalling. Mutation of Cys93 to Alanine had no effect on signalling with an untagged protein (Tang et al., 2012).

Modification of the conserved Serine residue may be important for both Wnt3a and Wg since it is required for association with the Wnt chaperone protein - Evi (Coombs et al., 2010; Tang et al., 2012)(Herr and Basler 2011). Mutation of the conserved Serine in all *Drosophila* Wnts (excluding WntD) prevents Evi localisation to the Golgi, which is used as a read out for Wg/Evi association (Herr and Basler 2011). Therefore, lipid modification is important for secretion of Wg from cells in conjunction with Evi.

A beautiful illustration of the importance of this modification came to light in 2012, when the crystal structure of *Xenopus* Wnt8 in complex with the mouse Fz8 cysteine-rich domain (CRD) was solved (Janda et al., 2012). Co-expression of XWnt8 and the Fz8 CRD facilitated purification of the complex in the absence of detergent because binding to the Fz8 CRD was shielding the lipid modification on XWnt8 (Janda et al., 2012). This lipid was found to be attached to the conserved Serine residue (in XWnt8 Ser187) and was predicted to be a palmitoleic acid. In XWnt8 the equivalent of the conserved Cys77 in Wnt3a (XWnt8 Cys55) is involved in a di-sulphide bond, which is predicted to be conserved across all Wnts, and therefore is not suggested to be acylated (Janda et al., 2012). This is consistent with the data discussed above and appears to indicate that acylation of Wnts at the conserved Serine site is the single modification required and existing.

It was initially thought (in the case of Wg), that the hydrophobic Wnt/ECM interactions were dependent on Wg glycosylation through the action of an ER-resident, multipass transmembrane protein called Porcupine (Porc)

that is required for Wnt secretion (Kadowaki et al., 1996; Tanaka et al., 2002; van den Heuvel et al., 1993). Subsequent sequence analysis predicted that Porc is a member of a family of membrane-bound O-acyltransferases (Hofmann, 2000). This would suggest that Porc is involved in acylation rather than glycosylation of Wg. Porc has subsequently been shown to both bind and transfer palmitoleate to Wnt3a (Rios-Esteves et al., 2014), and is responsible for the Ser209 acylation (Rios-Esteves et al., 2014; Takada et al., 2006).

1.3.2 Glycosylation of Wnt

Wnt proteins are N-glycosylated upon multiple Asparagine (Asn) residues, the details of which vary in number and position between family members (Tang et al., 2012). In *Drosophila*, Wg was demonstrated to be N-glycosylated at two major sites: Asn103 and Asn414 (Tanaka et al., 2002), though more may be present. Mutation of both glycosylation sites produced a form of Wg with slightly reduced signalling activity compared to wild type, but generally N-glycosylation appeared dispensable for Wg function (Tang et al., 2012). These results are consistent with work on mouse Wnt1, which retains its ability to function in the absence of glycosylation, albeit with a slight reduction in signalling (Doubravska et al., 2011). N-glycosylation of Wg has also been shown to be dispensable for association with Evi (Herr and Basler 2011). There is some controversy surrounding the requirement for glycosylation of Wnt proteins, since it has been reported that glycosylation of Wnt3a is required for efficient secretion (Komekado et al., 2007). However, these findings also claim that Wnt3a requires glycosylation for palmitoylation to happen (Komekado et al., 2007). Their read-out of palmitoylation was the modification of Cys77, which as discussed above does not occur, making these results unreliable. A subsequent study found that whilst non-glycosylated Wnt3a is less active than wild type, it is signalling competent and therefore glycosylation is not required in the same fashion as acylation of the conserved Serine (Doubravska et al., 2011; Takada et al., 2006). From analysis of the structure, three potential

glycosylation sites can be identified in XWnt8 for the addition of N-glycans (Janda et al., 2012).

The most important modification of Wnts is the acylation of a conserved Serine residue (Janda et al., 2012), which is required for efficient secretion and activity. The role in secretion is likely due to the fact that acylation at the Serine is needed for association with Evi (Herr and Basler 2011). Without such association, Wnt proteins are not secreted and therefore are unable to signal (Herr and Basler 2011). N-glycosylation of Wnt is dispensable for association with Evi, since glycosylation-deficient Wnt is secreted (Tang et al., 2012)(Herr and Basler 2011). Interestingly, *Drosophila* WntD is secreted and signals in both a Porc and Evi independent manner (Ching et al., 2008). Further analysis of WntD indicated that it is not lipid modified (Ching et al., 2008). This highlights the link between lipidation of Wnts and the requirement of Evi for efficient secretion.

1.4 The Wg Secretory Route

As a lipidated hydrophobic protein, Wg follows a well-controlled secretory route to facilitate trafficking to the cell surface. Several important factors involved in this process have been identified and are discussed below:

1.4.1 Porcupine (Porc)

The segment polarity gene *porc* was initially identified as an important contributor to Wg secretion, since Wg is confined to the expressing cells in *porc* embryos suggesting a secretion defect (van den Heuvel et al., 1993). As discussed above, Porc is predicted to be an ER-resident (Kadowaki et al., 1996) O-acyltransferase (Hofmann, 2000) involved in Wnt processing (Tanaka et al.,

2002), specifically in the palmitoylation of a conserved Serine residue (Takada et al., 2006). Mutation of this conserved Serine in some *Drosophila* Wnts phenocopies a *porc*$^{-/-}$ mutant (Herr and Basler 2011). Porc has recently been shown to bind and modify the conserved Ser209 of Wnt3a through addition of a palmitoleate (Rios-Esteves et al., 2014). Porcupine (Porcn) is also required for Wnt secretion in mice (Barrott et al., 2011; Biechele et al., 2011). Lipid modification of Wnts through the action of Porc has been shown to have important functions in Wnt trafficking and distribution. Wnt1 is sorted into detergent-resistant microdomains (lipid rafts) and it has been suggested that this is dependent on lipidation (Zhai et al., 2004). Binding of Wnts to Evi also requires the Porc-dependent modification, therefore sorting into membrane microdomains may be dependent on association with Evi (Tang et al., 2012)(Herr and Basler 2011). In this context, it is hypothesised that Evi could shield the hydrophobic palmitoleate group attached to Wnts to facilitate their movement through the secretory pathway (Yu et al., 2014).

1.4.2 Evi – The Wnt Chaperone

The main player guiding Wg secretion is thought to be Evenness interrupted (Evi)/Wntless (Wls)/Sprinter (Srt) (Banziger et al., 2006; Bartscherer et al., 2006; Goodman et al., 2006). *Evi* encodes a predicted eight-pass transmembrane protein that is found at the plasma membrane as well as the ER, Golgi and in endosomes (Banziger et al., 2006; Port et al., 2008; Yu et al., 2014). *Drosophila* embryos lacking maternal and zygotic Evi (*evi*^{2}) closely resemble *wg*$^{-/-}$ mutants (Bartscherer et al., 2006). Evi is specifically required within the Wg expressing cells, and is not required for secretion of non-Wnt signalling proteins such as Hh (Banziger et al., 2006; Bartscherer et al., 2006). The requirement for Evi in Wnt secretion is conserved across species; MOM-3 the *C. elegans* Evi homologue is also required for MOM-2 (Wnt homologue) secretion (Goodman et al., 2006). Human Evi also affects the secretion of Wnt3a in cell culture (Banziger et al., 2006).

Evi mRNA is ubiquitously expressed in the *Drosophila* wing imaginal disc. However, the level of basolateral Evi is specifically increased in Wg producing cells (Figure 1.5 D') (Port et al., 2008). This is not due to Wg signal transduction; instead it is likely a consequence of the presence of Wg itself (Port et al., 2008)(Herr and Basler 2011). For the purposes of this thesis, I shall refer to the altered localisation as "enrichment".

Evi containing a C-terminal V5 tag in S2 cells is described to predominantly accumulate in the Golgi, leading to the suggestion that it may facilitate trafficking of Wg from the Golgi to the cell surface (Belenkaya et al., 2008; Franch-Marro et al., 2008b). This Golgi localisation was also observed via antibody staining of endogenous Evi in the *Drosophila* wing imaginal disc (Port et al., 2008). However, recent analysis suggests that Wnt3a and Evi may meet in the ER rather than the Golgi (Yu et al., 2014). Comparison of endogenous Evi, with Evi-V5 tagged at the C-terminus, shows differences in subcellular Evi localisation (Yu et al., 2014). Localisation of Evi within the ER overlaps with Porc, and Evi found in ER cellular fractions was bound to Wnt3a in a lipid-dependent manner (Yu et al., 2014). The ER is diffuse within both *Drosophila* S2 cells and the wing imaginal disc (unpublished observations), which may explain why Port et al. (2008) missed the ER localisation and indicated the Golgi as the site for Evi and Wg association. In the *Drosophila* wing imaginal disc, the majority of Wg and Evi colocalisation is observed in the apical region of Wg expressing cells (Figure 1.5 D). This is consistent with the idea that Evi may function to transport palmitoylated Wnts from the ER to the apical cell surface (Herr and Basler 2011).

Figure 1.5: Distribution of Wg and Evi within the *Drosophila* wing imaginal disc.

Wild type discs were stained with anti-Wg and anti-Evi. RNA in situ hybridisation shows the expression pattern of *wg* mRNA. Confocal optical sections in the apical plane (A and D) and in the basolateral plane (B and C) are shown. YZ reconstructions are oriented so that the apical surface is at the top. (A) *Wg* mRNA is tightly apically localised within the Wg expressing cells. (B) Total Wg protein (intra and extracellular) is observed at highest levels in the apical region of expressing cells. (B') Wg puncta are also observed in receiving cells. (C) The majority of extracellular Wg is found on the basolateral surface of the wing imaginal disc where it forms a gradient. (D) Total Wg is expressed in a stripe of cells along the D/V boundary. Total Evi is expressed throughout the disc, with a particular enrichment in the Wg expressing cells (D' inset). (D''') Within these cells the majority of Wg and Evi colocalisation is observed in the apical region. Scale bars represent 24um.

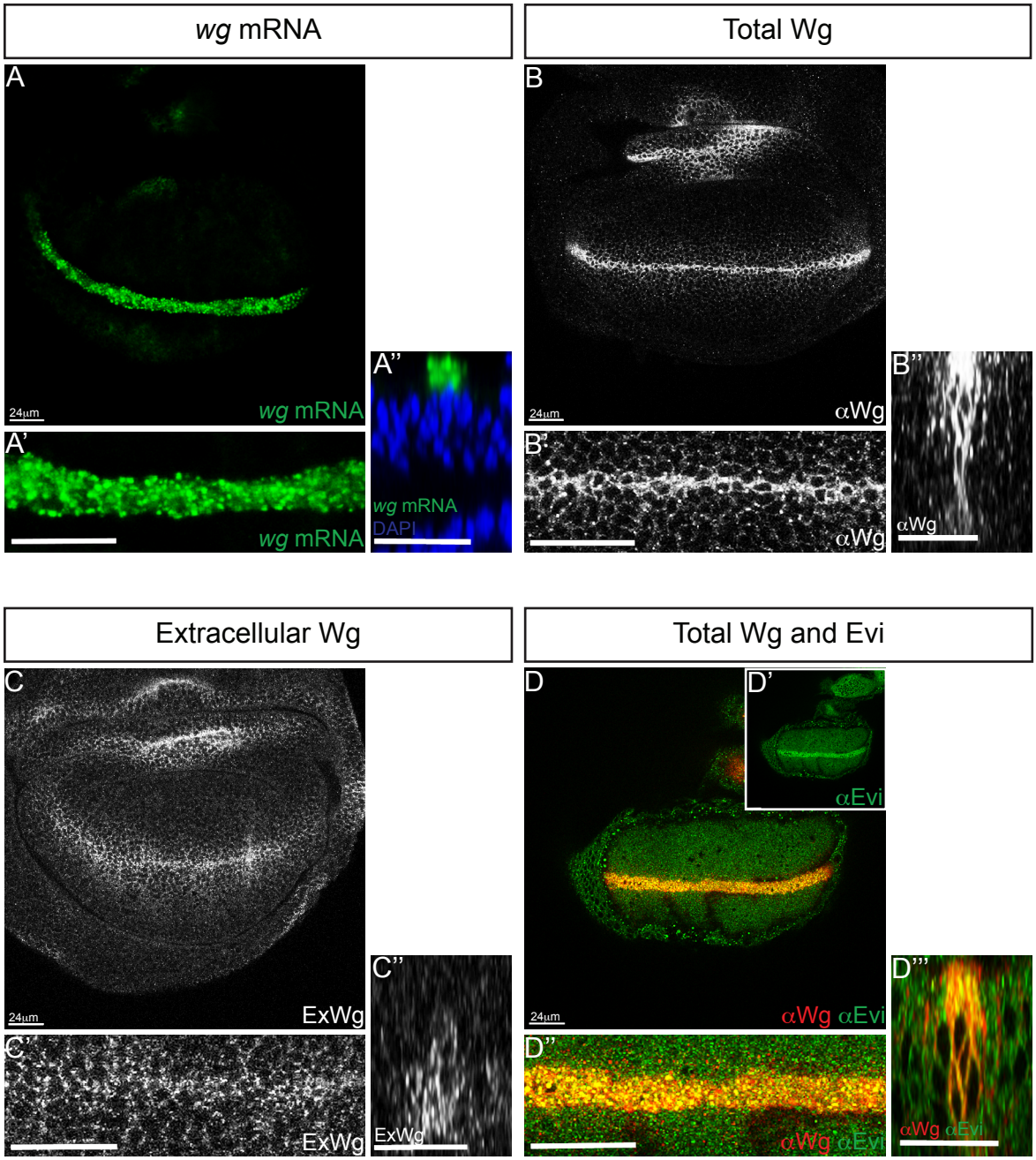
wg mRNA
Total Wg
A
24µm
wg mRNA
A'
wg mRNA
A''
wg mRNA
DAPI
B
24µm
αWg
B'
αWg
B''
αWg
Extracellular Wg
Total Wg and Evi
C
24µm
ExWg
C'
ExWg
C''
ExWg
D
D'
αEvi
24µm
αWg αEvi
D''
αWg αEvi
D'''
αWg αEvi

1.4.3 p24 Proteins

p24 proteins form a family of ER chaperones that bind many different cargoes, and have been shown to bind Wg (and other Wnts) in a lipid independent fashion. They are then guided to COP-II coated vesicles for exit from the ER (Beuchling T., 2011; Port et al., 2011). p24 proteins appear to act as cargo recognition receptors independently of Evi, since WntD secretion is also affected by a reduction in p24 protein levels (Beuchling T., 2011). Two separate studies have implicated several members of the p24 family as playing redundant roles in this process (Beuchling T., 2011; Port et al., 2011), but differed in opinion as to which p24 proteins were involved. However, both groups identified CHOp24/Emp24 as essential for Wg secretion (Palmer et al. 2011). p24 proteins have also been implicated in the trafficking of GPI-anchored proteins (Strating and Martens, 2009) and proteins residing in membrane-microdomains (lipid rafts) (Fujita et al., 2011; Strating and Martens, 2009). This is consistent with the lipid-dependent membrane microdomain localisation of Wnts observed by Zhai et al. (2004).

The discovery of p24 proteins as specialised cargo receptors, along with the lipidation of Wnts by Porc, and the requirement for the Wnt-specific chaperone Evi, indicate that a specialised secretory route for Wnt proteins begins in the ER and may involve targeting Wnts to lipid microdomains and therefore specialised ER exit sites (Palmer et al. 2011).

1.4.4 Retromer and COP-I dependent Evi Recycling

Once packaged into specialised ER exit sites, Wnt proteins (bound by their chaperone Evi) presumably traffic through the Golgi, undergo final N-glycan modification, and move to the plasma membrane for release. Wnt secretion has been shown to require retromer, since loss of components of this complex causes Wnt accumulation within expressing cells (Belenkaya et al., 2008; Franch-Marro et al., 2008b; Pan et al., 2008; Port et al., 2008; Yang et al., 2008). This was shown to be due to the requirement for retromer in Evi

recycling in *Drosophila* (Belenkaya et al., 2008; Franch-Marro et al., 2008b; Port et al., 2008), *C. elegans* (Pan et al., 2008; Yang et al., 2008) and mammalian cells (Belenkaya et al., 2008; Franch-Marro et al., 2008b; Port et al., 2008). As discussed previously, the retromer complex consists of several subunits, including the core "cargo recognition" complex of Vps26, Vps29 and Vps35 which mediate endosome to Golgi recycling (Burd, 2014; Johannes and Popoff, 2008). In *Drosophila*, disruption of the Vps35 component of the retromer complex causes a reduction of Evi within expressing cells (Port et al., 2008). However, there is an increase in Evi within MVBs compared to wild type, consistent with increased Evi trafficking to the lysosome for degradation (Franch-Marro et al., 2008b). This indicates that without retromer-dependent recycling, Evi undergoes degradation and is not able to facilitate Wg secretion. The classical retromer complex includes SNX-BAR pairs such as SNX1-SNX2 and SNX5-SNX6 (Cullen, 2008). Evi recycling does not require the classical SNX-BAR complexes (Harterink et al., 2011; Zhang et al., 2011). Instead, a specialised SNX, SNX3 forms part of the retromer complex required for Evi recycling (Harterink et al., 2011; Zhang et al., 2011). The SNX3 retromer complex sorts Evi into a recycling pathway distinct from that mediated by classical SNX-BAR complexes (Harterink et al., 2011). This indicates that Evi may undergo a specialised recycling route. This may be because, as suggested by Yu et al. (2014), the final destination for Evi in this recycling process is not the Golgi, but the ER. In the C-terminal region of Evi is an ER targeting sequence, which facilitates retrograde trafficking of Evi from the Golgi to the ER in a COP-I dependent manner (Yu et al., 2014). This process is also dependent on the small GTPase ARF (Yu et al., 2014). Once in the ER, Evi is presumably correctly positioned to facilitate movement of more Wnt through the secretory pathway.

Clathrin and dynamin-dependent endocytosis of Evi is also required for proper Wnt secretion (Belenkaya et al., 2008)(Gasnereau et al. 2011). Evi contains an AP2 binding motif (YEGL) in an intracellular loop, which is required for internalisation (Gasnereau et al. 2011). Upon mutation of this motif, Evi

accumulates on the surface of HeLa cells. The same mutation causes a reduction in Wg secretion and signalling in the *Drosophila* wing imaginal disc (Gasnereau et al. 2011). Therefore, proper Wnt secretion and signalling is dependent on the endocytosis of Evi. Some Evi protein is recycled while the rest is degraded. However, enough Evi must be recycled via retromer and COP-I retrograde transport to the ER to facilitate the movement of more Wnt to the cell surface.

1.4.5 The Non-polarised Secretory Model

One current model outlining Wg secretion is depicted in Figure 1.6. This is also likely to be applicable to most other Wnts. Wg is produced in the ER where it undergoes lipid modification by Porc (Takada et al., 2006) and subsequently associates with Evi in a lipid-dependent manner (Herr and Basler 2011). Wg/Evi cargo is selected by p24 proteins, which chaperone Wg/Evi into specialised COP-II vesicles for transport to the Golgi (Palmer et al. 2011). Wg and Evi transit the Golgi for movement to the plasma membrane, and Wg release. In parallel, Evi is endocytosed in an AP2-dependent manner into early endosomes (Gasnereau et al. 2011). From here Evi can either be degraded (via the lysosome), or is recycled from endosomes in a retromer and SNX3-dependent manner (Harterink et al., 2011; Port et al., 2008). Upon returning to the Golgi, Evi undergoes further retrograde recycling through a COP-I mediated pathway for return to the ER and another round of Wg secretion (Yu et al., 2014) (Figure 1.6).

Figure 1.6: A model of Wg secretion in non-polarised cells.
Potential model for the non-polarised secretion of Wg via the action of Evi. Wg is produced in the ER where it undergoes Porc-dependent lipidation, associates with Evi and is packaged into COP-II vesicles for movement to the Golgi via p24 proteins. Wg and Evi transit through the Golgi for movement to the surface and Wg release. Evi is then endocytosed in an AP2-dependent manner and is recycled from endosomes via a retromer/SNX3-mediated pathway to the Golgi. COP-I retrograde transport facilitates Evi movement back to the ER to begin the cycle again. Adapted from (Bartscherer and Boutros, 2008).

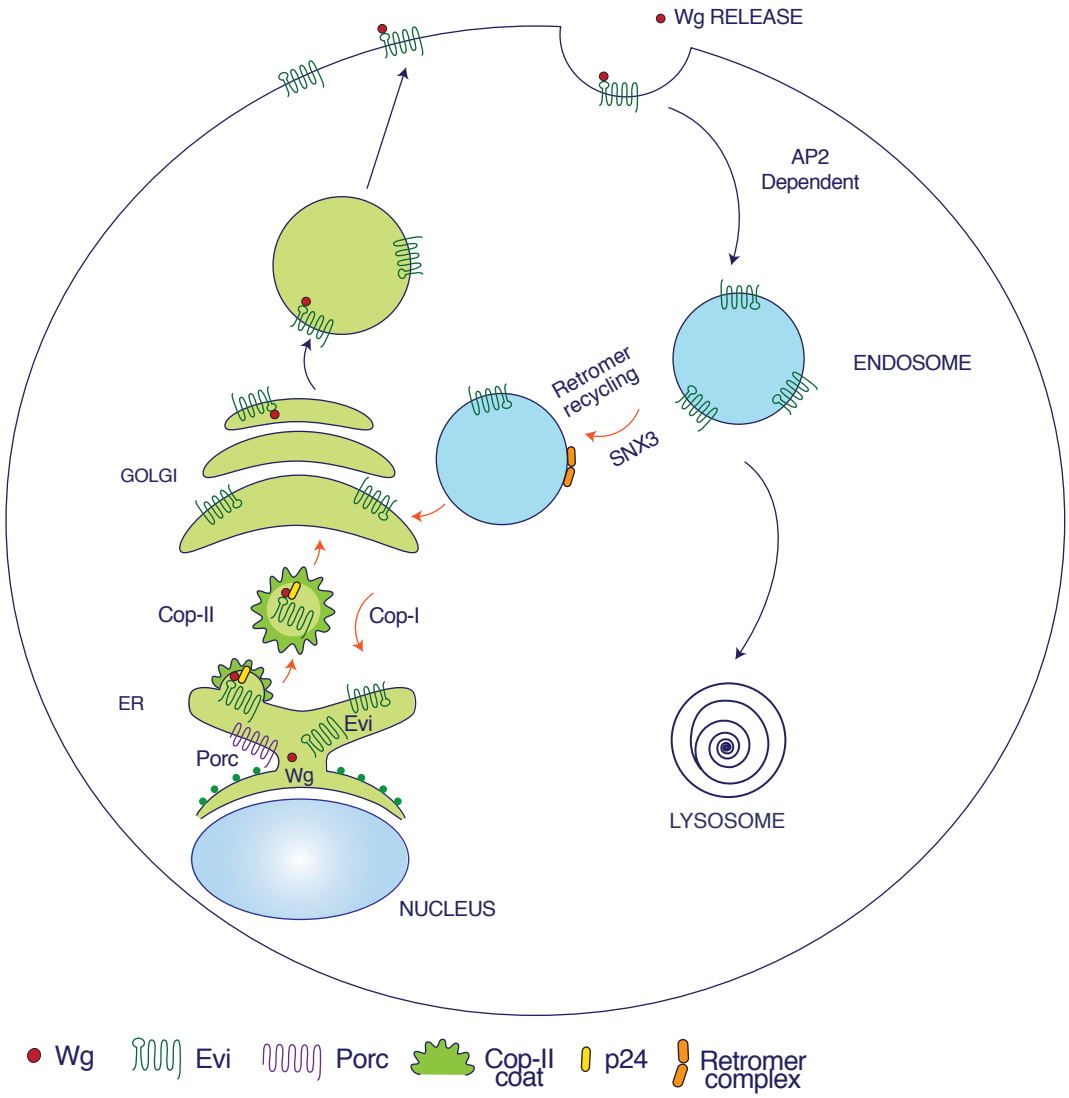
Wg RELEASE
AP2
Dependent
ENDOSOME
Retromer
recycling
SNX3
GOLGI
Cop-II
Cop-I
ER
Evi
Porc
Wg
LYSOSOME
NUCLEUS
Wg
Evi
Porc
Cop-II
coat
p24
Retromer
complex

1.5 Secretion of Wg from Polarised Wing Imaginal Disc Cells

One shortcoming of the model shown in Figure 1.6 is that it does not take into account the polarised nature of *Drosophila* wing imaginal disc cells. There are dramatically different distributions of Wg protein on the apical and basolateral surface of the Wg expressing cells, which indicates there may be an added layer of complexity to Wg movement within these cells.

1.5.1 Polarised Secretion

Epithelial cells often carry out functions within the host tissue that are dependent on their ability to distinguish between their two distinct apical and basolateral surfaces (Rodriguez-Boulan et al., 2005). Separation of these surfaces occurs due to the presence of junctions, which segregate the apical from the lateral surface of cells (Rodriguez-Boulan et al., 2005).

Extensive study has taken place in this area utilising the MDCK cell line, which can form a tight epithelium in cell culture (Cereijido et al., 1978). In these cells apical/basolateral sorting was traced back to the Golgi complex (Rodriguez-Boulan et al., 2005). A polarised secretory route within epithelial cells of an intact tissue has also been described in the *Drosophila* follicular epithelium (Lerner et al., 2013). This occurs via a basolaterally localised mRNA that is translated in a basolateral ER compartment and moves through a basolateral Golgi cluster to the basolateral surface for release. This polarised basolateral secretory pathway is dependent on Rab10 for restricted delivery (Lerner et al., 2013). As previously described, polarised sorting of protein cargo within REs may also be required for correct trafficking of proteins (Thompson et al., 2007). REs sort endocytosed cargo into specific membrane subdomains for polarised transport within epithelial cells (Thompson et al., 2007). Therefore, in epithelial cells, polarised sorting at both the secretory and

endocytic level is important for correct protein targeting to either the apical or basolateral surface.

1.5.2 Polarised mRNA distribution

Polarised mRNA distribution is also thought to contribute to the polarised secretion of several proteins. In the example described above, in the *Drosophila* follicular epithelium, basolateral localisation of the *colIV* mRNA and localised translation in a basolateral tER-Golgi unit was described to enhance the basolateral delivery of basement membrane components (Lerner et al., 2013). Polarised localisation of a *Drosophila* mRNA to distinct tER-Golgi units has also been described for the gene *gurken* (Herpers and Rabouille, 2004). Synthesis and transport of Gurken protein occurs only in tER-Golgi units in the Dorsal-Anterior corner of developing *Drosophila* oocytes, where *gurken* mRNA localises (Herpers and Rabouille, 2004). mRNA mislocalisation caused abnormal expression of Gurken protein indicating that it is mRNA localisation that dictates the ultimate site for Gurken synthesis and secretion (Herpers and Rabouille, 2004). In *Drosophila* embryos, *wg* mRNA is tightly apically localised (Simmonds et al., 2001). Apical localisation of the *wg* mRNA appears to be important for the ability of Wg to function, since mislocalisation of *wg* mRNA not only affects Wg protein localisation but also signalling (Simmonds et al., 2001). Therefore, when considering polarised protein production, the mRNA localisation may well dictate the site of synthesis and production.

1.5.3 Distribution of *wg* mRNA and Wg protein within polarised Wg secreting cells

As is the case in *Drosophila* embryos, *wg* mRNA is tightly apically localised within the *Drosophila* wing imaginal disc (Figure 1.5 A). This apical localisation may be important for signalling. The *wg* 3'UTR is thought to be responsible for apical mRNA localisation (Simmonds et al., 2001). Several *wg* localisation elements (WLEs) have been identified in the *wg* 3'UTR, which

facilitate apical transcript localisation (dos Santos et al., 2008; Simmonds et al., 2001). However, it is slightly contentious as to which of the WLEs is required for apical localisation. Regardless, the 3'UTR of *wg* is recognised as the element that confers this apical localisation (dos Santos et al., 2008; Simmonds et al., 2001).

Consistent with the apical localisation of the *wg* mRNA, the majority of total Wg protein visualised (with disc permeabilisation) is found in the apical region of Wg expressing cells (Figure 1.5 B), where it colocalises with the Wg chaperone protein Evi (Figure 1.5 D). This would suggest that *wg* mRNA and subsequent protein production works in a similar fashion to Gurken, and that the apical localisation of the *wg* mRNA dictates which tER exit site and subsequent tER-Golgi unit subset Wg utilises. In contrast, extracellular Wg (detected without permeabilisation) localises mainly to the basolateral surface of Wg expressing cells and across the disc (Figure 1.5 C). An efficient protocol for detecting extracellular Wg was first developed by Strigini et al. (2000), and they also observed an enrichment of extracellular Wg on the basolateral surface of wing imaginal disc cells. A small amount of apical extracellular Wg can be detected on the surface of the Wg expressing cells, however this is present at much lower levels than basolateral extracellular Wg (Figure 1.5 C''). This suggests that the majority of Wg in secreting cells is apical, whilst the extracellular gradient forms basolaterally (schematic shown in Figure 1.7 Box 1). As the junctions prevent extracellular Wg movement from the apical to basolateral surface, we need to understand how apical Wg is trafficked basolaterally to form an extracellular gradient.

1.5.4 Transcytosis Model of Wg Secretion

One possible model that may resolve the differences between total and extracellular Wg localisation is shown in Figure 1.7 Box 2. Wg would still be produced in the apical ER and undergo modification to allow its association with Evi. Evi then acts to chaperone Wg to the apical surface as previously

described, however instead of being released there to form the gradient, the Wg/Evi complex is endocytosed in an AP2 dependent manner. Wg and Evi are then moved across the cell in a process called transcytosis for basolateral Wg release. A recent study has suggested that the movement of Wg and Evi from the EE for transcytosis basally may be dependent on the protein Myopic (Mop) (Pradhan-Sundd and Verheyen, 2014). Gallet et al. (2008) hypothesised that Wg undergoes transcytosis as described above, but they suggest that the HSPG Dally-like protein (Dlp) is responsible for guiding Wg movement from the apical to basolateral surface of producing cells (Gallet et al., 2008).

Transcytosis as a trafficking mechanism has been most extensively studied in cell culture, specifically in MDCK cells (Rodriguez-Boulan et al., 2005), however still relatively little is known about the mechanistic basis of this process. A Rab11-positive RE has been implicated in the transcytotic process in several systems, as polarised sorting of cargo proteins in REs is required for movement to the correct surface (Casanova et al., 1999; Rojas and Apodaca, 2002). However, the exact regulation of this process appears to vary between systems (see Section 1.2.4). Another molecule that has been suggested to undergo transcytosis in a similar manner is Hh (Callejo et al., 2011; Gallet et al., 2008). Hh is also a lipid-modified morphogen that forms a gradient in the *Drosophila* wing imaginal disc akin to Wg (Osterlund and Kogerman, 2006). In the disc, a similar apical accumulation of Hh in producing cells with the formation of a basolateral gradient is observed. It has been suggested that apical Hh is re-internalised in the producing cells and targeted to the basolateral surface by Dispatched (a 12 pass transmembrane chaperone protein) for gradient formation to occur (Callejo et al., 2011). Similarly, it is possible that apical Wg may be moved via transcytosis for basolateral release via the action of Evi (a 8 pass transmembrane chaperone protein) (Figure 1.7 Box 2).

Figure 1.7: Model of Wg secretion in polarised epithelial cells.

Box 1 – Schematic of Wg distribution in secreting cells. Total Wg (intra and extracellular) is present mainly in the apical region, however the majority of extracellular Wg is observed on the basolateral surface. Box 2 - Potential model for Wg transcytosis through a polarised epithelial cell of the wing disc. Wg is produced in the ER, in the apical region of the cell, where it undergoes Porc-dependent lipidation, associates with Evi and is packaged into COP-II vesicles for movement to the apical Golgi via p24 proteins. Wg and Evi transit the Golgi for movement to the apical surface, but then are re-endocytosed and transcytosed for Wg release at the basolateral surface. This movement may involve the action of the protein Mop. Evi is recycled (orange arrows) via a retromer/SNX3-mediated pathway to the Golgi. COP-I retrograde transport facilitates Evi movement back to the ER to begin the cycle again.

Box 1

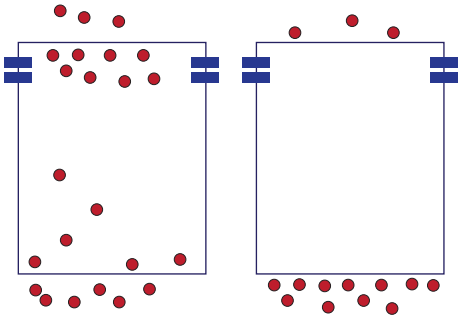

Box 2

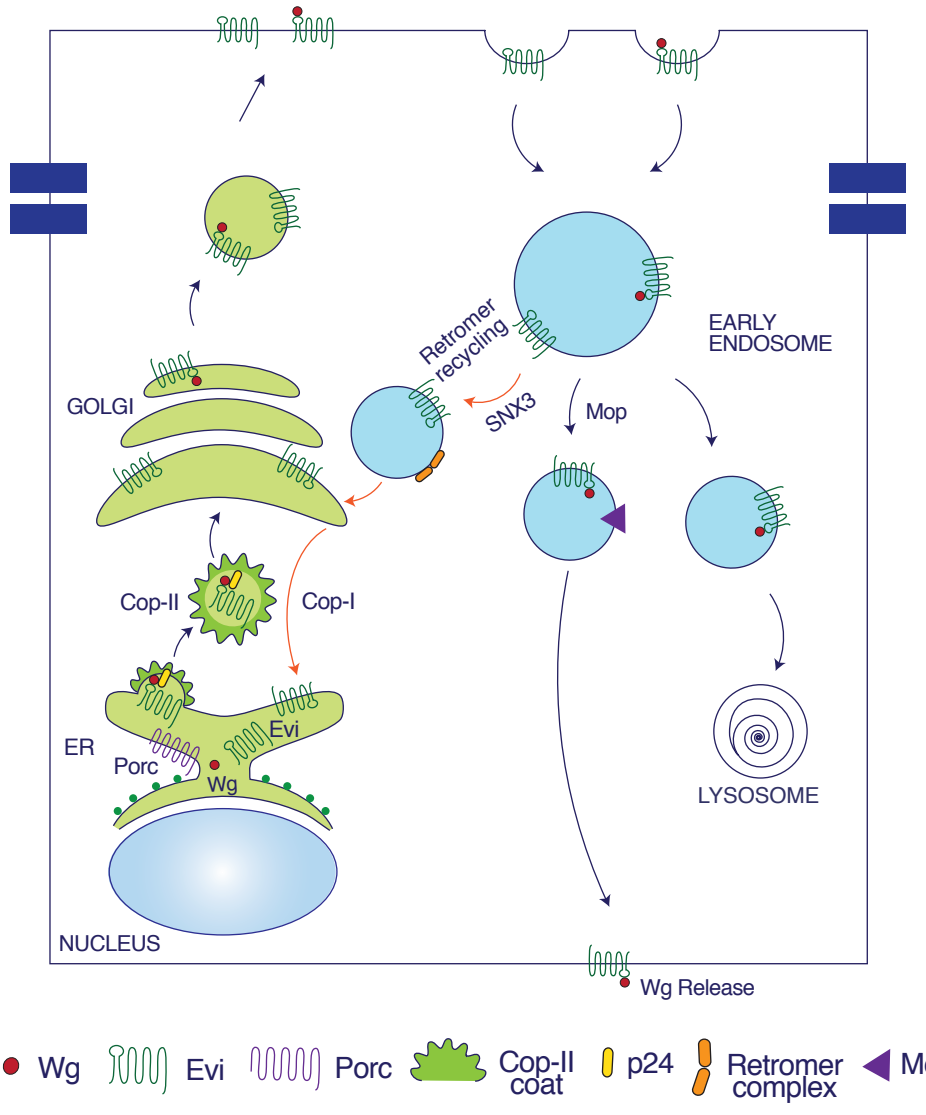
Retromer recycling
SNX3
Mop
EARLY ENDOSOME
GOLGI
Cop-II
Cop-I
ER
Porc
Evi
Wg
LYSOSOME
NUCLEUS
Wg Release
Wg
Evi
Porc
Cop-II coat
p24
Retromer complex
Mop

1.6 Packaging of Wg for release and long distance Transport

Since Wg is hydrophobic it has been proposed that there must be packaging mechanisms that allow it to travel along the tissue. To date, several models have been proposed, but none have yet been conclusively proven. It is possible that there are multiple pools of Wg, which may require different packaging mechanisms depending on their intended destination.

1.6.1 Lipoprotein Particles

Lipoprotein particles (LPPs) comprise a phospholipid monolayer surrounding a triglyceride and cholesterol filled inner core (Eaton, 2006). In insects these particles are called Lipophorins, and are produced in the fat body and travel systemically through the haemolymph (Eaton, 2006; Panakova et al., 2005). Lipid-linked morphogens such as Wg and Hh copurify with lipophorin, possibly due to the ability of lipophorin to shield their lipid moieties (Panakova et al., 2005). RNAi-mediated knockdown of lipophorin in the fat body causes a reduction in extracellular Wg spread and long-range signalling (Panakova et al., 2005). However, these treatments also inhibit growth, which could contribute to this phenotype. In mammalian cells, Wnt3a has been found to co-fractionate with LPPs, and in particular is associated with the high-density LPPs (Neumann et al., 2009). These observations have led several groups to suggest that LPPs may play a role in Wg packaging and long-range transport (Figure 1.8 A).

1.6.2 Argosomes and Exosomes

Argosomes are small exovesicles consisting of a membrane bilayer, which may facilitate the transport of hydrophobic molecules within the *Drosophila* wing imaginal disc (Greco et al., 2001). The main evidence for this is colocalisation between Wg and argosomes marked with membrane-localised GFP (Greco et al., 2001). It was initially suggested that these may be exosomes

or exovesicles, however, later work from the same group determined that argosomes do not colocalise with the exosome marker CD63, and concluded they were not exosomes but LPPs (Panakova et al., 2005). However, unlike LPPs, argosomes contain a lipid-bilayer therefore their similarity to exosomes cannot be completely discounted (Greco et al., 2001).

Exosomes are 50-100nm vesicles that are formed inside MVBs and are released by MVB fusion with the plasma membrane (Figure 1.8 B) (Bobrie et al 2011). Wg-containing 100nm vesicles have been visualised within and associated with MVBs in Wg producing cells in *Drosophila* embryos in vivo, suggesting that Wg resides in the correct site for exosome formation (van den Heuvel et al., 1989). As previously described, Wnt1 is found preferentially in detergent-resistant microdomains due to its ability as a lipidated protein to partition with cholesterol and sphingolipids (Zhai et al., 2004). Exosomes themselves contain cholesterol and ceramide-rich regions (Subra et al., 2007; Trajkovic et al., 2008), suggesting membrane domains in which Wnts reside contain potential exosome components. Sphingolipid depletion however does not cause a decrease in extracellular Wg spread (Pepperl et al., 2013), which would be expected if it were involved in exosome formation. Instead sphingolipid depletion prevents movement of Wg into RE or LE within receiving cells and hence affects signalling (Pepperl et al., 2013). Another potential exosome protein that is associated with microdomains, Flotillin-2, has been shown to promote spreading of Wg and Hh in the *Drosophila* wing imaginal disc (Katanaev et al., 2008), but does not affect exosome formation in *Drosophila* cell culture (Beckett et al., 2013). These data indicate that whilst there is the possibility of a role for exosomes in Wnt secretion, it is by no means definite.

The strongest hint that Wnt may be released on exosomes was the finding that Evi is secreted on exosomes both in vivo and cell culture (Beckett et al., 2013; Gross et al., 2012; Koles et al., 2012; Korkut et al., 2009). Studies of the *Drosophila* neuromuscular junction (NMJ) have shown that Evi is required for

Wg release at the NMJ, and that Evi is transported with Wg on exosomes for movement across the synapse (Koles et al., 2012; Korkut et al., 2009). MVBs containing Evi-positive vesicles with exosome size and morphology were identified in the NMJ by Electron microscopy (EM) (Koles et al., 2012). Using EM, Evi-containing exosomes were also identified in *Drosophila* S2 cells (Koles et al., 2012). Therefore, it is likely that Evi can be located on exosomes. However, whether Wnt is present with Evi on exosomes in the wing imaginal disc, and the importance of these exosomes in the release of Wnt are contentious issues. Active Wnt proteins are present on exosomes in both *Drosophila* and human cell lines, and purified Wnt-containing exosomes can stimulate signalling (Beckett et al., 2013; Gross et al., 2012). However, a study by Beckett et al. (2013) found that whilst Wg is secreted on exosomes in *Drosophila* S2 cells, only a small subset of total secreted Wg resides in these structures so it is likely that other pools of secreted Wg exist. Gross et al. (2012) suggest that secretion of both Wg and Evi also occurs on exosomes in the *Drosophila* wing imaginal disc. They claim that Wg and Evi are secreted from expressing cells and colocalise to spread across the tissue, and observe a high proportion of Wg on exosomes within the wing imaginal disc (Gross et al., 2012). However, Beckett et al. (2013) found this not to be the case, and suggest that exosome formation is not important for Wg movement in the wing imaginal disc.

Evi and Wg release at the NMJ was shown to be a Rab11-dependent process (Koles et al., 2012). Rab11 was also shown to be required for Wg and Evi-containing exosome release in *Drosophila* S2 cells (Beckett et al., 2013; Koles et al., 2012), but Rab11 is not required for formation of the extracellular Wg gradient (Beckett et al., 2013). Gross et al. (2012) claim that Wg and Evi are secreted from expressing cells and spread along the tissue via exosomes. They suggest that this requires Ykt6, since RNAi against Ykt6 causes a reduction in extracellular Wg spread in the wing imaginal disc. Ykt6 RNAi also blocks release of Wnt3A and Evi in cell culture (Gross et al., 2012). Subsequent research has

identified the "specific" exosome secretion factor Ykt6, as a SNARE required for general protein trafficking between the ER and Golgi (Flybase). Adequate controls were not performed by this group to determine that Ykt6 RNAi was not conferring a global secretion block, and recent work in the lab has indicated that this in fact is the case (K. Beckett, unpublished observations).

The Evi release observed by Gross et al. (2012) in imaginal discs could be due to overexpression. Expression of an extracellularly tagged form of Evi at endogenous levels showed no Evi release from the Wg expressing cells (Beckett et al., 2013). Gross et al. (2012) utilised a form of Evi tagged with Cherry at the C-terminus, which as described previously masks an important ER retrieval sequence in the Evi C-terminal tail (Yu et al., 2014). Therefore, overexpression caveats combined with a form of Evi that traffics incorrectly, might imply a role for Evi release, which is not present in a wild type situation. Therefore, it appears that whilst Evi and Wg can be released on exosomes in cell culture and at the NMJ, they do not play a role in gradient formation within the wing imaginal disc, and further investigation is required to determine whether there are other places where these may function.

1.6.3 Extracellular Chaperone Proteins: SWIM

In 2011 Mulligan et al. identified a lipocalin called Secreted Wingless-interacting Molecule (Swim), which directly binds Wg. Lipocalins are proteins that facilitate the extracellular transport of hydrophobic molecules by masking the lipid moiety, and purified Swim is required for Wg solubility and subsequent signalling (Mulligan et al., 2011). A reduction in Swim (via RNAi) causes a decrease in extracellular Wg spread and a reduction of the long-range Wg target *dll* (Mulligan et al., 2011). This suggests that Swim may be involved in long-range Wg transport to facilitate movement of Wg (Figure 1.8 C).

Figure 1.8: Potential modes of Wg packaging for release.
(A) Wg is proposed to associate with Lipoprotein particles (LPPs). This could occur at the cell surface or in an endocytic compartment. Wg transfer to LPPs may be mediated by palmitoleate/lipid-based interactions. (B) Wg could be released on exosomes by MVB fusion with the plasma membrane, or from plasma membrane budding of exovesicles. (C) Wg could associate with a chaperone protein such as Swim at the cell surface. Transfer of Wg to Swim may also be mediated by binding of the Swim lipocalin motif to the palmitoleate modification. (D) Wg could be transferred on cellular projections called cytonemes across many cell diameters.

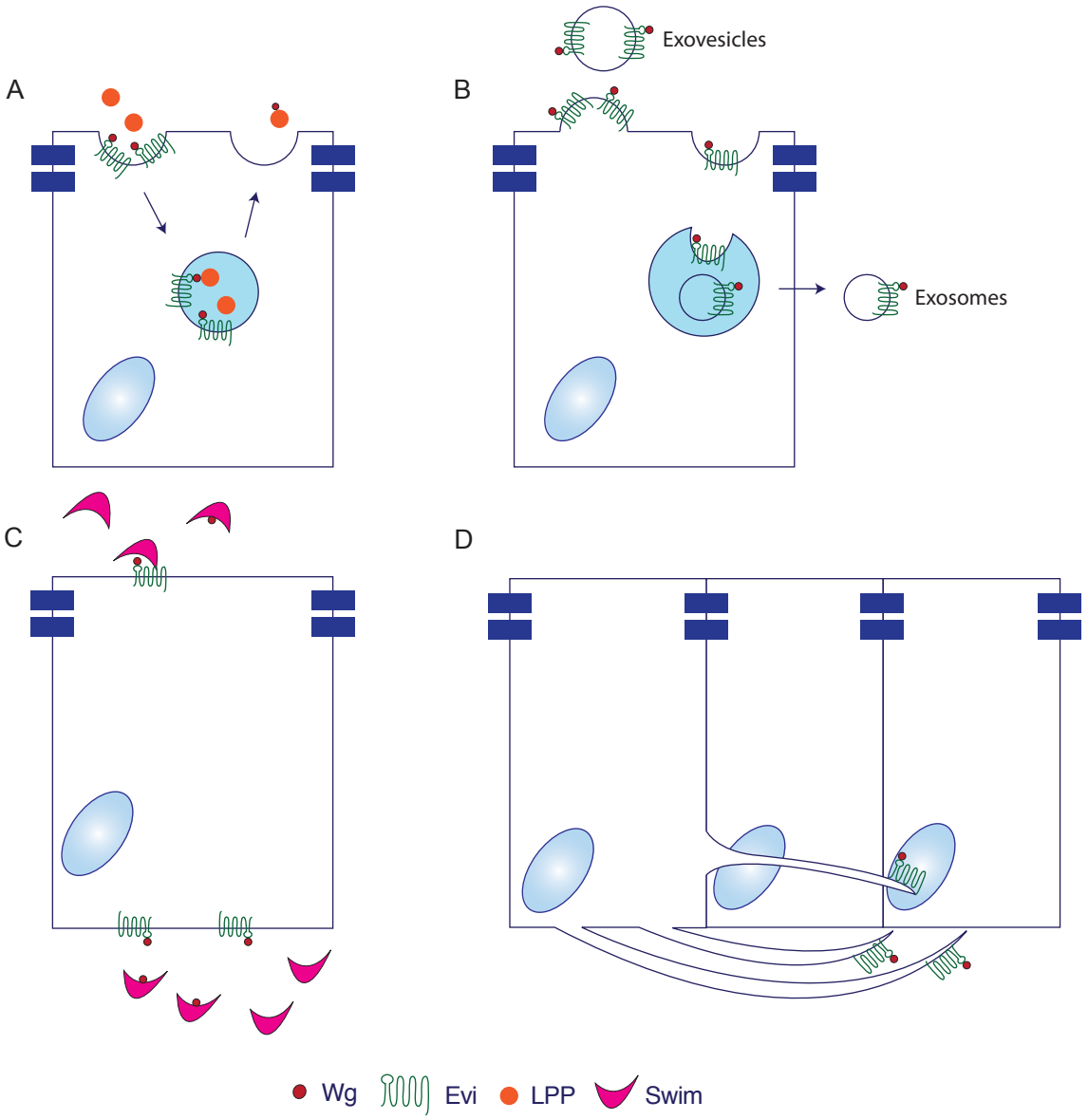
A
B
Exovesicles
Exosomes
C
D
Wg
Evi
LPP
Swim

1.6.4 Cytonemes

Cytonemes are dynamic, actin-based protrusions, which facilitate protein transfer between cells without the need to diffuse (Figure 1.8 D) (Ramirez-Weber and Kornberg, 1999). These protrusions have been mostly characterised in *Drosophila* tissues (wing imaginal disc, air-sac primordia and abdominal epidermis). However, the mouse limb bud has also been shown to produce cytonemes (Ramirez-Weber and Kornberg, 1999). It has been suggested that cytonemes may function to deliver morphogens to cells. Examples include Dpp and Hh (Bischoff et al., 2013; Roy et al., 2014). Overexpressed Dpp-GFP is present on cytonemes, often alongside its receptor Thickveins (Tkv), and it has been suggested that in certain contexts Dpp signalling requires cytoneme formation (Roy et al., 2014). In the *Drosophila* wing imaginal disc, Hh producing cells generate cytonemes suggesting they may participate in delivering the Hh morphogen to the receptor to activate signalling (Bischoff et al., 2013). However, in order to visualise these structures membrane-tethered GFP-fusion proteins are overexpressed which may localise to all membranous structures, regardless of their importance in vivo. Overexpression of these proteins could also boost the formation of these structures. Since Wnts are lipid modified morphogens that show many similarities to Hh, it is possible that Wnt transport may occur via cytonemes, although currently there is no evidence to suggest this is the case. In the *Drosophila* wing imaginal disc cytoneme protrusions are only observed perpendicular to the A/P boundary, where Dpp and Hh are expressed (Bischoff et al., 2013; Ramirez-Weber and Kornberg, 1999). For cytonemes to be relevant to Wg transport they would need to be present extruding from the Wg expressing cells perpendicular to the D/V boundary. Despite extensive attempts to test this using overexpression of Evi-V5 or Evi-GFP, these protrusions cannot be observed (K. Beckett, unpublished data), therefore currently Wg movement via cytonemes is unlikely.

1.7 Wingless Gradient Formation in the *Drosophila* wing imaginal disc

After Wg packaging and release, movement of Wg across the wing imaginal disc occurs. This is required to form the gradient observed in an extracellular Wg staining (Strigini and Cohen, 2000). Several factors are involved in the capture and spread of Wg across the basolateral surface of the disc to shape the gradient.

1.7.1 HSPGs: Dally and Dlp

Wnt proteins are secreted glycoproteins, which are lipidated and modified at a number of N-glycosylation sites (Bartscherer and Boutros, 2008). From early biochemical data it has been ascertained that Wnts are generally associated with the ECM (van den Heuvel et al., 1993), and Wnt1 has been found to preferentially associate with lipid raft membrane microdomains, which are also regions of GPI-anchored protein clustering (Zhai et al., 2004). Association between Wnt proteins and cell surface microdomains via the ECM may be due to the interaction of Wnt proteins with Heparan sulphate proteoglycans (HSPGs). *Sugarless* encodes the *Drosophila* homologue of UDP-glucose dehydrogenase, which is essential for proteoglycan biosynthesis (Hacker et al., 1997). *Drosophila sugarless*$^{-/-}$ mutants display segment polarity phenotypes, indicating that proteoglycans are required for proper Wg signalling (Hacker et al., 1997). *Sulfateless* encodes a *Drosophila* homologue of a heparan sulphate transferase, required for HSPG modification (Lin and Perrimon, 1999). S*ulfateless*$^{-/-}$ mutants display a similar segment polarity phenotype to that of a *sugarless*$^{-/-}$ mutant, indicating that it is HSPGs specifically that are involved in Wg signalling (Lin and Perrimon, 1999).

There are two main HSPGs found in the *Drosophila* wing imaginal disc that have roles in Wg gradient formation, *division abnormally delayed (dally)*

and *dally-like protein (dlp)*, which are both GPI-anchored glypicans (Baeg et al., 2001; Lin and Perrimon, 1999). Dlp has been shown to localise basolaterally (unpublished observations) and Dally localisation is unknown. These HSPGs have been shown to modulate the extracellular Wg gradient in the wing imaginal disc (Baeg et al., 2001; Han et al., 2005). *Dally*$^{-/-}$, *dlp*$^{-/-}$ mutant clones cause a reduction in the spread of extracellular Wg, presumably since Wg uses the HSPGs for retention along the basolateral surface of the disc (Han et al., 2005). Accordingly, Dally and Dlp would modulate basolateral Wg diffusion via "restricted diffusion" (Han et al., 2005). The importance of Dally and Dlp in Wg gradient modulation is highlighted by the presence of a secreted enzyme called Notum. Notum is a Wg target gene thought to modify both Dally and Dlp (Giraldez et al., 2002). It is hypothesised that Notum cleaves the GPI anchor of the Dlp glypican in a manner similar to the GPI anchor-cleaving enzyme PI-PLC, leading to the moulting of Dlp (Kreuger et al., 2004). In this fashion, Wg controls the shape of its own extracellular gradient through the expression of Notum (Kreuger et al., 2004).

Other proteins have also been shown to require stabilisation via the action of HSPGs. Hh requires HSPGs to restrict its movement through the ECM (Callejo et al., 2006). Without Dlp, which resides mainly on the basolateral surface of the disc, the majority of Hh moves apically in contrast to the wild type situation where Hh mostly moves basolaterally (Callejo et al., 2006). As discussed earlier, Dlp may also have roles in Wg gradient formation besides controlling extracellular Wg movement. It has been proposed to be involved in Wg secretion directly within Wg expressing cells (Gallet et al., 2008). In the Wg expressing cells, apical Dlp may undergo transcytosis with Wg, facilitating movement across the expressing cell for basolateral Wg release and subsequent extracellular gradient formation (Gallet et al., 2008). However, as previously described, Dlp mainly resides on the basolateral surface of the wing disc, and this conclusion rests on overexpressed, tagged Dlp casting doubt on its validity.

Whilst the role of Dlp in Wg transcytosis is still unclear, the role that the HSPGs play in Wg gradient formation and refinement is evident.

1.7.2 The Fz2/Arrow Receptor complex

The formation of a gradient requires the presence of both a "source" of morphogen and a "sink" for the removal of said morphogen (Marois et al., 2006). Removal of secreted morphogens from the surface of cells often occurs by receptor binding and endocytosis, leading to degradation. Therefore both the receptors and the endocytic pathway play important roles in gradient formation (Marois et al., 2006; Sorkin and von Zastrow, 2009). In the case of both Hh and Wg, dynamin is not required for spreading, which implies that the gradient forms by diffusion, and not planar transcytosis (Strigini and Cohen, 2000; Torroja et al., 2005). Extracellular Wg accumulates on the surface of dynamin mutant clones in the wing imaginal disc, implying that internalisation of Wg in a dynamin-dependent manner may be required to create a "sink" (Strigini and Cohen, 2000). Once internalised in receiving cells, Wg is found in both Rab5 and Rab7-positive endosomes suggesting targeting to degradation (Marois et al., 2006). Wg is not found in Rab11 recycling endosomes, indicating that the recycling branch of the endocytic pathway does not contribute to Wg spread (Marois et al., 2006).

In a similar fashion to dynamin mutant clones, Frizzled-2 (Fz2) overexpression within the *Drosophila* wing imaginal disc causes stabilisation of extracellular Wg, suggesting that Fz2 binding could contribute to long-distance Wg movement (Cadigan et al., 1998). This is consistent with the observation that Wg inhibits Fz2 expression in a negative feedback loop, presumably to allow movement along the disc (Cadigan et al., 1998). In this way Fz2 levels may shape the Wg morphogen gradient. Five *frizzled* genes exist in the *Drosophila* genome: Fz, Fz2 and Fz3 bind Wg, but, Fz2 binds with the greatest affinity (Wu and Nusse, 2002). Fz and Fz2 are both required for Wg signalling (Clevers and Nusse, 2012; Wu and Nusse, 2002). Structurally, the Frizzled

proteins are seven-pass transmembrane receptors with an extracellular CRD and a cytoplasmic tail (MacDonald and He, 2012; Wu and Nusse, 2002). As discussed previously, the crystallisation of XWnt8 would not have been possible but for its ability to bind the Fz8-CRD. The final structure shows that the palmitoleic acid inserts into a pocket in the Fz8-CRD. This suggests that the interaction between Wnt and Fz, and subsequent signalling may depend on the lipid (Janda et al., 2012).

Whilst Fz2 binds Wg, it is unable to signal without the presence of its co-receptor Arrow (Arr), the *Drosophila* homologue of mammalian LRP-5/6 (MacDonald and He, 2012; Piddini et al., 2005). Fz2 is required for Wg internalisation, but in concert with Fz2, Arr is required for directing internalised Fz2/Wg to a degradative branch of the endocytic pathway (Piddini et al., 2005). In the absence of both Fz2 and Arr, extracellular Wg accumulates due to the inability of these cells to internalise Wg (Baeg et al., 2004; Han et al., 2005).

Formation of the Wg morphogen gradient in the *Drosophila* wing imaginal disc therefore requires the presence of a Wg "source" (the expressing cells), and a "sink" for Wg removal (the endocytosis and degradation of Wg through the action of Fz2 and Arr). However, movement of Wg across the disc from "source" to "sink" is shaped by the presence of HSPGs Dally and Dlp. The combined contributions of the Wg receptors and HSPGs facilitate normal gradient formation (Baeg et al., 2004; Han et al., 2005). Both Dlp and Fz2 share similar expression patterns with downregulation observed around the D/V boundary. This facilitates movement of Wg away from the high concentration "source" domain across the disc for stabilisation and long-range signalling (Baeg et al., 2004). Most Dlp and Fz2 expression is observed on the basolateral surface of receiving cells (unpublished observations), which is consistent with the localisation of extracellular Wg (Strigini and Cohen, 2000). This suggests that Fz2 and Dlp may act together for Wg stabilisation and binding. Baeg et al. (2004) suggest a model where Dlp may act to trap/stabilise extracellular Wg

near to the Fz2 receptors to facilitate receptor binding and internalisation, therefore enabling both Wg signalling and the refinement of extracellular Wg gradient formation.

Aims of the Thesis and Overview of my work

The aim of this work is to uncover the secretory route taken by Wg and Evi within Wg-producing cells. I aimed to test whether Wg and Evi transit through the apical surface and then move to the basolateral surface for Wg release, and, if this is the case, to determine what relevant trafficking steps are involved.

To answer these questions I have used constructs expressing extracellularly tagged Wg and Evi at endogenous levels in vivo. I have designed a system to induce expression of tagged Wg at endogenous levels to enable its tracking through the secretory system. Using a reversible block of endocytosis in vivo, I determined where Wg and Evi localise upon perturbation of endocytosis, and their subsequent movement upon release of this block.

In Chapter 3 I describe the tools I have designed to achieve my aims. With these tools I have explored the movement of Wg within expressing cells, as described in Chapter 4. The role that the Wg chaperone protein Evi plays in this process is described in Chapter 5.

Chapter Two

Materials and Methods

2.1 *Drosophila* Genetics

2.1.1 Basic stock maintenance

Fly stocks were kept at 18°C, 25°C or 29°C on a standard medium consisting of agar, cornmeal and yeast. Crosses were performed at 25°C unless they involved tub-Gal80^{ts}, in which case they were kept at 18°C and moved to 29°C when required. Gal4/UAS-RNAi crosses were conducted at 29°C.

2.1.2 *Drosophila* strains

The stocks described below correspond to the original strains used to conduct experiments shown in this thesis. The origin of the stock is indicated along with several stocks produced in this study.

Genotype	**Origin and additional information**
Wild Type Stock	
yw	Wild type stock for all experiments
Tagged Wg Stocks	
Wg-Ex4-2HA BAC/TM6	Generated by C. Alexandre
Wg-Ex4-gly2HA BAC/TM6	Generated by C. Alexandre
Wg-Ex2-2HA BAC/TM6	Generated by C. Alexandre
Wg-Ex2-gly2HA BAC/TM6	Generated by C. Alexandre
wg{KO; Wg-Ex4-2HA}/CyO	Generated by C. Alexandre and A. Baena-Lopez
wg{KO; FRT-Wg-FRT-Wg-Ex4-2HA}/CyO	Generated in this study
wg{KO;FRT-Wg-Ex4-3OLLAS-FRT-Wg-Ex4-3HA}/CyO	Generated by C. Alexandre
Tagged Evi Stocks	
Evi-V5-Nterm BAC/TM6	Generated by C. Alexandre
Evi-EC3-V5 BAC/TM6	Generated by C. Alexandre

Evi-EC3-glyV5 BAC/TM6	Generated in this study
Evi-EC3-glyOLLAS BAC/TM6	Generated in this study
UAS-Evi-Nterm-V5/TM6	Generated in this study
UAS-Evi-FLV5/TM6	Generated by C. Alexandre
UAS-Evi-ECD8V5/TM6	Generated by C. Alexandre
Tagged Evi and Wg Stocks	
actin-FRT-Cerulean pA-FRT-Evi-EC3-OLLAS-2A-Wg-Ex4-HA/TM6	Generated in this study
actin-FRT-Plum pA-FRT-5'UTR-Evi-EC3-OLLAS-2A-Wg-Ex4-HA/TM6	Generated in this study
Additional Stocks	
KB19	Testes specific Flp – from K. Basler
ywhsflp;sp/SM6-6B	From P. Langton
wg^{KO}/CyO	Generated by C. Alexandre and A. Baena-Lopez
wg^{CX4}/CyO	From Bloomington stock centre
evi^{2}/TM3	From M. Boutros
Hh-Gal4 UAS-Flp/TM6	Lab stock
En-Gal4/CyO	Lab stock
shibire^{ts}	From C. O'Kane
En-Gal4 UAS-GFP/CyO; tub-Gal80^{ts}	Lab stock
En-Gal4 UAS-Flp/CyO; tub-Gal80^{ts}	Lab stock
Hh-Gal4 tub-Gal80^{ts}/TM6	Lab stock (recombined by C. Alexandre)
actin-FRT-stop-FRT-lacZ/TM6	Lab stock
UAS-Flp (II)	Lab stock
UAS-Flp (III)	Lab stock
tubulin-Rab5:YFP/TM6	From S. Eaton
UAS-Evi RNAi	From VCRC – CG6210, line no. 5214
FRT42D $vps35^{MH20}$/CyO	From X. Franch-Marro
FRT42D M(2)arm-lacZ/CyO	From Bloomington stock centre
FRT2A ubi-GFP/GlBc	From P. Langton
FRT2A $dlp^{-/-}$, $dally^{-/-}$	From P. Langton

2.1.3 Controlling the inducible system

Conditions for heat shocks:

Larvae were heat shocked for 20min at 37°C either 72hr after egg laying (AEL) and fixed 48hr later, or heat shocked under the same conditions at 120hr AEL and fixed either 3hr or 6hr later.

Conditions for Gal4 tub-Gal80^{ts} experiments:

Crosses were kept at 18^{o}C until larvae were wandering L3. At this stage larvae were moved to 29^{o}C for the required time period prior to fixation.

2.1.4 Blocking endocytosis using *shibire^{ts}*

Shibire^{ts} wandering L3 larvae were placed on a grape juice plate in either a 37^{o}C or 34^{o}C waterbath for the required time period and fixed afterwards. It was found that the effect of blocking endocytosis at 37^{o}C or 34^{o}C was equivalent (data not shown), so the majority of experiments were conducted at 34^{o}C. If an endocytic chase was needed, the grape juice plate and larvae were then placed back at 18^{o}C for the relevant time period before fixation. Control discs in these conditions expressed En-Gal4 UAS-CD8GFP.

2.1.5 Production of *dlp$^{-/-}$*, *dally$^{-/-}$* clones

Larvae were heat shocked 48hr AEL for 45min at 37^{o}C and fixed around 48hr later at wandering L3.

2.2 Molecular Biology

2.2.1 Producing a tagged Evi BAC using Recombineering

The Evi Bacterial Artificial Chromosomes (BACs) were designed using an Evi BAC clone (Ch321_67E05), containing 80kb of the *evi* locus. The BAC was electroporated into SW102 bacteria (NCI) to allow modification via recombineering. The pGalK vector was amplified by PCR using specific primers incorporating Evi sequence homologous for the region for insertion in the BAC (for primers see Appendix 1). This produced a fragment containing the GalK selection marker (selection for presence of this can be performed using minimal media + galactose plates) (Warming et al., 2005) flanked by arms

homologous to the region of Evi BAC for desired tag insertion. The GalK fragment with Evi BAC arms was purified (Gel extraction kit, Qiagen) and electroporated into competent SW102 Evi BAC containing cells. Cells were left to recover in LB for 1hr at 37^{o}C, washed in M9 salts and plated on minimal media + galactose plates to compete out non-GalK containing bacteria at 30^{o}C for 4 days. Positive colonies were selected for using McConkey plates and screened using GalK containing primers by PCR (Appendix 1) (Warming et al., 2005).

PCR products containing the tags of interest were made for the BAC insert using primers (Appendix 1), purified (Gel extraction kit, Qiagen) and electroporated into electrocompetant bacteria containing the Evi BAC-GalK. Cells were left to recover in Luria Broth (LB) for 3hr at 37^{o}C, washed in M9 salts and plated on minimal media DOG plates to compete out GalK containing bacteria at 30^{o}C for 4 days. Colonies containing the selected insert instead of the GalK were selected for using McConkey plates and screened using insert specific primers (Appendix 1). Positive colonies containing the insert were prepared and electroporated into EPI bacteria (NCI) which can express BACs at a higher copy number. Cells were left to recover in LB at 30^{o}C for 1hr and then plated on LB. DNA was prepared from EPI-BAC containing bacteria using a Pure-Link Maxi prep kit (Life Technologies) and sent for injection into the 65B2 attP site in transgenic flies (Rainbow Transgenics).

2.2.2 Creation of a UAS-Evi-NtermV5 construct

To create an Evi-NtermV5 tagged cDNA (tagged in the same region as shown in Figure 3.8 B), the Evi-NtermV5 BAC (C. Alexandre) was cut with unique restriction enzymes (Roche) to excise a piece of DNA containing the tagged N-terminal region. This was purified (Gel extraction kit, Qiagen) and ligated with a wild type cut Evi cDNA lacking that region in a TOPO vector (C. Alexandre, Life Technologies). This was then transformed and plated onto LB+Ampicillin. Positive colonies were screened for using V5 insert specific

primers (Appendix 1). Positive colonies were prepared and the entire Evi-NtermV5 insert was excised and ligated into a pUAS-attB vector. Positive colonies were screened for using specific primers (Appendix 1). DNA was prepared from these positive colonies using a Pure-Link Maxi prep kit (Life Technologies) and sent for injection into the 65B2 attP site in transgenic flies (Rainbow Transgenics).

2.2.3 Reinsertion of an inducible Wg cDNA into the *wg^{KO}*

To insert a modified cDNA into the attP site present in the *wg^{KO}*, the RIV$^{FRT.MCS.pA.FRT.MCS3}$ (Baena-Lopez et al., 2013) reinsertion vector was utilised. The wild type Wg cDNA was amplified from a Wg containing plasmid using primers either side of the 5'UTR and 3'UTR (Appendix 1) (C. Alexandre). The PCR product was then digested, purified (Gel extraction kit, Qiagen), cloned into the first MCS of the RIV$^{FRT.MCS.pA.FRT.MCS3}$ and plated on LB+Ampicillin. Positive colonies were screened using specific primers within Wg (Appendix 1) and this modified vector was used for the subsequent cloning steps. The Wg-Ex4-2HA cDNA (Figure 3.6) was synthesised (Genewiz) and then cloned in the same fashion into MCS3 in the reintegration vector. Positive colonies were screened for using specific primers within the HA tag (Appendix 1). DNA was prepared from these positive colonies using a Pure-Link Maxi prep kit (Life Technologies) and sent for injection into the attP site of the *wg^{KO}* flies (C. Alexandre, Rainbow Transgenics).

2.2.4 Creation of a construct to allow simultaneous production of Evi and Wg: The 2A system

Tagged versions of both Wg and Evi were synthesised (Genewiz) introducing the required restriction sites flanking both the Wg-Ex4-HA and Evi-EC3-OLLAS cDNAs. A pMT-2A-2A vector (C. Alexandre) was the recipient vector for these two cDNAs. They were digested (Roche), purified (Gel extraction kit, Qiagen), ligated (NEB), transformed and plated on LB+Ampicillin. Ligation of

the two tagged proteins was performed in both orders: Wg-2A-Evi and Evi-2A-Wg. Positive colonies were screened for using insert specific primers (Appendix 1) and positive colonies were grown up and the DNA was transfected into *Drosophila* S2R+ cells to analyse expression.

Following cell stainings, since both proteins were expressed, cloning was continued using pMT-Evi-EC3-OLLAS-2A-Wg-Ex4-HA. The Evi-2A-Wg fragment was excised from the pMT vector and inserted into an actin-FRT-Cerulean pA-FRT-attB vector that was previously designed and synthesised in the lab (C. Alexandre and A. Baena-Lopez). Positive colonies were screened for by PCR with relevant primers (Appendix 1). DNA was prepared from these positive colonies using a Pure-Link Maxi prep kit (Life Technologies) and sent for injection into the 65B2 attP site in transgenic flies (Rainbow Transgenics).

A modified version of this actin-FRT-Cerulean pA-FRT-Evi-EC3-OLLAS-2A-Wg-Ex4-HA construct was made, to include a 5'UTR and to change the fluorophore from earlier stages in the cloning process:

A PCR product of the Evi 5'UTR was made using specific primers (Appendix 1) with the Evi BAC (Ch321_67E05) as a template. This PCR fragment was cloned in front of Evi using unique sites in the pMT-Evi-EC3-OLLAS-2A-Wg-Ex4-HA vector. Positive colonies were screened for using relevant primers (Appendix 1). The actin-FRT-Cerulean pA-FRT-attB vector (C. Alexandre and A. Baena-Lopez) was also modified. Using unique sites either side of the Cerulean the fluorophore was exchanged for a Plum cDNA, which was a PCR fragment produced using specific primers (Appendix 1) from a template DNA provided by R. Makki. Positive colonies were screened for using relevant primers (Appendix 1). The 5'UTR-Evi-EC3-OLLAS-2A-Wg-Ex4-HA module was then excised from the pMT vector and cloned after the final FRT in the modified actin vector. Positive colonies were screened for using relevant primers (Appendix 1). DNA was prepared from these positive colonies using a Pure-Link Maxi prep kit (Life Technologies) and sent for injection into the 65B2 attP site in transgenic flies (Rainbow Transgenics).

2.3 Immunohistochemistry

2.3.1 Total wing disc stainings

Discs were dissected from wandering L3 larvae in Phosphate Buffered Saline (PBS) and fixed in 4% formaldehyde in PBS for 20min, permeabilised with TritonX-100 0.5% in PBS (PBTriton 0.5%) for 10min and blocked in 4% Foetal Bovine Serum (FBS)-PBTriton 0.5%. Permeabilisation for anti-Evi stainings was done using a higher concentration of TritonX-100 1%. Discs were incubated in primary antibody diluted in 4% FBS-PBTriton 0.5% overnight, washed in PBTriton 0.5% and then incubated in secondary antibody diluted in 4% FBS-PBTriton 0.5% for 2hr at room temperature. Final washes in PBTriton 0.5% were performed before mounting using Vectashield (Vector Labs).

2.3.2 Extracellular wing disc stainings

Discs were dissected from wandering L3 larvae chilled on ice at 4^{o}C and then incubated in primary antibody on ice at 4^{o}C for 2hr in Schneiders medium (see 2.4 Cell Culture for recipe). Discs were then washed and fixed in 4% formaldehyde in PBS for 40min at 4^{o}C. PBTriton 1% was used to permeabilise discs for 10min at room temperature and blocked in 4% FBS-PBTriton 0.5%. Discs were incubated in secondary antibody in 4% FBS-PBTriton 0.5% overnight, then washed and mounted in Vectashield (Vector Labs). Modified from (Strigini and Cohen, 2000), personal comm. Sophie Hamel.

2.3.3 List of Antibodies

Primary antibodies used in the following experiments:

Antibody	Animal raised in	Dilution: Total Staining	Dilution: Extracellular staining	Origin:
anti-Wg	Mouse	1:1000	1:300	DSHB, 4D4
anti-HA	Mouse	1:500	1:200	AbCam
anti-HA	Rabbit	1:1000	1:50	Cell signalling
anti-RFP	Rabbit	1:100	N/A	AbCam
anti-Evi	Rabbit	1:1000	N/A	K. Basler
anti-OLLAS	Rat	1:10	1:2	Abnova
anti-V5	Rabbit	1:500	1:200	AbCam
anti-Boca	Guinea-pig	1:500	N/A	R. Mann
anti-GMAP	Rabbit	1:1000	N/A	P. Therond
anti-D-Lamp	Rabbit	1:200	N/A	AbCam
anti-GFP	Chick	1:1000	N/A	AbCam
anti-Bgal	Chick	1:1000	N/A	AbCam
anti-GMAP	Goat	1:1000	N/A	S. Munro
anti-Cut	Mouse	1:20	N/A	DSHB, 2B10
anti-Dlp	Mouse	1:50	1:20	DSHB, 13G8

Secondary antibodies used in the following experiments:

2^{o} Antibody	Alexa fluorophores
anti-Mouse	488, 555
anti-Rat	488, 555
anti-Rabbit	488, 555
anti-Guinea pig	488
anti-Chick	488, 555, 647
anti-Goat	488, 555, 647

All Alexa secondary antibodies (Life Technologies) were used at 1:500 except Alexa-647, which is used at 1:200. For extracellular stainings all Alexa secondary antibodies (Life Technologies) were used at 1:250 except Alexa 647, which was used at 1:100. DAPI (Life Technologies) was used to stain nuclei at 1:1000.

2.3.4 Imaging conditions and analysis

Wing disc images were taken on a Leica SP5 confocal microscope. Z stacks were taken at 1-2 micron intervals. Images were processed using Adobe Photoshop and Volocity.

Analysis of images to allow quantification for Figures 4.3, 4.4 and 4.10: Independent triplicates were obtained for each condition and apical and basolateral sections were chosen using Volocity and exported as Tiff files. These tiff files were analysed using Fiji by drawing a line of 100pixel width from the top to the bottom of the wing pouch and this information was used to plot a Z-axis profile. The numerical values from this plot were then analysed using Excel (Microsoft) to create averages for each condition. These were normalised according to the background staining measured in regions of the pouch away from the Wg expressing cells. These were then plotted on a graph using Excel.

Analysis of images to allow quantification for Figures 4.9 and 5.7: Independent triplicates were obtained for each condition and entire Z stacks were analysed using Fiji. A box of defined size was drawn around the area of interest and this information was used to plot a Z-axis profile. The numerical values from this plot were then analysed using Excel to create averages for each condition. These were normalised according to an equivalent control box Z-axis profile, which was measured in a region of the pouch away from the Wg expressing cells to remove background staining. These averages were then plotted on a graph using Excel.

2.4 *Drosophila* Cell Culture

2.4.1 Maintenance of cell lines and transient transfection

Drosophila S2 and S2R+ cells (*Drosophila* Genomics Resource Centre, DGRC) were cultured at 25^{o}C in Schneiders medium + L-Glutamine (Sigma) containing 10% (v/v) Fetal Bovine Serum (FBS; Life Technologies) and 0.1 mg/ml Pen/Strep (Life Technologies). Transient transfections were performed using the Effectene transfection kit (Life Technologies). For constructs under the control of MT promoter, expression was induced using 500uM Copper Sulphate 24hrs post transfection.

2.4.2 Production of cell lysates

Cell lysates were produced using Triton Extraction Buffer (TEB): 50mM Tris pH7.5, 150mM NaCl, 1mM EDTA, 1% Triton-X100. Cells were incubated in cold TEB for 10min on ice then spun at 14,000rpm for 10min at 4^{o}C to remove remaining cell debris. The subsequent supernatant was the cell lysate.

2.4.3 Immunostaining of cells

For cell stainings, 48hrs after transfection S2R+ cells were washed in PBS, then fixed in 4% Paraformaldehyde (PFA) in PBS for 10min. Cells were washed in PBS, quenched using 50mM NH_4Cl in PBS for 10min, permeabilised using Triton-X100 0.1% for 10min and blocked in 2% FBS in PBS. Cells were then incubated with primary antibody for 60mins, washed in PBS, then incubated in the appropriate secondary antibody for 30mins at previously described concentrations. Cells were washed in PBS and coverslips were mounted in Prolong Gold (Life Technologies) and visualized as previously stated.

2.5 Western Blots

Cell lysates were mixed with 4x LDS sample buffer (Life Technologies) and heated at 95^{o}C for 5mins. 50mM DTT was added and samples stored at -20^{o}C. Samples were run on 4-12% Bis-Tris NuPage gels with MOPS buffer alongside SeeBlue Plu2 Pre-Stained Standard molecular weight marker (Life Technologies). Proteins were transferred onto PVDF membrane (Millipore) using semi-dry transfer apparatus (Bio-Rad). Transfer buffer used contained 10X blot, 1:10 methanol and antioxidant (Life Technologies). Soaking buffer contained 10X blot and 1:1000 SDS. Semi-dry transfer was completed using PVDF membrane and whatmann paper at 14V for 30min. Membranes were stained with Ponseau to assess protein loading and transfer and then washed in dH_20 to remove stain. Membranes were blocked in 5% dry milk in PBTween (Phosphate Buffered Saline + 0.1% Tween-20) and incubated in primary antibody diluted in 5% milk overnight at 4^{o}C. Membranes were washed in PBTween prior to incubation in HRP-conjugated secondary antibodies (anti-mouse 1:5000, Bio-Rad) for 2hrs at room temperature. Membranes were washed again in PBTween, developed using ECL (Amersham) and exposed to film (Amersham).

Chapter 3

Creating tagged versions of Wingless and Evi that are expressed at endogenous levels.

3.1 Introduction

Wingless (Wg) is produced in a stripe of cells in the *Drosophila* wing imaginal disc and spreads from these secreting cells across the tissue to form a gradient. Data from several publications has elucidated a basic trafficking route that Wg may take in these expressing cells (Figure 1.6). However, this may be over-simplified since this route does not take into account that secreting cells are polarised. Tools to elucidate the movement of Wg have not been accurate enough to give us insight into what is happening in the expressing cells. Most experimental approaches have relied on overexpression of proteins fused with fluorophores or epitope tags. Both overexpression, and/or the incorrect positioning of the tag could affect the movement and trafficking of the protein, causing deviation from the normal secretory route. We are fortunate to have a good antibody against Wg (van den Heuvel et al., 1989) that can detect both total and extracellular Wg expression at endogenous levels. Unfortunately, for the Wg chaperone protein Evenness Interrupted (Evi), the only antibody available (Port et al., 2008) is raised against an intracellular portion of this transmembrane protein. Therefore, we have been unable to detect extracellular Evi. In this chapter I describe improved tools to track Wg and Evi movement.

3.2 Results

3.2.1 Production of a tagged Wg BAC.

We wanted to create a tagged version of Wg that is expressed at endogenous levels in an experimentally controlled fashion. Thus, we would be able to produce a step of tagged Wg at the time of our choosing and follow its progress through the secretory pathway. To do this we created a 67kb *wg* Bacterial Artificial Chromosome (BAC) that contains the *wg* promoter, and most of the upstream elements to allow *wg* expression at endogenous levels. We then inserted a 9AA Haemagglutinin (HA) tag into specific sites in the Wg coding region to create several distinct BACs (Figure 3.1). The site in Exon 2 was chosen as another group had previously inserted a HA tag there in an overexpression construct (Hays et al., 1997) (Figure 3.1 C, D). The region surrounding the site in Exon 4 is not present in vertebrate Wnt (Hays et al., 1997; Miller, 2002), so seemed a suitable candidate region for tag insertion (Figure 3.1 A, B). HA tags both with (Figure 3.1 B, D) and without (Figure 3.1 A, C) flanking Glycines were inserted into these sites. It was hypothesised that insertion of Glycines either side of the tag would facilitate proper tag and protein folding, and better antibody recognition.

To control expression of our tagged BACs a stop cassette was inserted between the *wg* promoter and translational start site. This stop cassette consisted of a *cherry* cDNA (with a PolyA) flanked by Flp Recombinase Target (FRT) sites (Figure 3.1). When intact this cassette expresses Cherry under the control of the *wg* promoter and Wg-HA is not expressed. However, upon Flp expression from a different transgene, FRT recombination occurs, excising the stop cassette and initiating Wg-HA expression under its endogenous promoter.

Flies carrying the BACs were crossed to flies expressing a source of Flp in either the germline (Figure 3.1 F) or the P compartment (Figure 3.1 G-I). Discs from the offspring of those crosses were analysed and production of Wg-

HA was observed (Figure 3.1 F-I). Insertion of the HA tag in Exon 2 gives poor production of Wg-HA. Upon Flp expression in the P compartment of discs using En-Gal4 UAS-Flp, the Cherry stop cassette was excised from both BACs in the P compartment of the disc. However, the Wg-Ex2-2HA BAC produced no detectable Wg-HA and the Wg-Ex2-glyHA BAC produces very low levels of Wg-HA (Figure 3.1 H, I). Insertion of the HA tag into Exon 4 gives better expression of Wg-HA compared to Exon 2. Expression of the Wg-Ex4-glyHA BAC has aberrant Wg-HA stabilisation in the pouch region suggesting some problem with the stop cassette insertion (Figure 3.1 G). Despite this stabilisation, expression levels of the Wg-Ex4-glyHA BAC were comparable to the wild type (Figure 3.1 G). However, expression of the Wg-Ex4-2HA BAC reproduces the distribution of wild type Wg (Figure 3.1 E, F). Therefore, Exon 4 was determined as the best region to tag the Wg BAC.

Figure 3.1: Insertion of a HA tag in Exon 4 of a *wg*-containing BAC reproduces wild type expression.

(A-D) Different BAC constructs were made to express a tagged version of Wg. Two copies of a HA tag were inserted into the non-conserved region of Exon 4 with (B) or without (A) Glycines, or into a previously utilized site in Exon 2 (Hays et al., 1997), with (D) or without (C) flanking Glycines. An FRT flanked Cherry-PolyA stop cassette was inserted upstream of exon 1. When intact, Cherry is expressed under control of the Wg promoter. However, upon expression of a source of Flp, FRT recombination occurs removing Cherry and replacing expression with that of tagged Wg. (E) Wild type disc stained with the Wg antibody to show normal expression. (F-I) Expression of tagged Wg was induced using either germline Flp (F) or En-Gal4 UAS-Flp in the P compartment of discs (G-I). The remaining Cherry expression in the A compartment is shown in red using an anti-RFP antibody. (F) Wg-Ex4-2HA BAC expression is almost identical to the wild type. (G) Addition of Glycines flanking the HA tag in exon 4 causes lower levels of production, and stabilisation in the wing pouch. (H) The Wg-Ex2-gly2HA BAC expresses low levels of Wg-HA. (I) Wg-Ex2-2HA gives no detectable expression. Scale bars are shown on relevant panels.

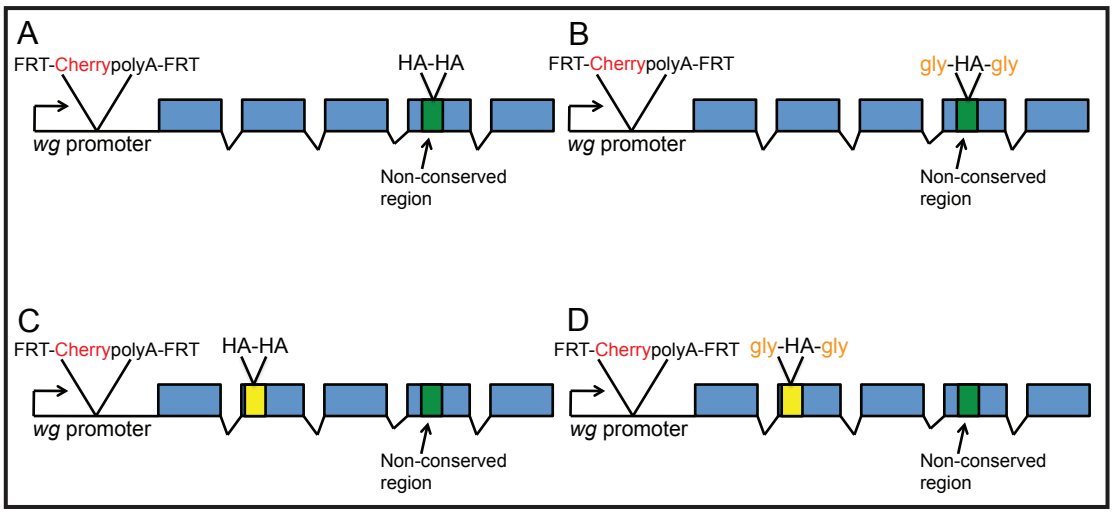
A
FRT-CherrypolyA-FRT
HA-HA
wg promoter
Non-conserved region
B
FRT-CherrypolyA-FRT
gly-HA-gly
wg promoter
Non-conserved region
C
FRT-CherrypolyA-FRT
HA-HA
wg promoter
Non-conserved region
D
FRT-CherrypolyA-FRT
gly-HA-gly
wg promoter
Non-conserved region

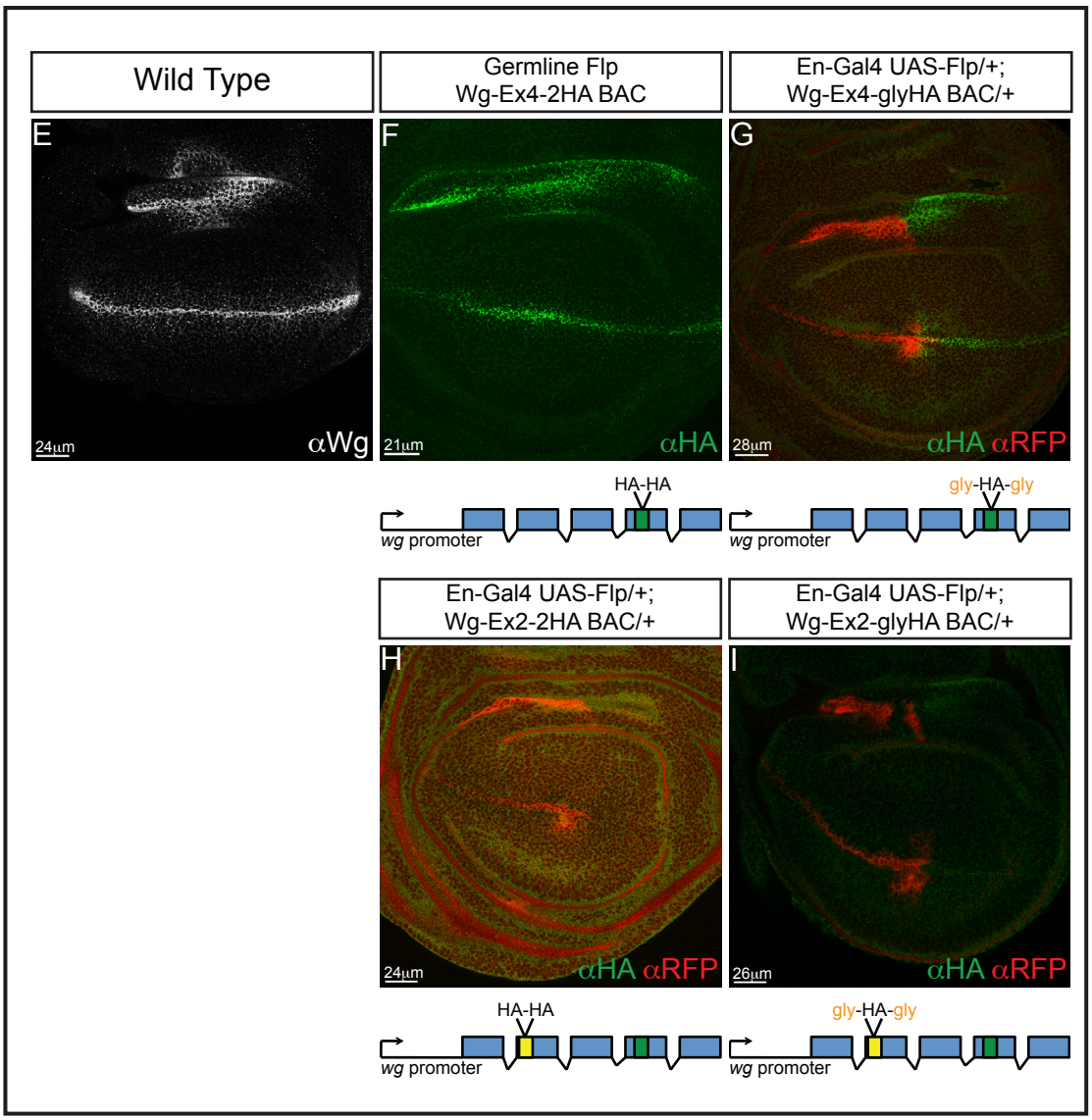
Wild Type
Germline Flp
Wg-Ex4-2HA BAC
En-Gal4 UAS-Flp/+;
Wg-Ex4-glyHA BAC/+
E
24µm
αWg
F
21µm
αHA
G
28µm
αHA αRFP
HA-HA
wg promoter
gly-HA-gly
wg promoter
En-Gal4 UAS-Flp/+;
Wg-Ex2-2HA BAC/+
En-Gal4 UAS-Flp/+;
Wg-Ex2-glyHA BAC/+
H
24µm
αHA αRFP
I
26µm
αHA αRFP
HA-HA
wg promoter
gly-HA-gly
wg promoter

3.2.2 Characterisation of the Wg-Ex4-2HA BAC.

I wanted to ensure that the Wg-Ex4-2HA BAC reproduces wild type Wg expression and signalling, and that the position of the tag does not affect the expression of Wg-HA compared to endogenous Wg. A fly was created where larvae expressed two copies of the Wg-Ex4-2HA BAC, where the stop cassette had been flipped out in the germline (Figure 3.2 A). These larvae therefore constitutively express Wg-HA. As already discussed, Wg-HA formed a gradient similar to that of wild type Wg (Figure 3.2 B-E). In addition, Wg-HA forms a basolateral extracellular gradient comparable to the wild type (Figure 3.2 F, G), and colocalises with Evi (Figure 3.2 H, I). Finally, expression of the Wg-Ex4-2HA BAC rescues a *wg* null mutant (wg^{CX4}) to viability. The only phenotype observed was loss of some bristles at the wing margin (Figure 3.2 J). Since bristle formation requires very high levels of Wg signalling it appears that Wg-HA produced by this BAC has only a small reduction in signalling activity. This could be due to tag positioning, or the 67kb *wg* BAC may not contain all the elements required to completely replicate endogenous levels of Wg signalling. However, the ability of Wg-HA to form a gradient and rescue mutant animals to adulthood suggests that Wg-HA has near wild type activity, and undergoes trafficking and secretion in the same fashion as wild type Wg.

Figure 3.2: The Wg-Ex4-2HA BAC acts like wild type Wg and almost fully rescues a *wg* null mutant.

A fly was made where larvae encoded two copies of the Wg-Ex4-2HA BAC (A) where the stop cassette had been flipped out in the germline of both copies. (C, E, G, I) In these larvae a Wg-HA gradient that is comparable to that of wild type Wg is formed (B, D, F, H) where discs expressing the BAC and wild type discs are stained with anti-HA and anti-Wg respectively. The extracellular concentration gradient is also comparable between expression of the Wg-Ex4-2HA BAC (G) and wild type Wg expression (F). Wg-HA also colocalises with Evi (I) in the same fashion as wild type Wg (H). The Wg-Ex4-2HA BAC construct was able to almost completely rescue a wg^{CX4} mutant (K). Slight loss of bristles at the wing margin in (K) was observed compared to the wild type (J). All scale bars for the Wg-Ex4-2HA BAC represent 21um and for the wild type represent 24um.

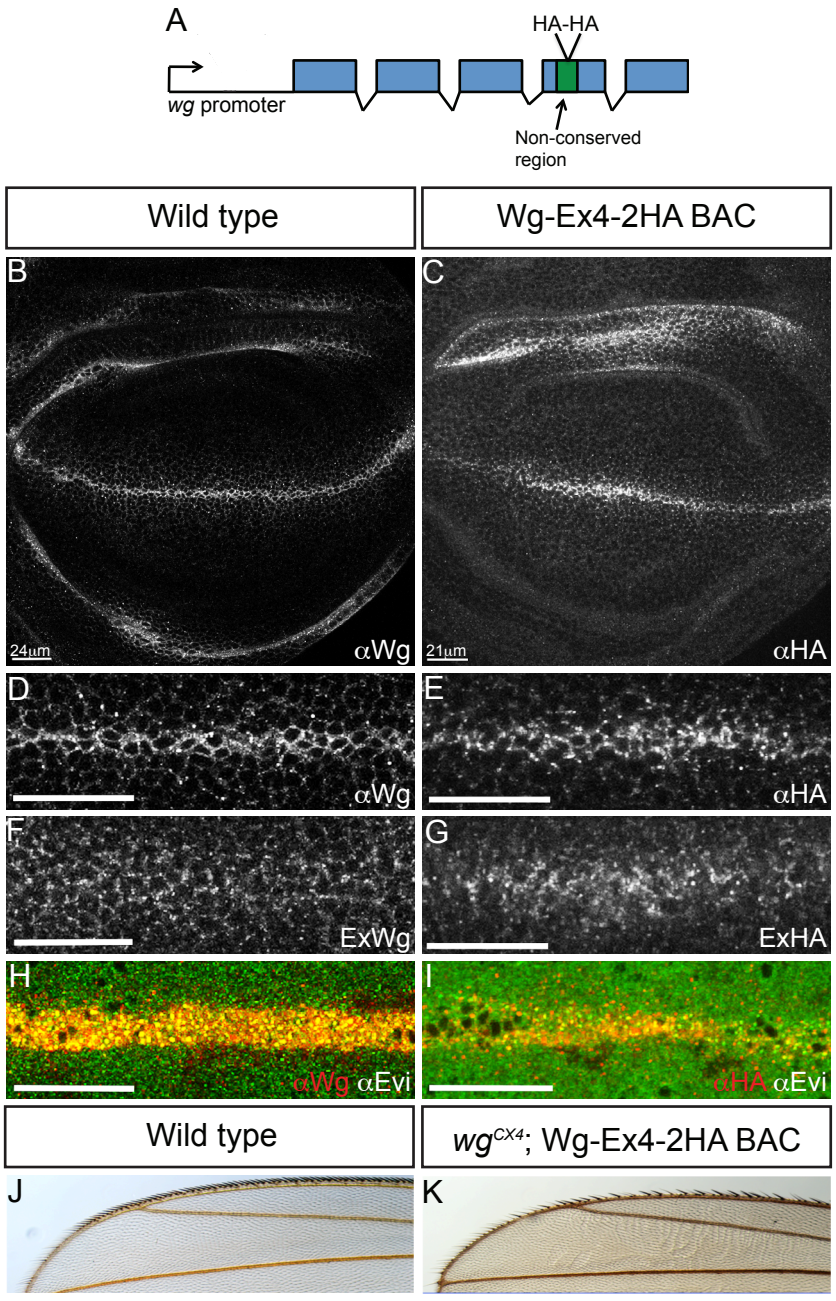
A
HA-HA
wg promoter
Non-conserved region
Wild type
Wg-Ex4-2HA BAC
B
24µm
αWg
C
21µm
αHA
D
αWg
E
αHA
F
ExWg
G
ExHA
H
αWg αEvi
I
αHA αEvi
Wild type
wgCX4; Wg-Ex4-2HA BAC
J
K

3.2.3 Optimisation of the heat shock induced expression of the Wg-Ex4-2HA BAC.

I next wanted to ensure that I could get expression of Wg-HA from the Wg-Ex4-2HA BAC in a controlled manner. To do this, I decided to use a heat shock inducible Flp to cause excision of the Cherry stop cassette from the BAC. Following a 20min heat shock at 37^{o}C and fixation 48hr later I was able to see effective excision of the stop cassette and production of Wg-HA (Figure 3.3). Wg-HA replaces Cherry in areas of the Wg stripe where excision has occurred (Figure 3.3 C-E), and the HA signal appears in a gradient with clear puncta in receiving cells (Figure 3.3 D', E'). From this I concluded that control of Wg-HA production via heat shock works effectively.

I then set out to optimise the heat shock conditions to achieve tight control of the Wg-HA step for further trafficking studies. First, I found that the presence of two copies of the Wg-Ex4-2HA BAC greatly increased detectable HA signal compared to one copy, especially at the basolateral surface of expressing cells (Figure 3.4 Box 1). This is unsurprising, since this boosts the number of HA copies in the system allowing better antibody recognition. However, it is important to recognise that the two copies of the BAC can excise the stop cassette independently and focus needs to be on the cells where both BACs undergo cassette excision (Figure 3.4 D-F). Cells where both copies of the BAC have excised their stop cassette can be identified by the absence of Cherry (Figure 3.4 D-F).

I also wanted to investigate how the timing of heat shock and fixation affected the HA signal. As seen previously in Figure 3.3, with a 20min heat shock and fixation 48hrs later, large regions of the Wg stripe are flipped out and produce Wg-HA. Signal is also detected along the apical-basolateral axis of the expressing cells and in the receiving cells (Figure 3.3 D', E'). With a 20min heat shock at 3rd instar and fixation after either 3 or 6hrs, the regions expressing Wg-HA are much smaller (Figure 3.4 Box 2). Under these conditions Cherry can still be detected in Wg-HA producing cells indicating there is not enough time

for the Cherry protein to degrade with such a late heat shock. Although Cherry is present throughout the Wg expressing cells, regions where the stop cassette has excised are marked by Wg-HA production (Figure 3.4 G', J'). Fixation 3hr after heat shock gives only very faint Wg-HA expression at the apical surface of the expressing cells where wild type Wg is normally strongest (Figure 3.4 G'). Fixation 6hr after heat shock gives increased Wg-HA expression at the apical surface compared to after 3hr (Figure 3.4 G', J'). Faint Wg-HA expression is also observed in the lateral region of the expressing cells (Figure 3.4 K'). This suggests that Wg-HA is progressing through the secretory pathway from the apical surface to a more basolateral region.

As described above, levels of Wg-HA detected using this BAC system are very low and hard to image. There was also variability in the number of cells in which heat shock mediated excision was observed. With heat shocks at 3rd instar (e.g. 3hr or 6hr), regions of Wg-HA expression are very small which makes them hard to visualise. The heat shock Flp used sometimes expressed Flp without heat shock causing complete excision of the stop cassette leading it to be considered "leaky". In some flies the cassette was excised in all cells presumably due to excision in the parental germline (data not shown). This is a problem for my experiments as it is important that I have tight control over the production of Wg-HA. Overall, these results were encouraging as they suggested that we had made a controllable source of Wg-HA which appeared to progress from the apical surface over time.

Figure 3.3: Expression of the Wg-Ex4-2HA BAC can be controlled using heatshock induced Flp.

Hsflp;;Wg-Ex4-2HA BAC 2nd instar larvae were heatshocked for 20min at 37^{o}C, and fixed 48hrs later. Production of tagged Wg was detected using an anti-HA antibody and found in regions where Cherry was absent due to excision of the stop cassette (B). Cherry was detected using an anti-RFP antibody (A, C, D, E). Panels C-E are close up views of the disc shown in panel A showing different planes within the disc, from apical, lateral and basolateral regions. The HA signal is higher in the apical and lateral sections (C', D') as is seen with wild type Wg. In the lateral and basolateral sections (D', E') puncta of Wg-HA can be seen forming the Wg concentration gradient. All scale bars represent 24um.

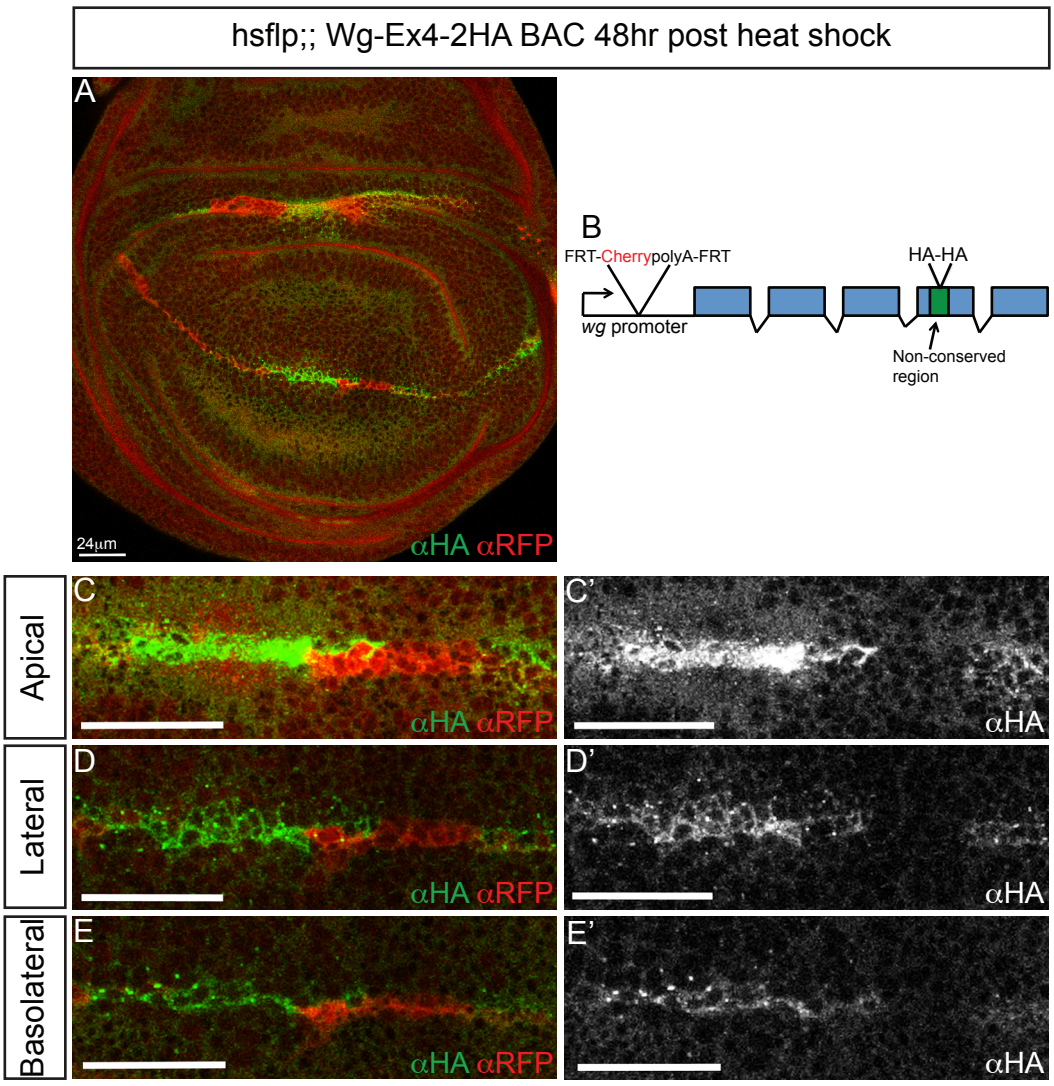
hsflp;; Wg-Ex4-2HA BAC 48hr post heat shock
A
24µm
αHA αRFP
B
FRT-CherrypolyA-FRT
HA-HA
wg promoter
Non-conserved region
Apical
C
αHA αRFP
C'
αHA
Lateral
D
αHA αRFP
D'
αHA
Basolateral
E
αHA αRFP
E'
αHA

Figure 3.4: Optimisation of heat shock conditions and Wg-HA signal detection.

All images are single confocal sections taken from the same region of the same disc at different planes along the apical-basolateral axis. Production of tagged Wg was detected using an anti-HA antibody and loss of anti-RFP staining indicates stop cassette excision. Box 1 – Wg-Ex4-2HA BAC heterozygous or homozygous 2nd instar larvae were heatshocked for 20min at 37^{o}C, and fixed 48hr later. (A-C) In Wg-Ex4-2HA BAC heterozygotes, HA signal can be detected at the very apical surface (A') where Wg levels are normally highest but less signal is seen at the lateral surface (B') and no signal can be detected at the basolateral surface (C'). (D-F) However, in homozygous Wg-Ex4-2HA discs, HA signal can be detected throughout. HA is detected at highest levels at the apical surface (D'), but gradient formation can also be seen at the basolateral surface (F'). Box 2 –Wg-Ex4-2HA BAC homozygous 3rd instar larvae were heatshocked for 20min at 37^{o}C and fixed either 3hr or 6hr later as indicated. (G-I) After 3hrs Wg-HA was produced but only at very low levels in small regions at the very apical surface (G'). No signal can be seen at either the lateral (H') or basolateral (I') surfaces. (J-L) But with fixation after 6hr production at the very apical surface is brighter and visible in more regions (J'). Some signal can also be detected at the lateral surface (K'). Scale bars are shown on relevant panels.

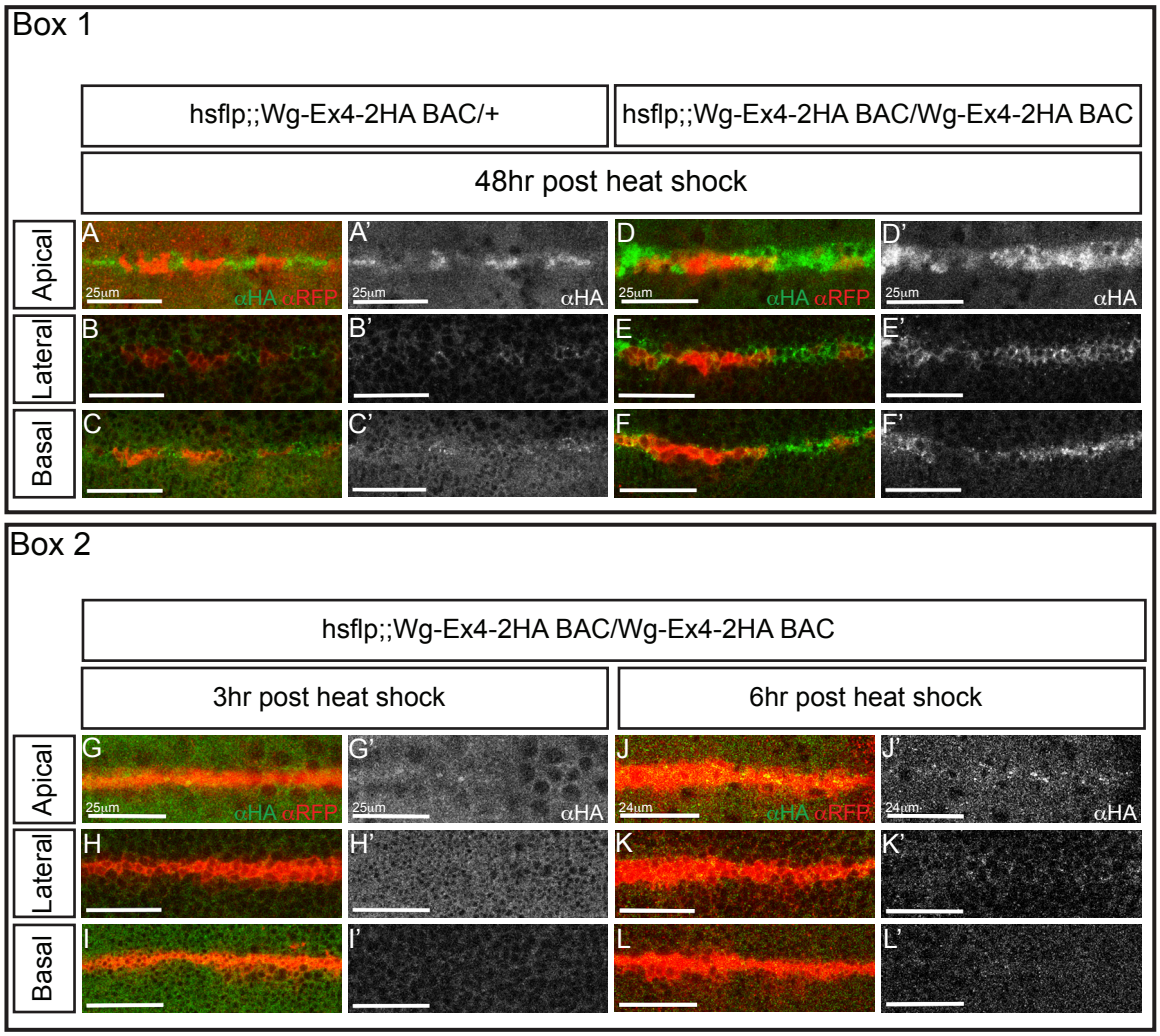
Box 1
hsflp;;Wg-Ex4-2HA BAC/+
hsflp;;Wg-Ex4-2HA BAC/Wg-Ex4-2HA BAC
48hr post heat shock
Apical
Lateral
Basal
A
A'
D
D'
B
B'
E
E'
C
C'
F
F'
25µm
αHA αRFP
αHA
Box 2
hsflp;;Wg-Ex4-2HA BAC/Wg-Ex4-2HA BAC
3hr post heat shock
6hr post heat shock
G
G'
J
J'
H
H'
K
K'
I
I'
L
L'
24µm

3.2.4 Production and characterisation of the *wg{KO; Wg-Ex4-2HA}*.

In the lab, Cyrille Alexandre and Alberto Baena-Lopez were developing an improved system to create gene knockouts, by removing the translational start sequence of a gene and replacing it with an attP site allowing subsequent cDNA insertion using the attP/attB recombination system (Figure 3.5) (Baena-Lopez et al., 2013). A knock out was generated using this technique in the *wg* locus, and we inserted a Wg-Ex4-2HA cDNA (with the tag in the same position as in the Wg-Ex4-2HA BAC) into the wg^{KO} to determine whether we would get better rescue compared to the BAC (Figure 3.5, C. Alexandre).

The Wg-Ex4-2HA cDNA was inserted into the attP site in the *wg* locus to make *wg{KO; Wg-Ex4-2HA}* flies (Figure 3.6 A). Expression of *wg{KO; Wg-Ex4-2HA}* provides a single copy of Wg to rescue over a *wg* null mutant chromosome (wg^{CX4}) to viability. These flies have normal wing bristles compared to the wild type (Figure 3.6 B, C) indicating that even the highest levels of Wg signalling are present. Wg-HA forms a gradient comparable to that of wild type Wg as detected using both the anti-HA and anti-Wg antibodies (Figure 3.6 D-G), and it also replicates expression of wild type extracellular Wg (Figure 3.6 H, I). These data suggested that for future experiments the *wg{KO; Wg-Ex4-2HA}* flies would be more suitable than the Wg-Ex4-2HA BAC flies. For both these constructs the HA tag is in the same position, so this led me to consider the reason for the difference in ability of these constructs to rescue. In selecting the 67kb BAC around the *wg* locus, we may have missed some of the regulatory elements that control the high levels of Wg signalling specifying wing margin bristles. Using the wg^{KO}, the Wg-Ex4-2HA cDNA is reinserted into the endogenous locus, therefore all regulatory elements are present and the highest levels of signalling can occur.

Figure 3.5: Generation of a *wg* knockout via homologous recombination.
(A) Schematic representation of the *wg* locus, not to scale. (B) To insert an attP site into the *wg* locus with the subsequent loss of the translation start site in Exon 1, arms homologous to the sequence either side of the region for deletion were designed (pink shaded boxes). This site entered the genome via homologous recombination deleting the translational start site and replacing it with an attP recombination site. (C) Once the attP site was inserted in the genome; a *wg* null mutant (wg^{KO}) was generated. Using the attP/attB recombination system we reinserted cDNAs back into the attP site to modify the locus and rescue the mutant phenotype. Selection for reinsertion of the cDNA was conducted using a selection marker incorporated into the reinsertion vector. (D) Once inserted, the cDNA of choice will be expressed under the control of the endogenous *wg* promoter. Tagged versions of Wg can be reinserted to rescue the wg^{KO} background. Modified from (Baena-Lopez et al., 2013).

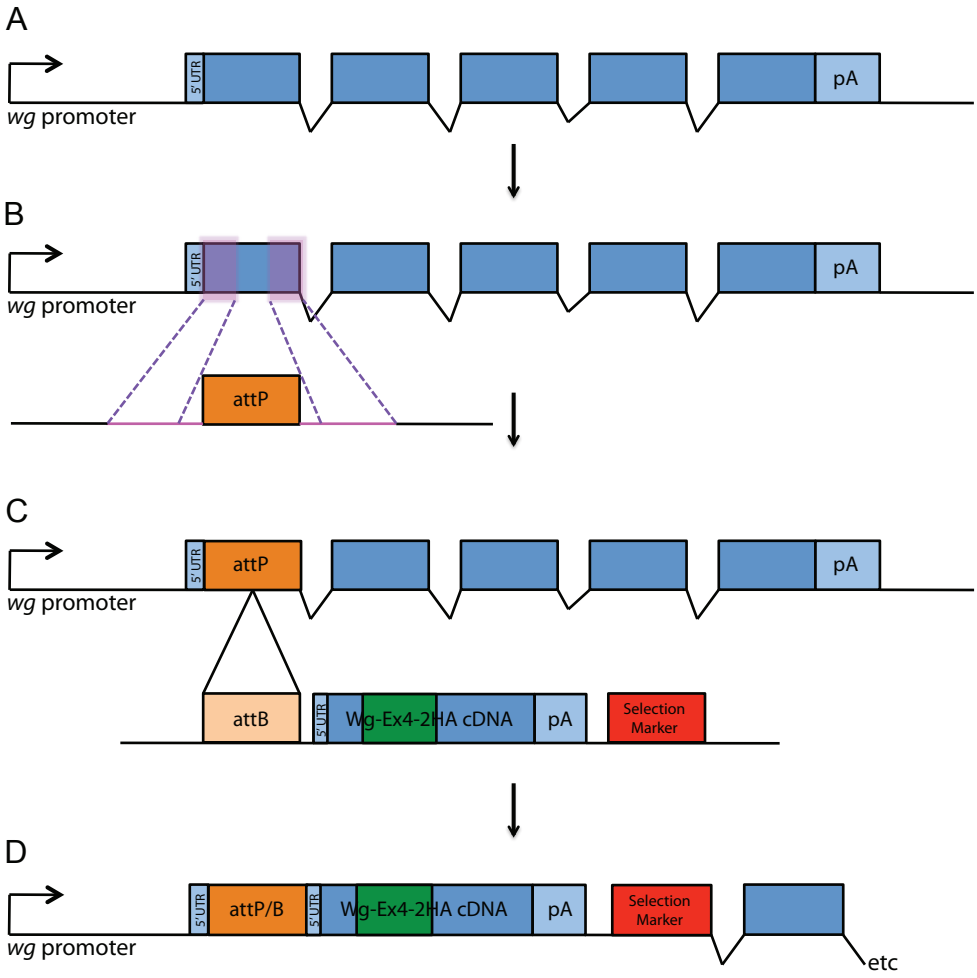
A
5' UTR
pA
wg promoter
B
5' UTR
pA
wg promoter
attP
C
5' UTR
attP
pA
wg promoter
attB
5' UTR
Wg-Ex4-2HA cDNA
pA
Selection Marker
D
5' UTR
attP/B
5' UTR
Wg-Ex4-2HA cDNA
pA
Selection Marker
wg promoter
etc

Figure 3.6: *wg{KO; Wg-Ex4-2HA}* acts like wild type Wg and fully rescues a *wg* null mutant.

(A) A *wg* cDNA with 2HA tags in exon 4 was then inserted into an attP site in the *wg* locus to make *wg{KO; Wg-Ex4-2HA}* flies. (B-C) Expression of this cDNA is able to completely rescue a *wg* null mutant and give a normal wing with all the bristles (C) compared to wild type (B). (D-E) Larvae homozygous for *wg{KO; Wg-Ex4-2HA}* stained with an antibody against HA (E) form a comparable Wg gradient to wild type Wg (D). In these homozygous larvae the only source of Wg is Wg-HA, and total and extracellular stainings in this genotype using the anti-Wg antibody (G and I) are comparable to wild type Wg (F and H) indicating that *wg{KO; Wg-Ex4-2HA}* acts akin to wild type Wg. Scale bars for (F-I) represent 24um for the wild type and 26um for the *wg{KO; Wg-Ex4-2HA}*.

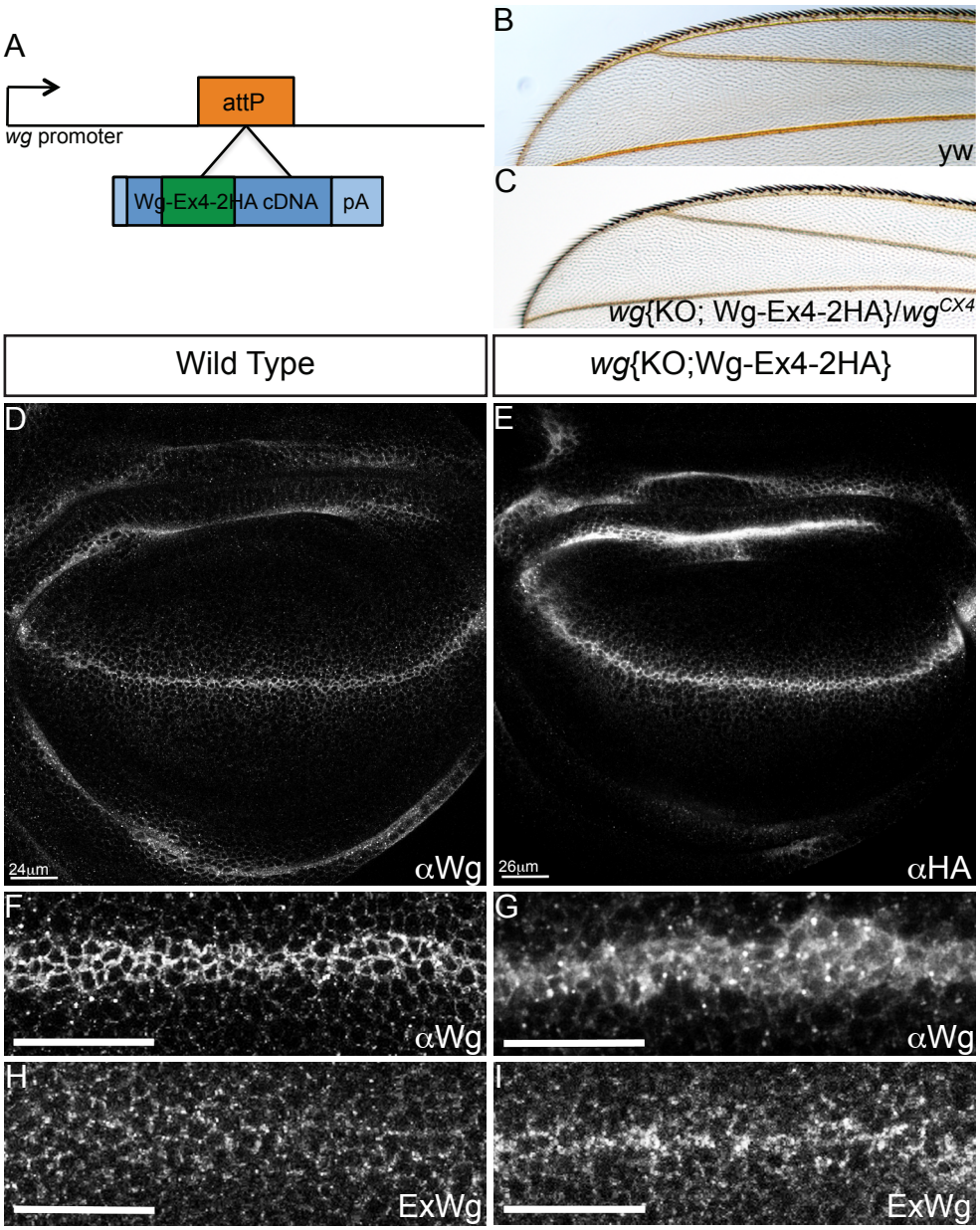
A
attP
wg promoter
Wg-Ex4-2HA cDNA
pA
B
yw
C
wg{KO; Wg-Ex4-2HA}/wg^CX4
Wild Type
wg{KO;Wg-Ex4-2HA}
D
24µm
αWg
E
26µm
αHA
F
αWg
G
αWg
H
ExWg
I
ExWg

3.2.5 Modification of *wg{KO; Wg-Ex4-2HA}* to allow controlled expression of Wg-HA.

To create a controlled step of Wg-HA expression in the Wg expressing cells as we had previously managed with the Wg-Ex4-2HA BAC (Figure 3.3), we needed to further modify the *wg{KO; Wg-Ex4-2HA}* construct. Unlike the Wg-Ex4-2HA BAC we were unable to insert a stop cassette before Wg-HA to control expression, since in the wg^{KO} background this would create a *wg* null allele. This would be a problem since *wg* null mutants die as embryos (van den Heuvel et al., 1993). Instead, I inserted a wild type version of Wg flanked by FRTs in front of tagged Wg-HA (Figure 3.7 A). In this way, wild type Wg is expressed throughout development, and it is also acting as a "stop cassette" which prevents Wg-HA expression. If Flp is expressed in the P compartment of discs containing the *wg{KO; FRT-Wg-FRT-Wg-Ex4-2HA}*, there is excision of the first wild type copy of Wg and replacement with Wg-HA (Figure 3.7 C). Anti-Wg can also recognise Wg-HA in this situation since the antibody is raised against a region of Wg present in Wg-HA (Figure 3.7 C'').

C. Alexandre created a further construct with the same premise as *wg{KO; FRT-Wg-FRT-Wg-Ex4-2HA}*, except in *wg{KO; FRT-Wg-Ex4-3OLLAS-FRT-Wg-Ex4-3HA}* flies both versions of Wg are tagged (Figure 3.7 D). By using two different tagged versions of Wg we hoped to create a cleaner way to visualise Wg movement by focusing on the movement of the boundary between anti-OLLAS and anti-HA immunoreactivity in the secretory pathway. If a source of Flp is expressed in the P compartment of discs expressing *wg{KO; FRT-Wg-Ex4-3OLLAS-FRT-Wg-Ex4-3HA}*, then excision of Wg-OLLAS is observed and it is replaced with Wg-HA expression (Figure 3.7 F). Importantly, both of these inducible, tagged Wg constructs (Figure 3.7 A, D) are able to rescue a *wg* null mutant to viability with no wing bristle phenotype (Figure 3.7 B, E). We have therefore managed to create an improved system, with better rescue and expression levels compared to the BAC, in which we will be able to conduct future experiments to follow the trafficking of a step of Wg in expressing cells.

Figure 3.7: Creating inducible, tagged forms of Wg-HA that rescue a *wg* null mutant.

(A, D) Two tagged cDNAs were inserted in the attP site in the *wg* locus to make either *wg{KO; FRT-Wg-FRT-Wg-Ex4-2HA}* (A) or *wg{KO; FRT-Wg-Ex4-3OLLAS-FRT-Wg-Ex4-3HA}* flies (D). (B, E) Expression of either of these forms of Wg rescues to viability and wing margin bristles in a *wg* null mutant background compared to wild type (as seen in (B) Figure 3.6). (C'', F'') In discs where a source of Flp is expressed in the P compartment using Hh-Gal4 UAS-Flp in the presence of either inducible Wg construct, FRT mediated excision of the first copy of Wg and replacement with a second tagged version of Wg occurs in the posterior compartment. (C) In the indicated genotype, Flp-mediated replacement of a wild type version of Wg with Wg-HA is detected using an anti-HA antibody (C'). (C'') The anti-Wg antibody also recognises Wg-HA expression in this situation since the epitope is present in the tagged protein. (F) In the indicated genotype, replacement of Wg-OLLAS (detected using anti-OLLAS antibody) (G) with that of Wg-HA (detected using anti-HA) (G') occurs upon expression of a source of Flp. Scale bars are shown on relevant panels.

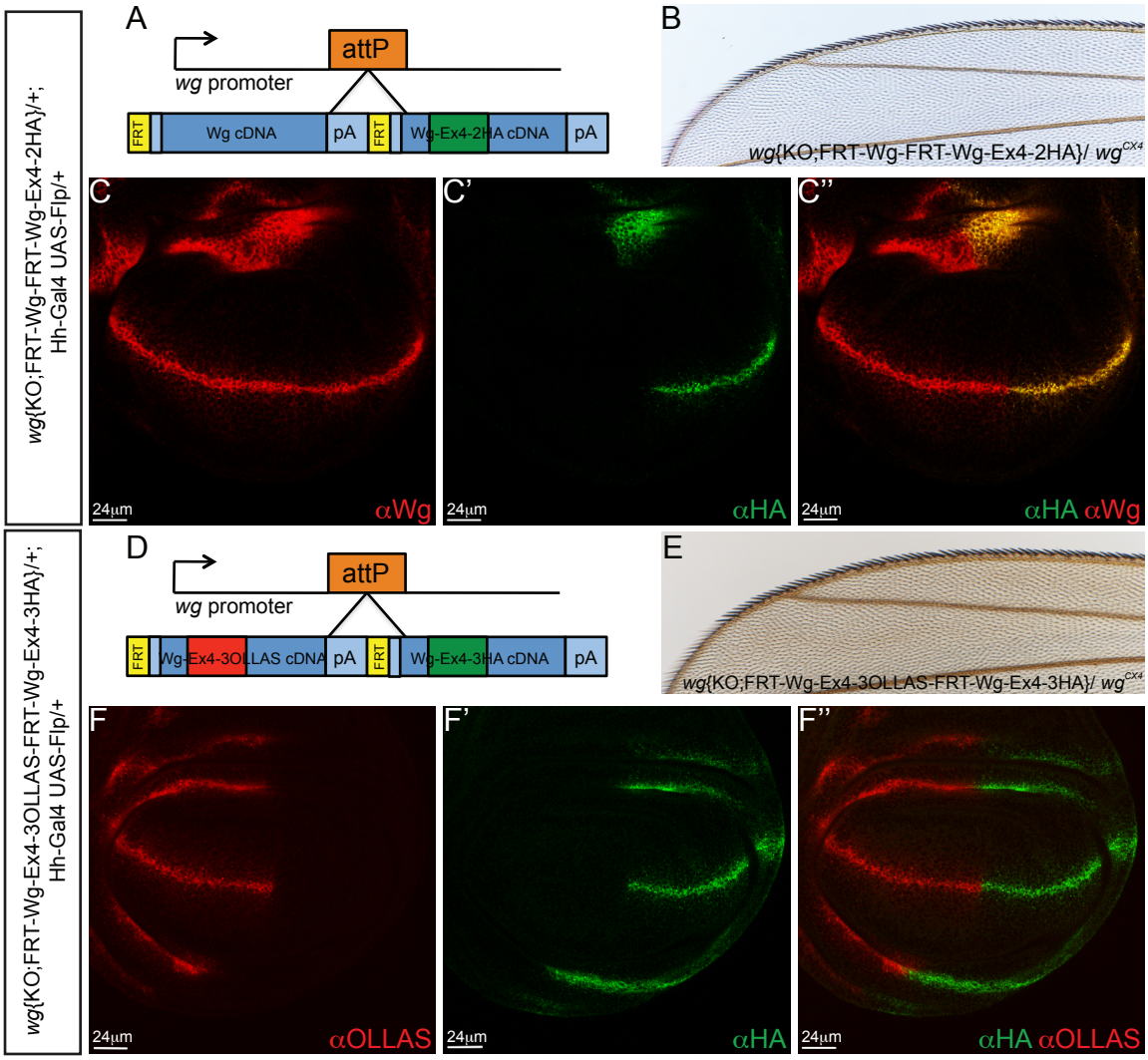
wg{KO;FRT-Wg-FRT-Wg-Ex4-2HA}/+;
Hh-Gal4 UAS-Flp/+
A
attP
wg promoter
FRT
Wg cDNA
pA
FRT
Wg-Ex4-2HA cDNA
pA
B
wg{KO;FRT-Wg-FRT-Wg-Ex4-2HA}/ wgCX4
C
24μm
αWg
C'
24μm
αHA
C''
24μm
αHA αWg
wg{KO;FRT-Wg-Ex4-3OLLAS-FRT-Wg-Ex4-3HA}/+;
Hh-Gal4 UAS-Flp/+
D
attP
wg promoter
FRT
Wg-Ex4-3OLLAS cDNA
pA
FRT
Wg-Ex4-3HA cDNA
pA
E
wg{KO;FRT-Wg-Ex4-3OLLAS-FRT-Wg-Ex4-3HA}/ wgCX4
F
24μm
αOLLAS
F'
24μm
αHA
F''
24μm
αHA αOLLAS

3.2.6 Production of a tagged Evi BAC.

In a similar fashion to the Wg-Ex4-2HA BAC, we wanted to produce a tagged version of the Wg chaperone protein Evi. An extracellularly tagged Evi BAC would be an important tool since the available antibody for Evi is raised against an intracellular region, and thus is not compatible with the extracellular labelling required for some trafficking studies. A very small amount of antibody raised against an extracellular region of Evi is available, but this is limited and is not viable for long-term experimental use. We have attempted to produce antibodies against the extracellular region of Evi but have been unsuccessful. We obtained an *evi* BAC containing 80kb around the *evi* locus that would hopefully contain most regulatory elements. Initially, a V5 tag was inserted at an N-terminal position between the predicted Wg binding domain (Coombs et al., 2010) and the second transmembrane (TM) region (Figure 3.8 B, C. Alexandre). When expressed in flies, this gave no Evi-V5 signal (Figure 3.8 B). In parallel, I created a UAS overexpression construct encoding the same Evi-Nterm-V5 (Figure 3.9). En-Gal4 was used to overexpress UAS-Evi-Nterm-V5 in the P compartment of discs, but Evi-V5 did not appear to traffic to the cell surface under these conditions (Figure 3.9 C). Levels of Evi-Nterm-V5 were also reduced on a Western blot in comparison to another form of overexpressed Evi indicating that it was not efficiently secreted (Figure 3.9 H). Through a process of elimination using intracellular markers for the Golgi, Lysosome and ER we determined that Evi-Nterm-V5 was accumulating in the ER (Figure 3.9 E-G). This affected the trafficking of both total and extracellular Wg (Figure 3.9 A-D).

Since the N terminal extracellular domain of Evi seemed unsuitable for tag insertion, a V5 tag was inserted in Extracellular Loop 3 (EC3) of Evi (Figure 3.8 C). EC3 is the least conserved domain of Evi (Banziger et al., 2006) and therefore the best candidate region for tag insertion. Expression of the Evi-EC3-V5 BAC gave uniform levels of Evi staining and had much high levels of signal in comparison to the Evi-Nterm-V5 BAC (Figure 3.8 B, C). However, Evi-V5 was not enriched in the Wg expressing cells like wild type Evi (Figure 3.8 A, C).

Further modification was required, so I created two new BAC constructs. Both had tags inserted in EC3, but one BAC contained a V5 tag flanked by Glycines (Figure 3.8 D) and the other an OLLAS tag (Park et al., 2008) flanked by Glycines (Figure 3.8 E). These BACs were initially tested in *Drosophila* S2 R+ cells and both were expressed (Figure 3.10 G, H), however the staining patterns showed differences. Evi-V5 mainly appeared in puncta within the cells (Figure 3.10 G'), whereas Evi-OLLAS was at very high levels at the cell membrane (Figure 3.10 H'). The latter was encouraging, since wild type Evi is present at the plasma membrane as would be expected with a transmembrane protein. The Evi-EC3-glyV5 BAC gave good uniform Evi-V5 expression, however enrichment of Evi-V5 in the Wg stripe was only observed at low levels in apical sections of the disc (Figure 3.10 B, C). In contrast, expression of the Evi-EC3-glyOLLAS BAC produces both uniform Evi-OLLAS staining and also enrichment of Evi-OLLAS in the Wg expressing cells (Figure 3.10 D, E) in a comparable fashion to wild type Evi (Figure 3.8 A). From these results I concluded that both the location and nature of the tag influence Evi expression. A comparison of all constructs indicated that the Evi-EC3-glyOLLAS BAC best recapitulates wild type Evi expression and localisation, including the enrichment of Evi in Wg producing cells. Therefore, I decided to continue using this BAC for future trafficking experiments.

Figure 3.8: Insertion of an OLLAS tag in EC Loop 3 of an Evi containing BAC reproduces wild type Evi expression.

(A) Wild type Evi expression was detected using an anti-Evi antibody raised against the cytoplasmic C-terminus of the protein. Uniform levels of Evi are observed across the wing disc, however additional Evi enrichment is observed in a stripe corresponding to the Wg expressing cells. (B-E) Discs expressing the BAC constructs listed were stained using antibodies against their corresponding epitope tags as indicated. (B) Insertion of the V5 tag into the extracellular N-terminal region of Evi produced a construct that gave no V5 expression. Insertion of the V5 tag into ECLoop3 with (D) or without Glycines (C) produced constructs able to reproduce the uniform Evi staining in a similar fashion to wild type (A), but without the enrichment in the Wg expressing cells. (E) Only the Evi-EC3-glyOLLAS BAC has both the uniform staining and Evi enrichment in Wg expressing cells directly comparable to wild type Evi (A). Scale bars are shown on relevant panels.

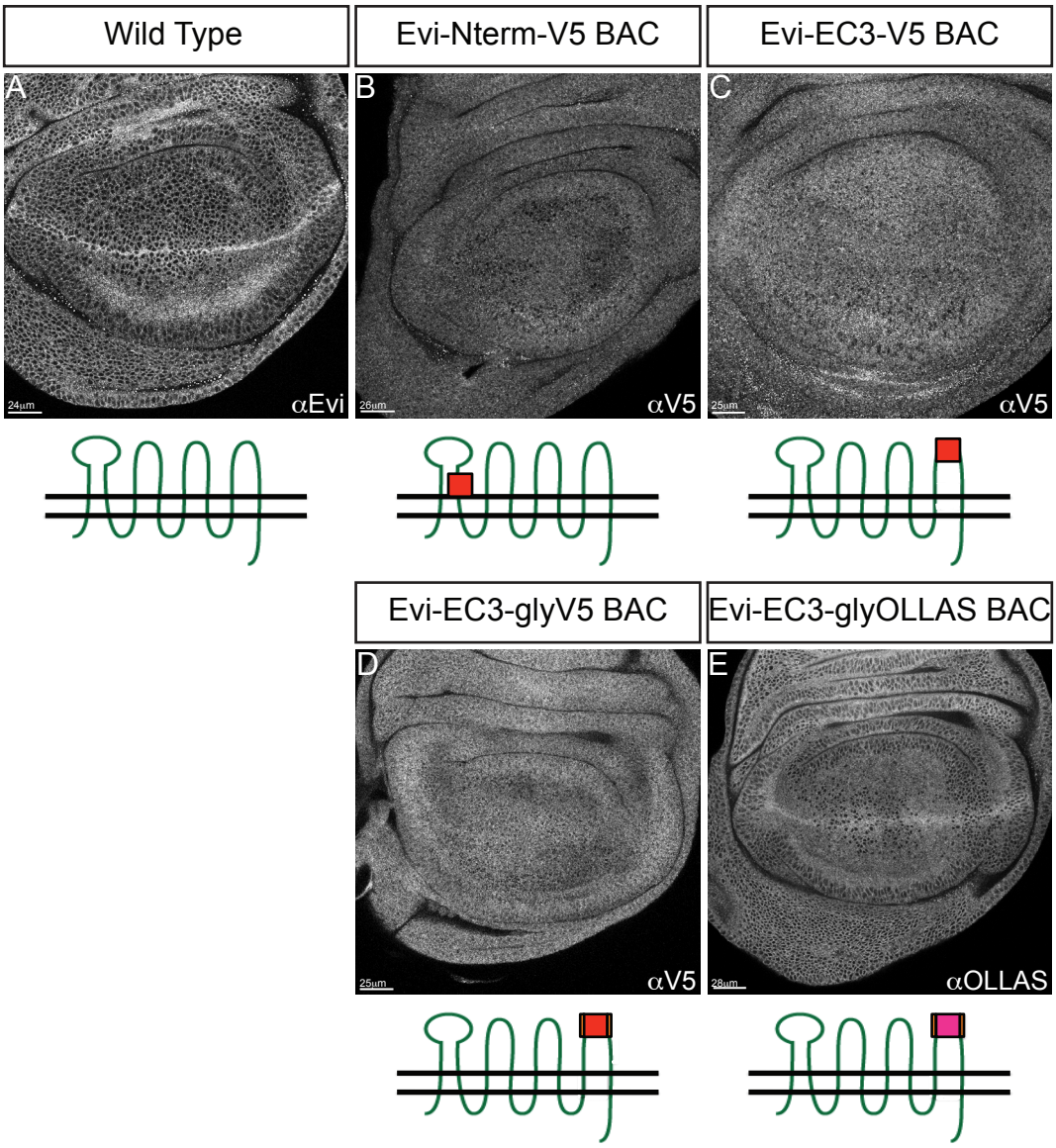
Wild Type
Evi-Nterm-V5 BAC
Evi-EC3-V5 BAC
A
B
C
24µm
αEvi
26µm
αV5
25µm
αV5
Evi-EC3-glyV5 BAC
Evi-EC3-glyOLLAS BAC
D
E
25µm
αV5
28µm
αOLLAS

Figure 3.9: Evi-Nterm-V5 is not secreted and interferes with Wg trafficking.

(A-G) En-Gal4/+; UAS-Evi-Nterm-V5/+ discs express the Evi-Nterm-V5 (with the V5 tag inserted in the same region as (B) Figure 3.8) in the P compartment of the disc as shown. Wg was detected using an anti-Wg antibody and Evi-V5 was detected using an anti-V5 antibody. (A-B) Overexpression of UAS-Evi-Nterm-V5 caused increased Wg retention and a reduction in gradient formation. (C-D) An extracellular Wg staining also showed a reduction in the basolateral extracellular Wg gradient (D'). Extracellular anti-V5 staining is not observed in these discs (C'). (E-G) Colocalisation with intracellular markers indicated that Evi-V5 was not detected in the Golgi (anti-GMAP, F) or lysosomes (anti-D-LAMP, G), but colocalised with the ER marker anti-BOCA (E) as indicated by arrows. (H) Western blot of cell lysates from *Drosophila* S2 cells transfected with a copper inducible Gal4 producing UAS-Evi-Nterm-V5 probed with anti-V5. Levels of UAS-Evi-Nterm-V5 production are greatly decreased compared to another full length Evi UAS construct tagged at the C-terminus (as used in Figure 5.3). All scale bars represent 24um.

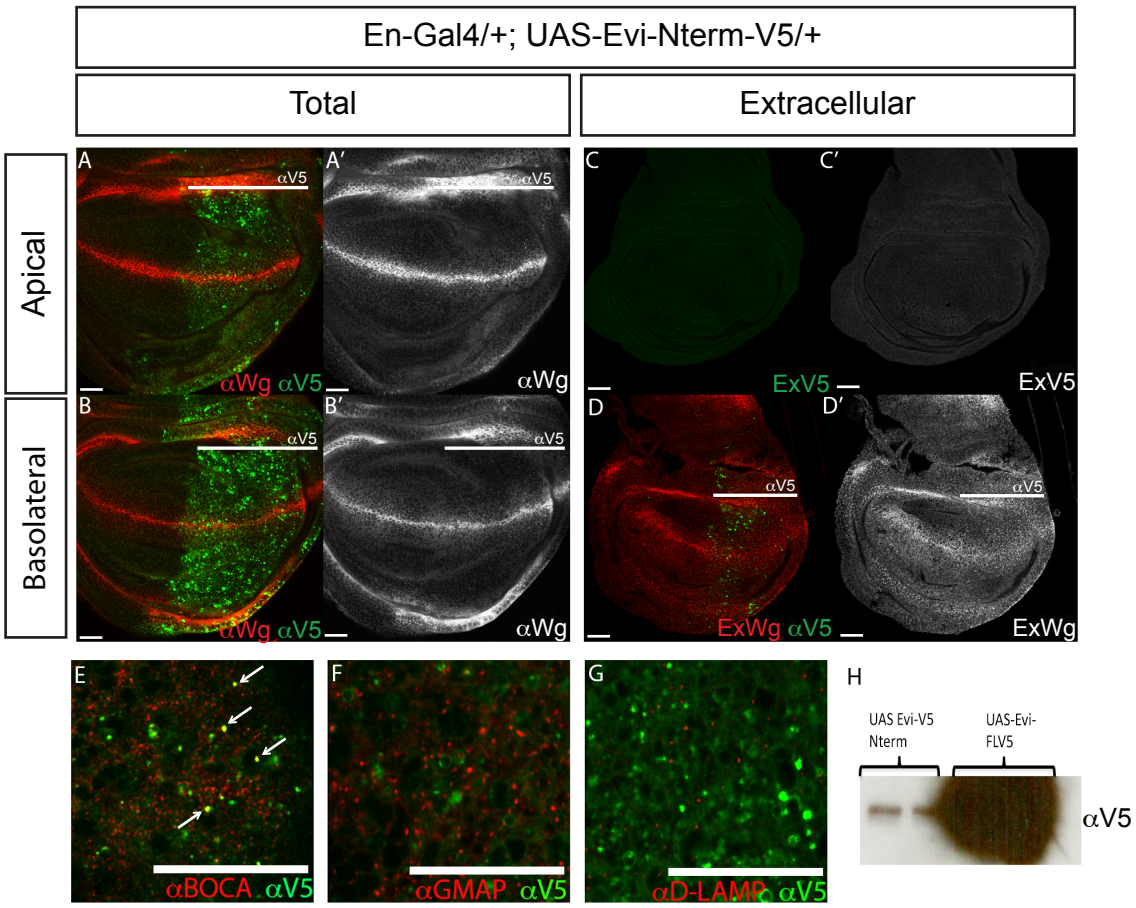
En-Gal4/+; UAS-Evi-Nterm-V5/+
Total
Extracellular
Apical
Basolateral
A
αV5
αWg αV5
A′
αV5
αWg
C
C′
ExV5
ExV5
B
αV5
αWg αV5
B′
αV5
αWg
D
αV5
ExWg αV5
D′
αV5
ExWg
E
αBOCA αV5
F
αGMAP αV5
G
αD-LAMP αV5
H
UAS Evi-V5 Nterm
UAS-Evi-FLV5
αV5

Figure 3.10: Tag composition as well as location is important for Evi expression levels from Evi BAC constructs.

Evi-V5 and Evi-OLLAS were detected using anti-V5 and anti-OLLAS antibodies respectively. (A, D) Schematic showing insertion of either gly-V5 or gly-OLLAS into Evi ECLoop3. (B-F) In discs expressing either BAC uniform Evi expression both apically and basally was observed. (E-F) Enrichment in the Wg stripe as seen with wild type Evi only occurred with the Evi-EC3-glyOLLAS BAC, see detail in next figure. (B-C) Weak Evi-V5 enrichment is observed at the very apical surface of the Wg expressing cells (B), but levels are dramatically reduced compared to those observed in the OLLAS tagged BAC (E). (G-H) Different localisation of Evi between the constructs was also seen in *Drosophila* S2R+ cells transfected with each BAC. The Evi-EC3-glyV5 BAC is predominantly seen in puncta inside the cells (G'), whereas the Evi-EC3-glyOLLAS BAC is seen mainly at the cell membrane (H'). Scale bars are shown on relevant panels.

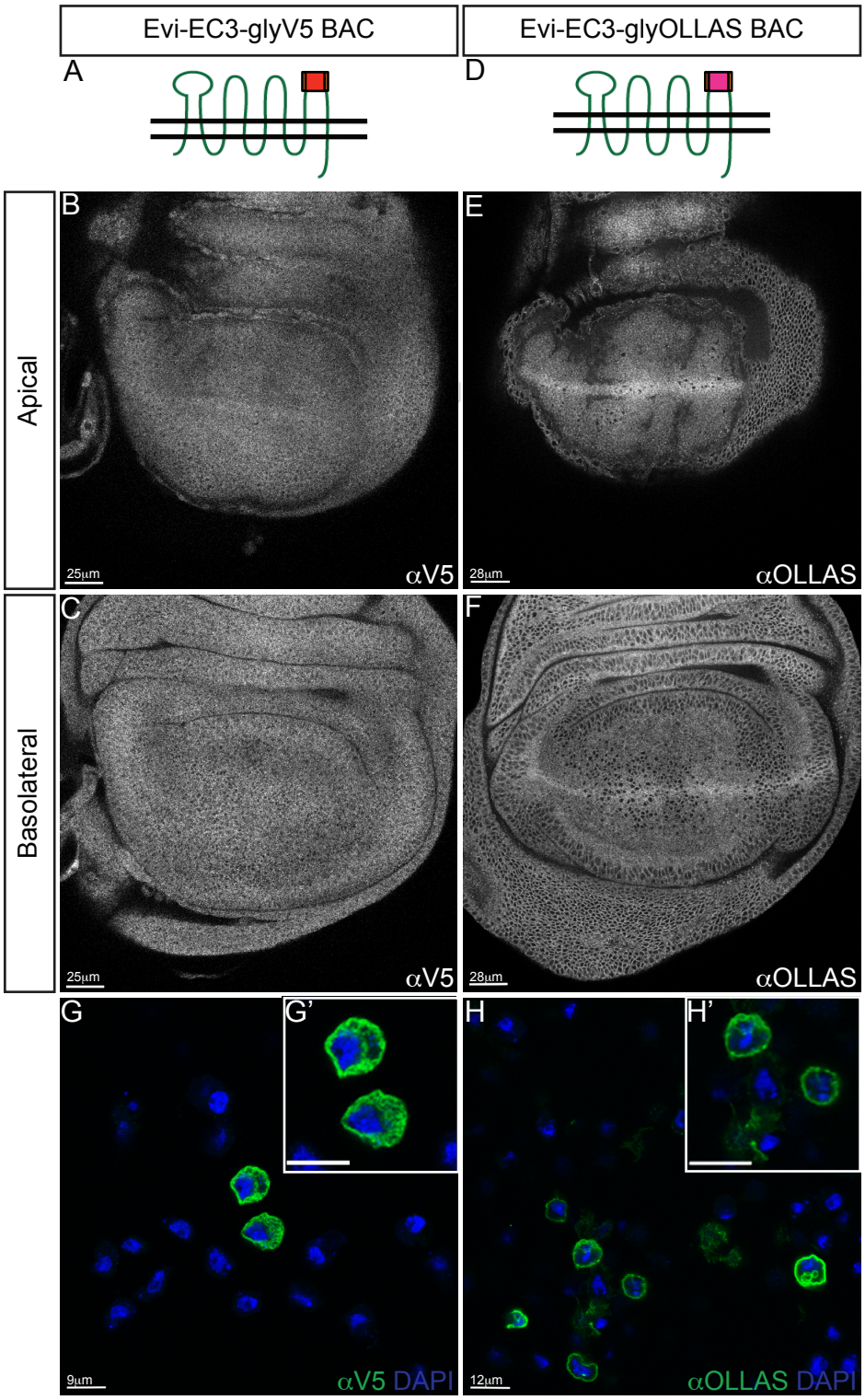
Evi-EC3-glyV5 BAC
Evi-EC3-glyOLLAS BAC
A
D
Apical
Basolateral
B
E
C
F
G
G'
H
H'
25µm
αV5
28µm
αOLLAS
25µm
αV5
28µm
αOLLAS
9µm
αV5 DAPI
12µm
αOLLAS DAPI

3.2.7 Characterisation of the Evi-EC3-glyOLLAS BAC.

I next wanted to ensure that the Evi-OLLAS protein was behaving like wild type Evi and therefore could be relied upon to follow the endogenous trafficking route in subsequent experiments. As already discussed, expression of Evi-OLLAS from the BAC gives a staining comparable to wild type Evi (Figure 3.11 D, E). To further confirm this, Evi-OLLAS was shown to colocalise with Wg across the dorsal-ventral boundary of the wing imaginal disc (Figure 3.11 F). Colocalisation of Evi- OLLAS and Wg is observed using both OLLAS and Evi antibodies (Figure 3.11 G-I). Finally, expression of the Evi-EC3-glyOLLAS BAC rescues an *evi* null mutant (evi^2) to viability. Importantly, these flies have no wing bristle phenotype indicating that the Evi-OLLAS protein produced by this BAC facilitates production of even the highest levels of Wg signalling (Figure 3.11 B, C). We have therefore managed to create an extracellularly tagged version of Evi that is produced at endogenous levels and fully rescues an *evi* mutant. Now, for the first time we will be able to detect extracellular Evi, and hopefully this will give us an insight into its trafficking route in tandem with Wg.

Figure 3.11: The Evi-EC3-glyOLLAS BAC is expressed like wild type Evi and fully rescues an *evi* null mutant.

Expression of the Evi-EC3-glyOLLAS BAC (A) rescues viability and the wing margin in an evi^{2} null mutant (C) compared to wild type (B). (D-E) Expression of the Evi-EC3-glyOLLAS BAC as detected using the anti-OLLAS antibody is comparable to wild type Evi detected using the anti-Evi antibody. (F-F'') Evi-EC3-glyOLLAS BAC expression colocalises with Wg across the D/V boundary of the wing disc, detected using the anti-Wg antibody. (G-I) The majority of Evi and Wg colocalisation occurs in the apical region of the Wg expressing cells. (G) In a wild type situation Evi and Wg colocalise in the apical region of Wg expressing cells, and this expression pattern is replicated using the same antibodies in a situation where the only source of Evi in the disc is that of the Evi-EC3-glyOLLAS BAC (H). (I) There is also colocalisation between expression of the Evi-EC3-glyOLLAS BAC and Wg as detected using the anti-OLLAS antibody. Scale bars are shown on relevant panels, for (G-I) scale bars represent 24um.

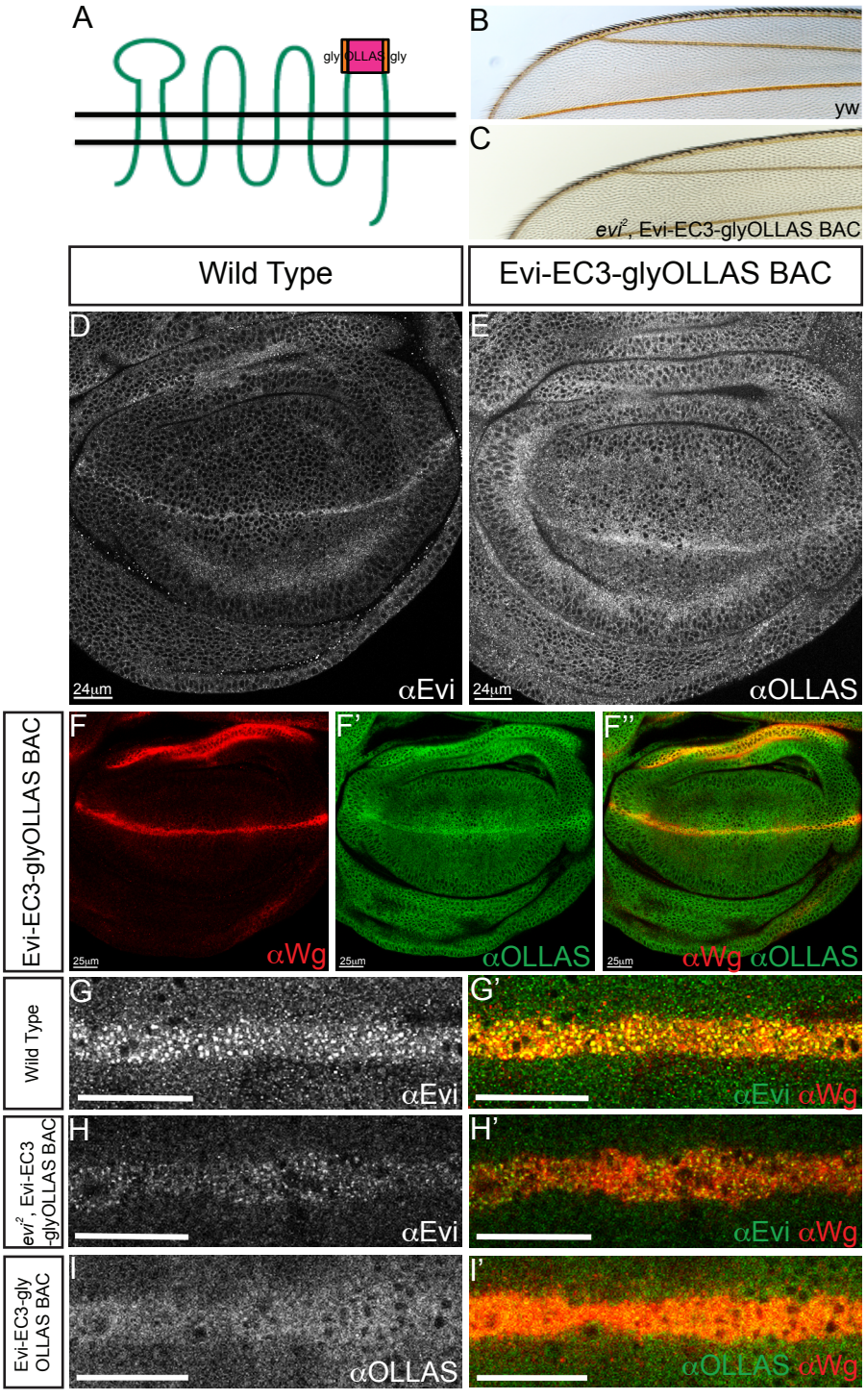
A
glyOLLASgly
B
yw
C
evi2, Evi-EC3-glyOLLAS BAC
Wild Type
Evi-EC3-glyOLLAS BAC
D
αEvi
E
αOLLAS
Evi-EC3-glyOLLAS BAC
F
αWg
F'
αOLLAS
F''
αWg αOLLAS
Wild Type
G
αEvi
G'
αEvi αWg
evi2, Evi-EC3 -glyOLLAS BAC
H
αEvi
H'
αEvi αWg
Evi-EC3-gly OLLAS BAC
I
αOLLAS
I'
αOLLAS αWg

3.3 Discussion

The results presented in this chapter highlight the large number of factors that need to be taken into account when designing a tagged construct expressed at endogenous levels. In this study I used two different techniques: BAC recombineering and cDNA re-insertion in a gene knockout. Both these techniques facilitate endogenous levels of protein production, however, as seen with the Wg-Ex4-2HA BAC this technique is perhaps not as effective as creating a knock out. When designing the Wg-Ex4-2HA BAC we isolated a 67kb region around the *wg* locus, but even this large BAC apparently did not contain all of the regulatory elements required for the highest levels of Wg signalling. This was manifested by an inability to fully rescue wing margin specification in a *wg* null mutant. When the same tag position was used in a cDNA reinserted into a wg^{KO} background (*wg{KO; Wg-Ex4-2HA}*), then there was full rescue in a *wg* mutant. This indicates within this construct it is not the tag insertion that affects the ability of Wg-HA protein to signal, but rather a problem with expression levels. The wg^{KO} contains all regulatory elements intact compared to the 67kb *wg* BAC. We were therefore fortunate in the case of the 80kb Evi-EC3-glyOLLAS BAC that this BAC contained all regulatory elements required for Evi-OLLAS to give full rescue in a *evi* null mutant.

With the accelerated homologous recombination technique developed in our lab (Baena-Lopez et al., 2013), it now takes roughly the same length of time to make a knockout in a gene of interest and reinsert a tagged cDNA compared to inserting a tag into a BAC using recombineering and making a transgenic fly. The added advantage with creating a knockout is that by inserting an attP site into the gene locus it is then easier to re-insert many different tagged cDNAs. Whereas, when modifying the Evi BAC a new recombineering protocol was undertaken for each tag, and a new transgenic was made. If required to create a new, tagged protein with endogenous expression levels in the future, I would

choose to follow the gene knockout method. However, for the purposes of this study the Evi-EC3-glyOLLAS BAC is a good tool for our approach.

Once a suitable BAC/knockout strategy is designed, both tag position and composition need to be considered in producing a fully functional protein. In this study we have shown that previous sites for tag insertion in overexpression constructs for both Wg and Evi, are not suitable sites for tag insertion at endogenous levels (Wg-Ex2-HA BAC Figure 3.1, (Hays et al., 1997)) (Evi-FLV5 BAC, unpublished data). C-terminally tagged Evi is published to rescue the Wg secretion defect in a *vps35*$^{\backslash -}$ mutant when overexpressed ((Franch-Marro et al., 2008b), see Figure 5.4), however when a tag is inserted into the C-terminal domain of an *evi* BAC it is unable to rescue in an *evi* null mutant background (data not shown). This highlights the limitations in using an overexpression approach, especially in trafficking studies that require such careful control over protein expression levels and function. In using tagged, overexpressed proteins not only is the secretory pathway artificially loaded with protein that would not usually exist at such high levels, but also often retention in intracellular compartments or incorrect protein folding occurs due to improper tag placement (Figure 3.9). This may lead to proteins following a trafficking pathway they would not follow under endogenous conditions. A certain amount of luck and perseverance is required to find suitable sites for tag insertion at endogenous levels within proteins (for this great thanks must go to my constant collaborator C. Alexandre). However, as we showed for both Wg and Evi, insertion into the least conserved domains of the protein is a good place to start. Once a good site for insertion is found, composition of the tag also needs to be considered. In the Evi BAC both gly-V5 and gly-OLLAS were inserted in the same site in EC3, but the Evi-EC3-glyOLLAS BAC gave better expression levels and recapitulated wild type Evi localisation, while the Evi-EC3-glyV5 BAC did not (Figure 3.10). The V5 tag contains more Proline residues than the OLLAS tag, so it may be that by incorporating more inflexible amino acid residues into EC3 improper folding of either the Evi protein or the tag itself

occurs. Specificity of recognition between the tag and its cognate antibody should also be taken into account. Endogenous proteins are expressed at much lower levels than traditional overexpression constructs, so tags that can be recognised in overexpressed proteins are often much harder to detect at endogenous levels. This can lead to a lower signal to noise ratio and high background therefore a good tag-antibody pairing is essential.

Ultimately, in this chapter I have shown that we have successfully tagged both Wg and Evi expressed at endogenous levels, and expression of both these constructs gives full rescue in their respective mutant backgrounds. We are now able to detect extracellular Evi with the insertion of an OLLAS tag in EC3, and we have developed a system in which we are able to produce a controlled step of tagged Wg. These tools can now be used to further explore the trafficking pathways that these proteins take in Wg expressing cells.

Chapter Four

Characterisation of the trafficking route taken by Wg in secreting cells.

4.1 Introduction

As shown in the previous chapter, I have developed several tools that can be used to further dissect the trafficking route taken by Wg in secreting cells. Observations in the lab and in previous studies (Strigini and Cohen, 2000) have described the polarised distribution of Wg within expressing cells, with the majority of total Wg protein seen in the apical region. However, extracellular Wg is predominantly observed on the basolateral surface ((Strigini and Cohen, 2000), unpublished observations). We were interested in finding out whether intracellular apical Wg gives rise to the extracellular basolateral Wg, and if so, what route does Wg take within the expressing cells to reach its destination. To explore these questions, I initially adopted a rudimentary approach of blocking global endocytosis and then looking at Wg localisation. This gave us some clues about where Wg transits. Then, to explore this movement in more detail, I used the inducible Wg production system I described in the previous chapter to follow a controlled step of tagged Wg through the secretory pathway of expressing cells.

4.2 Results

4.2.1 Inhibition of endocytosis using *shibire^{ts}* causes accumulation of Wg within expressing cells.

Shibire^{ts} is a temperature sensitive dynamin mutant that at the permissive temperature of 18^{o}C undergoes endocytosis. However, at the restrictive temperature of 34^{o}C dynamin is non-functional and all dynamin-dependent processes cease (Figure 4.1). Thus, endocytosis can be effectively and reversibly blocked in *shibire^{ts}* mutant discs and resultant changes in Wg localisation can be observed. Initially, I decided to optimise conditions for an endocytosis block in *shibire^{ts}* mutant discs, and to confirm that such a block would cause Wg accumulation within expressing cells. Dynamin has been reported to also function in the scission of vesicles within the Golgi (Jones et al., 1998). Therefore upon a *shibire^{ts}*-dependent endocytic block Wg may accumulate within the Golgi, as well as at the cell surface as predicted by our model (Figure 4.1).

In wild type Wg expressing cells, the majority of Wg colocalises with the Golgi in the apical region (Figure 4.2 B), whereas little colocalisation is observed in more basolateral regions (Figure 4.2 F). After 3hr at 34^{o}C in *shibire^{ts}* mutant discs there is a substantial Wg secretion block (Figure 4.2 C, D, G, H). Wg is observed in large puncta within expressing cells (Figure 4.2 D') and does not move across the tissue to form the basolateral gradient (Figure 4.2 H'). In the apical region of expressing cells especially, these large Wg puncta often colocalise with the Golgi (Figure 4.2 D). This suggests Wg is blocked in the Golgi due to a lack of dynamin-dependent vesicle scission. More Wg and Golgi colocalisation is present in basolateral regions of the disc compared to wild type (Figure 4.2 F, H).

These results firstly corroborate previously published results indicating that Wg undergoes dynamin-dependent endocytosis within expressing cells

(Strigini and Cohen, 2000). They also show that, in *shibire*^{ts} mutant discs, Wg secretion is blocked and basolateral spreading no longer occurs, suggesting that Wg is not released in these conditions. A large proportion of this accumulated Wg appears to colocalise with the Golgi indicating that a lack of functional dynamin within the Golgi is preventing Wg movement and subsequent secretion. This is in accordance with reports in the literature (Jones et al., 1998). These results were encouraging as they suggested that this endocytic block could be utilised to explore how Wg reached the basolateral surface.

Figure 4.1: Predictions from my model: at restrictive temperature a block in endocytosis causes Wg accumulation.

Shibire^{ts} encodes a temperature sensitive dynamin mutant protein that at the permissive temperature of 18^{o}C allows normal endocytosis. However, upon shifting to the restrictive temperature of 34^{o}C the dynamin becomes non-functional. Our model would predict that this would create a block of Wg on the apical surface of expressing cells, since endocytosis would be required for movement to the basolateral surface. This process would be reversible, as upon shifting from 34^{o}C back to the permissive temperature of 18^{o}C, dynamin becomes functional once again.

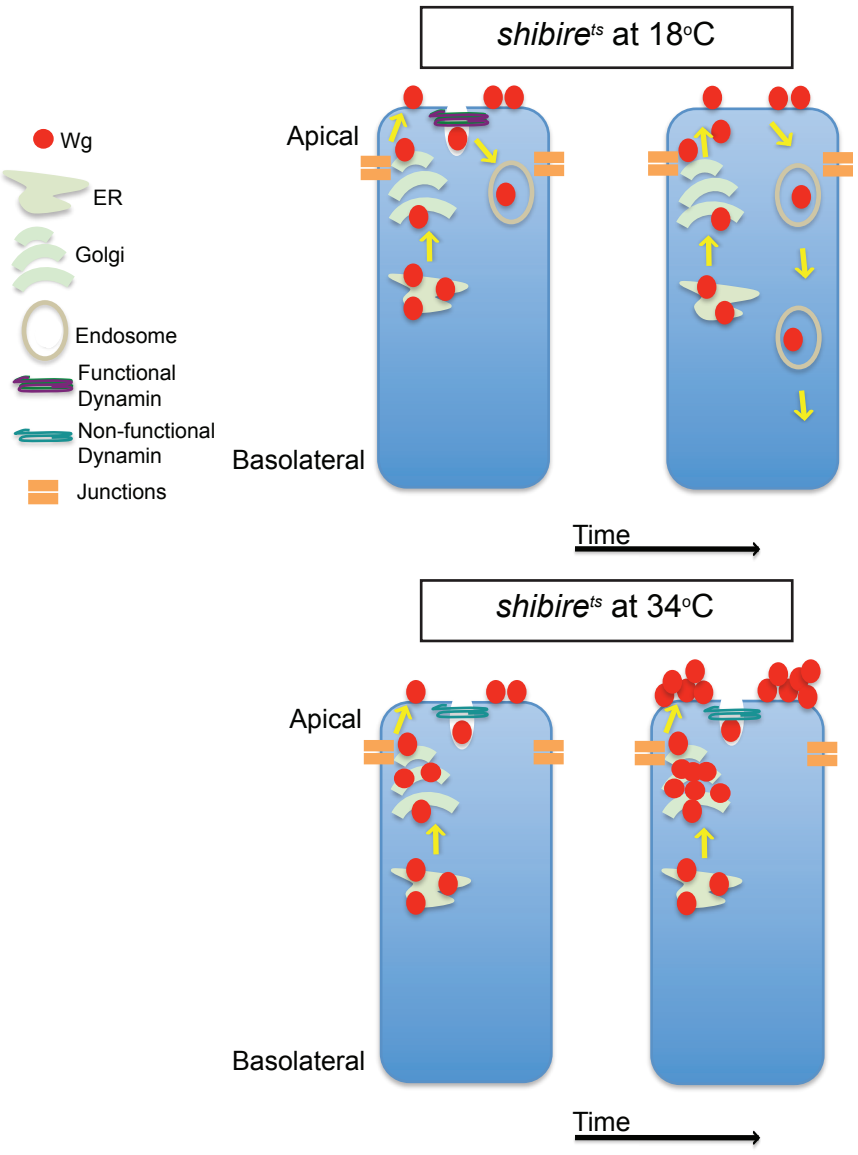
shibire^ts at 18°C
Apical
Basolateral
Time
shibire^ts at 34°C
Apical
Basolateral
Time
Wg
ER
Golgi
Endosome
Functional Dynamin
Non-functional Dynamin
Junctions

Figure 4.2: Endocytic block causes accumulation of total Wg in the Golgi of Wg expressing cells.

In all discs Wg protein was detected using anti-Wg, and Golgi were marked using anti-GMAP. Confocal settings are comparable. Apical (A-D) and basolateral (E-H) confocal sections are shown for each disc. Close ups of the Wg expressing cells are also shown (B, D, F and H). (A) In wild type discs the majority of Wg and Golgi colocalise in the apical region of the Wg expressing cells (B). Wg can be occasionally observed in the Golgi within more basolateral regions of the disc (E, F). In *shibire*^{ts} flies kept at 34^{o}C for 3hr, Wg accumulates in large puncta throughout the disc (C, D', G, H'). These large puncta often correlate with anti-GMAP (D, D') and the majority of this colocalisation is seen in the apical region of the expressing cells (D). Wg and Golgi colocalisation is increased in more basolateral regions of the disc after a 3hr endocytic block (H) compared to the wild type (F) situation. Scale bars represent 24um.

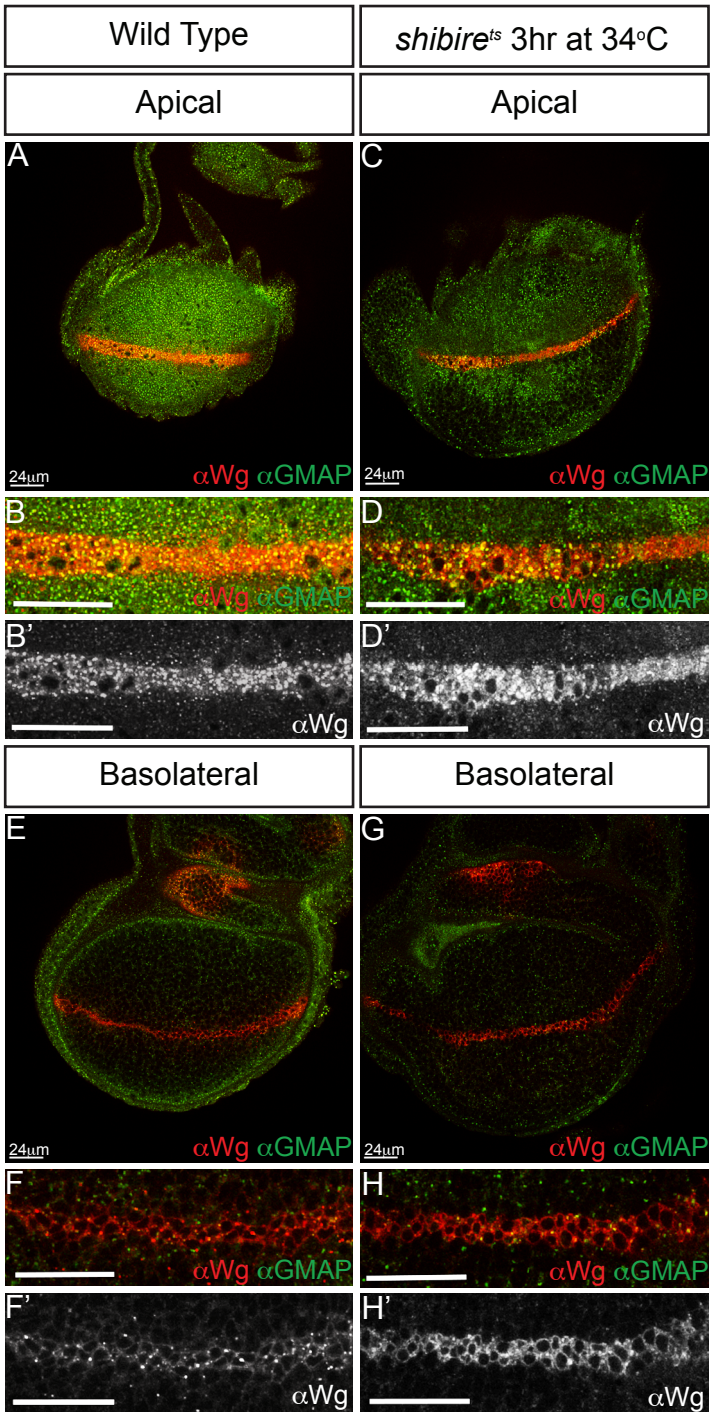
Wild Type
shibire^ts 3hr at 34°C
Apical
Apical
A
C
24µm
αWg αGMAP
24µm
αWg αGMAP
B
D
αWg αGMAP
αWg αGMAP
B'
D'
αWg
αWg
Basolateral
Basolateral
E
G
24µm
αWg αGMAP
24µm
αWg αGMAP
F
H
αWg αGMAP
αWg αGMAP
F'
H'
αWg
αWg

4.2.2 Inhibition of endocytosis causes apical accumulation of extracellular Wg and loss of basolateral extracellular Wg.

According to my model, if Wg does transit through the apical surface to form the basolateral extracellular Wg pool then upon an endocytosis block Wg will become stuck on the apical surface of expressing cells (Figure 4.1). With this idea in mind, I decided to do a timecourse in *shibire^{ts}* mutant larvae.

From previous results (Figure 4.2) I know that after 3hrs at 34^{o}C a Wg secretion block occurs in a *shibire^{ts}* mutant. Therefore I decided to start my timecourse at an earlier point to observe the initial extracellular Wg accumulation. In discs that have always been at the permissive temperature of 18^{o}C, extracellular Wg is mostly on the basolateral surface (Figure 4.3 A'). A small amount of apical extracellular Wg can be detected, but at low levels (Figure 4.3 A). However, after 15min endocytosis block at 34^{o}C, an apical accumulation of extracellular Wg can be observed (Figure 4.3 B). This accumulation is maintained after 30min, 60min (and 120min – data not shown) at 34^{o}C (Figure 4.3 C, D). Apical extracellular Wg accumulation upon an endocytic block is accompanied by the loss of basolateral extracellular Wg over time (Figure 4.3 A', B', C' D'). These observations are quantified in graphical form in Figure 4.3 E and F. Quantification supports the observations shown in Figure 4.3 A-D, that, after an endocytic block apical Wg accumulation can be observed in all samples compared to the 0min sample (Figure 4.3 E). This is shown by a steep increase in extracellular apical Wg signal. And over time, the extracellular Wg signal from the basolateral pool decreases below that of the 0min sample (Figure 4.3 F).

These results support the predictions from my working model. Upon a short endocytic block apical extracellular Wg accumulates, which would be consistent with a need to transit from the apical surface for the formation of the basolateral extracellular Wg pool. Extracellular Wg is lost from the basolateral surface of *shibire^{ts}* mutant discs over time suggesting that Wg is no longer supplied to this surface. It is possible that basolateral extracellular Wg is

degraded or removed from the surface of cells in a process that is not well understood.

4.2.3 Release of an endocytic block allows re-establishment of the basolateral extracellular Wg gradient.

As previously shown, upon a block of endocytosis extracellular Wg accumulates on the apical surface of expressing cells, with the concomitant loss of the basolateral gradient (Figure 4.3). I next decided to test how the localisation of extracellular Wg changes upon the release of this block. As described previously (Figure 4.1), the *shibire*^{ts} mutant system is reversible, so if larvae are returned to 18^{o}C after an endocytic block at 34^{o}C, then dynamin will begin to function again. If as suggested by my model, it is the pool of apical extracellular Wg that undergoes transcytosis to become basolateral extracellular Wg, then by releasing the endocytosis block the apical extracellular accumulation of Wg should disappear and replenishment of the basolateral extracellular Wg pool should begin.

After a 60min endocytic block at 34^{o}C a large apical accumulation of Wg is observed with loss of basolateral extracellular Wg compared to 0min at 34^{o}C as previously shown (Figure 4.4 B). After a 30min chase at 18^{o}C, the apical accumulation of extracellular Wg has disappeared and basolateral extracellular Wg is replenished (Figure 4.4 C). This basolateral extracellular Wg replenishment continues over time as it spreads across the tissue to form a gradient (Figure 4.4 D', E'). There is also a slight increase in apical extracellular Wg compared to the 0min situation in both the 60min and 90min at 18^{o}C chase samples (Figure 4.4 D, E). These observations are quantified in graphical form in Figure 4.4 F and G. Quantification supports the observations shown in Figure 4.4 B, that after an endocytic block of 60min, apical Wg accumulation can be observed compared to the 0min situation (Figure 4.4 F). Upon release of this block, apical accumulation of Wg decreases, however it does not completely return to wild type levels over time (Figure 4.4 F). After an endocytic block of

60min extracellular basolateral Wg has decreased below 0min levels (Figure 4.4 G), and with a release of the block at 18^{o}C, levels are restored back to those of 0min over time (Figure 4.4 G).

These results support the predictions of my working model. Upon an endocytic block at 34^{o}C apical extracellular Wg accumulates and basolateral extracellular Wg decreases, but upon release of the block at 18^{o}C the accumulated apical extracellular Wg decreases and the amount of basolateral extracellular Wg increases. This would be consistent with the idea that once shifted to 18^{o}C, the accumulated apical extracellular Wg is endocytosed and moved to the basolateral surface for release.

Results gathered from the above experiments using *shibire^{ts}* mutant discs (Figure 4.1-4.4) support my current working model that Wg traffics from the apical to basolateral surface of expressing cells (Figure 1.7). However, using *shibire^{ts}* mutants causes a global block in endocytosis that comes with the caveat that all trafficking processes are disrupted. In an attempt to follow Wg trafficking in a less disruptive manner, I decided to return to the inducible system developed in Chapter 3 to follow Wg-HA movement through the secretory pathway.

Figure 4.3: Endocytosis block causes a large accumulation of apical extracellular Wg with the concomitant loss of basolateral extracellular Wg.

In all conditions extracellular Wg was detected using the anti-Wg antibody. Confocal settings are comparable. Reconstructed YZ sections are oriented so that the apical surface is to the top. (A) In *shibire*^{ts} larvae at the permissive temperature, a small amount of extracellular Wg can be detected apically (A), but the majority of extracellular Wg is found on the basolateral surface (A'). (B) Upon an endocytosis block of 15min, *shibire*^{ts} mutant discs show a large accumulation of apical extracellular Wg (B, B''), but Wg protein is still detectable basolaterally (B'). (C) After a 30min endocytosis block, *shibire*^{ts} mutant discs still display the apical Wg accumulation (C, C''), however Wg is reduced at the basolateral surface (C'). (D) After an endocytosis block of 60min, *shibire*^{ts} mutant discs maintain apical accumulation of Wg (D, D''), but display a loss of Wg protein from the basolateral surface (D', D''). Data were pooled and quantified (n=3). Results are plotted in graphs shown in panels E and F. (E) A large increase in apical Wg signal in *shibire*^{ts} discs at 34^{o}C for 15min, 30min and 60min is observed compared to the permissive temperature. (F) The amount of basolateral Wg detected after endocytic block also dipped to below 0min levels in both the *shibire*^{ts} 30min and 60min discs as seen in (C' and D'). Scale bars for XY views represent 24um, YZ views (A'',B'',C'',D'') represent 16um.

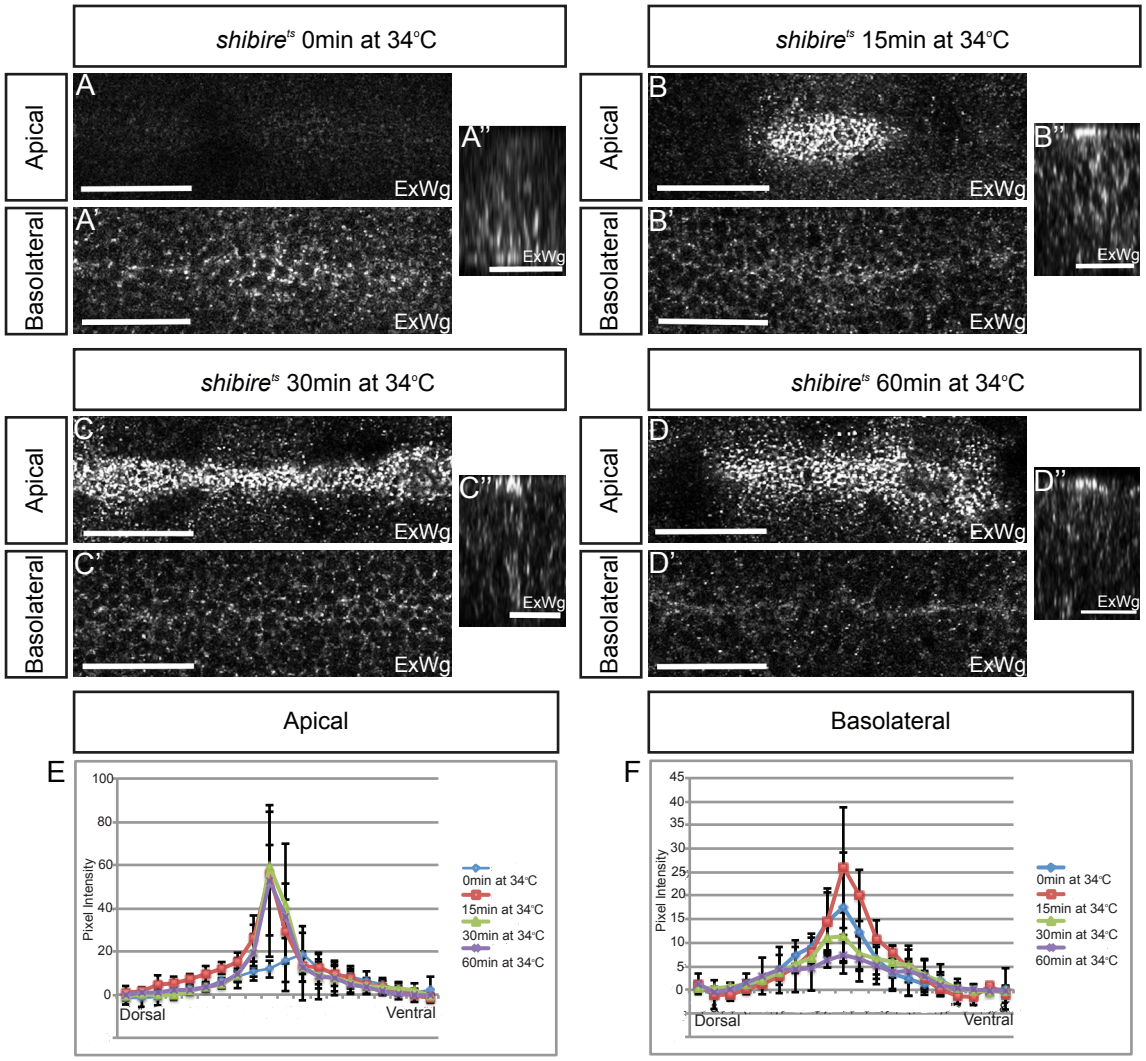
shibire^ts 0min at 34°C
shibire^ts 15min at 34°C
shibire^ts 30min at 34°C
shibire^ts 60min at 34°C
Apical
Basolateral
A
A'
A''
B
B'
B''
C
C'
C''
D
D'
D''
ExWg
E
F
Apical
Basolateral
Pixel Intensity
Dorsal
Ventral
0min at 34°C
15min at 34°C
30min at 34°C
60min at 34°C

Figure 4.4: Release of an endocytic block leads to the relief of the apical build up of extracellular Wg and replenishment of the basolateral gradient.

In all conditions, extracellular Wg was detected using anti-Wg. Reconstructed YZ sections are oriented so that the apical surface is to the top. (A) When *shibire*^{ts} larvae are at the permissive temperature, a small amount of extracellular Wg can be detected apically (A), but the majority of extracellular Wg is found at the basolateral surface (A'). (B) After an endocytosis block of 60min, discs display a large apical accumulation of Wg (B), but Wg protein is lost from the basolateral surface (B'). (C) After a 30min chase at 18^{o}C, the apical accumulation of Wg subsided (C compared to B), while basolateral extracellular Wg was replenished (C' compared to B'). At this time, the basolateral rise remains confined to the surface of Wg expressing cells (C'') and does not spread across the tissue as it did before the endocytosis block (A', A''). (D) After a 60min chase at 18^{o}C, apical Wg decreased sharply below pre block level. An increase in basolateral extracellular Wg can be observed (D'), which is greater than that seen after 30min chase (C'). At this time, Wg can be seen spreading along the basolateral surface of receiving cells (D', D'') similar to the 0min (A', A''). (E-E'') After a 90min chase, a small amount of Wg can be observed on the apical surface of the expressing cells (E), comparable to that seen before the endocytic block (A). The basolateral Wg pool also appears to be replenished (E') to almost 0min levels (A') and there is spread across the tissue greater than after 60min (D') and to an extent that resembles 0min (A'). Data were pooled and quantified (n=3). Results are plotted in graphs shown in panels F and G. (F) A large increase is observed in apical Wg signal in *shibire*^{ts} discs at 34^{o}C for 60min compared to 0min. The apical signal is then lost in both the 30min and 60min chase situations, and is only re established to pre block levels at 90min (F). (G) The amount of basolateral Wg detected after endocytic block also dipped to below 0min levels in the *shibire*^{ts} 60min disc as seen in (B'). But this increases back to 0min levels over time (G). Scale bars for XY views represent 24um, YZ views (A'',B'',C'',D'',E'') represent 16um.

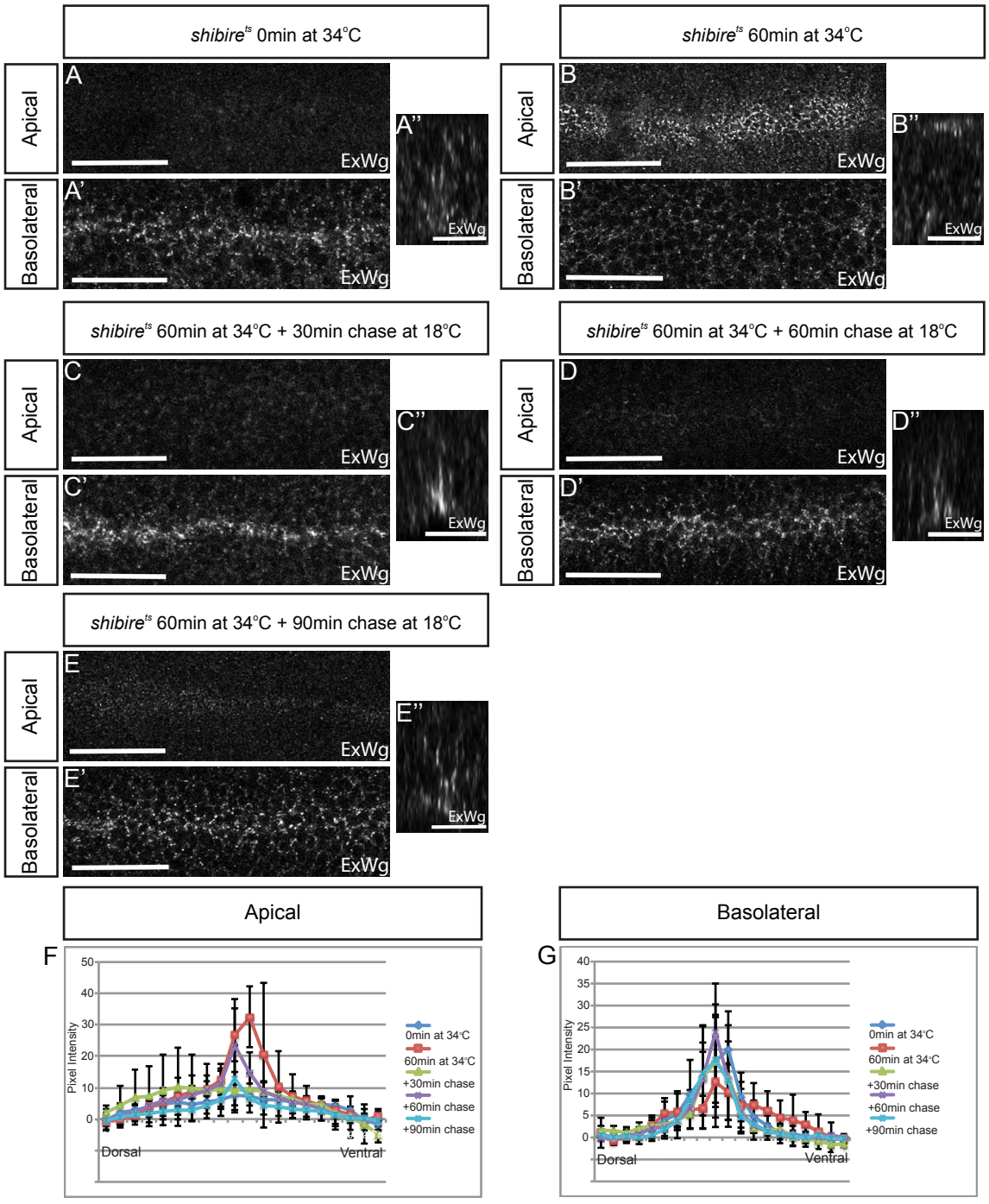
shibire^ts 0min at 34°C
shibire^ts 60min at 34°C
shibire^ts 60min at 34°C + 30min chase at 18°C
shibire^ts 60min at 34°C + 60min chase at 18°C
shibire^ts 60min at 34°C + 90min chase at 18°C
Apical
Basolateral
A
A'
A''
B
B'
B''
C
C'
C''
D
D'
D''
E
E'
E''
ExWg
Apical
Basolateral
F
G
Pixel Intensity
Dorsal
Ventral
0min at 34°C
60min at 34°C
+30min chase
+60min chase
+90min chase

4.2.4 Development and optimisation of the production of a Wg-HA step in the secretory pathway.

As described in the previous chapter, I have created two inducible Wg-HA constructs: *wg{KO; FRT-Wg-FRT-Wg-Ex4-2HA}* and *wg{KO; FRT-Wg-Ex4-3OLLAS-FRT-Wg-Ex4-3HA}*, which trigger expression of Wg-HA upon Flp production. From now onwards these will be referred to as *wg{KO; FRT-Wg-FRT-Wg-HA}* and *wg{KO; FRT-Wg-OLLAS-FRT-Wg-HA}* respectively. To further explore the trafficking route taken by Wg in expressing cells, I would like to produce a step of tagged Wg-HA and follow this step through the secretory pathway at different time points, to determine key trafficking steps (Figure 4.5). Upon Flp expression, excision of the first wild type copy of Wg in the *wg{KO; FRT-Wg-FRT-Wg-HA}* construct has been shown to be effective. However, a suitable source of Flp with a time-controlled method of production must be found. As discussed in Chapter 3, a heat shock controlled source of Flp was found to be "leaky" causing excision of the stop cassette without a heat shock induction. An alternative method of Flp production is to use UAS-Flp and the Gal4/Gal80^{ts} system. Gal80^{ts} is a temperature sensitive repressor of Gal4, which at the restrictive temperature of 18^{o}C prevents Gal4 activity so that UAS transgenes are not expressed. However, upon shifting to the permissive temperature of 29^{o}C, the repression of Gal80^{ts} is lifted and Gal4 can begin to activate UAS transgene (e.g. UAS-Flp) expression. A schematic representation of this process in the wing imaginal disc is shown in Figure 4.6 Box 1.

To use this system to control production of a Wg-HA step, I wanted to test different Gal4s to determine the time it would take for stop cassette excision following transfer to the permissive temperature (29^{o}C). Initially, En-Gal4 was used in conjunction with tub-Gal80^{ts}, UAS-Flp and Actin-FRT-stop-FRT-lacZ to provide a read-out of time taken for Flp-induced excision. Expression of β-gal indicates this excision has happened. Gal4 activity can be determined by expression of UAS-GFP. After 6hr at 29^{o}C the first faint GFP signal can be detected (Figure 4.7 B), however it is not until 16hr at 29^{o}C that

the first β-gal expression is detected (Figure 4.7 D'). This expression then increases over time, until 24hr at 29°C when the entire P compartment strongly expresses β-gal (Figure 4.7 F). Whilst it is encouraging that the Gal4/Gal80^{ts} system works effectively with the addition of a stop cassette-containing construct, for my purposes, this is a long time to wait for Wg-HA expression.

I decided to test a second source of Gal4 - Hh-Gal 4, in a similar fashion to that described above. With this driver, β-gal expression was first faintly detected after 2hr at 29°C (Figure 4.8 B') and increased levels of expression were observed both 4hr and 8hr later (Figure 4.8 C', D'). This expression is heterogeneous at such early timepoints, as only patches of the disc express β-gal. However, after 16hr at 29°C the entire P compartment expresses β-gal (Figure 4.8 E). These data indicate that Hh-Gal4 is more strongly expressed in the wing disc than En-Gal4, making it a more suitable driver for UAS-Flp. By minimising the time delay between transfer to permissive temperature and production of Wg-HA, I will reduce errors that could arise from heterogeneous excision within the stripe of Wg expressing cells.

Using Hh-Gal4 to express UAS-Flp under the temperature sensitive control of tub-Gal80^{ts}, I wanted to demonstrate that expression of Wg-HA from the *wg{KO; FRT-Wg-FRT-Wg-HA}* construct would occur as expected (Figure 3.7). A schematic of how this process works is depicted in Figure 4.6 Box 1. When larvae are kept constantly at the restrictive temperature of 18°C no Wg-HA expression is observed (Figure 4.6 A, B'). However, upon movement to 29°C for 8hrs, Wg-HA expression is observed in some of the Wg expressing cells (Figure 4.6 D). The majority of Wg-HA signal under these conditions is found in the apical region of the expressing cells, as is the case for wild type Wg (Figure 4.6 D''). After 24hr at 29°C the entire P compartment is expressing Wg-HA (Figure 4.6 E), and Wg-HA expression has spread from the apical to basolateral regions of expressing cells (Figure 4.6 F'').

I have shown that the Gal4/Gal80^{ts} system is an effective method of controlling the production of a step of Wg-HA. By choosing a Gal4 line that is expressed strongly in the wing imaginal disc I am able to get production of Wg-HA at as early a time as possible. Gal80^{ts} control of Gal4 was successful and at the restrictive temperature no Wg-HA is produced indicating this system is not "leaky". Upon Wg-HA production at 29^{o}C, HA signal is initially observed at highest levels in the apical region of expressing cells and it appears to move basolaterally over time. This is in accordance with predictions of my working model.

Figure 4.5: Proposed scheme for producing a step of tagged Wg within the secretory pathway.

Schematic illustrating the proposed scheme for following a step of tagged Wg in the secretory pathway. Without expression of Flp, Wg-HA is not produced. However upon expression of Flp, the stop cassette is removed and a step of Wg-HA starts to be expressed. By fixation at different timepoints and subsequent staining we can determine the route of movement through the cell.

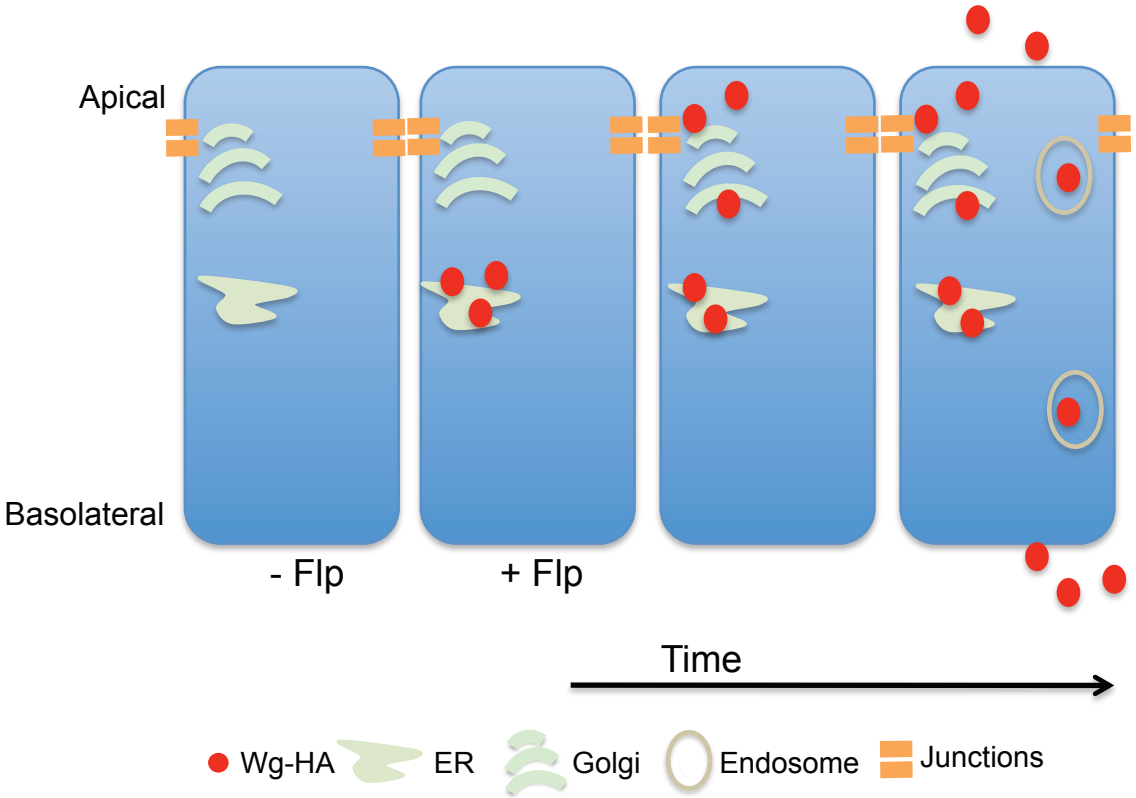
Apical
Basolateral
- Flp
+ Flp
Time
Wg-HA
ER
Golgi
Endosome
Junctions

Figure 4.6: A step of tagged Wg can be controlled using the Gal4/tub-Gal80^{ts} system.

Box 1 - An attP site was integrated in the *wingless* locus creating a null allele (*wg^{KO}*). A tagged cDNA was then inserted in the attP site to make *wg{KO; FRT-Wg-FRT-Wg-Ex4-2HA}* flies (as described in Figure 3.5 and Figure 3.7). Schematic showing the method for controlling the production of Wg-HA: Flp expression is activated in the P compartment at 29^{o}C using the Gal4/Gal80^{ts} system. This leads to excision of the wild type *wg* cDNA and expression of Wg-HA. Box 2 - 3rd instar larvae of the shown genotype were kept at 29^{o}C for various times before fixation and staining with anti-Wg and anti-HA to detect excision of wild type Wg and expression of Wg-HA. Confocal sections across a basal/lateral plane are shown. Reconstructed YZ sections are oriented so that the apical surface is to the top. (A-B'') No Wg-HA is produced in larvae kept at 18^{o}C. (C-D'') After 8hr at 29^{o}C regions of Wg-HA expression are visible indicating that excision of the stop cassette is occurring (C). Most of the HA signal is detected in the apical regions of these expressing cells (D''). Wg-HA signal is relatively weak at the basolateral surface (D''). (E-F'') After 24hr at 29^{o}C the whole posterior Wg stripe is producing Wg-HA (E). HA signal is again highest in the apical region (F'') but is also detectable at the basolateral surface of expressing cells (F''). Scale bars represent 24um.

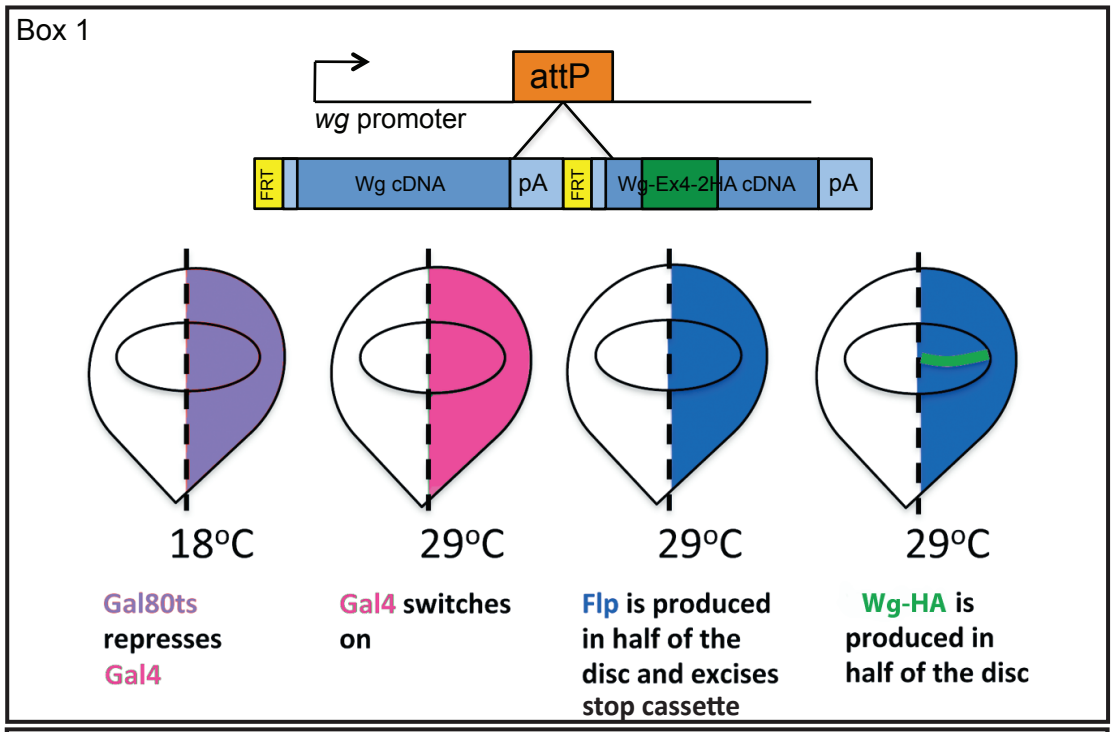
Box 1
attP
wg promoter
FRT
Wg cDNA
pA
FRT
Wg-Ex4-2HA cDNA
pA
18°C
29°C
29°C
29°C
Gal80ts represses Gal4
Gal4 switches on
Flp is produced in half of the disc and excises stop cassette
Wg-HA is produced in half of the disc

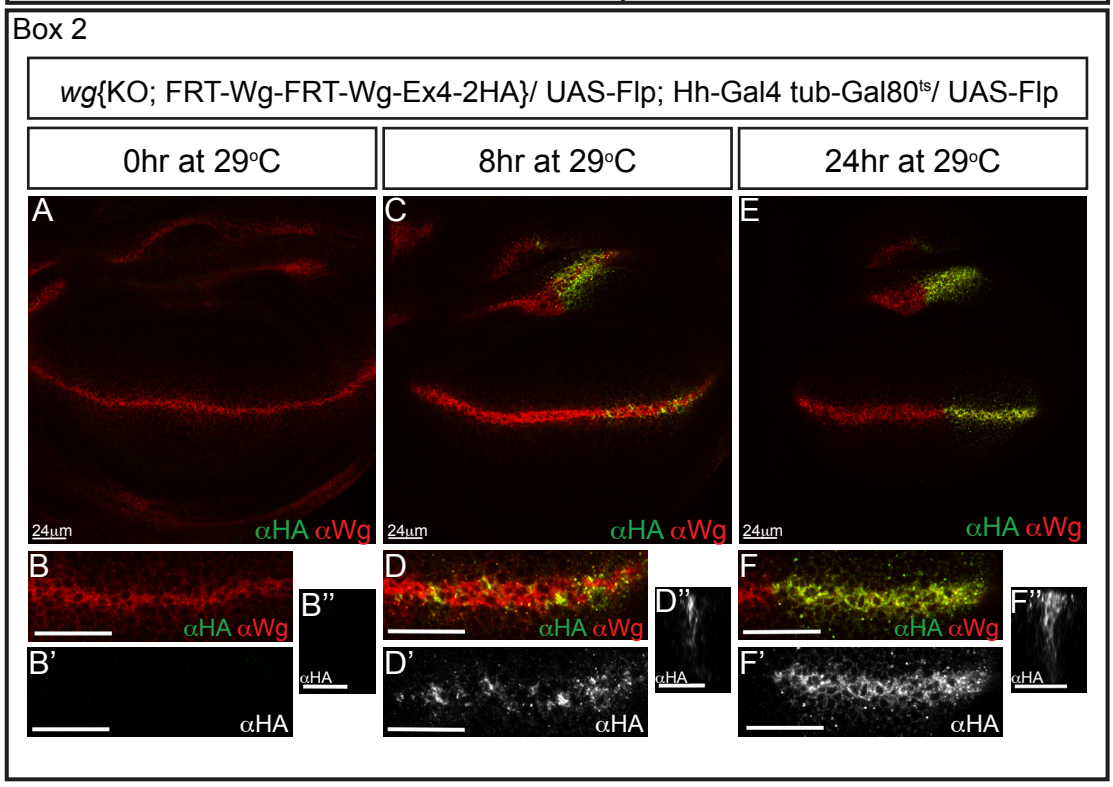
Box 2
wg{KO; FRT-Wg-FRT-Wg-Ex4-2HA}/ UAS-Flp; Hh-Gal4 tub-Gal80ts/ UAS-Flp
0hr at 29°C
8hr at 29°C
24hr at 29°C
A
C
E
24µm
αHA αWg
B
B'
B''
D
D'
D''
F
F'
F''
αHA

Figure 4.7: Identification of a suitable Gal4 driver: En-Gal4.
All discs express En-Gal4, which drives expression of UAS-GFP and UAS-Flp in the P compartment. Expression of UAS-Flp will cause FRT-mediated recombination of the Act-FRT-Stop-FRT-lacZ and subsequent lacZ expression. These discs also express a temperature-sensitive repressor of Gal4 - $Gal80^{ts}$ under the control of the tubulin promoter. This causes repression of Gal4 at 18°C, however at 29°C this repression is relieved and Gal4 activation of UAS-GFP and UAS-Flp will begin. As indicated, larvae have spent differing amounts of time at the permissive temperature of 29°C before fixation and staining for lacZ using an anti-β-gal antibody. (A) After 0hr at 29°C no expression of either GFP (a readout of Gal4 activity) or β-gal (showing excision of the stop cassette) can be detected. (B) After 6hr at 29°C Gal4 activity is present since weak GFP can be detected (B), but no β-gal is detected (B'). (C) After 12hr at 29°C strong GFP expression is observed (C), however β-gal can still not be detected (C'). (D) Weak β-gal expression can first be detected after 16hr at 29°C (D'). (E-F) From 20hr -24hr at 29°C the β-gal expression becomes stronger (E', F'). Scale bars are shown on relevant panels.

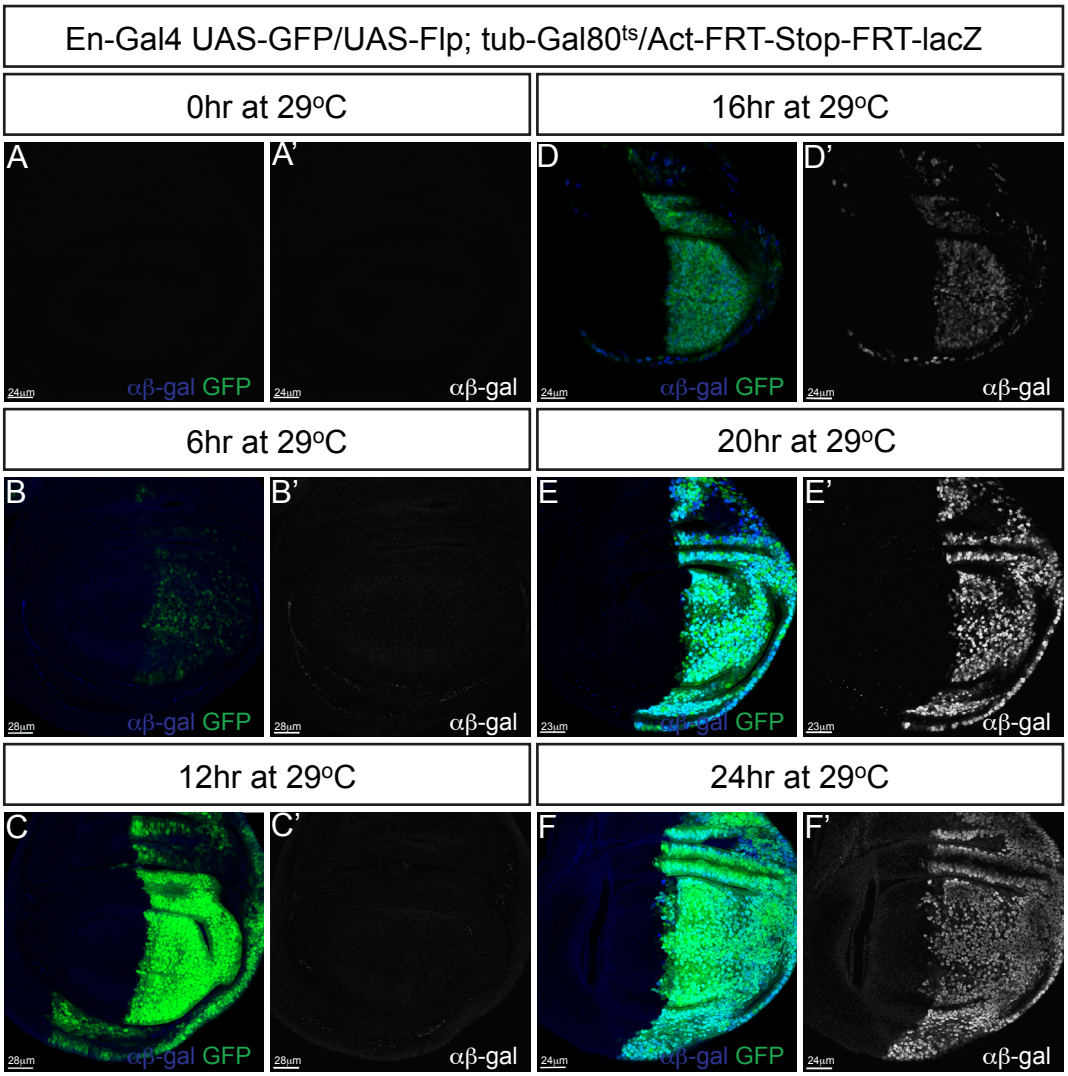
En-Gal4 UAS-GFP/UAS-Flp; tub-Gal80ts/Act-FRT-Stop-FRT-lacZ
0hr at 29ºC
16hr at 29ºC
A
A'
D
D'
24µm
αβ-gal GFP
αβ-gal
6hr at 29ºC
20hr at 29ºC
B
B'
E
E'
28µm
23µm
12hr at 29ºC
24hr at 29ºC
C
C'
F
F'

Figure 4.8: Identification of a suitable Gal4 driver: Hh-Gal4.

All discs express Hh-Gal4, which drives expression of UAS-Flp in the P compartment. Expression of UAS-Flp will cause FRT-mediated recombination of the Act-FRT-Stop-FRT-lacZ and subsequent lacZ expression. As before this is regulated by $Gal80^{ts}$. As indicated, larvae have spent differing amounts of time at the permissive temperature of 29°C before fixation and staining for lacZ using an anti-β-gal antibody. (A) After 0hr at 29°C there is no expression of β-gal. (B) After 2hr at 29°C β-gal is weakly detected (showing excision of the stop cassette and expression of lacZ) (B') but only in patches of the disc; production is not homogenous. (C-D) Between 4hr – 8hr at 29°C larger regions of the disc express β-gal (C', D') and the expression levels are stronger. (E) By 16hr at 29°C the entire P compartment is producing β-gal (E') and this expression pattern is comparable to the same conditions after 24hr at 29°C (F). Scale bars are shown on relevant panels.

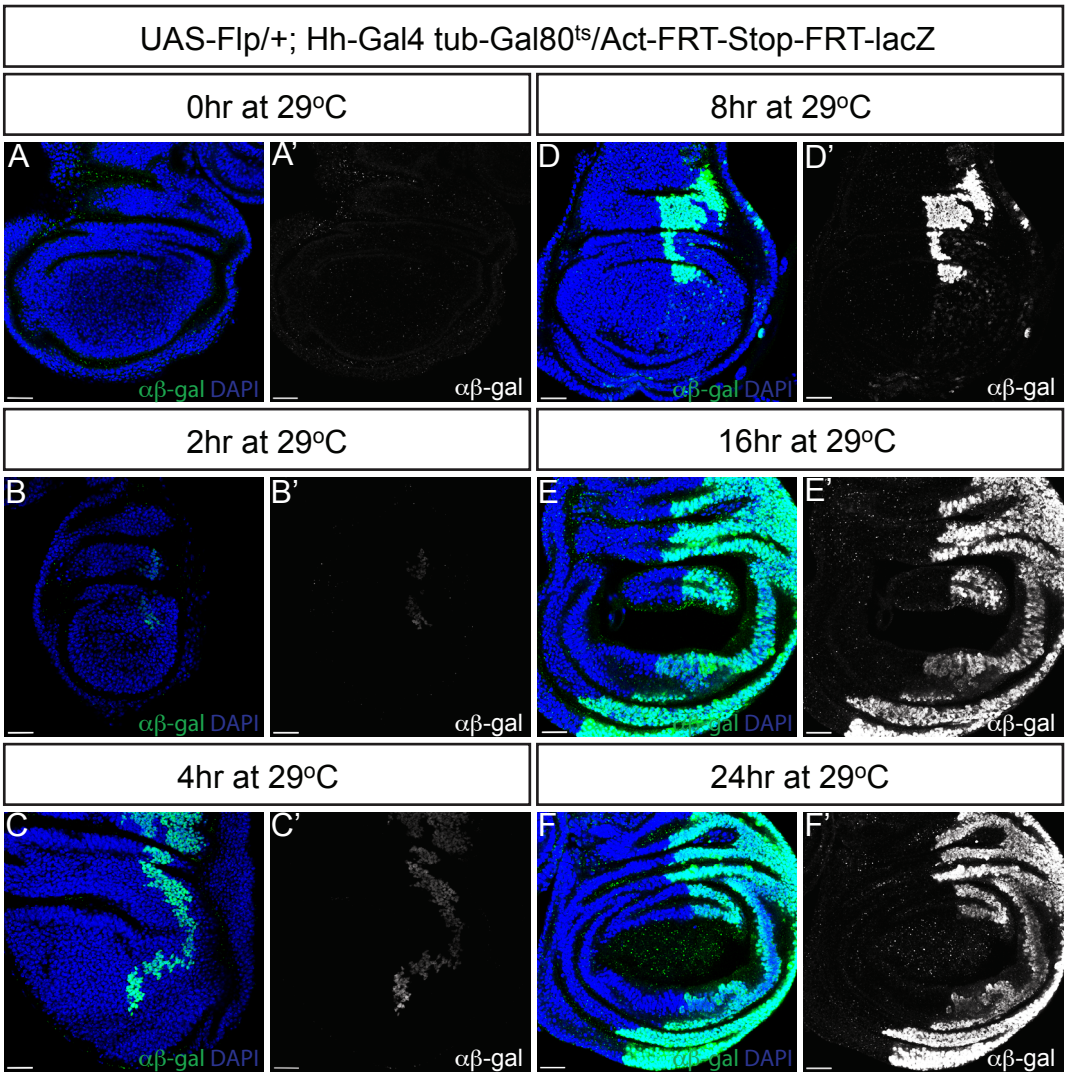
UAS-Flp/+; Hh-Gal4 tub-Gal80ts/Act-FRT-Stop-FRT-lacZ
0hr at 29ºC
8hr at 29ºC
2hr at 29ºC
16hr at 29ºC
4hr at 29ºC
24hr at 29ºC
A
A'
B
B'
C
C'
D
D'
E
E'
F
F'
αβ-gal DAPI
αβ-gal

4.2.5 Wg-HA moves basolaterally through the expressing cells over time.

Using the system described above to produce a controlled step of Wg-HA, I wanted to follow this step over time through the secretory pathway of expressing cells (Figure 4.5). To do this I used the *wg{KO; FRT-Wg-OLLAS-FRT-Wg-HA}* construct with the hope that this would give a clear boundary between Wg-OLLAS and Wg-HA, the movement of which could be followed through the secretory pathway. A timecourse was conducted using this construct and samples were fixed and stained using antibodies against their epitope tags.

After 0hr at 29^{o}C no Wg-HA is produced but Wg-OLLAS can be observed throughout the expressing cells (Figure 4.9 A). Wg-HA is first seen after 2hr at 29^{o}C in the apical region of expressing cells (Figure 4.9 B'). It moves more basally over time, as after 4hr at 29^{o}C Wg-HA can be observed in the apical, lateral and faintly in more basolateral regions of the cells (Figure 4.9 C'). After 8hr at 29^{o}C Wg-HA is expressed strongly along the entire apical-basolateral axis (Figure 4.9 D'), and after 16hr at 29^{o}C Wg-HA is expressed throughout the producing cell and HA positive puncta can be observed in receiving cells (Figure 4.9 E'). After 16hr at 29^{o}C most Wg-OLLAS has disappeared from the Wg-HA expressing cell presumably because it has passed through the secretory pathway and is no longer being expressed (Figure 4.9 E''). These observations are quantified in graphical form in Figure 4.9 F. All samples are not imaged using the same settings because absolute levels of Wg-HA vary greatly over the timecourse, and the gain had to be increased to detect the weak signal in some of the earlier samples. Therefore, when interpreting Figure 4.9 Graph F, the absolute levels of intensity cannot be considered. However, the relative amount of signal along the apical/basolateral axis (i.e. the shape and steepness of the apical/basolateral distribution) is meaningful. If Wg-HA is only concentrated in a small region of the cell then the apical/basolateral distribution will have a high peak and afterwards a steep gradient. However, if Wg-HA is present throughout the cell, then the apical/basolateral gradient will appear flatter with HA signal present throughout the cell. These phenomena can be observed in

Figure 4.9 F. For early timepoints (2hr, 4hr) a steep apical/basolateral gradient is observed. High levels of HA are present in the first 20% (apical region) of the cells, followed by a lack of signal in lateral and basolateral regions. However, for all later timepoints (8hr, 12hr, 24hr) the apical/basolateral gradient has a flattened profile indicating that signal is found throughout the cells. All profiles display a higher intensity value in the first 20% of the cell compared to the final 20% which is consistent with the higher levels of Wg that are always present in apical regions of expressing cells compared to more basolateral regions.

These results indicate that Wg-HA is produced in the apical region of expressing cells and it moves basolaterally over time. This is consistent with the tight apical localisation of *wg* mRNA (Figure 1.5 A), and with the idea that apical Wg may undergo transcytosis to form the basolateral extracellular Wg pool.

Figure 4.9: Wg-HA moves from the apical to basolateral region of expressing cells over time.

Using the same conditions as described in Figure 4.6, tub-Gal80^{ts} was used to control the production of Wg-HA. 3rd instar larvae of the genotype shown were kept at 29^{o}C for various times before fixation and staining with anti-OLLAS and anti-HA. Reconstructed YZ sections are oriented so that the apical surface is to the top. (A) Before transfer to 29^{o}C, no Wg-HA can be detected and Wg-OLLAS is detected predominantly apically as is the case for wild type Wg. (B) After 2hr at 29^{o}C Wg-HA is detected in the very apical region of the expressing cells (B') but not in lateral or basolateral regions. (C) After 4hr at 29^{o}C Wg-HA is detected strongly in both the apical and lateral regions of the cell (C') and weakly at the basolateral surface (C'). (D) After 8hr at 29^{o}C Wg-HA is detected throughout the expressing cells (D'). (E) After 16hr at 29^{o}C Wg-HA is also detected throughout the expressing cells (E') as well as in puncta spreading across the tissue (E'). Wg-OLLAS is mostly undetectable at this stage. Data were pooled and quantified (n=3). Results are plotted in a graph in panel F. (F) After both 2hr and 4hr at 29^{o}C, most Wg-HA is in the apical 20% of the cell but is largely undetectable in the basolateral 80% (F). Wg-HA continues to be enriched apically, but the apical/basolateral gradient progressively flattens after 8hr, 16hr and 24hr at 29^{o}C. This indicates movement from the apical to basolateral regions of the cell over time (F). Scale bars represent 19um.

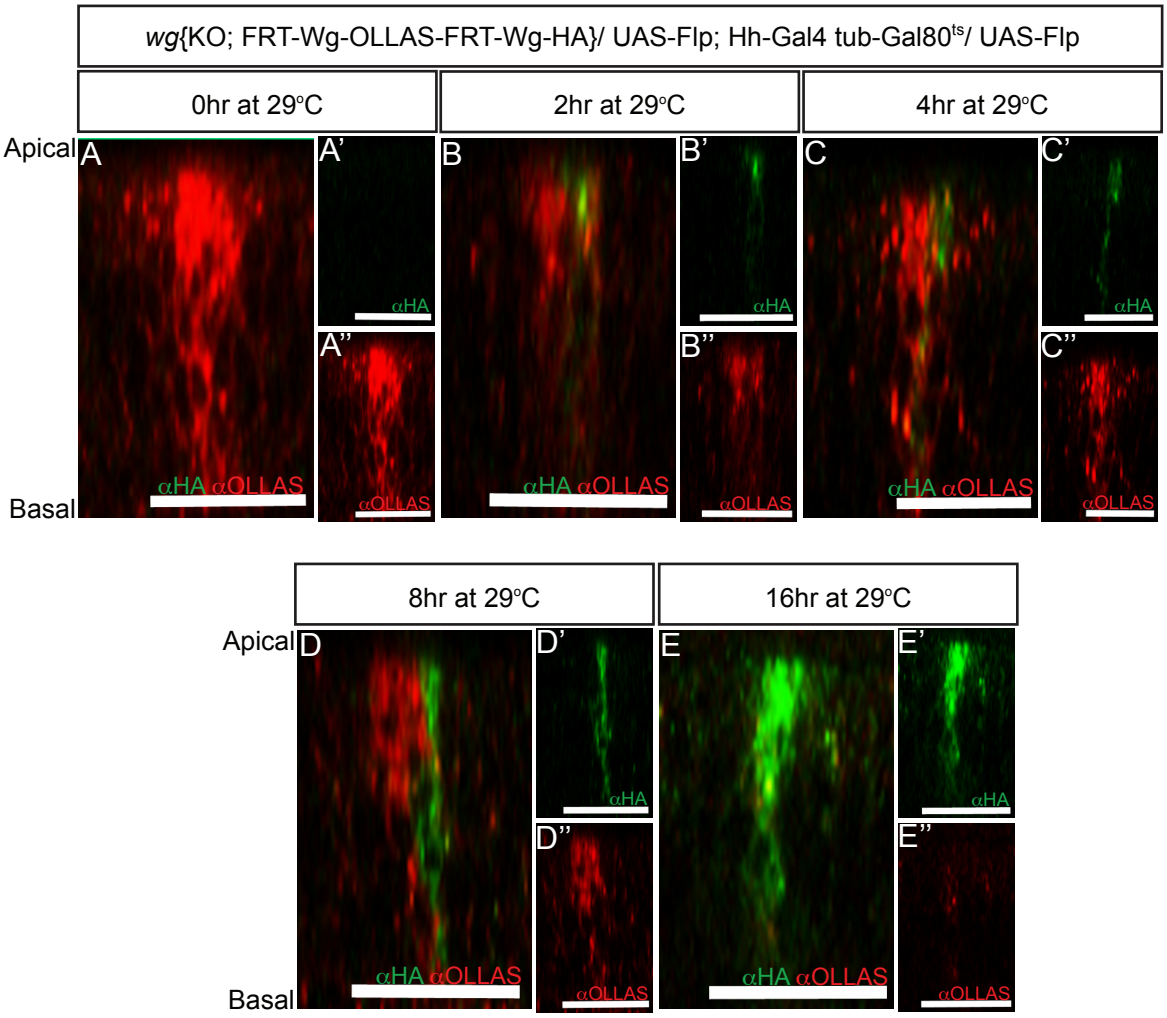
wg{KO; FRT-Wg-OLLAS-FRT-Wg-HA}/ UAS-Flp; Hh-Gal4 tub-Gal80ts/ UAS-Flp
0hr at 29°C
2hr at 29°C
4hr at 29°C
Apical
Basal
A
A'
A''
B
B'
B''
C
C'
C''
αHA αOLLAS
αHA
αOLLAS
8hr at 29°C
16hr at 29°C
D
D'
D''
E
E'
E''

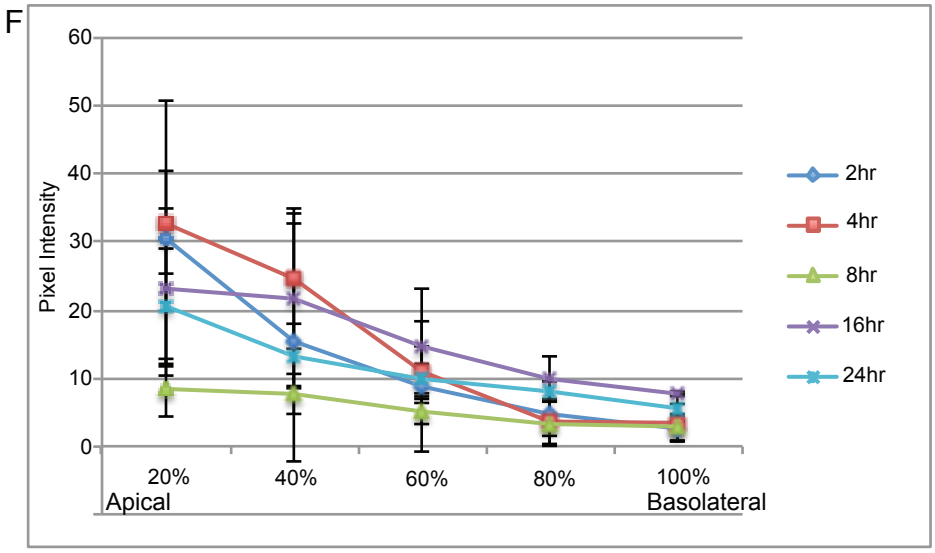
F
Pixel Intensity
60
50
40
30
20
10
0
20%
40%
60%
80%
100%
Apical
Basolateral
2hr
4hr
8hr
16hr
24hr

4.2.6 Extracellular Wg-HA spreads from expressing cells at the basolateral surface.

As shown above, a step of Wg-HA moves from the apical to basolateral region of expressing cells. I wanted to know what happened to Wg-HA after it reaches the basolateral surface. Previous results with *shibire*^{ts} suggested that Wg is released from the basolateral surface to form a gradient. I would like to find out if a Flp-induced step of Wg-HA behaves similarly.

This experiment was conducted in the same fashion as described above except extracellular Wg-HA was detected instead of total Wg-HA. After 2hr at 29^{o}C extracellular Wg-HA is first observed, and this is limited to the basolateral region of the Wg expressing cells (Figure 4.10 B). After 4hr at 29^{o}C more extracellular Wg-HA can be detected, but again this appears to be mostly limited to the basolateral surface of expressing cells (Figure 4.10 C). After 8hr and 12hr at 29^{o}C, larger regions of the disc contain extracellular Wg-HA (Figure 4.10 D, E). Wg-HA appears more diffuse, suggesting that spreading may have occurred (Figure 4.10 D, E). After 24hr at 29^{o}C extracellular Wg-HA has spread away from the surface of the Wg expressing cells to form an extracellular Wg gradient comparable to that of wild type Wg (Figure 4.10 F). These observations are quantified in graphical form in Figure 4.10 G. As before, samples were not imaged using the same settings because absolute levels of Wg-HA vary greatly over the timecourse. As shown in Figure 4.10 Graph G, at early timepoints (2hr, 4hr) the basolateral gradient is steep (Figure 4.10 G) indicating that extracellular Wg-HA does not spread within this timeframe. The profiles for 8hr and 12hr (at 29^{o}C) have a much flatter profile reaching into non-expressing cells (Figure 4.10 G). The profile for 24hr at 29^{o}C has a higher amplitude and at the same time reaches non-expressing cells, displaying gradient spread (Figure 4.10 G). Interestingly, the highest signal is broader than in earlier timepoints, presumably because after 24hr the gradient has reached equilibrium and high levels of extracellular Wg-HA expression are not just

found on the surface of the expressing cells, but also a few cells away (Figure 4.10 G).

These results support previous evidence I described in this chapter, to suggest Wg produced in the apical regions of expressing cells moves basally and is released to form the extracellular Wg gradient.

4.2.7 Wg-HA moves from apical Golgi into endosome-like sub-cellular compartments over time.

I have shown that Wg moves from the apical to basolateral surface of expressing cells, where it is released. But an interesting question remains – what is the route taken by Wg to complete this transcytotic step? Presumably, the first step from the apical surface would involve internalisation into a Rab5 positive endosome from whence it traffics basolaterally. To elucidate through which compartments Wg transits (as described in Section 4.2.5), I used sub-cellular compartment markers as guideposts.

Suitable markers were found for both the Golgi and Rab5 compartments: an antibody against GMAP was used to label the Golgi, and a transgenic fly line expressing Rab5 fused to the YFP fluorescent protein was used to label Rab5 positive endosomes. In wild type discs, the majority of Wg and GMAP colocalisation occurs in the apical region of expressing cells (Figure 4.11 A). This corresponds with previous results suggesting that production of Wg protein occurs apically (Figure 4.9). In tubulin-Rab5:YFP larvae, the majority of Wg and Rab5:YFP colocalisation was also found in the apical region of expressing cells (Figure 4.11 B). This would be consistent with the idea that Wg undergoes endocytosis from the apical region to move basolaterally. Using the same conditions as described in Section 4.2.5: Figure 4.9, I produced a controlled step of Wg-HA and followed its movement through expressing cells using anti-HA to visualise Wg-HA, and anti-GMAP to visualise the Golgi (Figure 4.11 Box 2). Before transfer to 29^{o}C no Wg-HA is produced (Figure 4.11 C). Golgi can be observed throughout the imaginal disc as detected by anti-GMAP

(Figure 4.11 C''). Wg-HA is first observed in the apical region of expressing cells after 2hr at 29^{o}C (Figure 4.11 D). Both hazy and punctate HA staining can be observed at this time (Figure 4.11 D'). All Wg-HA puncta colocalise with anti-GMAP within expressing cells, as indicated by white arrows (Figure 4.11 D). After 3hr at 29^{o}C, Wg-HA expression has moved more basally (Figure 4.11 E'). A subset of Wg-HA puncta colocalise with anti-GMAP under these conditions (white arrows), however anti-HA positive puncta that do not colocalise with anti-GMAP (blue arrows) can also be observed (Figure 4.11 E). These are mainly present in the apical region (Figure 4.11 E). This suggests that over time Wg-HA moves into a GMAP-negative compartment, most probably an early endosome.

These results support previous observations indicating the apical to basolateral movement of Wg. In steady state conditions Wg is observed apically in both Golgi and Rab5 sub-cellular compartments. Initially all Wg-HA puncta localise to apical Golgi, however over time Wg-HA puncta that are not stained with anti-GMAP appear. These are also mainly seen in the apical region suggesting that they may be Rab5-positive endosomes. This would be consistent with the need for Wg-HA to transit the apical surface via an early endosome before trafficking basolaterally.

Figure 4.10: Extracellular Wg-HA spreads away from the basolateral surface of producing cells over time.

As in Figure 4.6, tub-Gal80^{ts} allows temperature dependent control of Wg-HA production. 3rd instar larvae of the shown genotype were kept for various times as indicated before fixation and staining with extracellular anti-HA to detect Wg-HA movement. Basolateral confocal sections are shown. Reconstructed YZ sections are oriented so that the apical surface is to the top. (A) No extracellular Wg-HA is detected before the temperature shift. (B) After 2hr at 29^{o}C weak extracellular Wg-HA can be detected at the basolateral surface of expressing cells, but does not appear to spread across the tissue. (C) After 4hr at 29^{o}C extracellular Wg-HA signal has further increased on the basolateral surface of expressing cells. (D) After 8hr at 29^{o}C extracellular Wg-HA can be detected on an increasing number of cells. (E) After 12hr at 29^{o}C extracellular Wg-HA can be detected in large regions of the Wg stripe and appears to be spreading to neighbouring cells (E, E'). However the concentration and gradient span has not reached the levels of wild type. (F) After 24hr at 29^{o}C the distribution of basolateral extracellular Wg-HA resembles that of extracellular Wg in wild type discs. Data were pooled and quantified (n=3). Results are plotted in a graph in panel G. (G) This graph shows that extracellular basolateral Wg-HA is confined to the surface of expressing cells after 2-4hrs at 29^{o}C, and that at later times signal increases in intensity and appears to form a shallower gradient as extracellular Wg-HA begins to spread. Scale bars for XY views represent 24um, YZ views (B',C',D',E',F') represent 20um.

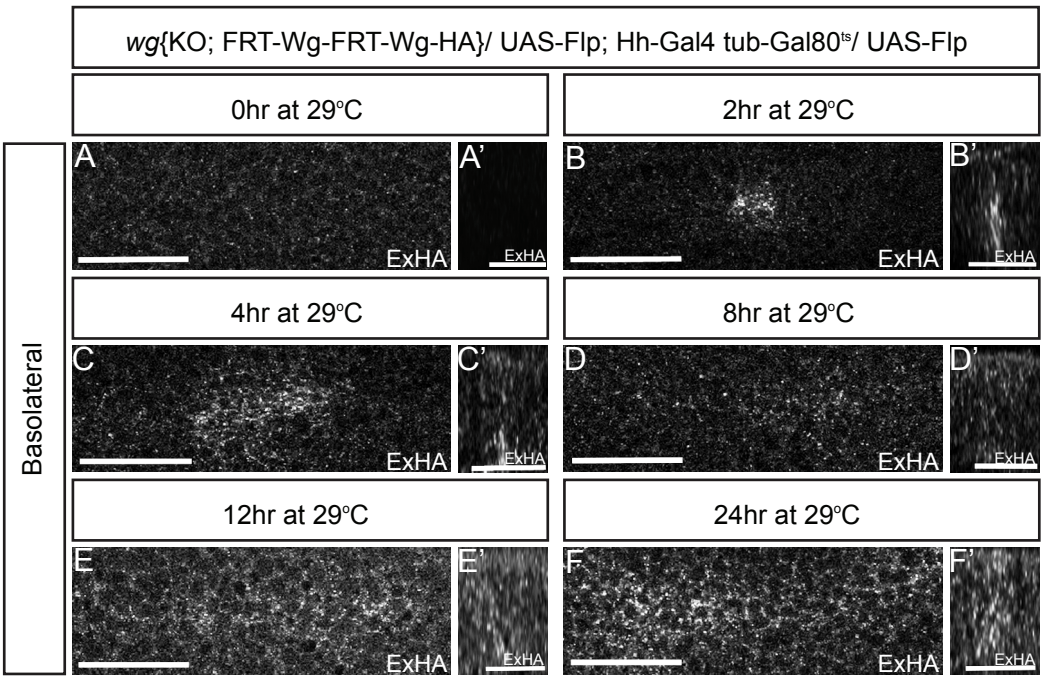
wg{KO; FRT-Wg-FRT-Wg-HA}/ UAS-Flp; Hh-Gal4 tub-Gal80ts/ UAS-Flp
0hr at 29°C
2hr at 29°C
4hr at 29°C
8hr at 29°C
12hr at 29°C
24hr at 29°C
Basolateral
A
A'
B
B'
C
C'
D
D'
E
E'
F
F'
ExHA

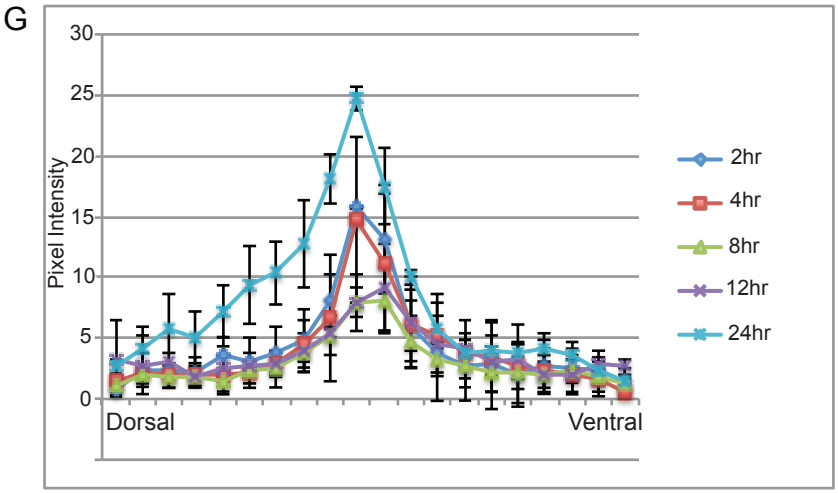
G
Pixel Intensity
30
25
20
15
10
5
0
Dorsal
Ventral
2hr
4hr
8hr
12hr
24hr

Figure 4.11: Wg-HA moves from apical Golgi into endosome-like structures over time.

Anti-Wg was used to detect Wg, Golgi were marked using anti-GMAP and a tubulin-Rab5:YFP transgenic line was used to mark Rab5 positive compartments. Reconstructed YZ sections are oriented so that the apical surface is to the top.

Box 1 - (A) In wild type discs the majority of Wg and Golgi colocalisation is observed in the apical region of the expressing cells (A, A''). Few basolateral Golgi-positive puncta of Wg can be observed (A') but at much lower levels. (B) In tubulin-Rab5:YFP larvae the majority of Wg and Rab5:YFP colocalisation is in the apical region of expressing cells (B, B''). There are considerably less Rab5:YFP-positive compartments in the basolateral regions of wing disc cells in general, and rarely Wg can be seen colocalising with these (B'). Box 2 – Using the same conditions as described in Figure 4.6, tub-Gal80^{ts} was used to control the production of Wg-HA. 3rd instar larvae of the genotype shown were kept at 29^{o}C for various times before fixation and staining with anti-HA. (C) No Wg-HA is detected before the temperature shift. (C'') Golgi are detected throughout the disc using anti-GMAP. (D) After 2hr at 29^{o}C Wg-HA is detected in the apical region of Wg expressing cells (D'). (D) All detectable Wg-HA puncta within expressing cells colocalise with anti-GMAP, indicating that Wg-HA transits through the apical Golgi. White arrows indicate colocalisation. (E) After 3hr at 29^{o}C Wg-HA is observed in Golgi-positive (white arrows) as well as Golgi-negative (marked by blue arrows) puncta in expressing cells. (E') These puncta mainly occur in the apical region of expressing cells suggesting these may represent endosomal compartments. Scale bars are shown on relevant panels, un-marked scale bars represent 20um.

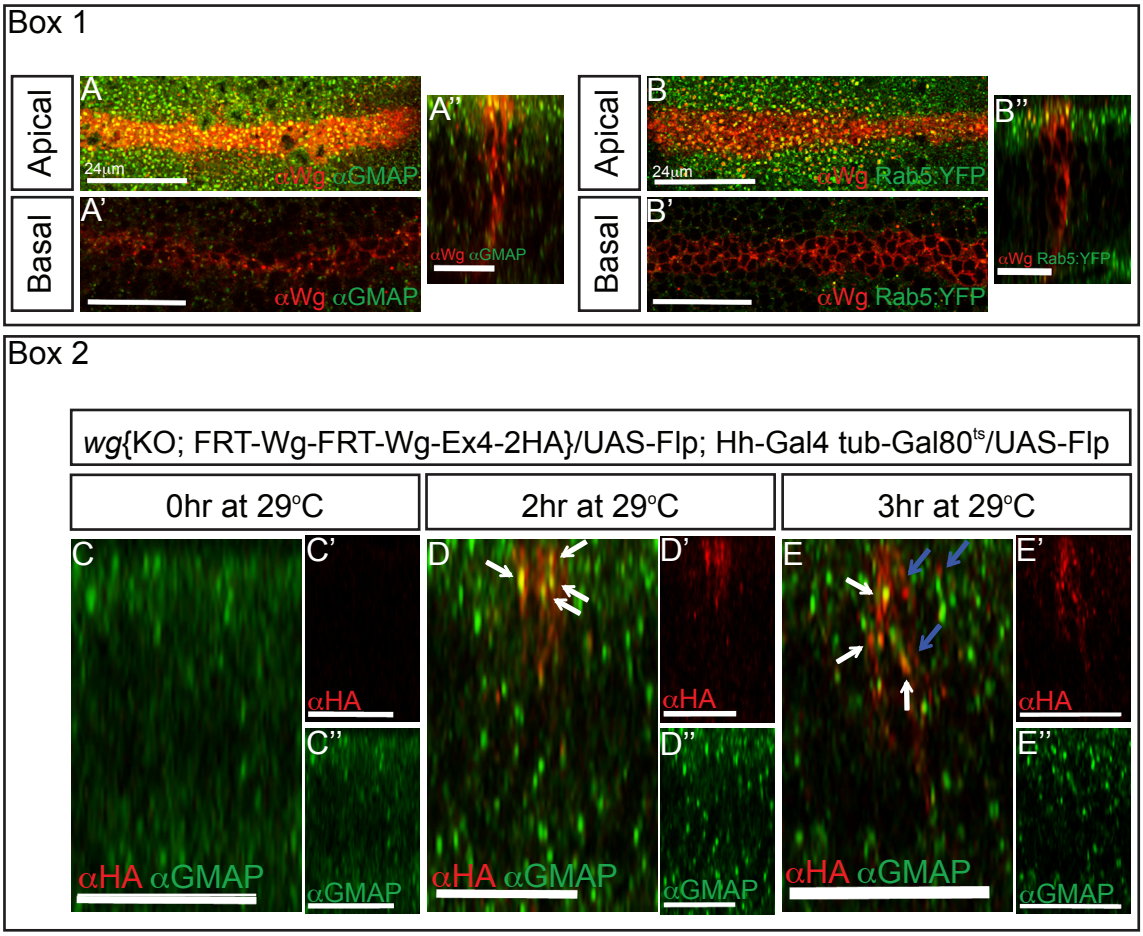
Box 1
Apical
Basal
A
A'
A''
24µm
αWg αGMAP
B
B'
B''
αWg Rab5:YFP
Box 2
wg{KO; FRT-Wg-FRT-Wg-Ex4-2HA}/UAS-Flp; Hh-Gal4 tub-Gal80ts/UAS-Flp
0hr at 29°C
2hr at 29°C
3hr at 29°C
C
C'
C''
D
D'
D''
E
E'
E''
αHA
αGMAP
αHA αGMAP

4.3 Discussion

In this chapter I have shown that upon an endocytosis block Wg accumulates on the apical surface of expressing cells, with the loss of the basolateral extracellular Wg pool. Upon release of this endocytosis block, the accumulated apical Wg returns to near wild type levels and the basolateral extracellular Wg pool is replenished, suggesting that Wg requires transit through the apical surface before basolateral release. Using a system to create a step of tagged Wg-HA, I have been able to follow Wg-HA movement over time. Wg-HA is produced in the apical region of expressing cells from whence it is trafficked to the basolateral surface for release and spread across the tissue over time. These results are consistent with our working model that Wg undergoes transcytosis in the expressing cells to move basolaterally for release.

The results presented in this chapter provide good evidence that Wg transits at the apical surface of expressing cells before moving basolaterally for release. However, there are caveats to consider. Endocytosis is such a fundamental process involved in all aspects of cell biology that perturbing this process might cause unrelated phenomena. A global endocytosis block using an agent like *shibire*^{ts} therefore is a tool that has to be used with caution.

Creating an endocytosis block using *shibire*^{ts} mutants provided us with information about the path taken by Wg. However, it was important in these experiments that larvae were kept at the restrictive temperature for as short a time as possible to avoid complications due to the ill health of the cells. Fortunately, the effects of a dynamin-dependent endocytosis block were very rapid and in most experiments samples were not submitted to times longer than 60min at 34^{o}C. Hopefully, with such an acute block there will not be unrelated consequences that may mask or alter the effect on Wg. DAPI staining of the nuclei was performed on all samples to observe the health of the cells and no apoptosis was observed under these conditions. Because of the role of

dynamin in the Golgi, Wg accumulated there upon shifting to 34°C in *shibire^{ts}* mutant larvae and Wg already released from the Golgi was accumulated on the extracellular apical surface. This was advantageous for two reasons: 1) A finite amount of Wg was blocked at the apical surface of expressing cells rather than a build up over time. This made visualisation of the surface of these cells easier, and it also increased the likelihood that the excess Wg would not be removed/trafficked in a fashion that would not occur in a normal situation. 2) Blockage of Wg in the Golgi and accumulation on the apical surface of expressing cells, created an artificial "pulse" of Wg trapped on the cell surface. When the endocytic block was released at the permissive temperature, this accumulated apical Wg was able to enter the cells rapidly. This allowed us to determine that it is the apical extracellular Wg that forms the basolateral extracellular gradient.

When releasing an endocytic block in *shibire^{ts}* mutant discs I found it took around 90min for the extracellular basolateral Wg gradient to reform. However, if this gradient is synthesised de novo using the Wg-HA step system it takes between 12-24hr for it to form. Speedier gradient formation in the *shibire^{ts}* mutant situation is probably because there are large stores of Wg in the Golgi that are rapidly released, a situation that would not usually be found in the wild type. This is represented in schematic form in Figure 4.12. The red lines indicate the amount of Wg available for gradient re-establishment at the onset of the experiment (Figure 4.12). Significantly more stored Wg is present in a *shibire^{ts}* mutant due to the accumulation of Wg in the Golgi (Figure 4.12). A further example of this is shown in chase experiments described in Figure 4.4. Upon movement of larvae from restrictive to permissive temperature, apical extracellular Wg levels do not return to the same level as before no endocytic block within our experimental timeframe. The increase in apical extracellular Wg observed after both 60min and 90min chase at 18°C, may also be due to an increase in intracellular Wg stored in the Golgi. Upon release of this block, more Wg than usual would be moving through the Golgi to the surface and only when

Figure 4.12: Re-establishment of the basolateral extracellular Wg gradient takes much longer when Wg-HA is synthesised de novo compared to the release of a *shibire^{ts}*-dependent block.

Schematic representation of why the basolateral Wg gradient is established within 1.5hr after release of an endocytosis block, while de novo Wg-HA expression leads to basolateral gradient formation only after 24hr. The red line represents intracellular stores of Wg within the Golgi. These are abundant after an endocytic block (A) but relatively scarce upon de novo synthesis (B).

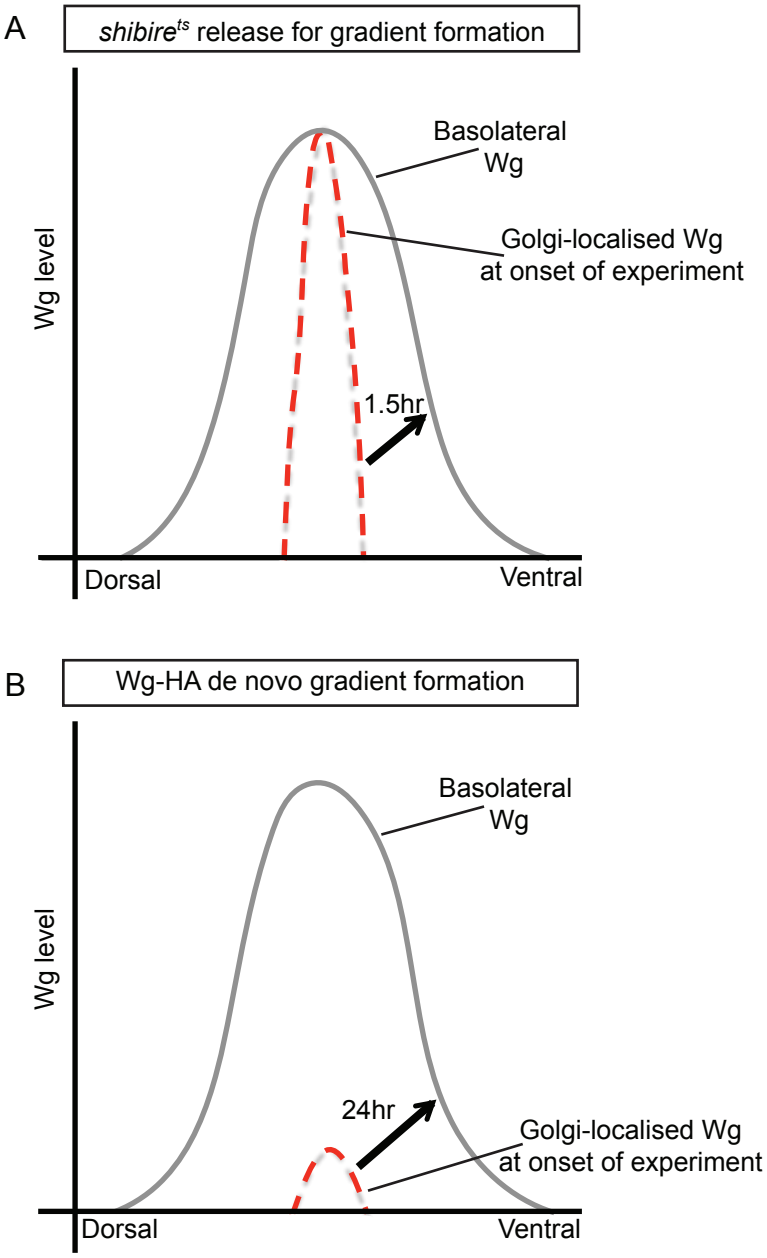
A
shibire^ts release for gradient formation
Basolateral
Wg
Golgi-localised Wg
at onset of experiment
Wg level
1.5hr
Dorsal
Ventral
B
Wg-HA de novo gradient formation
Basolateral
Wg
Wg level
24hr
Golgi-localised Wg
at onset of experiment
Dorsal
Ventral

this system is brought back into equilibrium would apical extracellular Wg levels return to those of the wild type. It appears that our experimental timeframe is not long enough for this to happen. These discrepancies highlight the importance of having multiple different methods to address the same question.

A less invasive technique to explore Wg trafficking was to produce a step of tagged Wg in the secretory pathway and follow its movement over time. Though effective, this method comes with some different caveats of its own. Hh-Gal4 UAS-Flp produces heterogeneous expression of Wg-HA. This is not such a problem at early timepoints, however, at later timepoints it means that a given disc may harbour multiple cells where Wg-HA has begun to be expressed at different times. We were fortunate that the expression and movement of Wg-HA happens quite rapidly so there is not a vast variation between Wg expressing cells, but this must be kept in mind for all these experiments.

Another challenge associated with any high-resolution study of trafficking in Wg secreting cells stems from their shape. These cells have a relatively wide apical surface and a narrow basolateral tip. Wg is present at higher levels in the apical region than at the basolateral surface, so the combination of lower Wg signal basally and a smaller basolateral area of the cells makes it difficult to visualise both surfaces at a given setting. This is further complicated when the Wg-HA signal is very weak as is the case for early timepoints. Therefore, sometimes Wg-HA may be present but undetectable in the basolateral region. For example, after 2hr at 29^{o}C in a total Wg-HA staining (Figure 4.9 B') expression appears to be mainly apical, but after 2hr in an extracellular Wg-HA staining (Figure 4.10 B) HA signal is observed on the basolateral surface of expressing cells. Therefore, there must be basolateral Wg present within 2hrs of induction, but this is not detectable with our staining and imaging protocols. This is a limitation I have been aware of throughout this project, and therefore realise that I can make no definitive statement about how long apical-basolateral movement of Wg-HA takes in these cells. I can only look

at the general flow of Wg-HA and comment accordingly. These variations in signal levels also mean that I have been unable to image all samples using the same confocal settings in my Wg-HA step experiments. The Wg-HA signal would either be undetectable or over saturated according to which settings I chose. This means again I am unable to comment on actual intensity of any of the images relative to each other, only on patterns of localisation observed.

I have attempted to remedy both the heterogeneity of Flp expression and differences in the imaging settings between samples by generating an unbiased sample of images and quantifying Wg-HA production across either the XY or YZ axis. I averaged different stop cassette excision events to ensure that the general trend over a larger number of cells and discs was fairly represented. This has also allowed me to even out late timepoint discrepancies resulting from multiple independent stop cassette excision events. Absolute intensity level gives no information in this context, since all samples were imaged using different settings. However, analysing the apical/basolateral distributions generated from these images can give us information about the trends these samples are following. Indeed such analysis corroborates the representative images shown.

Ultimately, in this chapter I have combined the use of both classical tools (*shibire*^{ts} mutant larvae) and the novel inducible Wg-HA system produced in Chapter 3 to explore Wg movement in expressing cells. Using a step of tagged Wg-HA produced at endogenous levels, I was able to determine the apical to basolateral movement of Wg within expressing cells. This is supported by data obtained from *shibire*^{ts} mutant discs, which upon an endocytic block show apical extracellular Wg accumulation, and by utilising the reversibility of this system I have also gathered evidence to suggest that this apical extracellular pool of Wg forms the basolateral extracellular Wg gradient. Thus multiple techniques lead to the same conclusion that Wg is first delivered to the apical surface, and then transcytosed to the basolateral surface for release.

Chapter Five

What role does Evi play in Wg trafficking and transcytosis?

5.1 Introduction

As discussed in previous chapters, I have provided evidence to suggest that Wg undergoes apical to basolateral movement through the secretory pathway in expressing cells. This route may have developed to facilitate movement of Wg from the site of its production (the apical region of expressing cells), to the site of Wg release (the basolateral surface of expressing cells). Evi is an important regulator of Wg trafficking and secretion (Banziger et al., 2006; Bartscherer et al., 2006). It has been suggested in the literature that Wg and Evi meet in the ER, and that Evi is required for the correct trafficking of Wg for release (Yu et al., 2014). Once Wg is released, Evi is recycled in a retromer-mediated fashion to the Golgi (Belenkaya et al., 2008; Franch-Marro et al., 2008b; Port et al., 2008), from whence it traffics back to the ER for another round of Wg transport to the cell surface (Figure 1.6) (Yu et al., 2014). This basic model may be over-simplified, as it does not take into account epithelial cell polarisation. With the new tools developed in Chapter 3, I aim to elucidate the role that Evi plays in Wg trafficking within producing cells. Using extracellularly tagged Evi, it can be determined for the first time where these proteins separate, and whether Evi spreads with Wg to form the gradient. I also want to determine what role (if any) Evi may play in Wg transcytosis.

5.2 Results

5.2.1 Extracellular Evi does not spread across the tissue with Wg to form the gradient.

As discussed in Chapter 3, I have created an extracellularly tagged *evi* BAC (Evi-EC3-glyOLLAS BAC) that expresses Evi-OLLAS at endogenous levels and fully rescues an *evi* null mutant (Figure 3.11). A very small amount of antibody raised against an extracellular region in Evi exists, however not enough is available for this to be considered a viable tool for Evi visualisation. The best available antibody for Evi is raised against an intracellular region therefore, it has not been possible to detect extracellular Evi localisation in the wing imaginal disc. Using Evi-OLLAS, I aim to determine both the extracellular distribution of Evi, and the relationship this may have with the distribution of extracellular Wg. If Wg and Evi spread across the tissue together there should be colocalisation of extracellular Wg and Evi forming the basolateral gradient. However, if Wg and Evi separate in the expressing cells, then Evi would not spread across the tissue with Wg.

In larvae harbouring both *wg{KO; Wg-Ex4-2HA}* and the Evi-EC3-glyOLLAS BAC, expression of Wg-HA and Evi-OLLAS is detected using the anti-HA and anti-OLLAS antibodies respectively (Figure 5.1 A-C). In a total staining, Wg-HA and Evi-OLLAS are seen to colocalise within the Wg expressing cells in a comparable fashion to the corresponding wild type proteins (Figure 5.1 C). As extracellular staining shows, Wg-HA spreads to form the basolateral gradient. However extracellular Evi-OLLAS remains on the surface of expressing cells and does not appear to spread (Figure 5.1 D). When the Wg expressing cells are marked using anti-Cut, extracellular Evi-OLLAS outlines these cells and does not spread to form a gradient (Figure 5.1 E). Some signal is observed outside of the expressing cells using the anti-OLLAS antibody. However, this is probably due to unspecific background from the antibody as suggested by the analysis of

discs expressing Evi RNAi, described below. The Evi BAC was recombined onto an *evi* null mutant chromosome so that Evi-EC3-glyOLLAS was the only source of Evi. In these larvae, Evi RNAi was expressed in the P compartment of wing discs using En-Gal4, and Evi-OLLAS was stained with anti-Evi and anti-OLLAS (Figure 5.2). Discs stained with the anti-Evi antibody display loss of Evi in the P compartment, indicating that the Evi RNAi is effective (Figure 5.2 A, B). Extracellular Evi-OLLAS signal was lost from the surface of the Wg expressing cells. However background OLLAS staining remained constant across the disc (Figure 5.2 C, D). This indicated that the extracellular OLLAS staining observed outside the Wg expressing cells is not Evi-dependent and therefore is not 'real' staining.

It can be concluded therefore, that Evi does not spread with Wg to form the gradient. Extracellular Evi is only detected on the surface of Wg expressing cells suggesting that Wg and Evi separate there for Wg release.

Figure 5.1: Extracellular Evi does not move with Wg to form the gradient.
(A) An attP site was integrated in the *wingless* locus to create a null allele (wg^{KO}). A tagged cDNA was then inserted in the attP site to make *wg{KO; Wg-Ex4-2HA}* flies. (B) An OLLAS tag was inserted in EC Loop 3 in a 80kb *evi* BAC. This was recombined with a null allele of *evi* (evi^{2}) so the only Evi expressed is tagged. Total and extracellular Wg-HA and Evi-OLLAS were detected using anti-HA and anti-OLLAS antibodies respectively. Basolateral confocal sections are shown. Reconstructed YZ sections are oriented so that the apical surface is to the top. (C) Tagged Wg-HA and Evi-OLLAS recapitulate the localisation of wild type Wg and Evi (Figure 3.11). (D) Extracellular Evi-OLLAS is only detected on the surface of Wg expressing cells and does not spread from secreting cells with Wg-HA. (E) Extracellular Evi-OLLAS is seen only on the basolateral surface of the Wg expressing cells as marked by anti-Cut. Scale bars are shown on relevant panels.

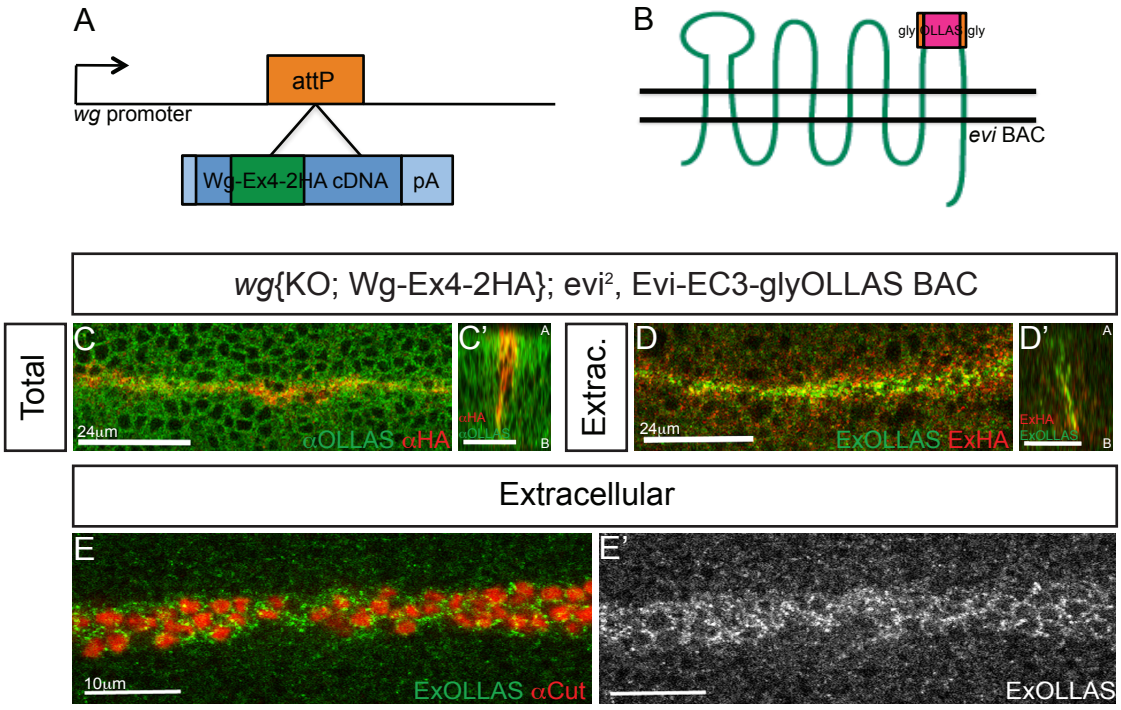
A
attP
wg promoter
Wg-Ex4-2HA cDNA
pA
B
glyOLLASgly
evi BAC
wg{KO; Wg-Ex4-2HA}; evi², Evi-EC3-glyOLLAS BAC
Total
C
24µm
αOLLAS αHA
C'
A
B
Extrac.
D
24µm
ExOLLAS ExHA
D'
ExHA
ExOLLAS
Extracellular
E
10µm
ExOLLAS αCut
E'
ExOLLAS

Figure 5.2: Extracellular Evi-OLLAS is only detected on the surface of Wg expressing cells; there is no uniform staining across the disc.

En-Gal4 was used to express UAS-Evi RNAi to knock down Evi expression in the P compartment. The only source of Evi in these discs comes from the Evi-EC3-glyOLLAS BAC, which has been recombined with the *evi (evi^{2})* mutant. 3rd instar larvae were fixed and stained with either anti-Evi to determine knockdown levels, or extracellular anti-OLLAS. (A, B) Total Evi staining shows knockdown of Evi in the posterior compartment of wing discs expressing UAS-Evi RNAi. (C, D) Extracellular OLLAS signal at the surface of Wg expressing cells disappears while low-level signal throughout the disc does not. I conclude the later represents non-specific background. Scale bars are shown on relevant panels.

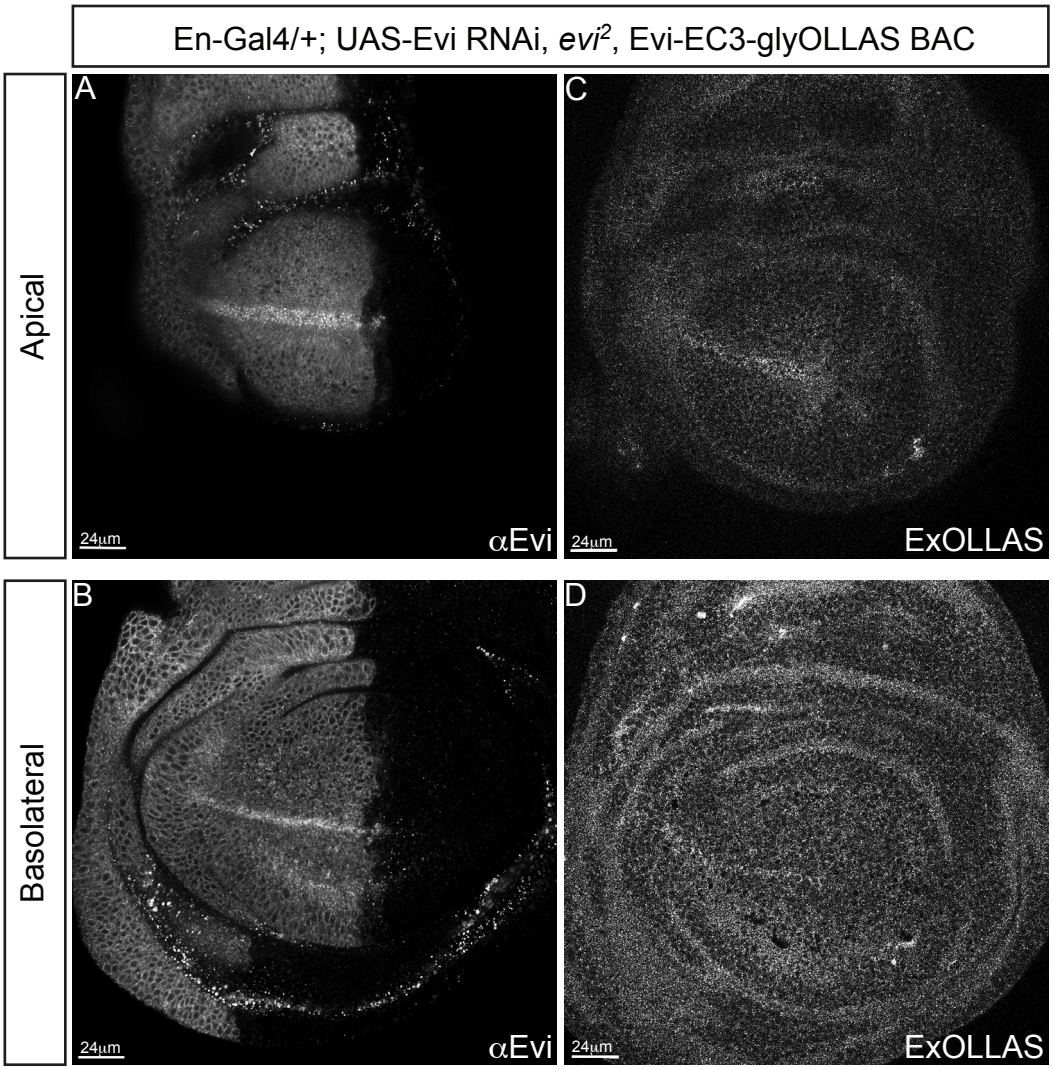
En-Gal4/+; UAS-Evi RNAi, evi2, Evi-EC3-glyOLLAS BAC
Apical
Basolateral
A
B
C
D
24μm
αEvi
ExOLLAS

5.2.2 Endocytosis of Evi may be required for Wg gradient formation.

As shown above, Evi is not released with Wg at the basolateral surface of expressing cells. This implies that Wg and Evi separate in the secretory pathway within the expressing cells. I wanted to determine where this separation might occur, so decided to explore whether Evi was required for the transcytotic movement of Wg. According to previous data shown in Chapter 4, there is probable endocytosis of Wg from the apical surface of expressing cells. If Evi were involved in this step then endocytosis of Evi would also be important for basolateral release of Wg and therefore gradient formation.

Thus, according to one scenario, Evi and Wg would co-traffic from the ER to the apical surface and part ways there. Alternatively, these two proteins could be co-internalised from the apical surface (presumably through an endocytic signal in Evi) and traffic together to the basolateral surface where Wg would be released. According to the first scenario, overexpression of endocytosis deficient Evi should fully rescue the Wg secretion defect present in *vps35*$^{-/-}$ mutant discs, relieving both the accumulation of Wg in the secretory pathway and guiding subsequent transport to the basolateral surface for gradient formation. However, according to the second alternative, Wg (and Evi) would accumulate at the apical surface in the same experimental condition. I therefore created UAS-Evi-ECD8V5, which is expected to bind Wg through the predicted N-terminal Evi binding site (Coombs et al., 2010) while lacking the other domains of Evi, including those that presumably mediate endocytosis. I also constructed UAS-Evi-FLV5, encoding full length tagged Evi as a control (Franch-Marro et al., 2008b). Both constructs were expressed in a *vps35*$^{-/-}$ background and the effect on intracellular and extracellular Wg was assayed. Both constructs are inserted at the same genetic locus using the attP/B system to avoid position effects.

I generated imaginal discs with P compartments that are *vps35*$^{-/-}$ mutant and overexpress UAS-Evi-FLV5 or UAS-Evi-ECD8V5. Total or extracellular anti-Wg was used to detect the extent of Wg trafficking rescue. A total Wg staining in

a *vps35*$^{-/-}$ mutant highlights the Wg secretion block in the P compartment as expected (Figure 5.4 A). This is rescued by overexpression of UAS-Evi-FLV5 (Figure 5.4 B) consistent with reports in the literature (Franch-Marro et al., 2008b). In addition Wg release from secreting cells is also restored (Figure 5.4 B). By contrast, overexpression of UAS-Evi-ECD8V5 does not rescue the Wg secretion block, or the basolateral release (Figure 5.4 C). Extracellular staining shows that surprisingly overexpression of UAS-Evi-FLV5 or UAS-Evi-ECD8V5 partially rescues the extracellular Wg gradient (Figure 5.4 D, E).

Unfortunately, within this experimental set up there are some fundamental problems. Neither overexpression construct has a tag inserted in an extracellular position, so I have been unable to ascertain whether UAS-Evi-ECD8V5 is truly endocytosis deficient via an extracellular staining or antibody uptake assay. If endocytosis of this construct occurs this may account for the partial rescue of the extracellular Wg gradient in a *vps35*$^{-/-}$ mutant by Evi-ECD8V5 overexpression. Addition of a CD8 domain to UAS-Evi-ECD8V5 may also alter the trafficking route taken by this construct through the secretory pathway compared to endogenous Evi. Insertions in the C-terminal region of Evi (similar to UAS-Evi-FLV5) have been shown to be an unsuitable region of tag insertion into the *evi* 80kb BAC (data not shown, C. Alexandre). This BAC could not rescue an *evi* null mutant. Therefore, tag placement may be affecting the ability of UAS-Evi-FLV5 to fully rescue the extracellular Wg gradient in a *vps35*$^{-/-}$ mutant. These issues are also compounded by the fact that this experiment involves overexpression, which as previously discussed creates problems of its own when observing protein secretion. To this end, I decided to adopt a different approach to explore the same question.

Figure 5.3: Experiment design to test the effect of Evi endocytosis on Wg gradient formation.

Overexpression constructs were designed to test the requirement for Evi endocytosis in Wg gradient formation. (A) UAS-Evi-CD8V5 is a truncated version of Evi containing only the putative Wg binding domain, a CD8 domain and a C-terminal V5 tag. (B) UAS-Evi-FLV5 is a full-length version of Evi with a C-terminal V5 tag, which should undergo endocytosis. (C) In a *vps35* mutant, Wg secretion is impaired because Evi fails to undergo retromer recycling. Overexpression of UAS-Evi-FLV5 is expected to rescue this defect (B, C) as shown previously – (Franch-Marro et al., 2008b). Overexpression of the full-length protein overcomes the lack of retromer recycling since Evi is constantly supplied by new biosynthesis. By assessing whether the endocytosis deficient form of Evi (A) allows Wg trafficking to the basolateral surface, we will be able to assess whether Evi contributes to the apical to basolateral transport of Wg.

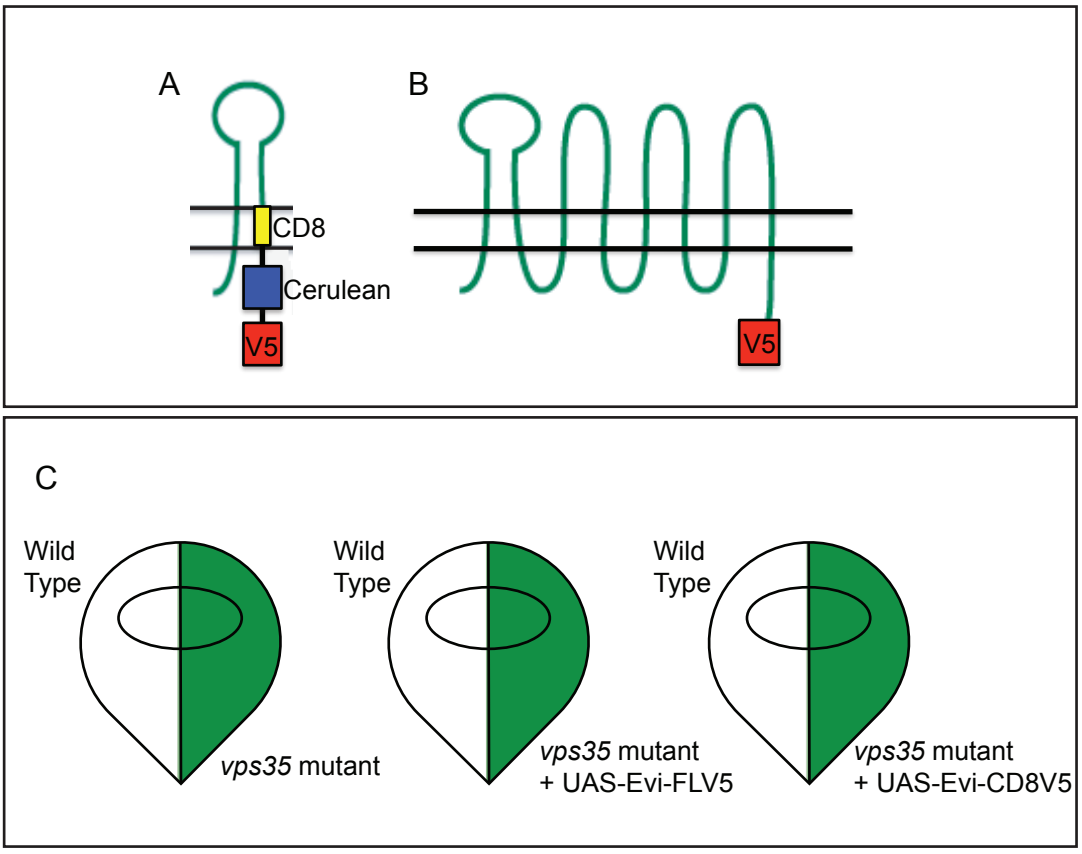
A
CD8
Cerulean
V5
B
V5
C
Wild
Type
vps35 mutant
Wild
Type
vps35 mutant
+ UAS-Evi-FLV5
Wild
Type
vps35 mutant
+ UAS-Evi-CD8V5

Figure 5.4: Overexpression of full length Evi-V5 rescues more effectively in a *vps35* mutant background than an endocytosis deficient form.

Genotypes are indicated above the images. Anti-Wg was used to recognise Wg and anti-V5 displays expression of the UAS-Evi constructs. Anti-β-gal labels wild type cells in the control half of the disc. Basolateral confocal sections are shown. Total Wg: (A) In *vps35* mutant P compartments (displayed by lack of β-gal) Wg secretion is impaired as indicated by build up in expressing cells (A'). (B) Overexpression of full length Evi-V5 rescues Wg gradient formation in a *vps35* mutant (B') compared to the relevant control (A'). (C) Overexpression of endocytosis deficient Evi-V5 (Evi-CD8V5) in a *vps35* mutant background does not fully rescue the Wg gradient (C'). Wg is still retained within expressing cells (C') but the phenotype is not as severe as a *vps35* mutant (A). Extracellular Wg: (D-E) Overexpression of both full length (D) and endocytosis deficient (E) Evi-V5 partially rescues extracellular Wg gradient formation. Scale bars are shown on relevant panels, they represent 36um.

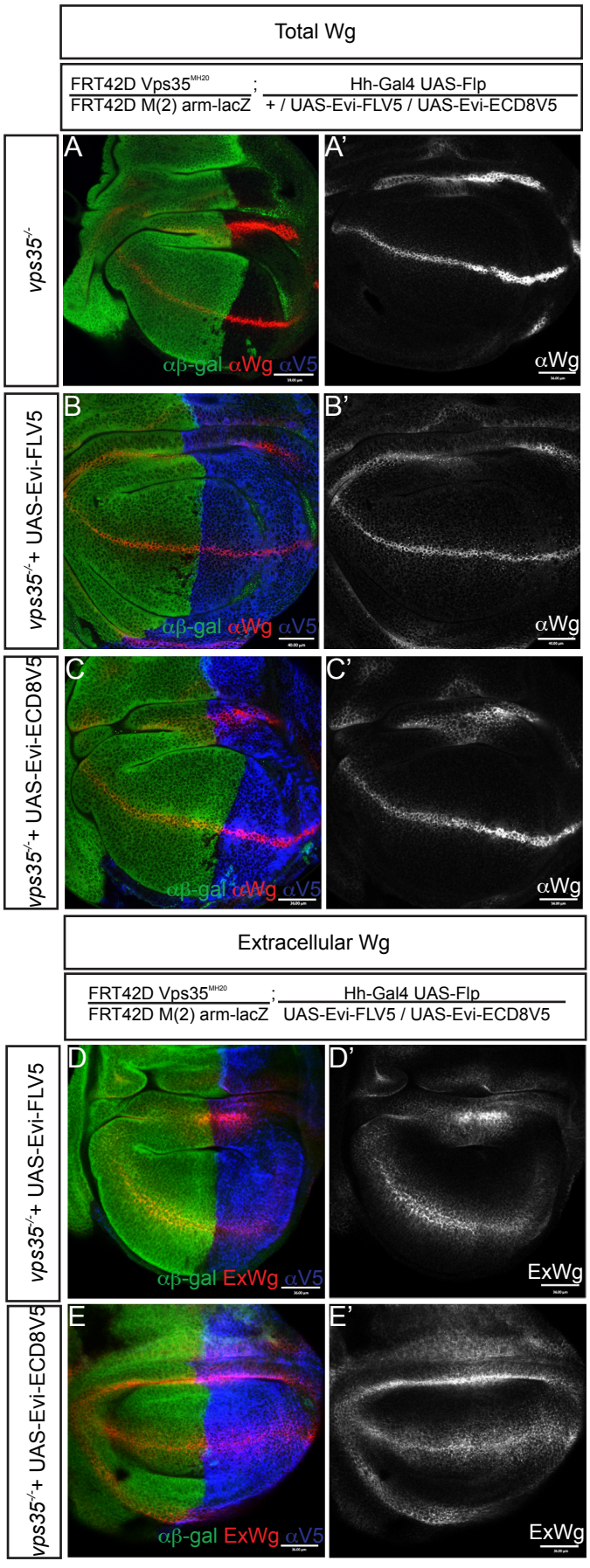
Total Wg
FRT42D Vps35MH20 / FRT42D M(2) arm-lacZ ; Hh-Gal4 UAS-Flp / + / UAS-Evi-FLV5 / UAS-Evi-ECD8V5
vps35-/-
A
αβ-gal αWg αV5
A'
αWg
vps35-/- + UAS-Evi-FLV5
B
αβ-gal αWg αV5
B'
αWg
vps35-/- + UAS-Evi-ECD8V5
C
αβ-gal αWg αV5
C'
αWg
Extracellular Wg
FRT42D Vps35MH20 / FRT42D M(2) arm-lacZ ; Hh-Gal4 UAS-Flp / UAS-Evi-FLV5 / UAS-Evi-ECD8V5
vps35-/- + UAS-Evi-FLV5
D
αβ-gal ExWg αV5
D'
ExWg
vps35-/- + UAS-Evi-ECD8V5
E
αβ-gal ExWg αV5
E'
ExWg

5.2.3 An endocytosis block causes accumulation of apical Evi, which colocalises with apical extracellular Wg.

To revisit the requirement for Evi endocytosis in Wg gradient formation I decided to adopt a similar approach to that used in Chapter 4, using *shibire^{ts}* to block endocytosis. Any effect on total and extracellular Evi localisation may give some indication of the surfaces where Evi transits, and how these relate to the position of Wg in the same experimental settings.

In this experiment discs are both mutant for *shibire^{ts}* and express the Evi-EC3-glyOLLAS BAC. When larvae have always been at the permissive temperature of 18^{o}C, total Evi-OLLAS staining is uniform across the disc, except in the Wg expressing cells where it is more abundant (Figure 5.5 A-D). In the Wg expressing cells, extracellular Evi-OLLAS is found mainly on the basolateral surface (Figure 5.5 I-J). Although a small amount of apical signal can also be detected (Figure 5.5 I', J'). Upon endocytosis block, basolateral enrichment of total Evi-OLLAS is lost, and Evi-OLLAS accumulates in the apical region of expressing cells (Figure 5.5 E-H). Extracellular Evi-OLLAS is seen around the whole Wg expressing cell (Figure 5.5 K-L), with a particularly high signal at the apical surface (Figure 5.5 K').

To explore the role of endocytosis in Wg and Evi localisation further, I introduced Wg-HA (*wg{KO; Wg-Ex4-2HA}*) and Evi-OLLAS (Evi-EC3-glyOLLAS BAC) into the *shibire^{ts}* mutant background. In discs that have always been at the permissive temperature of 18^{o}C, extracellular Wg-HA and extracellular Evi-OLLAS are observed predominantly on the basolateral surface of the Wg expressing cells (Figure 5.6 C, D). As expected, faint presence of Wg-HA and Evi-OLLAS can be observed on the extracellular apical surface of the expressing cells, however this is much lower than at the basolateral surface (Figure 5.6 A, B). As described previously, extracellular Wg-HA spreads to receiving cells on the basolateral surface, whereas extracellular Evi-OLLAS remains associated with the Wg expressing cells (Figure 5.6 D). Upon shifting to 34^{o}C, both extracellular Wg-HA and extracellular Evi-OLLAS accumulate and colocalise at

the apical surface of Wg expressing cells (Figure 5.6 E, F). Extracellular Evi-OLLAS is also present on the basolateral extracellular surface of the Wg expressing cells, whereas extracellular Wg-HA is not (Figure 5.6 G, H). This is consistent with results described in Chapter 4, indicating that the basolateral extracellular Wg gradient is lost upon an endocytosis block (Figure 4.3). However, extracellular Evi-OLLAS remains on the basolateral surface even after 1hr without endocytosis. This is consistent with the scenario that upon reaching the basolateral surface of expressing cells, Evi is not released with Wg and that it is also not recycled to the Golgi (then ER) because of the endocytic block.

Figure 5.5: In response to an endocytosis block total Evi accumulates throughout discs, while extracellular Evi accumulates only on the surface of the Wg expressing cells.

All larvae were *shibire*^{ts};;Evi-EC3-glyOLLAS BAC/+. Total Evi was detected using either the anti-Evi or anti-OLLAS antibody, extracellular Evi was detected using the anti-OLLAS antibody. (A-D) At the permissive temperature, total Evi is observed throughout discs with marked additional signal in Wg expressing cells especially in the basolateral region (C', D). (E-H) After 1hr endocytosis block, Evi accumulates in the apical region of the Wg expressing cells (E-F) at higher levels than at the permissive temperature (A-B). This is observed both with the anti-Evi antibody (E') and with the anti-OLLAS antibody (F). Basolateral enrichment of Evi within expressing cells is lost (G-H). (I-J) At the permissive temperature, extracellular Evi is exclusively on the apical and basolateral surfaces of the Wg expressing cells, with particular enrichment basolaterally (J). (K-L) After 1hr endocytosis block, extracellular Evi accumulates on the surface of the Wg expressing cells from the apical to basolateral surface (K, L). Elevated basolateral extracellular Evi is observed (L, L') compared to the situation at the permissive temperature (J'). Extracellular Evi is also accumulated at the apical surface (K, K'). Scale bars represent 24um.

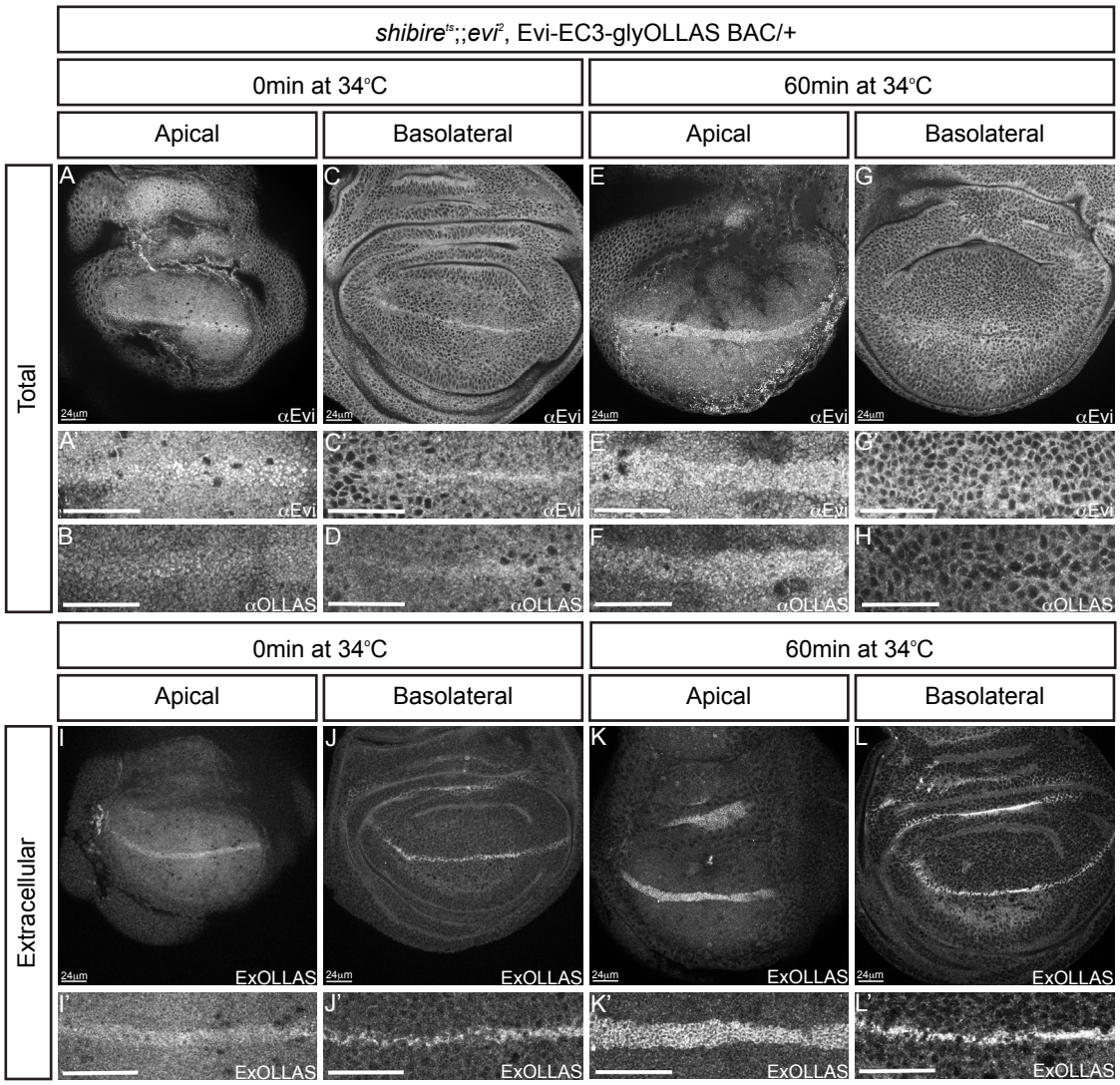
shibire^ts;;evi^2, Evi-EC3-glyOLLAS BAC/+
0min at 34°C
60min at 34°C
Apical
Basolateral
Apical
Basolateral
Total
A
C
E
G
24μm
αEvi
A'
C'
E'
G'
αEvi
B
D
F
H
αOLLAS
0min at 34°C
60min at 34°C
Apical
Basolateral
Apical
Basolateral
Extracellular
I
J
K
L
24μm
ExOLLAS
I'
J'
K'
L'
ExOLLAS

Figure 5.6: Endocytosis block causes accumulation of both extracellular Wg and Evi mainly at the apical surface of expressing cells.

All discs are *shibire*^{ts} mutant and express tagged forms of Wg and Evi. 3rd instar larvae were shifted to the restrictive temperature for the time indicated and then fixed and stained for extracellular Wg-HA and Evi-OLLAS using anti-HA and anti-OLLAS antibodies. (A-D) At the permissive temperature, extracellular Wg-HA and Evi-OLLAS are predominantly found on the basolateral surface (C-D''). Extracellular Wg-HA spreads to form a gradient (D') whereas extracellular Evi-OLLAS is restricted to the surface of the Wg expressing cells (D, D''). A small amount of apical extracellular Wg and Evi can be observed (A-B''), but at much lower levels than at the basolateral surface. (E-H) After a 1hr endocytosis block, both extracellular Wg-HA and extracellular Evi-OLLAS accumulate on the apical surface of Wg expressing cells (E-F'') at a much higher level than pre-block (A). The two proteins also appear to colocalise at the cell surface (E, F). Extracellular Evi-OLLAS accumulates on the lateral and basolateral surfaces of the expressing cells (G, H, H'') whereas the majority of extracellular Wg-HA has spread (H'). Residual extracellular Wg-HA at the surface of Wg expressing cells appears to coincide with extracellular Evi-OLLAS (H-H''). Scale bars represent 24um.

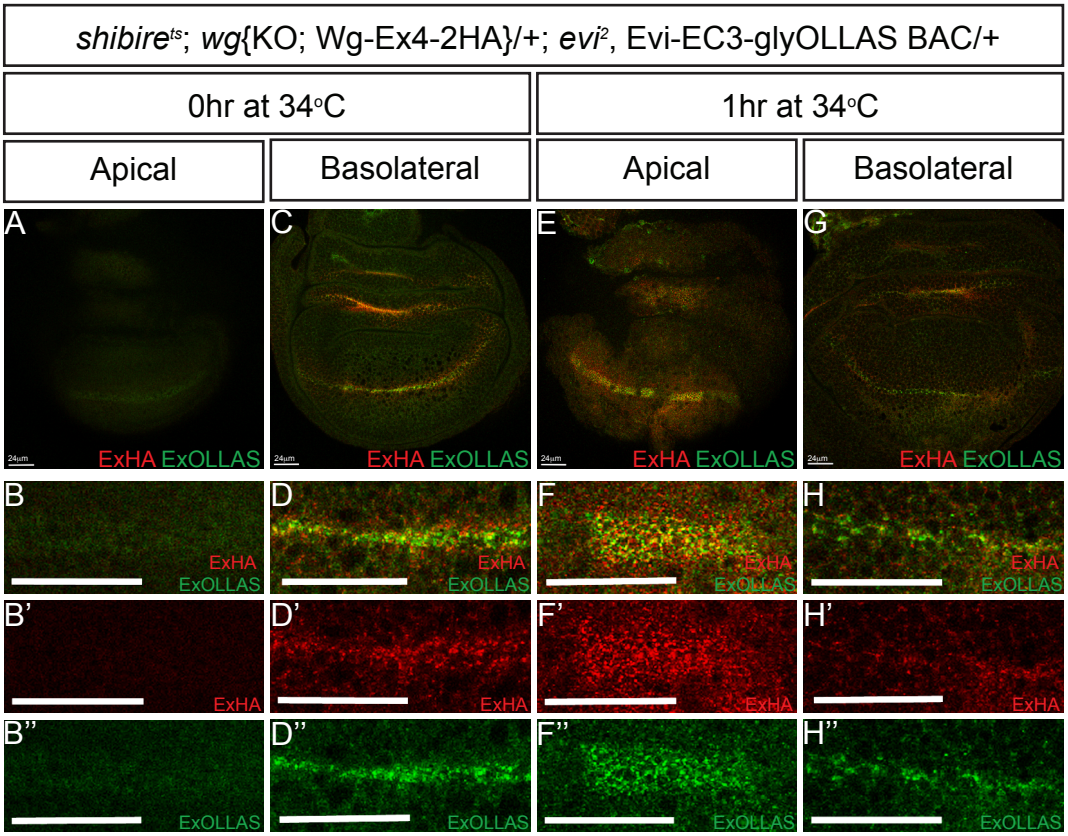
shibire^ts; wg{KO; Wg-Ex4-2HA}/+; evi^2, Evi-EC3-glyOLLAS BAC/+
0hr at 34°C
1hr at 34°C
Apical
Basolateral
Apical
Basolateral
A
C
E
G
24um
ExHA ExOLLAS
B
D
F
H
ExHA
ExOLLAS
B'
D'
F'
H'
ExHA
B''
D''
F''
H''
ExOLLAS

5.2.4 Upon release of the endocytosis block, the accumulation of extracellular Evi subsides.

As described above, Evi may be endocytosed along with Wg from the apical surface of expressing cells to reach the basolateral surface. I suggest that Evi could be endocytosed without Wg from the basolateral surface to allow recycling to the Golgi (and then ER). Using a similar approach to that used in Chapter 4, I capitalised on the reversibility of *shibire*^{ts} to assess the behaviour of extracellular Evi upon the release of the endocytic block (at 18^{o}C). According to my model, the apical accumulation of Evi should subside. Moreover, if basolateral Evi is recycled, release of the endocytic block should lead to a transient decrease in basolateral extracellular Evi. This would then later become replenished as apical Evi reaches the basolateral surface via transcytosis.

All experiments were conducted in *shibire*^{ts} discs expressing the Evi-EC3-glyOLLAS BAC. After a 60min endocytosis block at 34^{o}C an accumulation of extracellular Evi-OLLAS is observed both apically and basolaterally (Figure 5.7 B). After a 30min chase at 18^{o}C, the apical accumulation of extracellular Evi has disappeared and basolateral extracellular Evi levels also appear reduced (Figure 5.7 C). Replenishment of the basolateral extracellular Evi pool then occurs over time (60min, 90min chase) (Figure 5.7 D, E). In the time course of this experiment, levels of apical extracellular Evi do not return to pre-block levels (Figure 5.7 A, E). However, they have decreased relative to when endocytosis is blocked (Figure 5.7 B, E). These observations are quantified in graphical form in Figure 5.7 F. Quantification supports the observations shown in Figure 5.7 B, that apical extracellular Evi has risen after a 60min endocytosis block (Figure 5.7 F). Upon release of this block, apical extracellular Evi decreases but has not returned to pre-block levels within 90min (Figure 5.7 F). A decrease in basolateral extracellular Evi is also observed after endocytic block release (Figure 5.7 F). Levels of basolateral extracellular Evi are lowest after

30min at 18^{o}C, and expression has returned to levels comparable to 0min after 90min (Figure 5.7 F).

These results support the predictions of our working model. Upon an endocytic block at 34^{o}C extracellular Evi accumulates apically, but this subsides upon release of the block. Release of this block also causes a decrease in accumulated basolateral extracellular Evi, which is most striking after 30min at 18^{o}C. In summary, the behaviour of Evi upon changes in endocytic activity is consistent with the suggestion that Evi undergoes the transcytotic step with Wg from the apical to basolateral surface of expressing cells.

Figure 5.7: Release of an endocytic block leads to a relief of apically accumulated extracellular Evi and re-establishment of the basolateral Evi pool on the surface of Wg expressing cells.

All larvae were *shibire*^{ts};; Evi-EC3-glyOLLAS BAC/+ and extracellular Evi-OLLAS was detected using the anti-OLLAS antibody. Reconstructed YZ sections are oriented so that the apical surface is to the top. (A) At the permissive temperature, a small amount of extracellular Evi-OLLAS is detected apically (A) but the majority of extracellular Evi-OLLAS is observed on the basolateral surface (A') of Wg expressing cells. (B) After 60min at the restrictive temperature, extracellular Evi-OLLAS accumulates at the cell surface throughout the apical to basolateral axis (B), with particularly high signal at the very apical and basal ends (B''). (C) After a 30min chase at 18^{o}C, both the apical and basolateral accumulation subsides to reach a level that is lower than after 60min at 34^{o}C (B-B'') or at the permissive temperature throughout (A-A''). (D) After a 60min chase at 18^{o}C, extracellular OLLAS has almost returned to pre-block levels at the basolateral surface while it is still slightly elevated at the apical surface. (E) After a 90min chase at 18^{o}C, both the apical and basolateral Evi-OLLAS expression (E, E') appear to resemble those of the permissive temperature (A, A'). Data were pooled and quantified (n=3). Results are plotted in a graph in panel F. After a 60min endocytosis block the levels of extracellular Evi-OLLAS detected throughout the apical-basolateral axis of the cells is higher than all other samples (F). However, 30min after release, the levels of Evi dip below that of the permissive temperature (F) and after 60-90min these levels return to become comparable with the permissive temperature (F). Scale bars for XY views represent 24um, YZ views (A'',B'',C'',D'',E'') represent 19um.

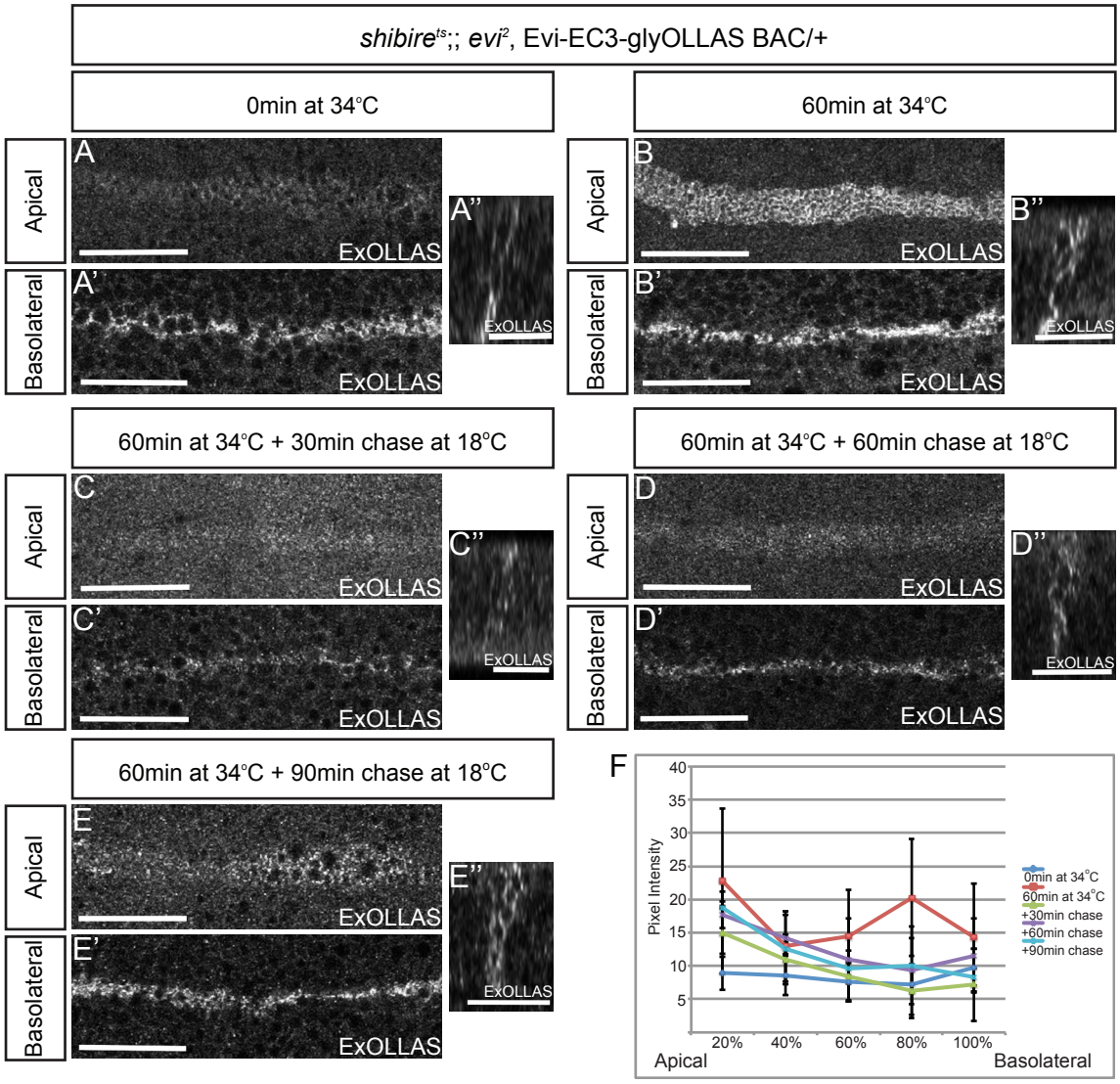
shibire^ts;; evi^2, Evi-EC3-glyOLLAS BAC/+
0min at 34°C
60min at 34°C
60min at 34°C + 30min chase at 18°C
60min at 34°C + 60min chase at 18°C
60min at 34°C + 90min chase at 18°C
Apical
Basolateral
A
A'
A''
B
B'
B''
C
C'
C''
D
D'
D''
E
E'
E''
ExOLLAS
F
Pixel Intensity
0min at 34°C
60min at 34°C
+30min chase
+60min chase
+90min chase
20%
40%
60%
80%
100%
Apical
Basolateral

5.2.5 Creating a construct allowing simultaneous production of tagged Wg and Evi.

It has been proposed that Wg and Evi bind in the ER and move from there to the cell surface (Yu et al., 2014). As already indicated our data suggest that Wg and Evi dissociate on the basolateral surface of expressing cells. However, this remains to be proven. It is therefore essential to further explore the trafficking route taken by Wg and Evi in expressing cells, especially where they join and separate.

To follow Wg and Evi simultaneously, I devised a system to produce the two proteins from the same transcript – The 2A system (Trichas et al., 2008). With this system, as the ribosome reaches the final amino acids of the 2A sequence (Asn-Pro-Gly-Pro) a peptide bond fails to form between the final Gly and Pro, and the ribosome "skips" to the next codon creating a "cleavage" and two separate proteins are produced (Trichas et al., 2008). Using this, Wg and Evi will be expressed at the same time and at the same levels. I inserted cDNAs encoding Wg-Ex4-HA and Evi-EC3-OLLAS on either side of the 2A site in a *Drosophila* cell culture expression vector (pMT) (Figure 5.8 A, B). Wg-Ex4-HA and Evi-EC3-OLLAS were inserted in either order (Figure 5.8 A, B). The order of protein insertion may prove to be important because a feature of the 2A system is that the short 2A sequence remains attached to the C-terminus of the first protein during translation, whereas the second protein remains unmodified (Trichas et al., 2008). Therefore, if either protein is sensitive to modification at its C-terminus it may require placing in the second position of this construct.

Induction of pMT-Wg-Ex4-HA-2A-Evi-EC3-OLLAS led to expression of Evi-EC3-OLLAS, but not Wg-Ex4-HA (Figure 5.8 C). However, with pMT-Evi-EC3-OLLAS-2A-Wg-Ex4-HA, both tagged proteins were expressed (Figure 5.8 D). Evi-OLLAS mainly localised to cell membranes while Wg-HA was observed in intracellular puncta with occasional colocalisation with Evi-OLLAS (Figure 5.8 D).

Further modifications were made to the pMT-Evi-EC3-OLLAS-2A-Wg-Ex4-HA (Figure 5.8 B) construct to allow controlled expression in transgenic flies (Figure 5.8 E). An FRT-flanked Cerulean-containing stop cassette was inserted in front of Evi-EC3-OLLAS-2A-Wg-Ex4-HA and the whole construct was inserted downstream of the ubiquitous actin promoter (Figure 5.8 E). Unfortunately, no expression of Cerulean could be detected in transgenic flies. Moreover excision of the stop cassette with En-Gal4 UAS-Flp did not trigger expression of Evi-OLLAS or Wg-HA. Since Evi-OLLAS and Wg-HA were expressed in S2 cells I conclude that somehow, a fault lies in the actin promoter and/or the stop cassette. However, others have successfully used the actin promoter in the lab suggesting that it may most likely be a problem with the stop cassette.

I therefore modified the construct as follows (Figure 5.8 E). An FRT-Plum pA-FRT stop cassette was exchanged for the Cerulean cassette in the hope that Plum would be detectable, as Cerulean is often poorly detectable in transgenic flies (personal communication, I. Salecker). There is also a possibility that in my initial construct upon stop cassette excision there may not be enough space between the promoter and the start of the *evi* cDNA for proper transcription to be initiated. Consequently, the 5'UTR of Evi was also inserted in front of the Evi-EC3-OLLAS-2A-Wg-Ex4-HA construct (Figure 5.9 A).

This newly modified actin-FRT-Plum pA-FRT-5'UTR-Evi-EC3-OLLAS-2A-Wg-Ex4-HA was transfected into *Drosophila* S2 R+ cells either with (Figure 5.9 C) or without (Figure 5.9 B) an actin-Flp plasmid. In the absence of Flp, no expression of Evi-OLLAS or Wg-HA is observed (Figure 5.9 B). In the presence of Flp, Evi-OLLAS and Wg-HA can be detected using the anti-OLLAS and anti-HA antibodies respectively indicating that stop cassette excision has occurred (Figure 5.9 C). This construct was then injected to make transgenic flies and combined with transgenics expressing Flp in the P compartment of the wing imaginal disc (Figure 5.9 D). Expression of Evi-OLLAS and Wg-HA was observed corroborating the results with S2 R+ cells (Figure 5.9 E). Evi-OLLAS can be

observed mainly at cell membranes, but also in intracellular puncta (Figure 5.9 E'') as is the case for endogenous Evi in wild type discs. However, expression of Wg-HA is at much lower levels than expected (Figure 5.9 E'). Localisation of Wg-HA appears to be correct as the majority of total Wg-HA is detected in the apical region of cells, which corresponds with wild type Wg (Figure 5.9 E').

In summary, I have created a construct that allows simultaneous Flp-dependent production of tagged Wg and Evi. However, this system requires further optimisation before it can be used to explore the question of where Wg and Evi separate in the secretory pathway.

Figure 5.8: Creating a construct that allows simultaneous production of tagged Wg and Evi.

(A, B) cDNAs encoding tagged Wg and Evi were linked with a 2A sequence and cloned into a pMT Cu^{2+} inducible vector (Trichas et al., 2008). Transfected *Drosophila* S2R+ cells were induced with Cu^{2+} to stimulate expression. Wg-HA and Evi-OLLAS were detected using the anti-HA and anti-OLLAS antibodies respectively. (C) Expression of Evi-OLLAS from pMT-Wg-Ex4-HA-2A-Evi-EC3-OLLAS is seen at the cell surface. However, Wg-HA is not produced at detectable levels (C). (D) When the pMT-Evi-EC3-OLLAS-2A-Wg-Ex4-HA construct is transfected into *Drosophila* S2R+ cells Evi-OLLAS is expressed marking the cell membranes and Wg-HA is also present in intracellular puncta (D). (E) Schematic of a vector for inducible expression of Evi-EC3-OLLAS-2A-Wg-Ex4-HA in transgenic flies An FRT-flanked Cerulean stop cassette was introduced before the transcriptional start. When intact the Cerulean stop cassette should be expressed under the control of the actin promoter. Expression of Flp will induce excision of the FRT flanked Cerulean and trigger expression of the Evi-EC3-OLLAS-2A-Wg-Ex4-HA module. Scale bars are shown on relevant panels.

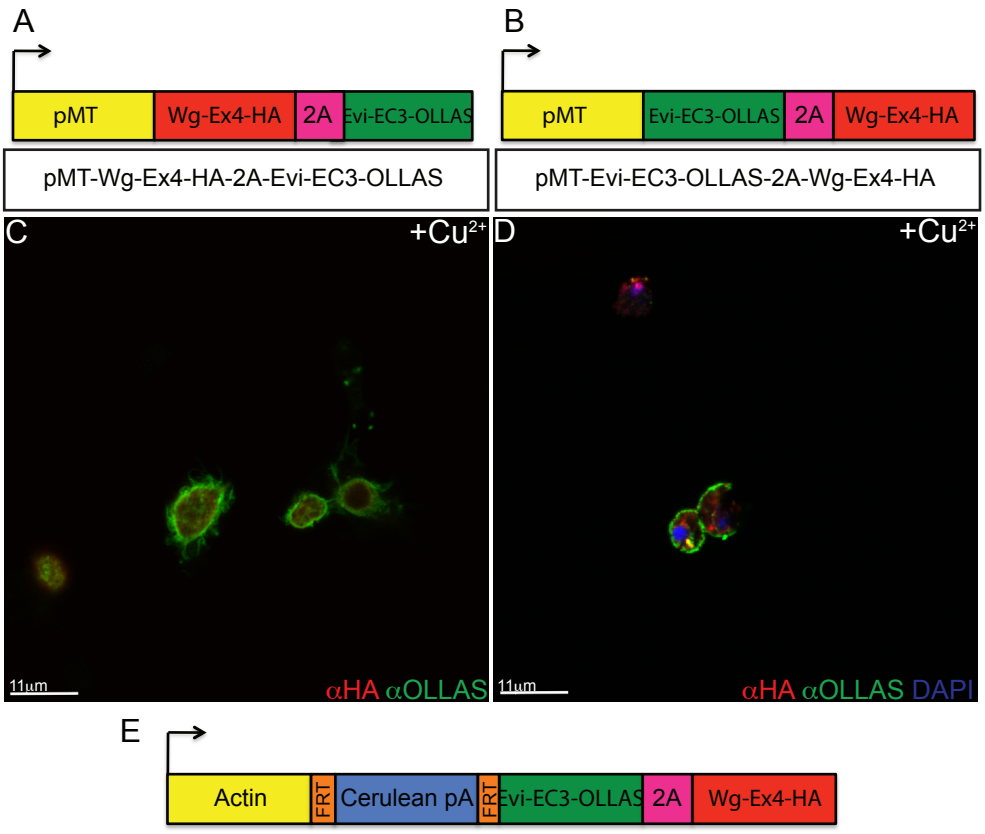
A
pMT
Wg-Ex4-HA
2A
Evi-EC3-OLLAS
pMT-Wg-Ex4-HA-2A-Evi-EC3-OLLAS
B
pMT
Evi-EC3-OLLAS
2A
Wg-Ex4-HA
pMT-Evi-EC3-OLLAS-2A-Wg-Ex4-HA
C
+Cu2+
11µm
αHA αOLLAS
D
+Cu2+
11µm
αHA αOLLAS DAPI
E
Actin
FRT
Cerulean pA
FRT
Evi-EC3-OLLAS
2A
Wg-Ex4-HA

5.9: Simultaneous expression of tagged Wg and Evi in vivo.

(A) Diagram of Actin-FRT-Plum-pA-FRT-5'UTR-Evi-EC3-OLLAS-2A-Wg-Ex4-HA construct for inducible expression of Evi-OLLAS and Wg-HA in transgenic flies and transfected cells. Wg-HA and Evi-OLLAS were detected using the anti-HA and anti-OLLAS antibodies respectively. Reconstructed YZ sections are oriented so that the apical surface is to the top. (B and C) The modified 2A construct was transfected into *Drosophila* S2R+ cells either with (C) or without (B) Actin-Flp. No Plum expression was observed in either sample (B and C). However, upon Actin-Flp co-transfection expression of Wg-HA and Evi-OLLAS was detected, indicating that stop cassette excision has occurred. Transgenic flies carrying this construct were crossed to flies expressing Flp in the P compartment. 3rd instar larvae of the indicated genotype were moved to 29^{o}C for 16hr to facilitate Flp expression. (D-E') Evi-OLLAS expression is similar to wild type (E''), however Wg-HA is expressed at lower levels than expected (E'). Scale bars are shown on relevant panels, scale bars for (E-E'') represent 20um.

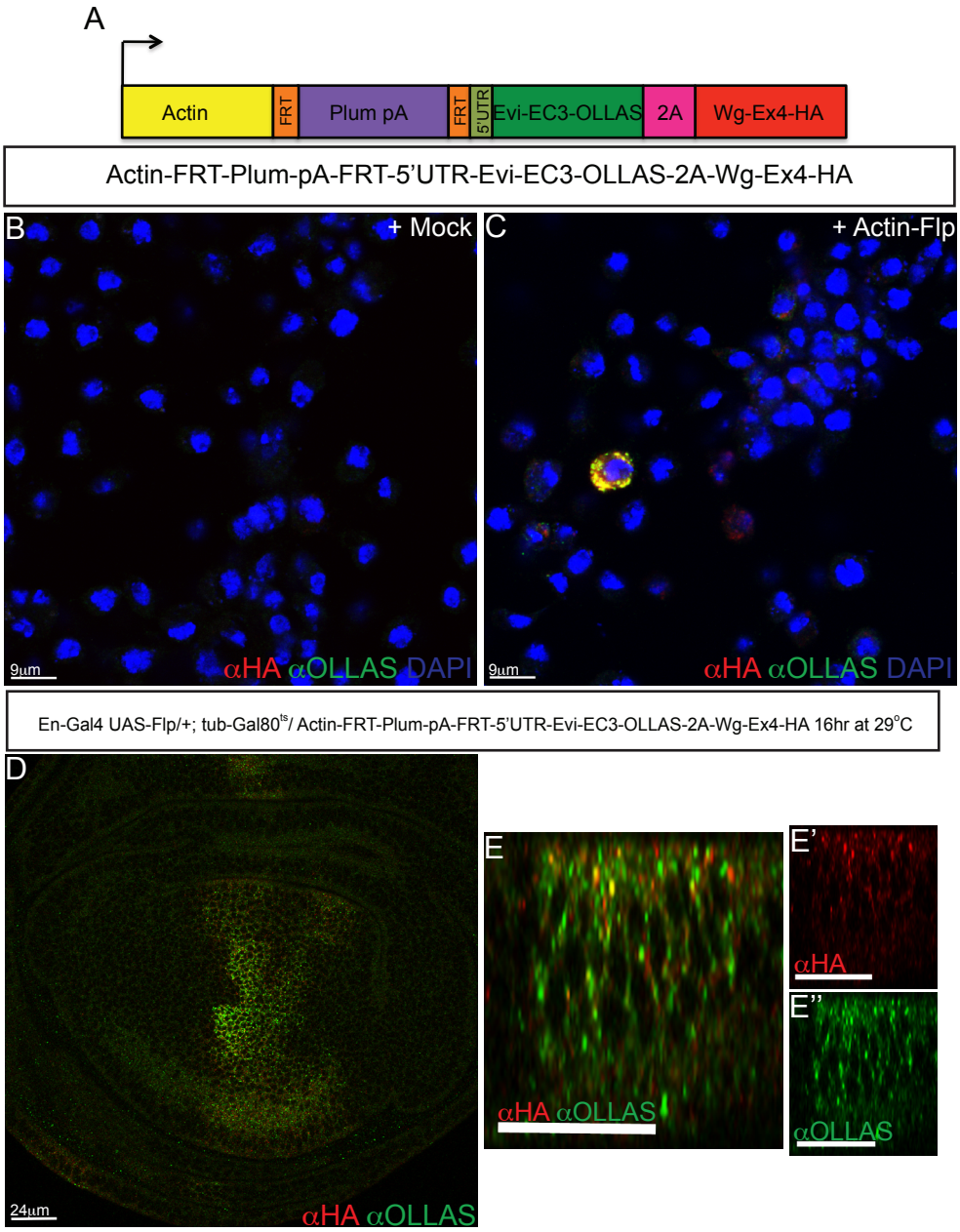
A
Actin
FRT
Plum pA
FRT
5'UTR
Evi-EC3-OLLAS
2A
Wg-Ex4-HA
Actin-FRT-Plum-pA-FRT-5'UTR-Evi-EC3-OLLAS-2A-Wg-Ex4-HA
B
+ Mock
9µm
αHA αOLLAS DAPI
C
+ Actin-Flp
9µm
αHA αOLLAS DAPI
En-Gal4 UAS-Flp/+; tub-Gal80ts/ Actin-FRT-Plum-pA-FRT-5'UTR-Evi-EC3-OLLAS-2A-Wg-Ex4-HA 16hr at 29°C
D
24µm
αHA αOLLAS
E
αHA αOLLAS
E'
αHA
E''
αOLLAS

5.2.6 Dlp and Dally HSPGs are not involved in Wg transcytosis.

Previous work has suggested that the HSPG Dlp is required for transcytosis of Wg to the basolateral surface of expressing cells (Gallet et al., 2008). Dlp is mainly known for its role in Wg gradient formation and spread (Baeg et al., 2004). Evidence for Dlp's involvement in transcytosis is based on assessing the distribution of overexpressed, tagged proteins (Gallet et al., 2008). Therefore, further exploration of this model is warranted. My own experimental results suggest that Evi is involved in Wg transcytosis, but it is possible that other factors could be involved. Therefore, I wanted to test the requirement of Dlp for Wg transcytosis.

Work from the Gallet et al. (2008) suggests that Dlp joins Wg on the apical surface of expressing cells and moves to the basolateral surface for Wg gradient formation. According to this model, if Dlp is the factor required for basolateral Wg movement, then in a $dlp^{-/-}$ mutant extracellular Wg should accumulate at the apical surface of expressing cells similar to what is seen with $shibire^{ts}$ at restrictive temperature.

In *Drosophila* two HSPGs have been reported to be involved in Wg gradient formation– Dlp and Dally (Han et al., 2005). Therefore to overcome potential redundancy, double $dlp^{-/-}$ and $dally^{-/-}$ mutant clones (marked by loss of GFP) were made in the disc. I confirmed that these double mutant clones do not contain any Dlp protein by staining the discs with anti-Dlp antibody (Figure 5.10 A). In mutant regions indicated by arrows no Dlp expression is detected by anti-Dlp (Figure 5.10 A'). This indicates that these clones are suitable to assess changes in extracellular Wg localisation. Within $dlp^{-/-}$ $dally^{-/-}$ mutant clones a subtle effect on basolateral extracellular Wg can be observed, with a slight reduction in spread (Figure 5.10 E). This is consistent with reports in the literature (Han et al., 2005; Strigini and Cohen, 2000). However, no apical extracellular Wg accumulation could be observed (Figure 5.10 C).

These results indicate that Dlp and Dally are not required for Wg transcytosis.

Figure 5.10: Dlp and Dally are not involved in Wg transcytosis.
Imaginal discs harbouring *dlp*$^{-/-}$ and *dally*$^{-/-}$ mutant clones are marked by loss of GFP. Clones were induced 48hr AEL and at 3rd instar larvae were dissected and stained for extracellular Wg with anti-Wg or for Dlp with anti-Dlp (A, A') No Dlp immunoreactivity is detected in mutant patches. Mutant regions are indicated with arrows. (B-E) Loss of Dlp and Dally has only a minor impact on extracellular Wg. In particular, extracellular Wg is mildly reduced on the basolateral surface (D-E') but appears unaffected at the apical surface (B-C'). Scale bars represent 24um.

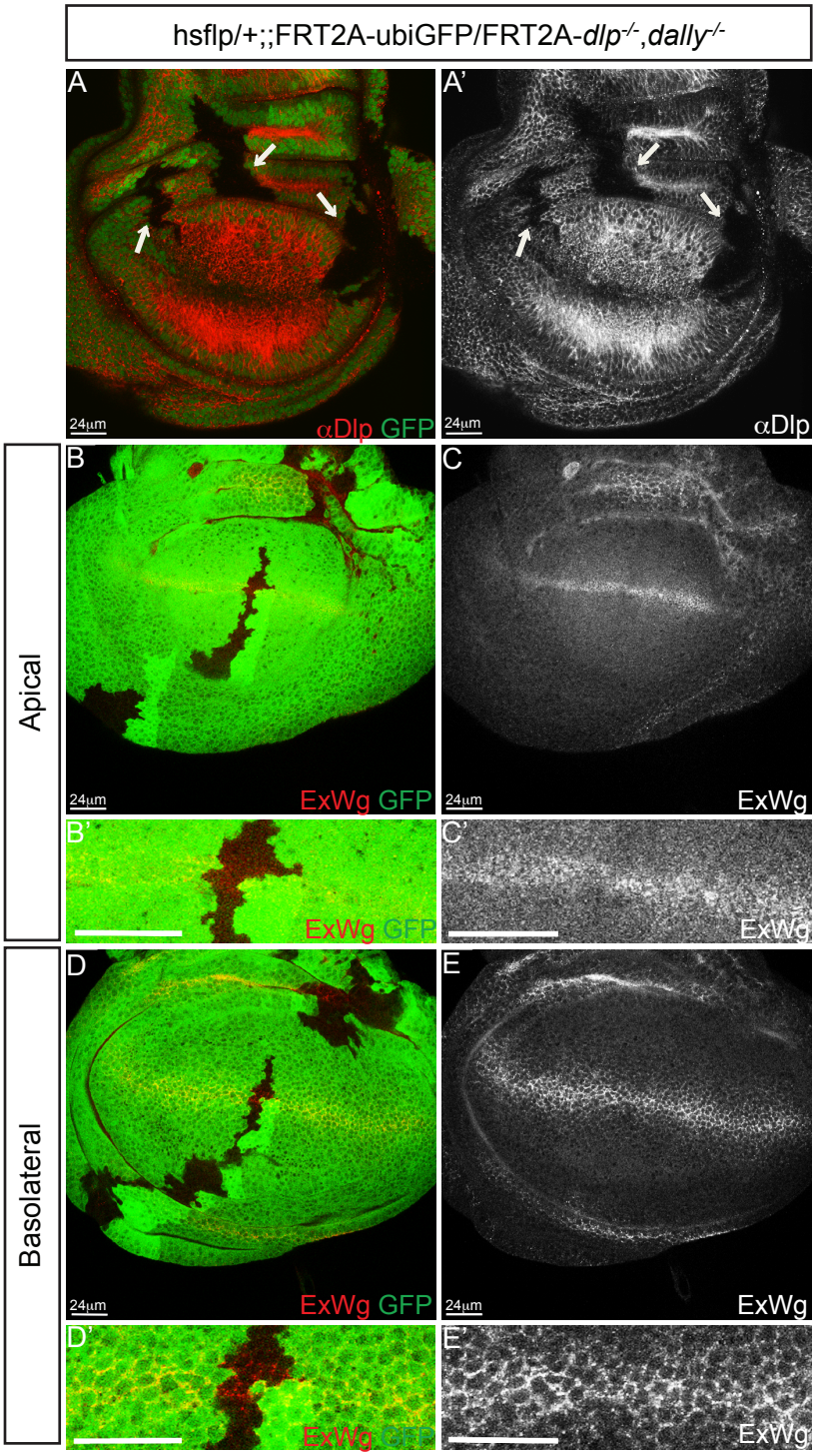
hsflp/+;;FRT2A-ubiGFP/FRT2A-dlp-/-,dally-/-
A
αDlp GFP
24μm
A'
αDlp
24μm
Apical
B
ExWg GFP
24μm
C
ExWg
24μm
B'
ExWg GFP
C'
ExWg
Basolateral
D
ExWg GFP
24μm
E
ExWg
24μm
D'
ExWg GFP
E'
ExWg

5.3 Discussion

In this chapter I have demonstrated that Evi is not released with Wg at the basolateral surface of Wg expressing cells. My data suggests that Evi undergoes apical endocytosis with Wg and that the two proteins could transcytose together to the basolateral surface. I suggest that they separate there, with Wg being released and Evi being recycled back to the Golgi (and then ER). I have also shown that Dlp is not required for Wg transcytosis, despite previous contrary suggestion by others.

The results presented in this chapter indicate the importance of extracellular protein detection. The extracellularly tagged Evi (Chapter 3), Evi-OLLAS expressed from the Evi-EC3-glyOLLAS BAC allowed me to show that extracellular Evi does not move with Wg to form the basolateral gradient. This finding has wider reaching implications for how we understand Wg release and spread since it contributed to the argument that Evi-containing exosomes are not important in Wg gradient formation in the wing disc (Beckett et al., 2013). Unfortunately, the anti-OLLAS antibody gives relatively high background with the extracellular staining protocol. This highlights the importance of tag and cognate antibody choice when devising tagged proteins. For my purposes I was unable to use an HA tag because this was used in the *wg{KO; Wg-Ex4-2HA}*. Moreover, a V5 tag impaired protein function (Figure 3.10), and the FLAG tag gives high background (unpublished observations), explaining why I settled for OLLAS.

The importance of extracellular tagging of proteins expressed at endogenous levels was also underlined in experiments utilising UAS-Evi-FLV5 and UAS-Evi-ECD8V5 (Figure 5.3 and 5.4). In this experiment, I aimed to design an endocytosis deficient version of Evi – UAS-Evi-ECD8V5, containing only the predicted Wg binding domain of Evi, the CD8 transmembrane domain and an intracellular tag (Figure 5.3 A). I expected the resulting protein to be

endocytosis deficient as it contains no predicted endocytosis motif, but this could not be demonstrated because of the absence of an extracellular tag. This experimental approach suffered from the additional unavoidable problems caused by the use of overexpression. However, this was required in order to overcome the lack of retromer-dependent recycling expected from an endocytosis-deficient form of Evi. In summary, I was unable to gain much information from this approach and it was abandoned.

Nevertheless, the issue of the requirement for Evi endocytosis in Wg gradient formation (and transcytosis) remains important to resolve. Data from experiments utilising a *shibire*^{ts} endocytosis block in conjunction with the Evi-EC3-glyOLLAS BAC suggested that endocytosis of Evi is involved in the transcytosis of Wg. However, a rigorous functional test is still required. Ideally, the role of Evi endocytosis should be tested with an endocytosis-deficient protein that better resembles the wild type form and harbours an extracellular tag. A predicted AP2 binding motif has been identified in the third intracellular loop of Evi, and upon mutation of this motif a non-endocytosable form of Evi is produced (Gasnereau et al. 2011). Expression of this mutant form of Evi does not fully rescue an *evi* null mutant. In particular the characteristic enrichment of basolateral Evi seen in the Wg expressing cells does not occur (Gasnereau et al. 2011). This phenotype is similar to that seen when endocytosis of Evi is inhibited with *shibire*^{ts} (Figure 5.5). As a further test of the role of Evi endocytosis, one could create an *evi*^{KO}, and re-insert a construct similar to that shown in Chapter 4, whereby a wild type version of Evi cDNA flanked by FRTs is inserted in front of one encoding extracellularly tagged *evi* with a mutated AP2 binding motif. In this fashion one could trigger production of a step of endocytosis-deficient Evi and observe the effect on Wg release over time. One could also follow the extracellular localisation of this form of Evi and determine which surfaces it accumulates on, and how this might affect extracellular Wg localisation.

In this Chapter, I also developed a system to allow expression of tagged Wg and Evi at the same time and at the same levels. One consideration when using the 2A system to co-express two proteins concerns the order of cDNA insertion. This is important because a short 2A sequence remains attached to the C-terminus of the first protein during translation, whereas the second protein remains unmodified (Trichas et al., 2008). This consideration was illustrated in the case of Wg. When in the first position Wg-HA was not expressed (Figure 5.8 C) however, when moved to the second position Wg-HA expression was observed (Figure 5.8 D). It has been previously described that modifications to the C-terminal tail of Wg cause the protein to become non-functional (Zecca et al., 1996). Therefore, addition of the short 2A sequence at the C-terminus of Wg could be the cause of the lack of Wg expression observed in Figure 5.8 C. This is not the case with Evi, as overexpression of a form of Evi tagged at the C-terminus rescues Wg secretion in a *vps35*$^{-/-}$ mutant (Franch-Marro et al., 2008b), therefore, the addition of the short 2A sequence to Evi presumably has no effect (Figure 5.8 D). During the course of my work I also realised the importance of the 5' and 3'UTRs. Without a 5'UTR Evi and Wg were not expressed even after stop cassette excision. Other factors must contribute to this lack of expression because even with the addition of the 5'UTR, the actin-FRT-Plum-pA-FRT-5'UTR-Evi-EC3-OLLAS-2A-Wg-Ex4-HA construct did not express Wg-HA at expected levels. This may be because the 3'UTR of the actin construct is different from the endogenous *wg* 3'UTR, which has been shown to be important for *wg* mRNA localisation and subsequent protein expression (Simmonds et al., 2001). The reduction in Wg-HA protein may be explained by the lack of its endogenous 3'UTR. All other constructs used in this study contain their endogenous 3'UTRs. Therefore, when considering construct design, cDNAs should be created that are as close to the endogenous gene as possible containing both the 5' and 3'UTRs.

Using tools developed during this study, I have been able to explore for the first time the extracellular distribution of Evi in the *Drosophila* wing

imaginal disc. I showed that Evi is not released with Wg to form the extracellular gradient, which is not only important for this study but also to understand gradient formation. Using *shibire*^{ts} mutant discs expressing tagged versions of both Wg and Evi, I showed that like Wg, extracellular Evi accumulates at the apical surface following an endocytosis block. Upon release of this block, it appears that the apical extracellular Evi transcytoses to form the basolateral Evi pool. This suggests that in a similar fashion as for Wg (Chapter 4), Evi transits between the apical and basolateral surfaces.

Chapter 6

General Discussion

6.1 Summary of results presented in this thesis

In this thesis I have produced new tools to allow the visualisation of Wg and Evi trafficking at endogenous levels. In addition, I have developed a system, which allows the controlled production of a step of tagged Wg-HA in the secretory pathway, also at endogenous levels. I have combined these tools with the *shibire*^{ts} system, which allows dynamin-dependent endocytosis to be controlled by changing the temperature.

Upon a block of endocytosis both Wg and Evi accumulate on the apical surface of Wg expressing cells, while the basolateral extracellular Wg gradient disappears (Figure 4.3, 5.6). This suggests that Wg and Evi move from the apical to basolateral region of expressing cells. To corroborate this suggestion, Wg-HA expression was induced as a step. Upon de novo production, Wg-HA is initially detected exclusively in apical Golgi, and then moves basolaterally over time until it is released and a basolateral extracellular gradient forms (Figure 4.9-4.11). Upon a block of endocytosis, Evi also accumulates at the apical surface but is not lost from the basolateral surface (Figure 5.6), suggesting that it is not released with Wg there (Figure 5.1). Upon release of the endocytic block, the extracellular apical accumulation of both Wg and Evi disappears, and over time the basolateral Wg gradient is re-established (Figure 4.4, 5.7). Basolateral extracellular Evi undergoes a transient decrease and then returns to wild type levels (Figure 5.7). This suggests that Evi could undergo endocytic uptake from the basolateral surface and recycle back to the Golgi (then ER).

A model summarising the Wg and Evi trafficking route predicted by this study, and combined with published data, is shown in Figure 6.1. Wg is produced in the apical ER where it associates with Evi in a lipid-dependent manner (Yu et al., 2014)(Herr and Basler 2011). Wg/Evi cargo is chaperoned via p24 proteins into COP-II coated vesicles for movement to the apical Golgi. Wg and Evi are then moved to the apical surface, where they undergo re-endocytosis in an AP2-dependent manner (Gasnereau et al. 2011), and are transcytosed for basolateral Wg release. Basolateral Evi is not released but instead is internalised and recycled back to the Golgi in a retromer-mediated manner (Belenkaya et al., 2008; Franch-Marro et al., 2008b; Port et al., 2008). Evi then undergoes further retrograde recycling through a COP-I mediated pathway for return to the ER and movement of more Wg (Yu et al., 2014).

Figure 6.1: Revised model of the Wg secretory route in polarised epithelial cells.

Model for the Wg secretory route through a polarised epithelial cell of the wing disc based on data presented in this thesis. Wg is produced in the ER where it undergoes Porc-dependent lipidation, associates with Evi, and is packaged into COP-II vesicles for movement to the Golgi via the action of p24 proteins. Wg and Evi transit the Golgi for movement to the apical surface, but are then re-endocytosed and transcytosed across the cell. Wg is released at the basolateral surface, and upon Wg release, Evi is subsequently re-endocytosed back into the cell for recycling via a retromer/SNX3-mediated pathway to the Golgi (orange arrows). COP-I retrograde transport facilitates Evi movement back to the ER to begin the cycle again (orange arrows).

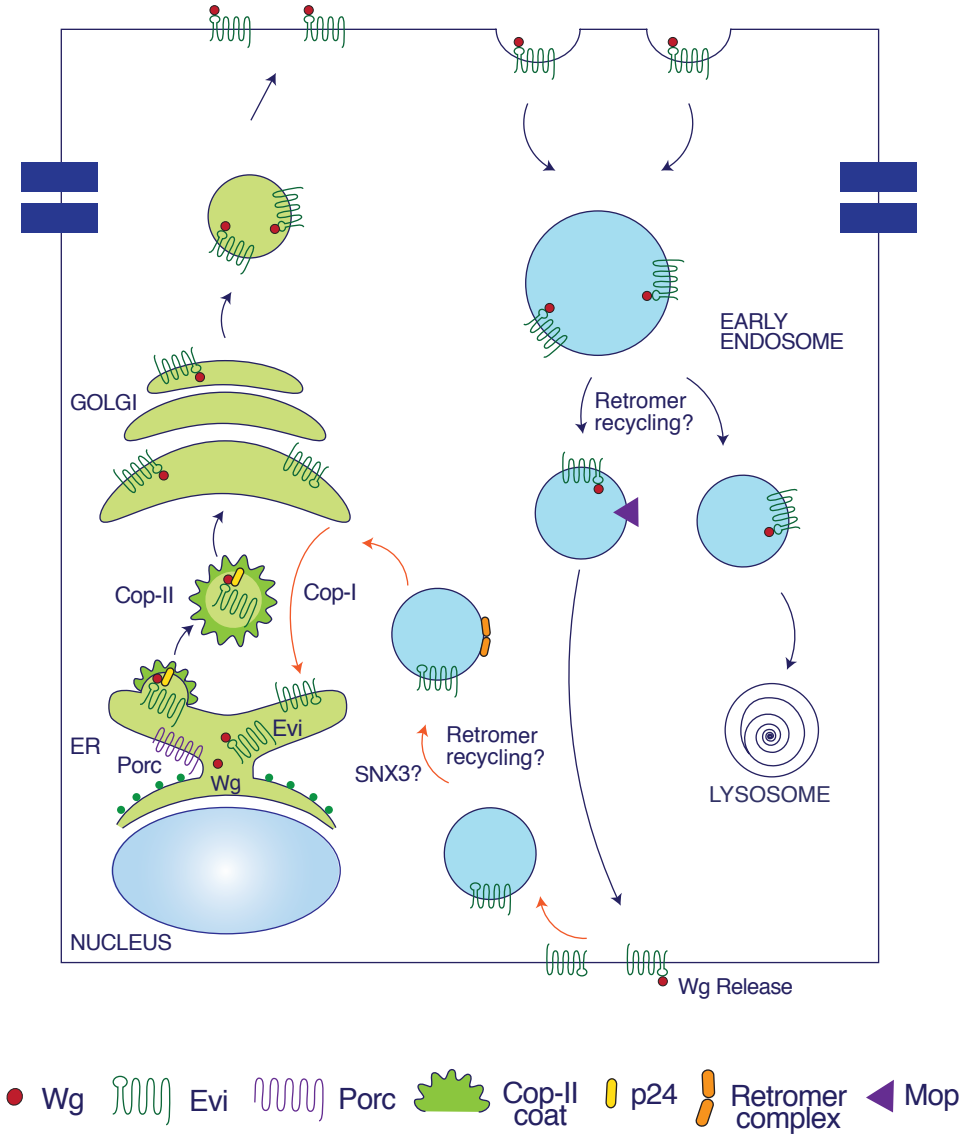
EARLY
ENDOSOME
Retromer
recycling?
GOLGI
Cop-II
Cop-I
ER
Porc
Evi
Wg
SNX3?
Retromer
recycling?
LYSOSOME
NUCLEUS
Wg Release
Wg
Evi
Porc
Cop-II
coat
p24
Retromer
complex
Mop

6.2 General Discussion

6.2.1 The importance of using extracellularly tagged proteins expressed at endogenous levels.

As discussed in Chapter 3, multiple factors need to be considered when designing a strategy for extracellular tagging of endogenously expressed proteins. Both the location and composition of selected tags can have an effect on the native protein. Upon insertion of an HA tag in either Exon 2 or Exon 4 of the Wg BAC, only Wg-Ex4-2HA was expressed in a similar manner to wild type Wg (Figure 3.1). Therefore choice of tag insertion site is important, presumably to allow proper protein folding and trafficking. The XWnt8 structure (Janda et al., 2012) has demonstrated how fortunate we were in our choice of tag site in Wg. Mapping of the HA tag site in Exon 4 onto the XWnt8 structure indicates its placement in a small helix on the periphery of the protein (Janda et al., 2012). When designing our tagging strategy we did not have the luxury of structural data to make an informed choice over tag placement. However, with the advent of the XWnt8 structure, more suitable sites for tag placement may be identified. It may also be possible to identify sites that could accommodate a larger tag than HA, perhaps even a fluorophore. This underlines the importance of structural information about proteins, which can give insight into both their functionality and regions for potential modification.

For this study, it was also important to identify a suitable extracellular site in which Evi could be tagged. Following a trial and error approach, we found that insertion of an OLLAS tag into EC3 was relatively innocuous (Figure 3.8). The Evi-EC3-glyOLLAS BAC recapitulates endogenous Evi expression and can rescue an *evi* null mutant (Figure 3.11). Tag composition was also important in this context since insertion of a V5 tag into this same site did not recapitulate wild type Evi expression (Figure 3.10). The V5 tag contains several Prolines that are relatively inflexible. Adding these structural constraints to Evi

may affect the ability of the protein to fold properly. Size, as well as tag composition can affect protein localisation. Indeed, we have been unable to insert fluorophores, which are typically in the region of 250AAs, into either site in Wg or Evi without affecting protein activity. Unfortunately, this means we are unable to follow trafficking of these proteins in live preparations. Hopefully, in the future with the advent of new technology, smaller fluorescent tags, which would not disrupt protein structure, will become available.

Most trafficking studies to date have been conducted with overexpressed proteins. Overexpression of proteins can cause artefacts due to the high levels of protein expression associated with these experiments. For example, UAS-Evi-FLV5 (Figure 5.3) can rescue Wg secretion in a *vps35*$^{-/-}$ mutant P compartment (Figure 5.4), suggesting that insertion of a C-terminal tag in Evi does not affect function. However, when the 80kb Evi BAC is tagged in the same position it does not recapitulate wild type Evi expression, and does not rescue an *evi* null mutant (C. Alexandre, unpublished data). Moreover, insertion of a C-terminal tag in Evi has recently been shown to mask the ER retrieval signal required for recycling of Evi back to the ER, and causes Evi mislocalisation to the Golgi (Yu et al., 2014). The rescue conferred by this construct is therefore probably due to constant replenishment of Evi in the ER. This is a consequence of the high levels of protein production caused by overexpression, not through the endogenous recycling route that Evi should take in a wild type situation. Insertion of this aberrant tag has led scientists to believe that Evi was localised to the Golgi for many years before this mistake was rectified. This underlines the importance of conducting trafficking studies at endogenous levels, and only utilising tagged proteins that recapitulate endogenous protein localisation and function.

6.2.2 Wg and Evi undergo transcytosis for Wg release.

I have demonstrated that Wg is produced in the apical region of expressing cells and is transcytosed for basolateral release. There is strong

evidence that Evi is also transcytosed, perhaps in association with Wg. As I have shown, Evi is not released at the basolateral surface with Wg. I propose that, instead, it may be recycled back to the Golgi and then ER for further rounds of Wg secretion (Figure 6.1). This model of Wg transcytosis is in agreement with the distribution of both intracellular and extracellular Wg in secreting cells (Figure 1.5). Evi protein is more abundant in Wg expressing cells compared to the rest of the disc (Figure 1.5 D'). This increase in Evi abundance is not transcriptional and is likely a consequence of Wg itself, although the underlying mechanism is not known. Inhibition of retromer-dependent recycling prevents Evi enrichment in Wg expressing cells (Port et al., 2008), although again the mechanism is unknown. With our new tools it would be interesting to explore this phenomenon in more detail, especially focusing on the distribution of extracellular Evi in a retromer mutant situation. Finally, it is worth pointing out that the Wg receptors Fz2 and Arr, and HSPGs Dlp and Dally are mainly found on the basolateral surface of disc cells (unpublished observations), which is consistent with Wg release and spread occurring basolaterally.

The movement of Wg across expressing cells via transcytosis is comparable to the behaviour of Hh, another lipid-modified protein (Callejo et al., 2011). Disp a multi-pass TM chaperone protein is required for Hh transcytosis and basolateral release (Callejo et al., 2011). It is possible that Evi and Disp may fulfil comparable roles. It has been suggested that via cooperation with Disp, Dlp may play a role in Hh transcytosis (Callejo et al., 2011). A previous study also implied that transcytosis of Wg might depend on the action of Dlp (Gallet et al., 2008). However, we found this not to be the case. In *dlp*$^{-/-}$, *dally*$^{-/-}$ mutant clones extracellular Wg did not accumulate apically, which would be expected if these proteins were required for Wg transcytosis (Figure 5.10). In addition, no colocalisation of Wg and Dlp can be observed with either a total or extracellular staining protocol (unpublished observations). This would also suggest that a functional interaction between the two proteins during transcytosis is unlikely.

Although examples of transcytosis do exist in the literature, relatively little is known about this process and its regulation. Several Rab proteins have been demonstrated to be involved, however this appears to be in a cell and protein-specific manner. Currently there is no consensus on a single main mode of transcytotic movement. The next step in this study will be to identify proteins involved in Wg transcytosis and thus begin to determine the mechanism. Two candidate proteins or complexes could be involved: Myopic (Mop) and the retromer complex. Mop is a protein tyrosine phosphatase, which has a role in the endosomal trafficking of Wg in secreting and receiving cells in the *Drosophila* wing imaginal disc (Pradhan-Sundd and Verheyen, 2014). Upon expression of Mop RNAi, Wg appears to be retained in an early endosomal compartment (Pradhan-Sundd and Verheyen, 2014). This could place Mop as a factor involved in the maturation and movement of Wg from early to recycling endosomes for transcytosis. Further characterisation of the sub-cellular localisation of Wg, Evi and other endocytic markers in this situation would be required to support this as a hypothesis. The retromer complex has previously been demonstrated to regulate the transcytosis of the polymeric immunoglobulin receptor (pIgR) in MDCK cells (Verges et al., 2004). The Vps35 subunit was identified as interacting with pIgR in endosomes via mass spectrometry (Verges et al., 2004). Depletion of Vps35 by RNAi reduces transcytosis of polymeric IgA (pIgA) (Verges et al., 2004). As discussed in Chapter 1, *vps35*$^{-/-}$ mutant wing imaginal discs display a Wg secretion defect due to the requirement for the retromer-complex in recycling of Evi (Belenkaya et al., 2008; Franch-Marro et al., 2008b; Port et al., 2008). However, detailed characterisation of the sub-cellular localisation of both Wg and Evi proteins upon retromer loss of function has not been performed. The possibility remains therefore, that there may be an additional role for retromer in transcytosis as well as Evi recycling to the Golgi.

The requirement of the Wg chaperone protein Evi for the transcytotic process must also be functionally tested. I have shown that Evi appears to

undergo transcytosis with Wg, however a stringent functional test is still required. As discussed in Chapter 5, an endocytosis-deficient form of Evi could be created by removal of an AP2-dependent endocytosis motif (Gasnereau et al. 2011). According to our model (Figure 6.1), expression of an endocytosis-deficient Evi would be predicted to block Wg secretion at the apical surface of expressing cells. Therefore, one could adapt this system to turn on the production of an endocytosis-deficient form of Evi in a controlled manner similar to that described for the production of Wg-HA in Chapter 4. Subsequently, the effect of an apical Evi endocytosis block on Wg transcytosis and basolateral release could be monitored to determine the role of Evi in transcytosis.

6.2.3 The importance of Wg apical localisation and transit through the apical surface.

As shown in Figure 1.5, the majority of total Wg protein is observed in the apical region of expressing cells, which is in accordance with the tightly apically localised *wg* mRNA. However, the importance and function of this apical localisation is not clear. Overexpression studies with embryos have suggested that the 3'UTR is the apical localising determinant (dos Santos et al., 2008; Simmonds et al., 2001). In the same study it was suggested that changing the *wg* mRNA localisation to a more uniform pattern affected the ability of UAS-Wg to rescue a *wg* null mutant, indicating a reduction in Wg signalling (Simmonds et al., 2001). Preliminary data from our lab suggests that this is not the case. We changed the endogenous Wg 3'UTR to an hsp70 3'UTR which should cause uniform expression of *wg* mRNA (C. Alexandre, unpublished data). This modified DNA was then inserted into the wg^{KO} to give *wg{KO; Wg-hsp70pA}* transgenic flies (C. Alexandre). Uniform wg^{hsp70} mRNA distribution was verified by in-situ hybridisation in embryos and wing discs (K. Beckett, unpublished data), but *wg{KO; Wg-hsp70pA}* homozygous flies were shown to be viable and fertile indicating that Wg signalling is normal (C. Alexandre,

unpublished data). However, intracellular Wg protein levels in the wing imaginal disc were dramatically reduced in *wg{KO; Wg-hsp70pA}* homozygous wing imaginal discs, whilst the extracellular Wg gradient was largely unaffected and signalling was apparently normal (L. Palmer, K. Beckett, unpublished data). This is consistent with a model by which, only the *wg* mRNA present in the apical region is translated leading to reduced yet sufficient protein levels. In other words, apical mRNA localisation is essential for normal Wg protein levels, but the levels of Wg protein required for normal development are much lower than previously thought.

As described above, it appears that Wg is produced in the apical region of expressing cells, suggesting that there may be a functional requirement for trafficking of Wg through the apical surface. Several possible reasons are outlined in Figure 6.2. Although my results suggest that Wg is released at the basolateral surface, I cannot exclude the possibility that some release takes place apically (Figure 6.2 A). It is also possible that two pools of Wg may exist, the short-range signalling may occur via apical release and long-range Wg signalling may occur via release from the basolateral surface (Figure 6.2 A). However, I have found no data indicating this to be the case. Wg may require transit through the apical surface because it undergoes modification there (Figure 6.2 B). This modification may be via the action of a Wg-interacting protein, or a physical modification. Wg may transit the apical surface to associate with packaging proteins like LPPs or Swim (Figure 6.2 C). Proteins involved in Wg packaging may be concentrated in the peripodial space at the apical surface of expressing cells, and therefore meet Wg there to undergo transcytosis for basolateral release and movement. Finally, I must also consider the possibility that transit through the apical surface may not be functionally important. The apical *wg* mRNA localisation in the wing disc may be due to the requirement for apical localisation in the embryonic epidermis (Simmonds et al., 2001). This constraint may be carried over in the wing disc and mechanisms may have evolved there to ensure final delivery of the protein to the basolateral

surface (Figure 6.2 D). With further elucidation of the Wg trafficking route and further experiments manipulating the Wg 3'UTR, and thus the *wg* mRNA localisation (as described above), we will hopefully begin to understand the relevance of this localisation.

Figure 6.2: Models for possible function of apical Wg transit.
(A) Wg could be released apically for movement across the apical surface, in addition to basolateral release. (B) Wg could become modified at the apical surface of expressing cells, and this modification could be required for subsequent basolateral transport or signalling. (C) Wg could interact with potential packaging proteins at the apical surface. LPPs (orange) or Swim (pink) could associate with Wg apically and undergo the transcytosis step to the basolateral surface with Wg for release. This could happen either with, or in the absence of Evi. (D) Wg could transit the apical surface due to the spatial restrictions imposed upon its production from the apical localisation of the *wg* mRNA. Wg protein may be produced in the apical ER due to mRNA localisation and then require subsequent basolateral targeting via transcytosis.

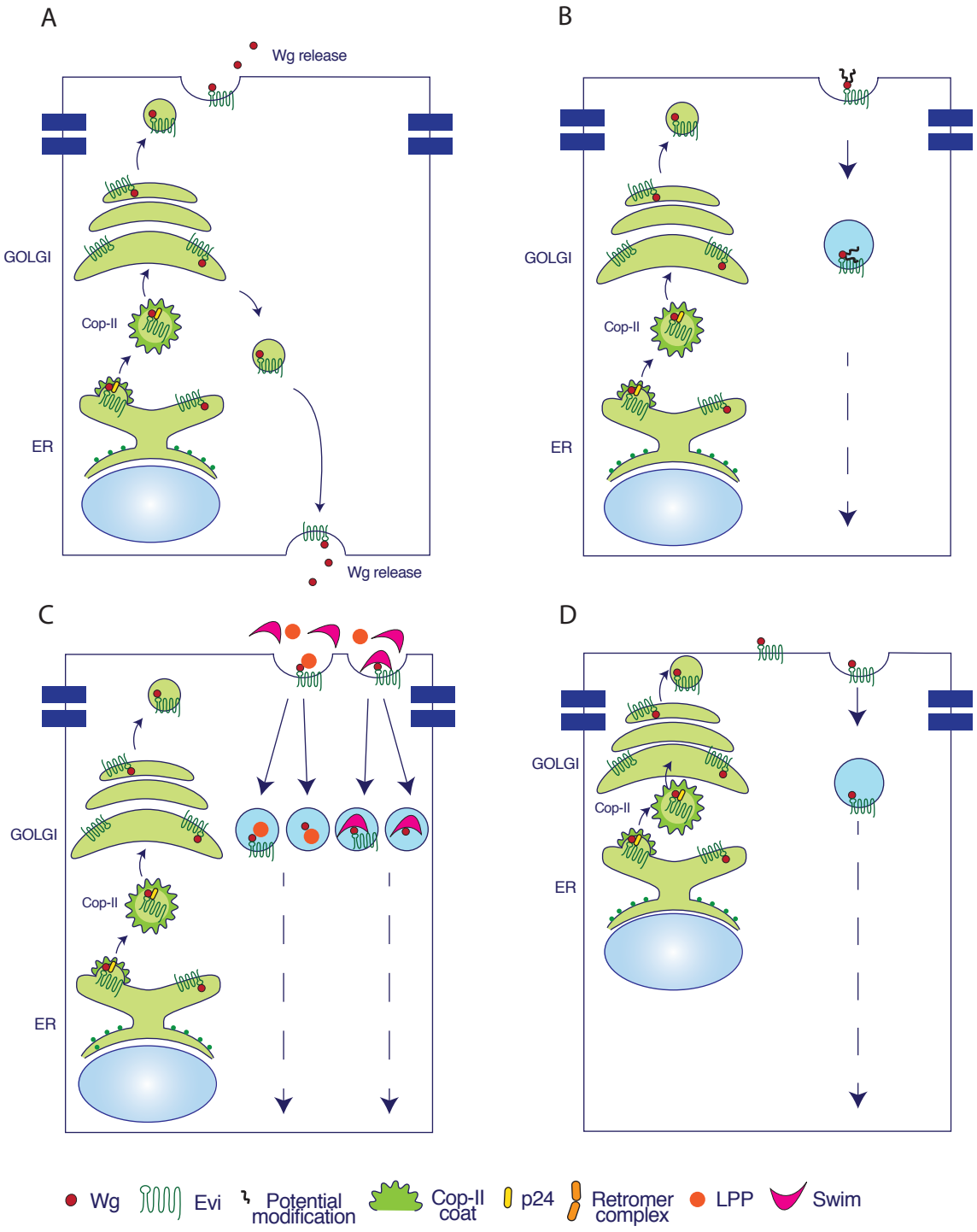
A
Wg release
GOLGI
Cop-II
ER
Wg release
B
GOLGI
Cop-II
ER
C
GOLGI
Cop-II
ER
D
GOLGI
Cop-II
ER
Wg
Evi
Potential modification
Cop-II coat
p24
Retromer complex
LPP
Swim

6.2.4 How is Wg packaged for basolateral release?

Data from experiments described in Chapter 4 suggest that Wg is released basolaterally from secreting cells and spreads along the surface of receiving cells to form a gradient (Figure 4.4, 4.10). As discussed above, there could be release of Wg from the apical surface of expressing cells, however I have no data to suggest that this is the case. Through an understanding of the trafficking route taken by Wg and Evi in expressing cells, we can begin to elucidate possible mechanisms for Wg packaging and release (as discussed in Chapter 1, Section 1.6). Determining that Evi is not released with Wg is an important piece of evidence indicating that Evi-containing exosomes do not play a role in Wg gradient formation in the *Drosophila* wing imaginal disc (Beckett et al., 2013). Further research in the lab indicates that Wg and LPPs do not colocalise within the imaginal disc, suggesting that LPPs also do not contribute to Wg gradient formation (K. Beckett, unpublished data). Since cytonemes have not been shown to emanate from the D/V boundary in wing imaginal discs, we are left with the possibility that another factor or process enables Wg release and diffusion. Swim is a lipocalin, which can spread over a long-range and is efficiently secreted (Mulligan et al., 2011)(K. Beckett, unpublished data). I have shown that upon a *shibire*^{ts}-dependent endocytosis block, basolateral extracellular Wg is lost from the surface of cells over time (Figure 4.3). This suggests that once it has reached the basolateral surface, Wg does not remain stably associated with the cell membrane. Loss of Wg from the basolateral surface in this situation could be due to several different factors. One possibility is that removal of extracellular Wg could be stimulated by a packaging protein such as Swim (Figure 6.3 A, B). Swim may then spread away from the surface of expressing cells into the basolateral interstitial space causing the dilution of signal observed in Figure 4.3 (Figure 6.3 B).

Once we have an understanding of Wg movement and its subsequent basolateral packaging and release, the next question for exploration concerns the delivery of Wg to its receptor. If Wg is transported via a packaging protein

such as Swim, which masks the lipid moiety, how is Wg transferred to Fz for lipid-dependent binding to the Fz-CRD? Using tools to track these proteins in a similar way as described in this study, one may be able to determine where and when these association and dissociation events occur. However, more sophisticated structural and biochemical analysis will surely be required to dissect the finer details of transfer.

Figure 6.3: The possible role of Swim in basolateral Wg release.
(A) Wg and Evi undergo transcytosis as described in Figure 6.1. Upon reaching the basolateral surface, Wg is removed from Evi via the action of Swim, and Evi undergoes re-endocytosis and retromer-dependent recycling as described above. Swim masks the lipid moiety of Wg to enable movement along the tissues basolateral surface to form the extracellular Wg gradient. (B) Upon a *shibire*^{ts}-dependent endocytosis block, Wg and Evi build up both in the Golgi and on the apical surface of expressing cells. Wg and Evi therefore cannot undergo transcytosis for basolateral Wg release. Wg transcytosed before the endocytosis block moves away with Swim from the surface of expressing cells and along the tissue, causing the loss of basolateral Wg observed in Figure 4.3. Evi is unable to undergo re-endocytosis and recycling from the basolateral surface due to the dynamin block, so accumulates basolaterally.

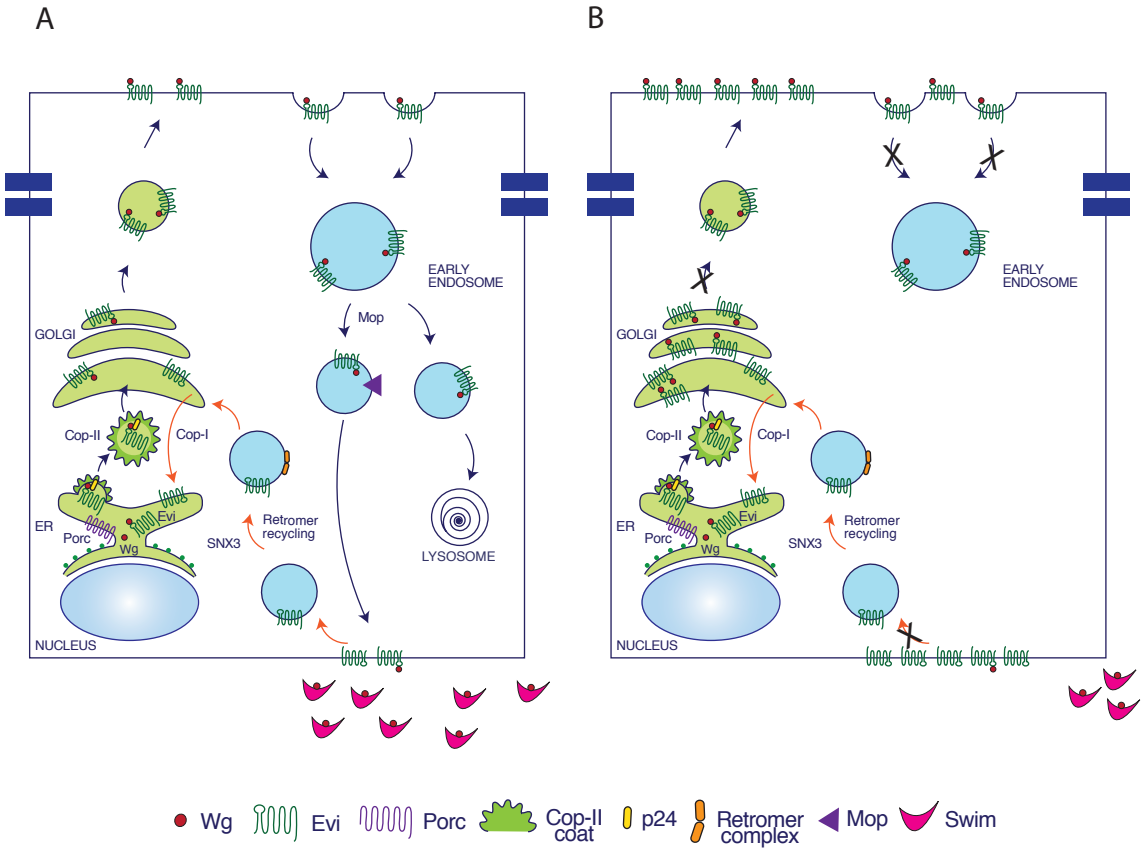
A
B
EARLY ENDOSOME
Mop
GOLGI
Cop-II
Cop-I
ER
Porc
Evi
Wg
SNX3
Retromer recycling
LYSOSOME
NUCLEUS
Wg
Evi
Porc
Cop-II coat
p24
Retromer complex
Mop
Swim

6.3 Concluding remarks

This thesis describes new approaches to study in vivo trafficking using tagged proteins expressed at endogenous levels within a tissue. By using endogenously expressed proteins with small epitope tags we can be confident that they move within the secretory and endocytic pathways in the same manner as their wild type counterparts. Using the *Drosophila* wing imaginal disc as our model system instead of cell culture, we are able to observe trafficking events in a situation where all relevant factors (ECM/glypicans/receptors etc.) are present. However, this comes with its own challenges, especially with detection and visualisation of proteins. The low endogenous expression levels, twinned with the pseudostratified nature of the epithelium make protein visualisation difficult. Nevertheless, we were able to show transcytosis, whereby Wg moves from the apical to basolateral surface of expressing cells, possibly facilitated by the action of the chaperone protein Evi. Transcytosis is not a well-understood process, so this study uncovers exciting possibilities to dissect the underlying mechanism. In particular, several proteins have been demonstrated to be important for Wg endosomal trafficking within secreting cells. Further study of these using our experimental system may help define the role of candidate proteins in transcytosis.

In this study I generated a novel tool, which allows the controlled production of a step of tagged protein expressed at endogenous levels. Using this system, I followed Wg-HA within secreting cells and elucidated its endogenous intracellular trafficking route. The ability to produce a controlled step of tagged protein may be a useful system to apply to other morphogens in the wing imaginal disc such as Hh and Dpp. The trafficking route of Hh, as examined previously, appears to be similar to that shown for Wg in this study. Using a hh^{KO} that we have developed in the lab, it may be interesting to adopt a similar strategy to observe movement of tagged Hh. However, as discussed

previously, identifying a site to insert a tag in Hh that gives rescue when expressed in a null mutant may be a challenge. In addition to the wing imaginal disc, Wg trafficking has also been well studied in both the NMJ and embryonic epidermis in *Drosophila* (Dubois et al., 2001; Korkut et al., 2009). It would therefore be interesting to apply the inducible system to other tissues and determine whether Wg traffics in a similar manner there. Controlled induction of a step of tagged Wnt could also be translated to other systems, to explore whether Wnt traffics in a similar fashion to *Drosophila* in other animals. This approach could be particularly appropriate with organoids, using drug-inducible Cre to produce a step of Wnt-HA.

Understanding the trafficking route taken by Wg and Evi also provides us with information about the spatial regulation of signalling between Wg expressing and receiving cells. The precise control of signal trafficking is required for detailed placement of signalling proteins in the correct places for their action. By determining where and how Wg is released we have been able to add more information to the controversial topic of Wnt signalling.

Appendix 1

Table of Primers used in this study

Primer Name	Primer Sequence
Section 2.2.3/3.2.5: *wg{KO; FRT-Wg-FRT-Wg-Ex4-2HA}*	
ScrChe R	GGGAAGGACAGCTTCAAGTAGTCG
ScrpGE F	GCACAATTCCGCTCGAATTGCCG
ScrWg300 R	AGTTTCTCGTCGAGCAGTTCCAGCG
ScrWg1400 F	GGCGGACGAAATGGACGTCGTCAGG
Section 2.2.1/3.2.6: Evi-EC3-glyV5 BAC and Evi-EC3-glyOLLAS BAC	
GalKeviEC3 F	CCCTTGTATGTGCAGCTCTGACCGTCGCCGGCTTCATTATGGG CCAAATGGCCGAGGGCCAGTGGGACTGGAACGACCCTGTTGA CAATTAATCATCGGC
GalKeviEC3 R	GAGCAGGGCGAAGATATAGATGTTCCACATGCCGTAGACGCC GGTCAGGAAGGCGGAAGTTGGCTGAATTGCCACATTTCAGCA CTGTCCTGCTCCTTGTG
ScrGalK F	CCTGTTGACAATTAATCATCGGCATAG
ScrGalK R	TCAGCACTGTCCTGCTCCTTGTGATGG
OLLASgly F	CAGCTCTGACCGTCGCCGGCTTCATTATGGGCCAAATGGCCGA GGGCCAGTGGGACTGGAACGACGGTGCAGGCGGAGGGAGTGG CTTTGCGAATGAATTGGGACCTAGG
OLLASgly R	ATAGATGTTCCACATGCCGTAGACGCCGGTCAGGAAGGCGGC CGTTGGCTGAATTGCCACATTCCCTCCACCGGCGCCCTTTCCC ATCAACCTAGGTCCCAATTCATTCG
V5gly F	TGCAGCTCTGACCGTCGCCGGCTTCATTATGGGCCAAATGGCC GAGGGCCAGTGGGACTGGAACGACGGTGCAGGCGGAGGGGGT AAGCCTATCCCTAACCCTCTCCTAG
V5gly R	AGATGTTCCACATGCCGTAGACGCCGGTCAGGAAGGCGGAAG TTGGCTGAATTGCCACATTCCCTCCACCGGCGCCCGTAGAATC GAGACCTAGGAGAGGGTTAGGGATA

ScrEC3 F	ACTATGATTCAATGTTGTATCCAGAAGCTCC
ScrEC3 R	TTAGAAAACAATAATTCGAGTCCTTCCGCC
Section 2.2.2/3.2.6: UAS-Evi-Nterm-V5	
NdeV5Evi F	GTTCGGCCATATGCACGATGGTAAGCCTATCCCTAACCCTCTC CTCGGTCTCGATTCTACGCTCACGCTGACAGCTATTC
SalEvi R	GCGAGCGAATGGTCGACTTGTTCGG
ScrUAS F	CCAGCAACCAAGTAAATCAACTG
Screvi420 R	GTCAACTGAAGTTCCCTGGGCG
Section 2.2.4/5.2.5: act-FRT-Cerulean-FRT-Evi-OLLAS-2A-Wg-HA	
ScrCer F	CGCTACCCCGACCACATGAAGCAGC
ScrCer R	GTTGGCCTTGATGCCGTTCTTCTGC
Scr2A F	GGAAGTCTGCTAACATGCGGTGACG
Scr2A R	ACCGCATGTTAGCAGACTTCCTCTGC
ScrEviNco F	GATCCCATGGCGTTTTTGATGCTGGCCACCCTTGTATG
ScrEviNco R	GATCCCATGGCCTTCCATATCATGTAGCACAGAAAGAG
Section 2.2.4/5.2.5: act-FRT-Plum-FRT-5'UTR-Evi-OLLAS-2A-WgHA	
SpeI5'UTR F	GATCGACTAGTTCACACTGCTTTGTTGATTCTTG
Eag5'UTREvi R	GCTGCACGGCCGACGGTCCGTTGGTTGCTCGAAGGTTTGGAG
Scr5'UTREvi F	CTTTACGCCCACCCAACTGTG
ScrEvi420 R	GTCAACTGAAGTTCCCTGGGCG
PmeIPlum F	GATCGAGTTTAAACATGGTGAGCAAGGGCGAGGAGGTCAT
PmeIPlum R	GATCATGTTTAAACTTAGGTGGAGTGGCGGCCCTCGGCG
General Screening Primers for all Cloning	
pMTChk F	CCGAGAGCATCTGGCCAATGTG

pMTChk R	ACTCATCAATGTATCTTATCATGTCTGG
ScrHAex4 F	TGCGAGTCGATACGCAAGAAGCC
ScrHAex4 R	TCGGGATTGTGCGGGTTCAGTTGG
ScrAct F	ACAAGTTAGTTTGTTATGACAATTGTACTTTGG

References

Alberts, B. (2002). Intracellular Compartments and Protein Sorting. In Molecular biology of the cell (Garland Science), pp. 689-709.

Alexandre, C., Baena-Lopez, A., and Vincent, J.P. (2014). Patterning and growth control by membrane-tethered Wingless. Nature *505*, 180-185.

Baeg, G.H., Lin, X., Khare, N., Baumgartner, S., and Perrimon, N. (2001). Heparan sulfate proteoglycans are critical for the organization of the extracellular distribution of Wingless. Development *128*, 87-94.

Baeg, G.H., Selva, E.M., Goodman, R.M., Dasgupta, R., and Perrimon, N. (2004). The Wingless morphogen gradient is established by the cooperative action of Frizzled and Heparan Sulfate Proteoglycan receptors. Dev Biol *276*, 89-100.

Baena-Lopez, L.A., Alexandre, C., Mitchell, A., Pasakarnis, L., and Vincent, J.P. (2013). Accelerated homologous recombination and subsequent genome modification in Drosophila. Development *140*, 4818-4825.

Baena-Lopez, L.A., Franch-Marro, X., and Vincent, J.P. (2009). Wingless promotes proliferative growth in a gradient-independent manner. Science signaling *2*, ra60.

Baena-Lopez, L.A., Nojima, H., and Vincent, J.P. (2012). Integration of morphogen signalling within the growth regulatory network. Current opinion in cell biology *24*, 166-172.

Banziger, C., Soldini, D., Schutt, C., Zipperlen, P., Hausmann, G., and Basler, K. (2006). Wntless, a conserved membrane protein dedicated to the secretion of Wnt proteins from signaling cells. Cell *125*, 509-522.

Barrott, J.J., Cash, G.M., Smith, A.P., Barrow, J.R., and Murtaugh, L.C. (2011). Deletion of mouse Porcn blocks Wnt ligand secretion and reveals an ectodermal etiology of human focal dermal hypoplasia/Goltz syndrome. Proceedings of the National Academy of Sciences of the United States of America *108*, 12752-12757.

Bartscherer, K., and Boutros, M. (2008). Regulation of Wnt protein secretion and its role in gradient formation. EMBO Rep *9*, 977-982.

Bartscherer, K., Pelte, N., Ingelfinger, D., and Boutros, M. (2006). Secretion of Wnt ligands requires Evi, a conserved transmembrane protein. Cell *125*, 523-533.

Beckett, K., Monier, S., Palmer, L., Alexandre, C., Green, H., Bonneil, E., Raposo, G., Thibault, P., Le Borgne, R., and Vincent, J.P. (2013). Drosophila S2 cells secrete wingless on exosome-like vesicles but the wingless gradient forms independently of exosomes. Traffic *14*, 82-96.

Bejsovec, A. (2013). Wingless/Wnt signaling in Drosophila: the pattern and the pathway. Molecular reproduction and development *80*, 882-894.

Belenkaya, T.Y., Wu, Y., Tang, X., Zhou, B., Cheng, L., Sharma, Y.V., Yan, D., Selva, E.M., and Lin, X. (2008). The retromer complex influences Wnt secretion by recycling wntless from endosomes to the trans-Golgi network. Dev Cell *14*, 120-131.

Beuchling T., C.V., Spirohn K., Weiss, M. and Boutros, M. (2011). p24 proteins are required for secretion of Wnt ligands. EMBO Reports.

Biechele, S., Cox, B.J., and Rossant, J. (2011). Porcupine homolog is required for canonical Wnt signaling and gastrulation in mouse embryos. Dev Biol *355*, 275-285.

Bischoff, M., Gradilla, A.C., Seijo, I., Andres, G., Rodriguez-Navas, C., Gonzalez-Mendez, L., and Guerrero, I. (2013). Cytonemes are required for the establishment of a normal Hedgehog morphogen gradient in Drosophila epithelia. Nature cell biology *15*, 1269-1281.

Bobrie, A., Colombo, M., Raposo, G., and Thery, C. (2011). Exosome secretion: molecular mechanisms and roles in immune responses. Traffic *12*, 1659-1668.

Brandizzi, F., and Barlowe, C. (2013). Organization of the ER-Golgi interface for membrane traffic control. Nat Rev Mol Cell Biol *14*, 382-392.

Burd, C. (2014). Retromer: A master conducter of Endosome sorting. In Endocytosis, S. Schmid, ed. (Cold Spring Harbour Lab Press), pp. 161-169.

Cadigan, K.M., Fish, M.P., Rulifson, E.J., and Nusse, R. (1998). Wingless repression of Drosophila frizzled 2 expression shapes the Wingless morphogen gradient in the wing. Cell *93*, 767-777.

Callejo, A., Bilioni, A., Mollica, E., Gorfinkiel, N., Andres, G., Ibanez, C., Torroja, C., Doglio, L., Sierra, J., and Guerrero, I. (2011). Dispatched mediates Hedgehog basolateral release to form the long-range morphogenetic gradient in the Drosophila wing disk epithelium. Proceedings of the National Academy of Sciences of the United States of America *108*, 12591-12598.

Callejo, A., Torroja, C., Quijada, L., and Guerrero, I. (2006). Hedgehog lipid modifications are required for Hedgehog stabilization in the extracellular matrix. Development *133*, 471-483.

Casanova, J.E., Wang, X., Kumar, R., Bhartur, S.G., Navarre, J., Woodrum, J.E., Altschuler, Y., Ray, G.S., and Goldenring, J.R. (1999). Association of Rab25 and Rab11a with the apical recycling system of polarized Madin-Darby canine kidney cells. Molecular biology of the cell *10*, 47-61.

Cereijido, M., Robbins, E.S., Dolan, W.J., Rotunno, C.A., and Sabatini, D.D. (1978). Polarized monolayers formed by epithelial cells on a permeable and translucent support. The Journal of cell biology *77*, 853-880.

Ching, W., Hang, H.C., and Nusse, R. (2008). Lipid-independent secretion of a Drosophila Wnt protein. J Biol Chem *283*, 17092-17098.

Clevers, H., and Nusse, R. (2012). Wnt/beta-catenin signaling and disease. Cell *149*, 1192-1205.

Coombs, G.S., Yu, J., Canning, C.A., Veltri, C.A., Covey, T.M., Cheong, J.K., Utomo, V., Banerjee, N., Zhang, Z.H., Jadulco, R.C.*, et al.* (2010). WLS-dependent secretion of WNT3A requires Ser209 acylation and vacuolar acidification. Journal of cell science *123*, 3357-3367.

Coudreuse, D., and Korswagen, H.C. (2007). The making of Wnt: new insights into Wnt maturation, sorting and secretion. Development *134*, 3-12.

Couso, J.P., Bishop, S.A., and Martinez Arias, A. (1994). The wingless signalling pathway and the patterning of the wing margin in Drosophila. Development *120*, 621-636.

Cullen, P.J. (2008). Endosomal sorting and signalling: an emerging role for sorting nexins. Nat Rev Mol Cell Biol *9*, 574-582.

De Matteis, M.A., and Luini, A. (2008). Exiting the Golgi complex. Nat Rev Mol Cell Biol *9*, 273-284.

Deborde, S., Perret, E., Gravotta, D., Deora, A., Salvarezza, S., Schreiner, R., and Rodriguez-Boulan, E. (2008). Clathrin is a key regulator of basolateral polarity. Nature *452*, 719-723.

Doherty, G.J., and McMahon, H.T. (2009). Mechanisms of endocytosis. Annual review of biochemistry *78*, 857-902.

dos Santos, G., Simmonds, A.J., and Krause, H.M. (2008). A stem-loop structure in the wingless transcript defines a consensus motif for apical RNA transport. Development *135*, 133-143.

Doubravska, L., Krausova, M., Gradl, D., Vojtechova, M., Tumova, L., Lukas, J., Valenta, T., Pospichalova, V., Fafilek, B., Plachy, J.*, et al.* (2011). Fatty acid modification of Wnt1 and Wnt3a at serine is prerequisite for lipidation at cysteine and is essential for Wnt signalling. Cellular signalling *23*, 837-848.

Dubois, L., Lecourtois, M., Alexandre, C., Hirst, E., and Vincent, J.P. (2001). Regulated endocytic routing modulates wingless signaling in Drosophila embryos. Cell *105*, 613-624.

Eaton, S. (2006). Release and trafficking of lipid-linked morphogens. Curr Opin Genet Dev *16*, 17-22.

Eaton, S. (2014). Cargo sorting in the endocytic pathway: A key regulator of cell polarity and tissue dynamics. In Endocytosis S. Schmid, ed. (Cold Spring Harbour Lab Press), pp. 443-456.

Farquhar, M.G., and Palade, G.E. (1998). The Golgi apparatus: 100 years of progress and controversy. Trends in cell biology *8*, 2-10.

Franch-Marro, X., Wendler, F., Griffith, J., Maurice, M.M., and Vincent, J.P. (2008a). In vivo role of lipid adducts on Wingless. Journal of cell science *121*, 1587-1592.

Franch-Marro, X., Wendler, F., Guidato, S., Griffith, J., Baena-Lopez, A., Itasaki, N., Maurice, M.M., and Vincent, J.P. (2008b). Wingless secretion requires endosome-to-Golgi retrieval of Wntless/Evi/Sprinter by the retromer complex. Nature cell biology *10*, 170-177.

Fu, J., Jiang, M., Mirando, A.J., Yu, H.M., and Hsu, W. (2009). Reciprocal regulation of Wnt and Gpr177/mouse Wntless is required for embryonic axis formation. Proceedings of the National Academy of Sciences of the United States of America *106*, 18598-18603.

Fujita, M., Watanabe, R., Jaensch, N., Romanova-Michaelides, M., Satoh, T., Kato, M., Riezman, H., Yamaguchi, Y., Maeda, Y., and Kinoshita, T. (2011). Sorting of GPI-anchored proteins into ER exit sites by p24 proteins is dependent on remodeled GPI. The Journal of cell biology *194*, 61-75.

Gallet, A., Staccini-Lavenant, L., and Therond, P.P. (2008). Cellular trafficking of the glypican Dally-like is required for full-strength Hedgehog signaling and wingless transcytosis. Dev Cell *14*, 712-725.

Galmes, R., Delaunay, J.L., Maurice, M., and Ait-Slimane, T. (2013). Oligomerization is required for normal endocytosis/transcytosis of a GPI-anchored protein in polarized hepatic cells. Journal of cell science *126*, 3409-3416.

Gasnereau, I., Herr, P., Chia, P.Z., Basler, K., and Gleeson, P.A. (2011). Identification of an endocytosis motif in an intracellular loop of Wntless protein, essential for its recycling and the control of Wnt protein signalling. J Biol Chem *286*, 43324-43333.

Giraldez, A.J., Copley, R.R., and Cohen, S.M. (2002). HSPG modification by the secreted enzyme Notum shapes the Wingless morphogen gradient. Dev Cell *2*, 667-676.

Gonzalez, F., Swales, L., Bejsovec, A., Skaer, H., and Martinez Arias, A. (1991). Secretion and movement of wingless protein in the epidermis of the Drosophila embryo. Mech Dev *35*, 43-54.

Gonzalez-Gaitan, M. (2003). Endocytic trafficking during Drosophila development. Mech Dev *120*, 1265-1282.

Goodman, R.M., Thombre, S., Firtina, Z., Gray, D., Betts, D., Roebuck, J., Spana, E.P., and Selva, E.M. (2006). Sprinter: a novel transmembrane protein required for Wg secretion and signaling. Development *133*, 4901-4911.

Gould, G.W., and Lippincott-Schwartz, J. (2009). New roles for endosomes: from vesicular carriers to multi-purpose platforms. Nat Rev Mol Cell Biol *10*, 287-292.

Grant, B.D., and Donaldson, J.G. (2009). Pathways and mechanisms of endocytic recycling. Nat Rev Mol Cell Biol *10*, 597-608.

Greco, V., Hannus, M., and Eaton, S. (2001). Argosomes: a potential vehicle for the spread of morphogens through epithelia. Cell *106*, 633-645.

Gross, J.C., Chaudhary, V., Bartscherer, K., and Boutros, M. (2012). Active Wnt proteins are secreted on exosomes. Nature cell biology *14*, 1036-1045.

Hacker, U., Lin, X., and Perrimon, N. (1997). The Drosophila sugarless gene modulates Wingless signaling and encodes an enzyme involved in polysaccharide biosynthesis. Development *124*, 3565-3573.

Han, C., Yan, D., Belenkaya, T.Y., and Lin, X. (2005). Drosophila glypicans Dally and Dally-like shape the extracellular Wingless morphogen gradient in the wing disc. Development *132*, 667-679.

Harterink, M., Port, F., Lorenowicz, M.J., McGough, I.J., Silhankova, M., Betist, M.C., van Weering, J.R., van Heesbeen, R.G., Middelkoop, T.C., Basler, K.*, et al.* (2011). A SNX3-dependent retromer pathway mediates retrograde transport of the Wnt sorting receptor Wntless and is required for Wnt secretion. Nature cell biology *13*, 914-923.

Hays, R., Gibori, G.B., and Bejsovec, A. (1997). Wingless signaling generates pattern through two distinct mechanisms. Development *124*, 3727-3736.

Henne, W. (2014). Molecular mechanisms of the membrane sculpting ESCRT pathway. In Endocytosis, S. Schmid, ed. (Cold Spring Harbour Lab Press), pp. 193-203.

Herpers, B., and Rabouille, C. (2004). mRNA localization and ER-based protein sorting mechanisms dictate the use of transitional endoplasmic reticulum-golgi units involved in gurken transport in Drosophila oocytes. Molecular biology of the cell *15*, 5306-5317.

Herr, P., and Basler, K. (2011). Porcupine-mediated lipidation is required for Wnt recognition by Wls. Dev Biol *361*, 392-402.

Hlsken, J., and Behrens, J. (2000). The Wnt signalling pathway. Journal of cell science *113 (Pt 20)*, 3545.

Hofmann, K. (2000). A superfamily of membrane-bound O-acyltransferases with implications for wnt signaling. Trends in biochemical sciences *25*, 111-112.

Janda, C.Y., Waghray, D., Levin, A.M., Thomas, C., and Garcia, K.C. (2012). Structural basis of Wnt recognition by Frizzled. Science *337*, 59-64.

Johannes, L., and Popoff, V. (2008). Tracing the retrograde route in protein trafficking. Cell *135*, 1175-1187.

Jones, S.M., Howell, K.E., Henley, J.R., Cao, H., and McNiven, M.A. (1998). Role of dynamin in the formation of transport vesicles from the trans-Golgi network. Science *279*, 573-577.

Kadowaki, T., Wilder, E., Klingensmith, J., Zachary, K., and Perrimon, N. (1996). The segment polarity gene porcupine encodes a putative multitransmembrane protein involved in Wingless processing. Genes Dev *10*, 3116-3128.

Kaiser, C. (2000). Thinking about p24 proteins and how transport vesicles select their cargo. Proceedings of the National Academy of Sciences of the United States of America *97*, 3783-3785.

Katanaev, V.L., Solis, G.P., Hausmann, G., Buestorf, S., Katanayeva, N., Schrock, Y., Stuermer, C.A., and Basler, K. (2008). Reggie-1/flotillin-2 promotes secretion of the long-range signalling forms of Wingless and Hedgehog in Drosophila. EMBO J *27*, 509-521.

Kicheva, A., Pantazis, P., Bollenbach, T., Kalaidzidis, Y., Bittig, T., Julicher, F., and Gonzalez-Gaitan, M. (2007). Kinetics of morphogen gradient formation. Science *315*, 521-525.

Kiecker, C., and Niehrs, C. (2001). A morphogen gradient of Wnt/beta-catenin signalling regulates anteroposterior neural patterning in Xenopus. Development *128*, 4189-4201.

Kirchhausen, T. (2014). Molecular structure, function and dynamics of Clathrin-mediated membrane traffic. In Endocytosis, S. S, ed. (Cold Spring Harbour Lab Press), pp. 11-31.

Koles, K., Nunnari, J., Korkut, C., Barria, R., Brewer, C., Li, Y., Leszyk, J., Zhang, B., and Budnik, V. (2012). Mechanism of evenness interrupted (Evi)-exosome release at synaptic boutons. J Biol Chem *287*, 16820-16834.

Komekado, H., Yamamoto, H., Chiba, T., and Kikuchi, A. (2007). Glycosylation and palmitoylation of Wnt-3a are coupled to produce an active form of Wnt-3a. Genes to cells : devoted to molecular & cellular mechanisms *12*, 521-534.

Kondylis, V., Goulding, S.E., Dunne, J.C., and Rabouille, C. (2001). Biogenesis of Golgi stacks in imaginal discs of Drosophila melanogaster. Molecular biology of the cell *12*, 2308-2327.

Kondylis, V., Tang, Y., Fuchs, F., Boutros, M., and Rabouille, C. (2011). Identification of ER proteins involved in the functional organisation of the early secretory pathway in Drosophila cells by a targeted RNAi screen. PloS one *6*, e17173.

Korkut, C., Ataman, B., Ramachandran, P., Ashley, J., Barria, R., Gherbesi, N., and Budnik, V. (2009). Trans-synaptic transmission of vesicular Wnt signals through Evi/Wntless. Cell *139*, 393-404.

Kreuger, J., Perez, L., Giraldez, A.J., and Cohen, S.M. (2004). Opposing activities of Dally-like glypican at high and low levels of Wingless morphogen activity. Dev Cell *7*, 503-512.

Lerner, D.W., McCoy, D., Isabella, A.J., Mahowald, A.P., Gerlach, G.F., Chaudhry, T.A., and Horne-Badovinac, S. (2013). A Rab10-dependent mechanism for polarized basement membrane secretion during organ morphogenesis. Dev Cell *24*, 159-168.

Levine, T., and Rabouille, C. (2005). Endoplasmic reticulum: one continuous network compartmentalized by extrinsic cues. Current opinion in cell biology *17*, 362-368.

Lin, X., and Perrimon, N. (1999). Dally cooperates with Drosophila Frizzled 2 to transduce Wingless signalling. Nature *400*, 281-284.

MacDonald, B.T., and He, X. (2012). Frizzled and LRP5/6 receptors for Wnt/beta-catenin signaling. Cold Spring Harbor perspectives in biology *4*.

Mallard, F., Tang, B.L., Galli, T., Tenza, D., Saint-Pol, A., Yue, X., Antony, C., Hong, W., Goud, B., and Johannes, L. (2002). Early/recycling endosomes-to-TGN transport involves two SNARE complexes and a Rab6 isoform. The Journal of cell biology *156*, 653-664.

Marois, E., Mahmoud, A., and Eaton, S. (2006). The endocytic pathway and formation of the Wingless morphogen gradient. Development *133*, 307-317.
Martinez Arias, A. (2003). Wnts as morphogens? The view from the wing of Drosophila. Nat Rev Mol Cell Biol *4*, 321-325.

Matsuoka, K., Morimitsu, Y., Uchida, K., and Schekman, R. (1998a). Coat assembly directs v-SNARE concentration into synthetic COPII vesicles. Molecular cell *2*, 703-708.

Matsuoka, K., Orci, L., Amherdt, M., Bednarek, S.Y., Hamamoto, S., Schekman, R., and Yeung, T. (1998b). COPII-coated vesicle formation reconstituted with purified coat proteins and chemically defined liposomes. Cell *93*, 263-275.

Maxfield, F.R., and McGraw, T.E. (2004). Endocytic recycling. Nat Rev Mol Cell Biol *5*, 121-132.

Mayor, S. (2014). Clathrin-independent pathways of endocytosis. In Endocytosis, S. Schmid, ed. (Cold Spring Harbour Lab Press), pp. 93-108.

McDowell, N., and Gurdon, J.B. (1999). Activin as a morphogen in Xenopus mesoderm induction. Seminars in cell & developmental biology *10*, 311-317.

McMahon, H.T., and Boucrot, E. (2011). Molecular mechanism and physiological functions of clathrin-mediated endocytosis. Nat Rev Mol Cell Biol *12*, 517-533.

Merrifield, C. (2014). Endocytic Accessory factors and regulation of Clathrin-mediated endocytosis. In Endocytosis, S. Schmid, ed. (Cold Spring Harbour Lab Press), pp. 37-48.

Miller, J.R. (2002). The Wnts. Genome biology *3*, Reviews 3001.

Mulligan, K.A., Fuerer, C., Ching, W., Fish, M., Willert, K., and Nusse, R. (2011). Secreted Wingless-interacting molecule (Swim) promotes long-range signaling by maintaining Wingless solubility. Proceedings of the National Academy of Sciences of the United States of America *109*, 370-377.

Musch, A. (2004). Microtubule organization and function in epithelial cells. Traffic *5*, 1-9.

Neumann, C.J., and Cohen, S.M. (1997). Long-range action of Wingless organizes the dorsal-ventral axis of the Drosophila wing. Development *124*, 871-880.

Neumann, S., Coudreuse, D.Y., van der Westhuyzen, D.R., Eckhardt, E.R., Korswagen, H.C., Schmitz, G., and Sprong, H. (2009). Mammalian Wnt3a is released on lipoprotein particles. Traffic *10*, 334-343.

Nickel, W., and Rabouille, C. (2009). Mechanisms of regulated unconventional protein secretion. Nat Rev Mol Cell Biol *10*, 148-155.

Nusse, R., Brown, A., Papkoff, J., Scambler, P., Shackleford, G., McMahon, A., Moon, R., and Varmus, H. (1991). A new nomenclature for int-1 and related genes: the Wnt gene family. Cell *64*, 231.

Nusse, R., and Varmus, H.E. (1982). Many tumors induced by the mouse mammary tumor virus contain a provirus integrated in the same region of the host genome. Cell *31*, 99-109.

Nusslein-Volhard, C., and Wieschaus, E. (1980). Mutations affecting segment number and polarity in Drosophila. Nature *287*, 795-801.

Osterlund, T., and Kogerman, P. (2006). Hedgehog signalling: how to get from Smo to Ci and Gli. Trends in cell biology *16*, 176-180.

Oving, I.M., and Clevers, H.C. (2002). Molecular causes of colon cancer. European journal of clinical investigation *32*, 448-457.

Palmer, L., Vincent, J.P., and Beckett, K. (2011). Wnts need a p(assport)24 to leave the ER. EMBO Rep *13*, 90.

Pan, C.L., Baum, P.D., Gu, M., Jorgensen, E.M., Clark, S.G., and Garriga, G. (2008). C. elegans AP-2 and retromer control Wnt signaling by regulating mig-14/Wntless. Dev Cell *14*, 132-139.

Panakova, D., Sprong, H., Marois, E., Thiele, C., and Eaton, S. (2005). Lipoprotein particles are required for Hedgehog and Wingless signalling. Nature *435*, 58-65.

Park, S.H., Cheong, C., Idoyaga, J., Kim, J.Y., Choi, J.H., Do, Y., Lee, H., Jo, J.H., Oh, Y.S., Im, W*., et al.* (2008). Generation and application of new rat monoclonal antibodies against synthetic FLAG and OLLAS tags for improved immunodetection. J Immunol Methods *331*, 27-38.

Pepperl, J., Reim, G., Luthi, U., Kaech, A., Hausmann, G., and Basler, K. (2013). Sphingolipid depletion impairs endocytic traffic and inhibits Wingless signaling. Mech Dev *130*, 493-505.

Piddini, E., Marshall, F., Dubois, L., Hirst, E., and Vincent, J.P. (2005). Arrow (LRP6) and Frizzled2 cooperate to degrade Wingless in Drosophila imaginal discs. Development *132*, 5479-5489.

Polakis, P. (2012). Wnt signaling in cancer. Cold Spring Harbor perspectives in biology *4*.

Port, F., Hausmann, G., and Basler, K. (2011). A genome-wide RNA interference screen uncovers two p24 proteins as regulators of Wingless secretion. EMBO Rep.

Port, F., Kuster, M., Herr, P., Furger, E., Banziger, C., Hausmann, G., and Basler, K. (2008). Wingless secretion promotes and requires retromer-dependent cycling of Wntless. Nature cell biology *10*, 178-185.

Pradhan-Sundd, T., and Verheyen, E.M. (2014). The role of Bro1 domain-containing protein Myopic in endosomal trafficking of Wnt/Wingless. Dev Biol.

Prasad, B.C., and Clark, S.G. (2006). Wnt signaling establishes anteroposterior neuronal polarity and requires retromer in C. elegans. Development *133*, 1757-1766.

Ramirez-Weber, F.A., and Kornberg, T.B. (1999). Cytonemes: cellular processes that project to the principal signaling center in Drosophila imaginal discs. Cell *97*, 599-607.

Reichsman, F., Smith, L., and Cumberledge, S. (1996). Glycosaminoglycans can modulate extracellular localization of the wingless protein and promote signal transduction. The Journal of cell biology *135*, 819-827.

Rijsewijk, F., Schuermann, M., Wagenaar, E., Parren, P., Weigel, D., and Nusse, R. (1987). The Drosophila homolog of the mouse mammary oncogene int-1 is identical to the segment polarity gene wingless. Cell *50*, 649-657.

Rios-Esteves, J., Haugen, B., and Resh, M.D. (2014). Identification of key residues and regions important for Porcupine-mediated Wnt acylation. J Biol Chem.

Rodriguez-Boulan, E., Kreitzer, G., and Musch, A. (2005). Organization of vesicular trafficking in epithelia. Nat Rev Mol Cell Biol *6*, 233-247.

Rojas, R., and Apodaca, G. (2002). Immunoglobulin transport across polarized epithelial cells. Nat Rev Mol Cell Biol *3*, 944-955.

Romer, W., Pontani, L.L., Sorre, B., Rentero, C., Berland, L., Chambon, V., Lamaze, C., Bassereau, P., Sykes, C., Gaus, K.*, et al.* (2010). Actin dynamics drive membrane reorganization and scission in clathrin-independent endocytosis. Cell *140*, 540-553.

Roy, S., Huang, H., Liu, S., and Kornberg, T.B. (2014). Cytoneme-mediated contact-dependent transport of the Drosophila decapentaplegic signaling protein. Science *343*, 1244624.

Rusten, T.E., Vaccari, T., and Stenmark, H. (2012). Shaping development with ESCRTs. Nature cell biology *14*, 38-45.

Schepers, A., and Clevers, H. (2012). Wnt signaling, stem cells, and cancer of the gastrointestinal tract. Cold Spring Harbor perspectives in biology *4*, a007989.

Schwank, G., Dalessi, S., Yang, S.F., Yagi, R., de Lachapelle, A.M., Affolter, M., Bergmann, S., and Basler, K. (2011). Formation of the long range Dpp morphogen gradient. PLoS biology *9*, e1001111.

Sharma, R.P., and Chopra, V.L. (1976). Effect of the Wingless (wg1) mutation on wing and haltere development in Drosophila melanogaster. Dev Biol *48*, 461-465.

Sheff, D.R., Kroschewski, R., and Mellman, I. (2002). Actin dependence of polarized receptor recycling in Madin-Darby canine kidney cell endosomes. Molecular biology of the cell *13*, 262-275.

Simmonds, A.J., dosSantos, G., Livne-Bar, I., and Krause, H.M. (2001). Apical localization of wingless transcripts is required for wingless signaling. Cell *105*, 197-207.

Sonnichsen, B., De Renzis, S., Nielsen, E., Rietdorf, J., and Zerial, M. (2000). Distinct membrane domains on endosomes in the recycling pathway visualized by multicolor imaging of Rab4, Rab5, and Rab11. The Journal of cell biology *149*, 901-914.

Sorkin, A., and von Zastrow, M. (2009). Endocytosis and signalling: intertwining molecular networks. Nat Rev Mol Cell Biol *10*, 609-622.

Springer, S., Chen, E., Duden, R., Marzioch, M., Rowley, A., Hamamoto, S., Merchant, S., and Schekman, R. (2000). The p24 proteins are not essential for vesicular transport in Saccharomyces cerevisiae. Proceedings of the National Academy of Sciences of the United States of America *97*, 4034-4039.

Stamos, J.L., and Weis, W.I. (2013). The beta-catenin destruction complex. Cold Spring Harbor perspectives in biology *5*, a007898.

Strating, J.R., and Martens, G.J. (2009). The p24 family and selective transport processes at the ER-Golgi interface. Biology of the cell / under the auspices of the European Cell Biology Organization *101*, 495-509.

Strigini, M., and Cohen, S.M. (2000). Wingless gradient formation in the Drosophila wing. Curr Biol *10*, 293-300.

Subra, C., Laulagnier, K., Perret, B., and Record, M. (2007). Exosome lipidomics unravels lipid sorting at the level of multivesicular bodies. Biochimie *89*, 205-212.

Tabata, T. (2001). Genetics of morphogen gradients. Nature reviews Genetics *2*, 620-630.

Takada, R., Satomi, Y., Kurata, T., Ueno, N., Norioka, S., Kondoh, H., Takao, T., and Takada, S. (2006). Monounsaturated fatty acid modification of Wnt protein: its role in Wnt secretion. Dev Cell *11*, 791-801.

Tanaka, K., Kitagawa, Y., and Kadowaki, T. (2002). Drosophila segment polarity gene product porcupine stimulates the posttranslational N-glycosylation of wingless in the endoplasmic reticulum. J Biol Chem *277*, 12816-12823.

Tang, X., Wu, Y., Belenkaya, T.Y., Huang, Q., Ray, L., Qu, J., and Lin, X. (2012). Roles of N-glycosylation and lipidation in Wg secretion and signaling. Dev Biol *364*, 32-41.

Thompson, A., Nessler, R., Wisco, D., Anderson, E., Winckler, B., and Sheff, D. (2007). Recycling endosomes of polarized epithelial cells actively sort apical and basolateral cargos into separate subdomains. Molecular biology of the cell *18*, 2687-2697.

Torroja, C., Gorfinkiel, N., and Guerrero, I. (2005). Mechanisms of Hedgehog gradient formation and interpretation. J Neurobiol *64*, 334-356.

Trajkovic, K., Hsu, C., Chiantia, S., Rajendran, L., Wenzel, D., Wieland, F., Schwille, P., Brugger, B., and Simons, M. (2008). Ceramide triggers budding of exosome vesicles into multivesicular endosomes. Science *319*, 1244-1247.

Traub, L. (2014). Cargo recognition in Clathrin-mediated endocytosis. In Endocytosis, S. Schmid, ed. (Cold Spring Harbour Lab Press), pp. 53-68.

Trichas, G., Begbie, J., and Srinivas, S. (2008). Use of the viral 2A peptide for bicistronic expression in transgenic mice. BMC Biol *6*, 40.

Ulloa, F., and Marti, E. (2010). Wnt won the war: antagonistic role of Wnt over Shh controls dorso-ventral patterning of the vertebrate neural tube. Developmental dynamics : an official publication of the American Association of Anatomists *239*, 69-76.

van den Heuvel, M., Harryman-Samos, C., Klingensmith, J., Perrimon, N., and Nusse, R. (1993). Mutations in the segment polarity genes wingless and porcupine impair secretion of the wingless protein. Embo J *12*, 5293-5302.

van den Heuvel, M., Nusse, R., Johnston, P., and Lawrence, P.A. (1989). Distribution of the wingless gene product in Drosophila embryos: a protein involved in cell-cell communication. Cell *59*, 739-749.

van der Bliek, A.M., Redelmeier, T.E., Damke, H., Tisdale, E.J., Meyerowitz, E.M., and Schmid, S.L. (1993). Mutations in human dynamin block an intermediate stage in coated vesicle formation. The Journal of cell biology *122*, 553-563.

Verges, M., Luton, F., Gruber, C., Tiemann, F., Reinders, L.G., Huang, L., Burlingame, A.L., Haft, C.R., and Mostov, K.E. (2004). The mammalian retromer regulates transcytosis of the polymeric immunoglobulin receptor. Nature cell biology *6*, 763-769.

Wandinger-Ness, A. (2014). Rab proteins and the Compartmentalization of the Endosomal system. In Endocytosis, S. Schmid, ed. (Cold Spring Harbour Lab Press), pp. 135-152.

Warming, S., Costantino, N., Court, D.L., Jenkins, N.A., and Copeland, N.G. (2005). Simple and highly efficient BAC recombineering using galK selection. Nucleic acids research *33*, e36.

Willert, K., Brown, J.D., Danenberg, E., Duncan, A.W., Weissman, I.L., Reya, T., Yates, J.R., 3rd, and Nusse, R. (2003). Wnt proteins are lipid-modified and can act as stem cell growth factors. Nature *423*, 448-452.

Wolpert, L. (1996). One hundred years of positional information. Trends in genetics : TIG *12*, 359-364.

Wolpert, L. (1998). Principles of Development. In Principles of Development (Oxford University Press), pp. 19-20.

Wu, C.H., and Nusse, R. (2002). Ligand receptor interactions in the Wnt signaling pathway in Drosophila. J Biol Chem *277*, 41762-41769.

Yang, P.T., Lorenowicz, M.J., Silhankova, M., Coudreuse, D.Y., Betist, M.C., and Korswagen, H.C. (2008). Wnt signaling requires retromer-dependent recycling of MIG-14/Wntless in Wnt-producing cells. Dev Cell *14*, 140-147.

Yu, J., Chia, J., Canning, C.A., Jones, C.M., Bard, F.A., and Virshup, D.M. (2014). WLS Retrograde Transport to the Endoplasmic Reticulum during Wnt Secretion. Dev Cell *29*, 277-291.

Zecca, M., Basler, K., and Struhl, G. (1996). Direct and long-range action of a wingless morphogen gradient. Cell *87*, 833-844.

Zeng, X., Goetz, J.A., Suber, L.M., Scott, W.J., Jr., Schreiner, C.M., and Robbins, D.J. (2001). A freely diffusible form of Sonic hedgehog mediates long-range signalling. Nature *411*, 716-720.

Zerial, M., and McBride, H. (2001). Rab proteins as membrane organizers. Nat Rev Mol Cell Biol *2*, 107-117.

Zhai, L., Chaturvedi, D., and Cumberledge, S. (2004). Drosophila wnt-1 undergoes a hydrophobic modification and is targeted to lipid rafts, a process that requires porcupine. J Biol Chem *279*, 33220-33227.

Zhang, P., Wu, Y., Belenkaya, T.Y., and Lin, X. (2011). SNX3 controls Wingless/Wnt secretion through regulating retromer-dependent recycling of Wntless. Cell Res *21*, 1677-1690.